



b
**UNIVERSITÄT
BERN**

Graduate School for Cellular and Biomedical Sciences

University of Bern

**Local immunosuppression
in Vascularized Composite Allotransplantation
using self-assembled hydrogel drug delivery systems**

PhD Thesis submitted by

Dzhuliya Dzhonova

from **Pazardjik , Bulgaria**

for the degree of

Ph.D. in Biomedical Sciences

Supervisor

Prof. Robert Rieben

Department for BioMedical Research, University of Bern, Bern,
Switzerland

Co-advisor

Prof. Praveen Vemula

Institute of Stem Cell Biology and Regenerative Medicine, Bangalore,
India

Accepted by the Faculty of Medicine, the Faculty of Science and the Vetsuisse
Faculty of the University of Bern at the request of the Graduate School for
Cellular and Biomedical Sciences

Bern, Dean of the Faculty of Medicine

Bern, Dean of the Faculty of Science

Bern, Dean of the Vetsuisse Faculty Bern

Abstract

Patients with hand amputations and severe face deformities today have the possibility of receiving a hand or face transplant. The successful esthetic and functional outcomes of this intervention, however, are countered by two persisting problems. First, current immunosuppression regimens often fail to completely prevent rejection of hand or face grafts. Recipients frequently experience multiple acute rejection episodes, and suffer in the long term from irreversible and untreatable chronic rejection, leading to graft loss. Second, and again an immunosuppression-related problem, is the high and frequent incidence of immunosuppression-related side effects, including malignancies, opportunistic infections, nephrotoxicity and a variety of metabolic disorders. Rejection due to under-immunosuppression and dangerous health impairment due to over-immunosuppression often occur concomitantly and signal that an accurate titration of immunosuppressants is crucial, yet difficult to achieve.

Localizing immunosuppression to the graft has been considered by many as a potential way to target immunosuppressants to the site of rejections, maintaining clinically relevant drug levels in the graft, while reducing the systemic exposure to the drugs.

In this work two different approaches for localized immunosuppression are investigated, using a rat hind-limb transplantation model:

- 1) An in situ forming implant for continuous release, loaded with rapamycin, and, as a main project of my PhD program:
- 2) A hydrogel loaded with TAC for enzyme-triggered drug release.

The findings described in this thesis indicate that substitution of systemic with localized immunosuppression is indeed feasible and yields better toxicological and immunological outcomes in the used animal model. In conclusion, localized immunosuppression is worth further investigation and development, both in terms of basic research, to establish control mechanisms for anti-graft immunity, and in terms of clinical application, to achieve efficient immunosuppression with reduced side effects.

Contents

1.	INTRODUCTION.....	1
1.1.	TRAUMA, AMPUTATION AND CURRENT SOLUTIONS.....	1
1.2.	VCA – FROM MYTH TO REALITY.....	3
1.3.	VCA – A XXI. CENTURY LANDSCAPE.....	6
1.4.	TRANSPLANTED VS. PROSTHETIC HAND.....	9
1.5.	IMMUNOBIOLOGY OF VCA REJECTION.....	10
1.5.1.	NEW INSIGHTS IN VCA REJECTION.....	11
1.5.2.	BEYOND CELL-MEDIATED REJECTION.....	12
1.6.	REGULATORY T CELLS IN TRANSPLANTATION.....	13
1.7.	A FINE LINE BETWEEN GVHD AND CHIMERISM.....	14
1.8.	IMMUNOSUPPRESSION IN VCA.....	15
1.8.1.	TAC, MMF AND CORTICOSTEROIDS.....	15
1.8.2.	ALTERNATIVE 1: MTOR INHIBITORS.....	18
1.8.3.	ALTERNATIVE 2: CO-STIMULATORY BLOCKADE.....	18
1.8.4.	ALTERNATIVE 3: ADOPTIVE CELL THERAPIES.....	19
1.9.	DRUG DELIVERY SYSTEMS.....	21
1.9.1.	BIOLOGICAL AND LIVING DDS.....	22
1.9.2.	MICRO- AND NANOPARTICLES.....	22
1.9.3.	SCAFFOLDS AND IMPLANTS.....	22
1.9.4.	ORGANO- AND HYDROGELS.....	23
1.9.5.	<i>IN SITU</i> FORMING IMPLANTS.....	26
2.	AIMS.....	27
3.	RESULTS.....	29
3.1.	LOCAL INJECTIONS OF TACROLIMUS-LOADED HYDROGEL REDUCE SYSTEMIC IMMUNOSUPPRESSION-RELATED TOXICITY IN VASCULARIZED COMPOSITE ALLOTRANSPLANTATION.....	31
3.2.	DELIVERY OF RAPAMYCIN USING <i>IN SITU</i> FORMING IMPLANTS INDUCES IMMUNOREGULATORY MECHANISMS PROMOTING VASCULARIZED COMPOSITE ALLOGRAFT SURVIVAL.....	73

<u>3.3. INTRA-GRAFT INJECTION OF TACROLIMUS PROMOTES SURVIVAL OF VASCULARIZED COMPOSITE ALLOTRANSPLANTATION</u>	<u>125</u>
<u>3.4. IN VIVO CHARACTERIZATION AND NON-INVASIVE MONITORING OF TACROLIMUS-LOADED HYDROGEL FOR LOCALIZED IMMUNOSUPPRESSION.....</u>	<u>137</u>
<u>4. DISCUSSION AND OUTLOOK.....</u>	<u>159</u>
<u>5. REFERENCES</u>	<u>162</u>
<u>6. ACKNOWLEDGEMENTS</u>	<u>174</u>
<u>7. CURRICULUM VITAE.....</u>	<u>175</u>
<u>8. PUBLICATIONS, ABSTRACTS, PRESENTATIONS</u>	<u>177</u>

1. Introduction

1.1. Trauma, amputation and current solutions

A major traumatic injury, requiring body part removal by amputation, leads to sudden and devastating loss of function and sensation of the lost part. This provokes changes in self-perception of the patient's body image, and in the assumed perception by others. The shocking loss of lifestyle and abilities taken for granted contributes to psychological maladjustment and long-term negative psychosocial consequences in nearly every amputee¹. The occurrence of psychiatric manifestations such as depression, anxiety, crying spells, insomnia, loss of appetite, suicidal ideas and psychotic behavior are alarmingly high in amputees².

To restore body completeness of amputees, prosthetics application has been documented in ancient Egypt, India, Greece, Rome and throughout the Middle Ages³. The first truly functional prosthetics were only developed in the 1500s by the French royal surgeon Ambroise Paré (**Figure 1a**)³. Ever since, prostheses increasingly sophisticated in functionality and design have become available. Today three main types of prostheses are on disposal to amputees:

- Cosmetic – used mainly during social events to improve appearance.
- Body-powered – functional, durable, require sufficient body strength.
- Myoelectric – controlled by electromyography (EMG) signals – contractions from the muscles of the residual limb. They trade their increased dexterity to a decreased grip strength⁴.



Figure 1. Cutting-edge hand prostheses then and now.
a) “Le Petit Lorrain” “a mechanical hand operated by catches and springs” in the 1500s³.



Figure 1b) 3D printable Adam Jensen bionic arm by Open Bionics.
<https://www.augmentedfuture.com>

XXI. century prosthetics research exploits advances in robotics, biomaterials and machine learning, to develop high-end commercially available bionics with multiple degrees of freedom, such as the BeBionic hand (<http://www.bebionic.com>), the Michelangelo hand (<https://www.ottobock.ch>), and the i-limb quantum (<http://www.touchbionics.com>)⁵. 3D printed low-cost bionic prosthetics are entering the market, promising open source, fully-customizable designer prosthesis that are fast and easy to produce⁶(**Figure 1b**).

The changes in prosthetics today are not merely technological, they are conceptual. The original goal of amputated body part reconstruction was to “include restoration of a socially acceptable presentation”⁷. Today the attitude has moved away from restoration and towards augmentation of the self, envisioning a biomechanical future, where humans are proudly “upgrading” their own imperfect body parts with more powerful and multi-functional bionic ones.

These futuristic aspirations however do not correspond to the reality of an average amputee here and now – many abandon their prostheses due to discomfort, pain and disappointing performance⁸. Lightweight, comfort, cost, functionality, improved strength and control, and resistance to environmental exposure are among the unmet needs of amputees^{8,9}. Until the technology is advanced enough to respond to the needs of amputees, there is one possibility that could restore not only appearance and function, but also sensation, the substitution of “like with like”, thanks to vascularized composite allotransplantation (VCA). VCA is the transplantation of fully functional units, like hands, face or abdominal wall, composed of multiple tissues, including skin, muscle, bone, fat, nerves, vessels, tendons etc.

1.2. VCA – from myth to reality

Perceived by some¹⁰ as an intermediate step between traditional prosthetics and futuristic bionics, VCA offers an adequate esthetic, functional and sensational recovery. Myths of similar interventions date back to AD 348, with the Saints Cosmas and Damian allegedly transplanting the leg of a dead Ethiopian man in place of the cancerous leg of a patient¹¹ (**Figure 2**). Centuries later, around 1885 – 1914 transplantations of vessels, heart, thyroid gland and parathyroids, adrenals, hypophysis, ovaries and testicles, kidney, spleen, pancreas, intestine, and prostate were attempted with limited success on animals and humans by Alexis Carrel, Jaboulay, Ullman and others¹². Autografts (grafts from the same person) and syngeneic grafts (grafts from genetically identical individuals) were always successful, while allografts (grafts procured from other donors of the same species) were typically rejected with various degrees of severity. Xenografts (donor and recipient are from different species) elicited the strongest immune response (today known as hyperacute rejection). The first proposals about the concept and importance of donor and recipient matching came from Masson's observations that blood group compatibility is important not only for successful blood transfusions, but also for skin grafting¹³. At that time Loeb hypothesized that the rejection process is driven by "individuality-differentials", and could show that the allograft rejection process is local and cell-mediated, driven primarily by lymphocytes¹⁴.



Figure 2. Miracle of Sts. Cosmas and Damian, “replacing a failed leg with a Moorish one” (fragment), Ditzingen, Kreis Ludwigsburg, early 16th century, Landesmuseum Württemberg, Stuttgart, Germany

In 1943 Gibson and Medawar observed that second skin grafts from the same donor were rejected much faster than the first grafts¹⁵. Medawar recreated the experiment with rabbits, moving the second set of grafts to the contralateral side of the body, to demonstrate that the observed acquired immunity was not local, but systemic and definitively concluded that the rejection process is a specific reaction of the host versus the graft¹⁶.

The student of Medawar – Rupert Billingham – however, demonstrated that rejection is not an unpreventable event. He inoculated mouse embryos with spleen cells from another mouse strain and when the delivered pups reached adulthood they accepted a skin graft from the strain donating the spleen cells, but not from other strains¹⁷. The mice became chimeras, meaning that in their circulation cells from both donor and recipient origin coexisted. At that time chimerism was considered an interesting finding, however without any clinical significance. Indeed, the first successful transplantation was achieved without the need of chimerism, by Murray and his team, who transplanted a kidney between identical twins on December 23rd, 1954¹⁸. Although technically the surgery was nothing new, it's success spurred a great interest in transplantation and in 1960 the first successful renal transplantations between non-twins were performed in France, using sublethal total body irradiation and corticosteroids¹⁹. However, patients treated that way still rejected their grafts, and none of them survived more than one year. Starzl changed that by using azathioprine and prednisone to successfully revert rejection episodes in kidney transplantation²⁰.

Inspired by Starzl, in 1964 a hand transplantation was attempted in Ecuador, using the same protocol, but within three weeks the graft was removed due to rejection²¹. Hand transplantation success had to be postponed until the discovery of modern immunosuppression (IS) – cyclosporine A (CsA) in 1980s²², tacrolimus (TAC) and mycophenolate mofetil (MMF) in 1990s^{23,24}. In 1985 Hewitt and Black published their successful extension of graft survival in a rat hind-limb allotransplantation model, treated with CsA^{25,26}, which led them to be referred to as the “Cosmas and Damian in the 20th century”²⁷. Finally, the first successful hand transplantation was performed on 18 September 1998 by Dubernard, followed by the first face transplantation on 27 November 2005 by Devauchelle. Key moments in the history of VCA are summarized in **Table1**.

Table 1. Key moments in the history of VCA

Pioneering VCA	Year	Lead surgeon	Survival
Digital flexor mechanism²⁸	1957	Peacock	Not reported
Hand – unilateral unsuccessful	1964	Gilbert	Removed in 3 weeks due to insufficient immunosuppression ²⁹
Knee-joint³⁰	1996	Hofmann	Maximum 56 months survival ³¹
Laryngotracheal³²	1998	Strome	Removed after 14 years due to chronic rejection ³³
Hand – unilateral³⁴ first short-term success	1998	Dubernard	Removed after 2 years, due to non-compliance ³⁵
Hand – unilateral³⁶ first long-term success	1999	Breidenbach	At least 12 years ³⁷ , likely ongoing
Hand - bilateral³⁸	2000	Dubernard	At least 13 years ³⁹ , likely ongoing
Uterus⁴⁰	2000	Fageeh	Removed after 99 days due to acute vascular thrombosis ⁴⁰
Abdominal wall⁴¹	Publis hed 2003	Levi	Out of 14 patients, 5 patients and 4 grafts were still surviving in 2009 (follow-up 2-7.1 years) ⁴²
Tongue⁴³	2003	Ewers	Patient died in one year ⁴³
Face – partial⁴⁴	2005	Devauchelle	Partial graft loss after 10 years followed by death of patient in 2016 from cancer ⁴⁵
Penis⁴⁶	2006	Hu	Removed on patient request in two weeks ⁴⁶
Face - total⁴⁷	2010	Barret	Ongoing
Leg⁴⁸	2011	Cavadas	Removed due to post-transplant lymphoproliferative disease ⁴⁹
Hand – pediatric bilateral⁵⁰	2015	Levin	Ongoing ⁵⁰

1.3. VCA – a XXI. century landscape

The International Registry on Hand and Composite Tissue Transplantation was founded in May 2002 by Dubernard, with the purpose to register hand and face transplantations worldwide, as well as their outcomes and side effects on a voluntary basis. By May 2017, 66 hand (18 unilateral and 38 bilateral) and 30 face transplantations have been registered⁵¹ by a growing amount of VCA centers. The reports of the registry together with case reports and studies initiated by the VCA centers themselves greatly facilitate evaluation of the VCA landscape today.

- Graft survival: Clinical cases of VCA are still too few to allow accurate estimation of the typical half-life of VCA grafts. What is known is that 86.6% of hand allografts reached a 10 year graft survival and 96.6% of face allografts reached 5 years, as of 2017⁵¹;
- Functional recovery: According to the Hand Transplantation Score System functional recovery is good for hand transplants (**Figure 3**), and face transplant recipients are mostly “very satisfied” with their grafts⁵¹;
- Graft rejection: Most hand and face transplant recipients experienced at least one acute rejection (AR) episode, 87.8% and 72.7%, respectively, in the first year post-transplantation, and up to 12 AR episodes per patient were recorded so far⁵¹. Nine of the hand and two of the face transplants performed so far developed chronic rejection (CR), requiring removal of 4 of the hand grafts⁵¹;
- Cross-center synchronization: There are no internationally accepted, standardized protocols for pre-operative use of graft perfusion solutions, induction or maintenance of IS, treatment of rejection episodes or guidelines to exit strategies. Most VCA centers apply their own sets of protocols, typically based on solid organ transplantation treatment regimens⁵², introducing wide variability in the small clinical volume of VCA.
- Graft acceptance: Unlike solid organs, VCA grafts must fulfill the esthetical and functional expectations of their recipients in order to be psychologically accepted as “own”. Disappointment in graft appearance and performance can contribute to frustration and abandonment of the graft. The recipient of the first penis transplant and his wife couldn't psychologically accept the graft and demanded it's removal⁴⁶, emphasizing

the importance of careful psychological screening for selection of appropriate VCA candidates.



Figure 3. Pediatric bilateral forearm transplantation, 9 months after surgery. Previously a quadruple amputee, Zion Harvey (pictured) could sense a light touch on his transplanted hands 6 months after transplantation, had muscle innervation 7-10 months after the surgery and was able to write, feed, toilet, and dress himself independently by the 18th month⁵⁰.

- Compliance: Non-adherence is a widespread cause of rejection and graft removal in solid organ transplantation and its impact in VCA begins to be estimated. The recipient of the first successful hand transplantation was not satisfied with the new hand, stopped adhering to his IS, resulting in graft rejection and amputation in 2001⁵³. A study from 2012 determined that 8 of 49 hand grafts were lost due to non-adherence, while only 4 grafts were lost due to other reasons⁵⁴.
- Side effects: According to the most recent report of the International Registry on Hand and Composite Tissue Transplantation, 41.5% of the registered hand transplant recipients experienced hyperglycemia, 26% had increased serum creatinine values, some leading to end-stage renal disease, hemodialysis and even kidney transplantation. Opportunistic bacterial, viral, and fungal infections during the first post-transplant year were experienced by 32.3%, 18.5%, and 12.3% of hand recipients, respectively. Post-transplant lymphoproliferative disease, basal cell carcinoma and various further complications were reported⁵¹. Similar was the situation with the face transplant recipients⁵¹. **Table 2** summarizes the major hand and face transplantation complications from the report⁵¹. The majority of these complications are secondary to the immunosuppressive drugs, used continuously to prevent or revert graft rejection.
- Cost: The cost-utility ratio for the different VCA modalities is highly variable. It has been estimated that the life-long economic impact of a unilateral hand transplantation in US is on average \$528,293 and for

bilateral \$529,315, the bulk of which consists of IS costs⁵⁵. A uni- and bilateral prosthesis for comparison has been calculated by the same study to cost \$20,653 and \$41,305, respectively, making apparent that more cost-effective IS is critical to bring such a life-enhancing procedure closer to an acceptable cost threshold in an already overwhelmed health care system.

Table 2. Complications in hand and face transplant recipients

Complications (%)		Hand transplantation		Face transplantation	
		First post-transplant year	Follow-up	First post-transplant year	Follow-up
Opportunistic infections	Bacterial infection	32	7.7	24.1	13.8
	Cytomegalovirus infection	12	1.5	13.8	6.9
	Herpes simplex infection	6	–	17.2	13.8
	Herpes zoster infection	2	9.2	–	–
	Epstein–Barr virus infection	–	1.5	3.4	–
	Fungal infection	12	1.5	17.2	6.9
Metabolic complications	Hyperglycemia/ Post-transplant Diabetes Mellitus (PTDM)	42	23.0	24.1	3.4
	Increased creatinine values	25	26.0	44.8	13.8
	Arterial hypertension	6	11.0	3.4	10.3
Malignancies		2	3.0	3.4	13.8

From this statistical digest it becomes apparent that the great promise of VCA is only undermined by the costly, life-long, systemic, IS and its direct toxicity and detrimental side effects on the health of the patients. Currently, IS works by nonspecifically reducing the number and activity of the main participants in acute rejection, the T lymphocytes. Inevitably, essential functions of the immune system, such as keeping infections and cancer cell progression in check, are halted – skyrocketing the risks for their respective development in the immunosuppressed patient. Additionally, higher and persistent doses of systemic IS have direct cytopathic effects, leading to nephrotoxicity, diabetes, hypertension and a variety of metabolic disorders. And despite all, modern IS fails to prevent AR episodes in VCA, nor can it stop the progression to CR.

1.4. Transplanted vs. prosthetic hand

Sober comparison of transplant versus prosthesis requires consideration of functional, esthetical, financial, psycho-social, health and many other factors and fall beyond the scope of this work. Level of amputation influences greatly the performance of both and additional factors, such as type of prosthesis or genetic differences between graft and recipient account for a tremendous variability. **Table 3** is a reductionist attempt to juxtapose the pros and cons of a transplanted hand versus those of a myoelectric prosthesis, largely consulted by the work of Salminger et al.⁵⁶. In addition, a small study comparing outcomes of 5 hand recipients and 7 prosthetic patients revealed that both offered similar functional outcomes. However, hand transplant recipient considered significantly better their vitality, emotional and mental health, and paradoxically – physical functioning, revealing that self-perception and not only function has importance when choosing between the two⁵⁷.

Table 3. Back-to-back comparison of hand transplantation vs. myoelectric prosthesis

Factor	Hand transplantation	Prosthetic hand
Appearance	Natural; differences in size, color and hair growth between recipient and graft remain obvious	Synthetic; inferior
Function	Depends on level of amputation and rehabilitation commitment; could decline with AR episodes incidence	Sufficient motor function to perform day-to-day activities; difficult to use for body hygiene and grooming
Sensation	Potentially complete recovery; Could decline with AR episodes incidence	None; requires constant visual control – not suitable for blind amputees
Psychological	Higher satisfaction	Lower satisfaction; frequent abandonment (estimated 1 out 5 users)
Surgery	Extensive, risky	Not necessary
Rehabilitation	Extremely demanding: 3-4h, 7 days/week in the first 4.25 ± 5.02 months, followed by 3-6h, 5 days/week for 11.1 6± 9.31 months	Rapid: 10-20h after a 3 month recovery period for the stump
Medication	Life-long, associated with elevated health hazards and risk of AR and CR	Not necessary
Follow up	Therapeutic drug monitoring, protocol biopsies, close monitoring of various health parameters	Not necessary
Return to normal life	Delayed due to extensive rehabilitation	Rapid due to short learning period to control the prosthesis
Cost	High; coverage by insurance providers depends on country	Variable; covered by insurance providers as standard of care
Miscellaneous	No need of de/re-attachment; no need of charging; Self-repairing	Frequent de/re-attachment, may require change of multiple attachments to perform different tasks; needs a power source; needs technical assistance or substitution when broken

1.5. Immunobiology of VCA rejection

Today we know that the “individuality-differentials” of Leo Loeb are products of histocompatibility genes, coding for Major Histocompatibility Complexes (MHC) and minor histocompatibility ones. The MHC present self- and foreign peptides (from viruses, bacteria, cancer cells, grafts) – and in the latter case – elicits strong immune responses. There are two classes of MHC: MHC-I, which is constitutively expressed on all nucleated cells, and MHC-II, which is only expressed on professional Antigen-Presenting Cells (APC) – dendritic cells (DC), B cells, as well as activated endothelial cells and macrophages. MHC-I presents peptides to CD8⁺ Cytotoxic T Lymphocytes (CTL), while MHC-II presents peptides to CD4⁺ T helper lymphocytes (Th)⁵⁸. These T cells are the main drivers of the rejection processes that Medawar observed⁵⁹.

Clinical evidence suggests that the majority of AR episodes in VCA are largely confined to the skin, macroscopically comprising of erythematous macules and histologically of dense perivascular dermal and epidermal CD3⁺ infiltrates^{53,60}. The Banff rejection classification system has been devised to stratify the advancement and severity of AR episodes based on their histological appearance (**Table 4**)⁶¹.

Table 4. A brief overview of Banff classification of acute rejection in VCA

Rejection Severity Grade (Banff)	Histological Manifestation
Grade 0 (no rejection)	No infiltration
Grade 1 (mild rejection)	Mild perivascular infiltration
Grade 2 (moderate rejection)	Moderate perivascular inflammation
Grade 3 (severe rejection)	Dense dermal and epidermal involvement
Grade 4 (necrotizing AR)	Frank skin necrosis

Skin has important protective functions to the underlying body, so keeping up its integrity is an important task for the immune system. It is densely populated with diverse immune cells, such as long-lived resident or migratory DC and T cell types. In fact skin hosts about twice as many lymphocytes as are circulating in the blood⁶². Resident dermal DC (Langerhans cells, classical dermal DCs, and Langerin⁺ dermal DCs) sample antigens, mediate tolerogenic effects on T cells, activate T cells, or imprint skin-homing phenotype on T cells⁶³. T cells in skin are over 95% CD45RO⁺ memory T cells (mostly effector memory T cells), the rest are passenger lymphocytes⁶². Skin DC can directly activate memory T cells in skin when encountering a known pathogen⁶⁴. Additionally circulating DC, such as interferon alpha (IFN- α) secreting plasmacytoid DC⁶⁵, and central memory T cells can be rapidly recruited when

damage associated molecular patterns (DAMPs) are released from the keratinocytes in the epidermis, in response to tissue damage (i.e. procurement, ischemia, transplantation). Other recruited cells, such as macrophages further release interleukins 1 and 6 (IL-1 and IL-6), which prompt nearby DC to traffic to the draining lymph node where they activate naïve alloreactive T cells. Those initiate proliferation, and differentiation into effector CTL or Th, which under the influence of specific skin-homing addressins migrate to the site of antigen exposure⁶⁶. Th kill graft cells via first apoptosis signal receptor and ligand (Fas-FasL) interactions, and produce pro-inflammatory cytokines, such as IFN- γ , IL-4 and tumor necrosis factor alpha (TNF- α), which attract macrophages and eosinophils. CTL deliver a “lethal punch” – a mixture of perforin and granzyme B digesting graft parenchymal cells and vasculature.

1.5.1. New insights in VCA rejection

The abovementioned mechanism of rejection has been dogmatic until recently, but new findings show that we have a lot more to learn about rejection. A study of 5 full facial transplants reported that contrary to expectations, the mononuclear infiltrates observed during AR in facial skin are dominated by donor derived resident immune cells, and not host ones. Possibly, the graft-infiltrating host immune cells are in turn presented to graft T cells, which mount a mirroring reaction, exacerbating the collateral tissue damage⁶⁷. This surprising finding prompts re-evaluation of the way we look at rejection, but more importantly it generates new avenues for treatment. Memory T cells are resistant to conventional IS, as they are less reliant on co-stimulation⁶⁸. There are two types of memory T cells – migratory central memory T cells (T_{cm}), and effector memory T cells (T_{em}). T_{cm} circulate for long periods and upon re-activation respond with vigorous proliferation, while T_{em} remain in the tissue and upon re-exposure to the same antigen mediate immediate effector functions^{69,70}. Although definitive studies are lacking, alloreactive memory T cells from both graft and recipient, could have essential roles in rejection, as reviewed by Beura et al.⁷¹. The study of Lian et al. provides an interesting suggestion that irradiation of the graft prior transplantation could reduce the amount of resident T cells and hopefully reduce the risk of AR⁶⁷.

Another novel point of skin rejection goes about the importance of microanatomical differences of skin. Rejection within different skin areas (i.e. skin with hairs on the arm versus hairless, thinner skin on the palms) appears to present distinct mechanisms. For example Schneeberger et al. distinguished

an “atypical” AR involving the nails and the palms, as opposed to the “typical” rejection pattern, sparing the palmar skin⁷². Another study employing a rat VCA model showed differences in cytokine expression between rejecting skin of the thigh versus rejecting skin of the footpad⁷³. To further complicate the picture, cross-reactive memory T cells originally activated by pathogens⁷⁴, environmental exposure to cold and dry weather⁷⁵ and frequent mechanical stress⁷² have also been related to skin rejection.

1.5.2. Beyond cell-mediated rejection

T cells can activate alloreactive B cell clones to produce donor-specific antibodies (DSA)⁷⁶, which can opsonize graft cells and initiate complement activation⁷⁷. DSA deposition on the graft’s vascular endothelium facilitates complement-, neutrophil- and macrophage-mediated vascular damage. DSA and deposition of the complement product C4d, are increasingly reported in VCA, especially after multiple AR episodes^{45,78,79}, however their diagnostic value is still a subject of debate. Antibody-mediated rejection (AMR) is a leading cause of graft loss in solid organ transplantation, mandating close attention to their role in VCA, as mentioned by Etra et al.⁸⁰. In addition to T and B cells, Natural Killer (NK) cells also have the ability to recognize and attack foreign cells and are increasingly recognized as important participants in graft rejection⁸¹.

Lymphoid neogenesis, the ectopic formation of lymphoid-like structures (called tertiary lymphoid organs, or TLO), have also been described in VCA⁷⁹. TLO arise under circumstances of persistent antigen presence and form discrete T cell and B cell zones, complete with high-endothelial venules and even germinal centers⁸². Not only structural are the similarities of TLO with lymph nodes, but also functional, as they serve as local sites for antigen presentation, T cell activation and antibody production.

DSA and TLO are suspected contributors to CR – a slow progressive process, challenging to detect as it develops in deep graft vessels in absence of symptoms. The mechanism behind CR in VCA is not clearly understood as only few clinical cases have been described^{45,83-85}. Generally persistent inflammation inflicts subclinical damage to vascular endothelium and stimulates proliferation of underlying intimal muscle layer of graft vessels. The resulting narrowing of the vascular lumen (accelerated graft arteriosclerosis) causes graft ischemia. The Banff classification for CR in VCA from 2007 included as clinical and histological features of CR vascular narrowing, loss of

adnexa, skin and muscle atrophy, fibrosis of deep tissue, myointimal proliferation and nail changes⁶¹. Non-compliance to IS and frequent preceding AR episodes coincide with CR, mandating strict control of IS. There is a troubling gap of knowledge on treating or preventing CR and the outcome is ultimately partial or later total removal of the graft.

1.6. Regulatory T cells in transplantation

One of the most discussed topics in transplantation revolves around a subset of T cells expressing forkhead box P3 (FOXP3⁺) transcriptional regulator⁸⁶, called regulatory T cells (Treg). Treg can inhibit activation and proliferation of effector T cells (Teff), such as Th and CTL, and their cytokine production. There are four general mechanisms, depending on their anatomical and inflammatory setting, that Treg employ to reach that goal are as reviewed by Vignali⁸⁷:

1. Secreting anti-inflammatory cytokines, such as IL-10, IL-35 and transforming growth factor beta (TGF- β)
2. Teff apoptosis induction by releasing granzymes and perforin
3. DC modulation
4. Metabolic disruption

Treg can affect Teff stimulated by weak T cell receptor signaling, but not if the signal is strong⁸⁸. This why Treg are permitting inflammation to unfold when necessary, but protect tissue homeostasis when inflammation can hurt more than help, as reviewed by Sakaguchi⁸⁹. Unsurprisingly, there is a big interest in harnessing and augmenting the immunosuppressive capacities of Treg as prognostic means and as adoptive cell immunotherapy in transplantation. A difficulty to the later is their flexibility in relation to their environment. T reg are a heterogeneous population, consisting of terminally committed, potential and transient lineages, with intrinsic plasticity to acquire or lose regulatory and Teff pathogenic phenotypes (called exTreg), as reviewed by Sawant and Vignali⁹⁰. Natural thymus-derived Tregs (tTreg) are considered committed to a stable FOXP3 expressing lineage⁹¹, while Treg generated in peripheral tissues (pTreg) in response to antigens bolster more promiscuous behavior. Treg suppressive function becomes destabilized when the ratio of Teff in respect to Treg is skewed⁹² and in presence of IL-6⁹³, which is abundant in inflammation. Moreover persistent inflammatory conditions can downregulate FOXP3 expression in Treg and convert them to pathogenic Teff phenotypes. This flexibility of Treg to adapt to intrinsic and extrinsic factors requires better understanding of the principles controlling their fate.

One additional factor affecting Treg in transplantation is IS. Mammalian target of rapamycin (mTOR) inhibitors, such as Sirolimus (rapamycin) support Treg expansion⁹⁴, and in clinics have been correlated to higher Treg levels and improved graft function⁹⁵. Calcineurin inhibitors, like TAC and CsA show dose-dependent effect on Tregs⁹⁶.

1.7. A fine line between GVHD and chimerism

The outcome of the relationship between graft and recipient immunity depends heavily on who has the upper hand. In a rat VCA model it has been shown that if more than 50% of the circulating cells come from the donor, 70-100% of the animals will develop graft-versus-host disease (GVHD)⁹⁷. As the name suggests, GVHD is a reaction of graft derived immune cells, against host tissues, particularly skin, liver and mucosal tissues, such as the gastrointestinal tract. GVHD, much like rejection, is a frequent clinical reality with acute and chronic forms. It shares remarkable similarities with graft rejection in both pathogenesis and treatments (nonspecific IS). GVHD can progress to a life-threatening condition and is a major risk of cell-based therapies, such as bone marrow transplantation or Treg transplantation.

Still, the lively exchange and replacement of cells between graft and recipient could facilitate a much more fortunate outcome. If as much as 20-50% of the immune cells circulating are donor derived, mixed hematopoietic chimerism takes place, and it is a reliable sign of good graft function and potentially tolerance⁹⁷. VCA grafts feature a significant own immune component within their skin, lymph nodes and vascularized bone, containing bone marrow (BM), raising possibilities for both GVHD and chimerism among VCA recipients. The quantity of BM depends on donor and recipient age, and kind/part of bone transplanted. With increasing age “red”, hematopoietic bone marrow is reduced to bones of the central skeleton and the epiphyses of long bones. Neither GVHD nor chimerism have been confirmed in clinical VCA even after an infusion of donor-derived hematopoietic stem cells without prior myeloablation⁷⁸.

1.8. Immunosuppression in VCA

IS in VCA begins prior or during the transplantation itself, with an induction therapy, aiming to prevent acute rejection in the early post-transplant period. It is consisting of poly- or monoclonal antibodies against various surface molecules on human T cells, and is followed by administration of high doses of TAC, MMF and steroids in the majority of cases⁵². The most trusted induction IS in VCA is the infusion of anti-thymocyte globulins (ATG), used in 57.9% of hand and 91.7% of face transplants⁵¹. ATG are polyclonal Immunoglobulin G (IgG) antibodies against human T cells, purified from rabbit or horse serum. They cause complement-mediated lysis of circulating T cells, as well as T and B cell apoptosis, as reviewed by Mohty⁹⁸. Since a common complication of ATG is cytokine release syndrome, increasingly monoclonal antibodies are chosen over ATG. Alemtuzumab (anti-CD52), Basiliximab (anti-CD25 – the α chain of the IL-2 receptor), and Daclizumab (another IL-2 receptor agonist) have been introduced in VCA⁵¹, although their advantage over ATG have not yet been confirmed^{99,100}. Induction therapies aggressively and profoundly deplete T cells, making the patients extremely vulnerable to infections and malignancies.

Maintenance IS includes the life-long daily or twice a day systemic IS, used as a prophylaxis against rejection. Maintenance IS in VCA today presents an interesting paradox. Rodent, porcine and non-human primate VCA models are successfully treated with an increasingly broad and sophisticated repertoire of novel drugs, cell-based therapies and intelligent drug-delivery systems (DDS). Meanwhile, in clinical setting, patients are almost invariably treated with the infamous mainstay triple therapy of TAC, MMF and corticosteroids⁵².

1.8.1. TAC, MMF and corticosteroids

Not long after its appearance in 1984, TAC²³ took the crown from the roughly 100 times weaker CsA as the most potent and used immunosuppressant¹⁰¹. The two drugs are structurally different and form complexes with different intracellular targets – CsA binds cyclophilin, while TAC binds FK-506 binding protein. Both complexes ultimately inhibit the same serine/threonine phosphatase – calcineurin.

Calcineurin is localized in the cytosol of cells in virtually any tissue and organ in the body, importantly so in T- and B-lymphocytes. In response to

increased cytosolic Ca^{2+} levels it dephosphorylates the cytosolic nuclear factor of activated T cells (NFAT), as detailed by Rusnak and Mertz¹⁰². Dephosphorylated NFAT translocates to the nucleus, where it meets nuclear transcription factors from the activator protein 1 family (AP-1)¹⁰³. The two form a complex, which binds to the promoter of the IL-2, 4, 10, 17 genes and initiates their transcription. The inhibition of this process by the calcineurin inhibitors CsA and TAC results in downregulation of these cytokines¹⁰⁴. As result of IL-2 downregulation, T cell activation and differentiation into effector subtypes is inhibited as summarized by Boyman and Sprent¹⁰⁵. In addition to NFAT, nuclear factor κ light-chain enhancer of activated B cells (NF- κ B) is also suppressed by calcineurin inhibition¹⁰⁶. NF- κ B regulates the expression of a variety of genes, including those coding TNF- β ¹⁰⁷ and IFN- γ ¹⁰⁸.

Independently of calcineurin, TAC and CsA inhibit the c-Jun N-terminal kinase (JNK) and p38 mitogen activated protein kinases (MAPK), which as well are regulating AP-1 activity and IL-2 gene expression¹⁰⁹. Some literature suggests also a role of CsA and TAC in upregulation of TGF- β , which as well inhibits T cell proliferation in an IL-2-dependent manner¹¹⁰.

In terms of pharmacokinetics, TAC is a class 2 drug according to the Biopharmaceutics Classification System (BCS) of the U.S. Food and Drug Administration (FDA). This means it has low solubility, high permeability, elimination via extensive metabolism (instead of urine or bile) and the effect of efflux transporters determines the bioavailability, rather than that of absorptive transporters¹¹¹. TAC has a poor oral bioavailability (the amount of drug reaching the circulation without being metabolized). Venkataramanan et al. summarized that TAC bioavailability in studied liver and kidney transplant cohorts is around 25%, meaning that the patient needs to take up to 4 times higher dose to achieve therapeutic systemic TAC levels¹¹². In addition, TAC has a narrow therapeutic window (therapeutic dose does not differ substantially from the toxic dose)¹¹³, and large inter- and intra-patient variability of absorption. The latter is dependent on patient age, race, hematocrit, albumin concentration, dose of accompanying corticosteroids, expression of cytochrome P450 (CYP) and P-glycoprotein (P-gp) and many others as reviewed by Staatz and Tett¹¹⁴.

TAC is administered orally, and is metabolized by CYP 3A¹¹⁵ and P-gp in the gastrointestinal tract, which pumps it out of the enterocytes (intestinal cells) and back into the intestinal lumen, as reviewed by Hebert¹¹⁶. From the intestines TAC enters the liver via the portal vein, where it is further metabolized to multiple products, most of which have weak to none IS

capabilities¹¹⁷. In the circulation majority of TAC binds to erythrocytes and plasma proteins, and only the non-bound TAC ultimately reaches the lymphocytes¹¹⁸.

TAC therapy is associated with multiple side effects, including nephrotoxicity, malignancies and infections and metabolic abnormalities. The most common and clinically significant adverse effect of TAC therapy is nephrotoxicity. Acute TAC-induced nephrotoxicity, manifested as increase in serum creatinine values, is typically reversible, while chronic nephrotoxicity is irreversible and is histologically observed as interstitial fibrosis and tubular atrophy, as skillfully exemplified in the 2017 Atlas of Renal Pathology by Lusco et al.¹¹⁹. TAC also stimulates the sodium chloride co-transporter, causing sodium retention and hypertension – another common complication of TAC therapy¹²⁰. Further, patients on TAC therapy are at increased risk of post-transplant diabetes mellitus as Jindal et al. summarized¹²¹. TAC suppresses glucokinase activity, leading to reduced ATP production and glycolysis and therefore reduction of insulin secretion and hyperglycemia¹²². An extensive list of adverse effects of TAC, including infections, malignancies, alopecia and gastrointestinal disturbances is available online at <https://www.uptodate.com/contents/pharmacology-of-cyclosporine-and-tacrolimus>.

To reduce risks of toxicity and ensure optimal IS, therapeutic drug monitoring of TAC trough levels in whole blood is helpful, but not perfect. A study of 90 liver transplant recipients showed that local intra-graft TAC levels and TAC levels in PBMCs (peripheral blood mononuclear cells, which are mostly lymphocytes) had both good correlation to rejection, but whole blood TAC levels didn't¹²³.

To minimize the administered TAC dose and AR risks, TAC is typically administered in conjunction with steroids, powerful anti-inflammatory drugs, inhibiting IL-1 production, and MMF, a selective inhibitor of *de novo* purine synthesis and thereby proliferation of T and B cells. The dosing of each drug varies across the different transplant centers, with daily TAC doses ranging between 8 and 25 ng/mL, steroids from 2.5 to 20mg and MMF between 500mg and 2g, as summarized by Howsare et al.⁵².

To reduce the adverse effects of this triple therapy many centers attempt strategies for minimization of IS with variable success. The latest report of the International Registry on Hand and Composite Tissue Transplantation reveals 10 hand transplant cases of MMF withdrawal, of which 4 were unsuccessful⁵¹. Further, in 12 hand and 5 face transplant cases there was an attempt for

steroid withdrawal, unsuccessful in 7 hand and 2 facial cases, respectively⁵¹. Finally, some groups took the courage to break out of the triple therapy scheme and attempt addition of, or conversion of one of its components to alternative IS drugs, such as rapamycin and Belatacept (see below), or even using cell-based therapies.

1.8.2. Alternative 1: mTOR inhibitors

Discovered in earth samples from the island Rapa Nui, rapamycin – a bacterial antifungal metabolite was described to have potent IS function. Similarly to TAC it forms a complex with FK-506 binding protein, which instead of calcineurin, binds to and specifically inhibits the mammalian target of rapamycin (mTOR). The mTOR is a master regulator of cell cycle progression and its inhibition halts activation and proliferation of T and B cells as well as endothelial cells, hepatocytes, and smooth muscle cells^{124,125}. Rapamycin is used as a substitute for TAC, CsA or MMF in solid organ transplantation, however whether it offers superior outcomes is controversial. As example one study analyzed 142 reports of kidney transplant recipients treated with calcineurin inhibitors or mTOR inhibitors and concluded that although mTOR inhibitors presented improved graft outcomes, the patient outcomes were actually worse¹²⁶.

In VCA, three hand transplant recipients had TAC dose lowered with addition of rapamycin, and three face transplant recipients were switched to rapamycin – two from TAC and one from MMF, respectively. In one face transplant recipient the treatment was based on Everolimus (derivative of rapamycin) and steroids, instead⁵¹. Future long-term follow-up reports should investigate whether the mTOR inhibitors are a better alternative to the triple therapy.

1.8.3. Alternative 2: Co-stimulatory blockade

The activation of T cells requires more than interaction of their T cell receptor¹²⁷ with the MHC-peptide complex¹²⁸. A second trigger is provided by interactions of co-stimulatory molecules, such as CD40 (expressed on APC) and its ligand CD40L (on activated T cells) or CD28 (on T cells) and its ligands CD80 and CD86 (on APC)¹²⁹. Other molecules can interact with those ligands, too, to provide the opposite – inhibitory effects. For example CTL

antigen-4 (CTLA-4) binds CD80/CD86¹³⁰ thereby blocking their interaction with CD28 on CTL. Loss of co-stimulation blocks CTL proliferation, making co-stimulatory blockade a subject of great interest in transplantation.

Belatacept – a recombinant antibody consisting of the extracellular domain of CTLA-4 and a fragment of a modified Fc portion of IgG1 to extend its half-life in the body – was recently approved as co-stimulatory blocker for T cells in kidney transplantation (2011)¹³¹. Recently it has been tested in 4 hand transplant recipients with mixed success. While three of the four patients tolerated the introduction of this medicament well and could achieve reduction of their daily TAC dose, the fourth developed an AR, which resulted in graft amputation¹³². A likely reason is that mature T cells down-regulate their CD28 expression and are less dependent on co-stimulation than naïve T cell, meaning that they can survive treatment with Belatacept and mediate rejection despite it¹³³.

The quest for novel IS drugs stagnates, due to inadequate regulatory endpoints for drug approval, lack of interest by the pharmaceutical industry, and other issues, as summarized by Stegall et al.¹³⁴. That re-directs the quest for improved welfare of patients and grafts to alternative strategies. One alternative strategy entering the bedside is switching from IS to immunomodulation – directing the immune response towards desired regulatory instead of effector behavior towards the graft. The two means to get there are namely increase in Treg and/or induction of chimerism. Rapamycin is an immunosuppressant with potentially immunoregulatory capabilities. For example a recent study in a small cohort of 15 liver transplant recipients converted from TAC to mTOR inhibitors reported on increase in their Treg count in peripheral blood¹³⁵. But while Treg promotion is a fortunate side effect of rapamycin treatment, it is the sole business of another approach – adoptive cell transfer therapies.

1.8.4. Alternative 3: Adoptive cell therapies

The most straightforward cell-based therapy concept is infusing Treg, to tip the immune balance towards tolerogenic instead of graft-reactive phenotype. An exciting new study employed Tregs with chimeric antigen receptor – CAR-Tregs. The CAR consisted of extracellular antigen-binding domain recognizing human leucocyte antigens, and an intracellular signaling domain, able to transmit T cell receptor and co-stimulatory signal to activate the Treg cell upon recognition of an HLA molecule. Infused in humanized mice with human skin grafts, the CAR-Tregs could prevent graft rejection for 40 days, after which the

experiment was stopped due to xenogeneic GVHD¹³⁶. The downsides of Treg infusion are, however, that Treg obviously couldn't prevent GVHD, suggesting that their action is strictly directed to the antigen they can recognize, and no other, and that under inflammatory conditions, Treg can switch to effector phenotype and contribute to graft damage, rather than protection.

Alternatively, mesenchymal stem cells (MSC) – a type of multipotent cell found in bone marrow, placenta, umbilical cord, umbilical cord blood, adipose tissue and Warton's jelly – have a multifactorial approach to taming immune reactions. They can suppress activation, proliferation and differentiation of T cells, as well as recruitment, maturation and function of DCs, as reviewed by Castro-Manrezza and Montesinos¹³⁷. MSCs have been described to prolong graft survival in a rat VCA model¹³⁸. Moreover, the "Pittsburgh protocol" – TAC monotherapy and infusion of donor bone marrow cells on day 14 after transplantation – have been reported in 5 hand transplant recipients to be a safe and permissive of reduction of IS⁷⁸. Future analyses should show what is the fate of those cells within the body under normal and inflammatory conditions and how do they exert their beneficial effects.

A third approach is to use APCs exposed to alloantigens *ex vivo* under tolerogenic conditions to polarize Th cells towards Treg phenotype. Unfortunately, DC are too rare to be purified from blood in relevant amounts and do not expand in culture¹³⁹. B cells on the other hand are abundant in blood and can be further expanded in culture¹⁴⁰. Taking advantage of these benefits, a study recently demonstrated *ex vivo* that B cells loaded with antigen nanoparticles, depending on the culture conditions could polarize Th cells to T_H1 or T_H2 phenotypes¹⁴¹. This discovery gives the exciting opportunity to cheaply and easily load multiple donor antigens onto B cells to expand the Treg pool in VCA recipients and create a tolerogenic environment to the graft.

Cell-based therapies require lab expertise, long time and high costs of preparation, which makes them unpractical for mass production. In contrast, a growing variety of biomaterials can be produced at low cost out of abundant and cheap materials, that can absorb and deliver already approved drugs and release them in a controlled fashion, to reduce their side target effects.

1.9. Drug delivery systems

The efficiency and toxicity of any drug is a function of its so-called ADME – absorption, distribution, metabolism and excretion. ADME depends on the route of drug delivery, which could be oral, intravenous or local. In VCA oral delivery of IS is the golden standard, but it requires a high drug dose to be acquired, so that sufficient amount can reach the target cells (lymphocytes). Much of the drug is inactivated while passing through various pH and enzymes in the gastrointestinal tract and extensive liver metabolism. Intravenous delivery results in high transient drug dose “dumping” in the circulation, from where majority of the drug reaches highly perfused organs, such as liver, heart and kidney and a fraction is carried to the VCA tissues, as well as any other part of the body. Localized IS has the potential to reduce the high systemic drug dose indispensable to oral and intravenous routes, and has therefore been thoroughly investigated as an opportunity to focus IS in the VCA graft, reduce collateral tissue exposure and minimize drug input. Moreover, localized IS creates an opportunity to target and inhibit resident APC presentation, resident memory T cell activation, trans-endothelial migration or egress of activated T and B cells from the draining lymph node.

The skin in VCA grafts offers the possibility for topical, transdermal, or subcutaneous IS. Topical IS has been used in conjunction with systemic IS to successfully combat AR episodes in VCA¹⁴² and has been shown to prevent skin rejection in a Wistar Furth-to-Lewis hind limb transplantation, maintaining high skin and low systemic drug levels¹⁴³. Transdermal approaches in VCA have not been described so far. Subcutaneous approaches for IS on the other side are many and mostly rely on innovative drug delivery systems (DDS) for controlled or on-demand release.

DDS for controlled release could reduce the number of applications of IS and thereby mitigate the problem of non-compliance. To do this they should be able to enclose therapeutically relevant amounts of drug and release it in a predictable and controllable manner over extended periods of time, providing therapeutically adequate levels of IS during that time. They should be composed of biocompatible and biodegradable products, which do not produce toxic and harmful substances in the process of their decomposition. Finally they should be easy to administer and do not cause discomfort to the patient. Ideally, they should be easy to remove or inactivate when necessary.

1.9.1. Biological and living DDS

Extracellular vesicles serve as cellular messengers, transferring miRNA, mRNA, growth factors and other molecules from one cell to another. A recent review discusses their potential to be exploited as DDS¹⁴⁴, which could be of great interest for IS delivery in VCA and transplantation in general. In addition, cells, such as erythrocytes, macrophages and lymphocytes can be used as living DDS, able to circulate and deliver drugs, enzymes and antigens in a sustained and/or targeted manner as reviewed by Pang et al.¹⁴⁵. One example relevant to VCA is using erythrocytes loaded with antigens to render C57BL/6 mice tolerant to these antigen, mediated by increase in Treg¹⁴⁶. These therapies, however, could prove costly and complicated to produce, which might reduce their marketability.

1.9.2. Micro- and nanoparticles

Micro- and nanoparticles can serve a similar purpose, and are easy to produce, administer, and provide sustained drug release. A combination of polylactic-co-glycolic acid (PLGA) microparticles releasing IL-2, TGF- β and rapamycin for 3-4 weeks in a sustained manner was shown to induce murine and human Treg *ex vivo*¹⁴⁷. Recently, PLGA microparticles loaded with TAC have been injected subcutaneously in Wistar Kyoto rats, reducing systemic IL-2 levels and maintaining low systemic TAC levels for 10 days¹⁴⁸. In another study TAC-loaded microspheres were injected subcutaneously in a Dark Agouti-to-Lewis rat liver transplantation model and could provide 88.6 ± 54.7 days survival with a single dose of 4.8 mg/kg¹⁴⁹. Testing their efficacy in a VCA transplantation model could shed light on their potential in VCA.

1.9.3. Scaffolds and implants

DDS can serve not only as vessels for IS, but also, as means for immunomodulation. As mentioned earlier, *ex vivo* expansion of Treg for Treg-based therapy is not a straightforward task. Treg are a minority of the circulating T cells, their purification requires sophisticated laboratory instrumentation, fetches high costs, and gives a low yield. Using safe and easy to fabricate scaffolds and implants that promote Treg expansion locally in the graft holds a great promise. Collagen, fibrin and decellularized extracellular

matrix are only few examples of biocompatible and biodegradable materials, which can serve as 3D scaffolds, as reviewed by Segers and Lee¹⁵⁰. Their ability to deliver a broad spectrum of substances could be used to modulate local immunity, or to support adhesion, survival, proliferation and differentiation of the transplanted cells in adoptive cell therapies. One recent example is a poly-lactide-co-glycolide (PLG) scaffold releasing TGF- β , which prolonged survival and function of pancreatic islets transplanted into diabetic mice¹⁵¹. One of the best examples of drug-delivery implants successful in a VCA setting is a TAC-loaded poly-capro-lactame disc, loaded with 40 mg TAC. Lewis rats receiving Brown-Norway hind limb grafts were pre-conditioned with anti-lymphocyte serum (polyclonal antibody depleting T cells), and received an implant subcutaneously in the ipsilateral groin. The disc could provide >180 days of graft survival despite sub-therapeutic blood TAC levels for extended periods of time¹⁵².

1.9.4. Organo- and hydrogels

A growing variety of biocompatible gelators (materials, able to form gels) are attracting the attention of biomaterial engineers, due to their ability to encapsulate hydrophobic drugs and release them in a predictable manner¹⁵³. The main focus of my doctoral work has been investigating injectable hydrogels for on-demand delivery of IS in VCA (see Results, part 3.1). The on-demand release concept seeks to further minimize the drug levels not only in space, but also in time. The drug release is triggered by an environmental switch, such as pH or enzymatic levels. Such smart systems are designed to instantly adjust the IS levels to the current requirements of their immediate surroundings (the graft), while sparing the systemic impact. We have developed a TAC-loaded triglycerol-monostearate hydrogel (TGMS-TAC) for subcutaneous injection. It has been shown to release TAC under the influence of inflammation-related enzymes, providing increased intra-graft levels of IS during rejection episodes (**Figure 4**). The possibility of a single injection of TGMS-TAC to prolong graft survival, along with its inflammation-triggered release have been demonstrated previously¹⁵⁴.

a

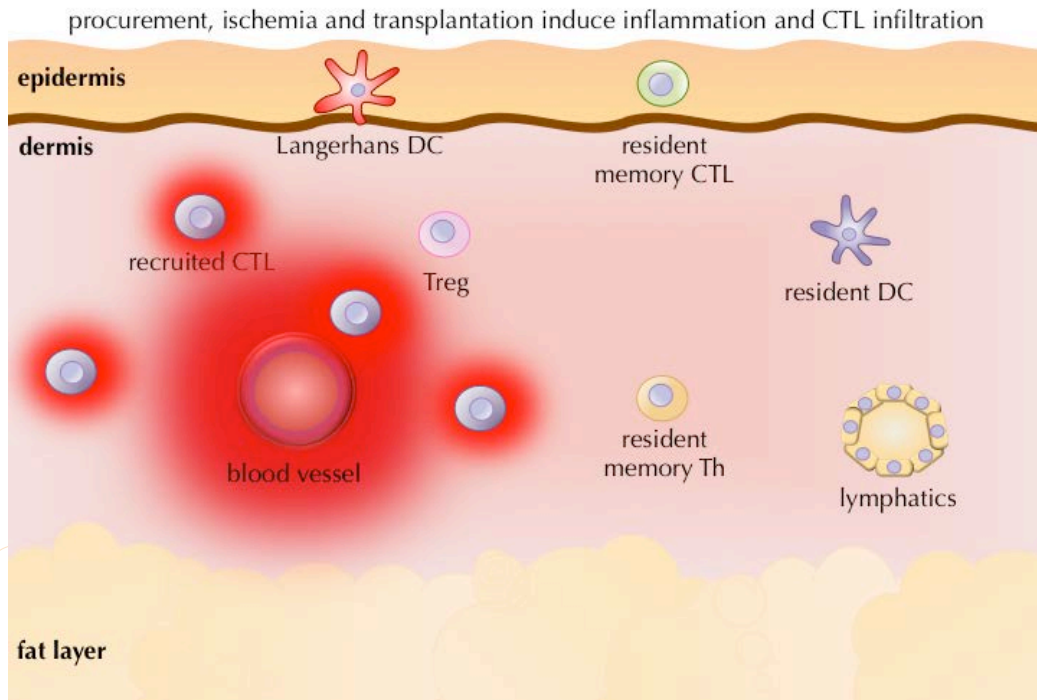


Figure 4. Mechanism of action of TGMS-TAC hydrogel in VCA. a) Procurement, ischemia-reperfusion injury, surgical trauma during transplantation, and rejection episodes lead to inflammation in graft tissue, especially in the skin. Pathological manifestations include perivascular inflammation (red halos) with recruitment of T_H1 on the site of inflammation.

b

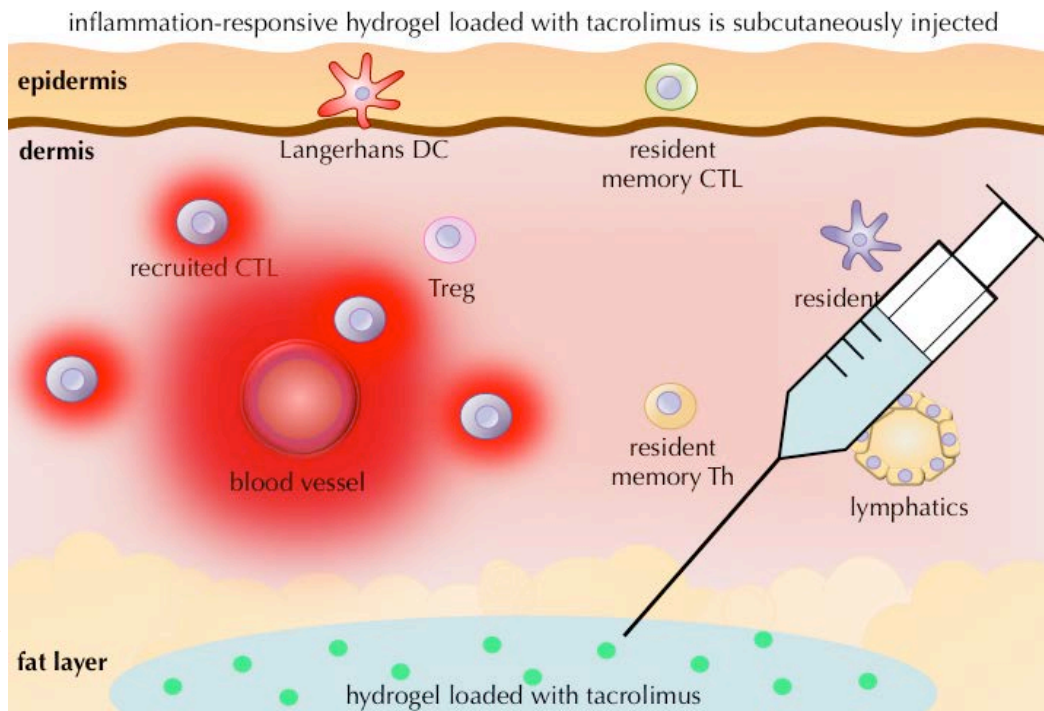


Figure 4. b) Subcutaneous injection of TGMS-TAC – a tacrolimus-loaded hydrogel. TGMS-TAC molecules are digested by enzymes, upregulated during inflammation.

c

tacrolimus is released from the hydrogel, taming the rejection, inflammation is controlled

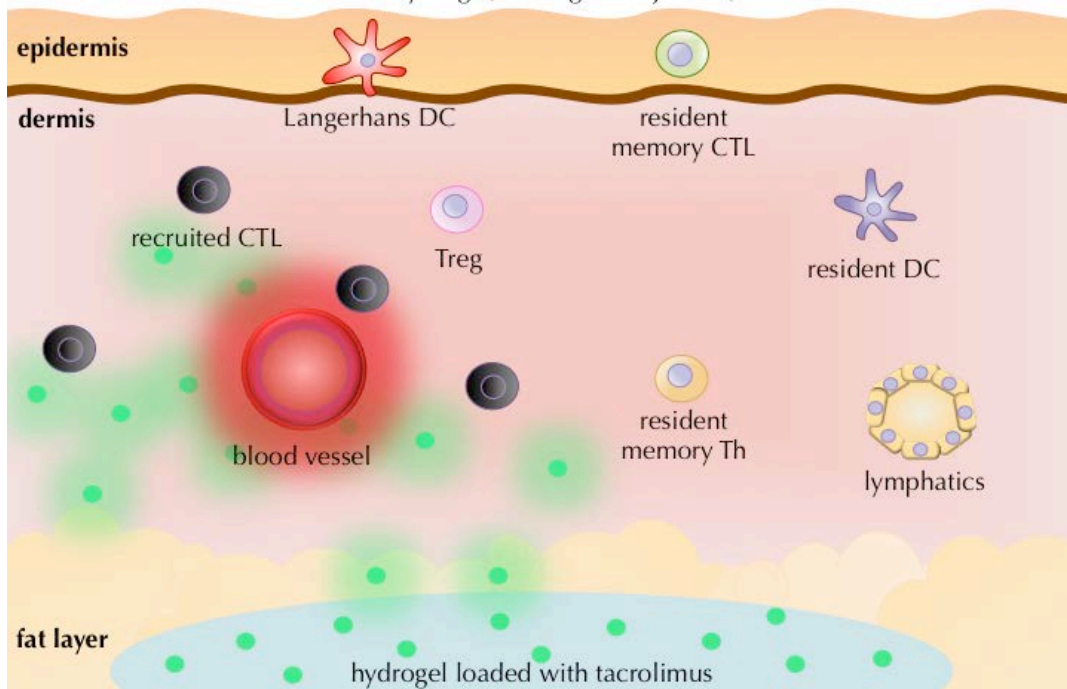


Figure 4. c) Enzymes upregulated during inflammation partially digest TGMS-TAC, thereby releasing tacrolimus (green bubbles) in the surrounding environment. Tacrolimus suppresses recruited Teff cells and counteracts rejection and inflammation.

d

inflammation and rejection are resolved, tacrolimus is retained in the hydrogel

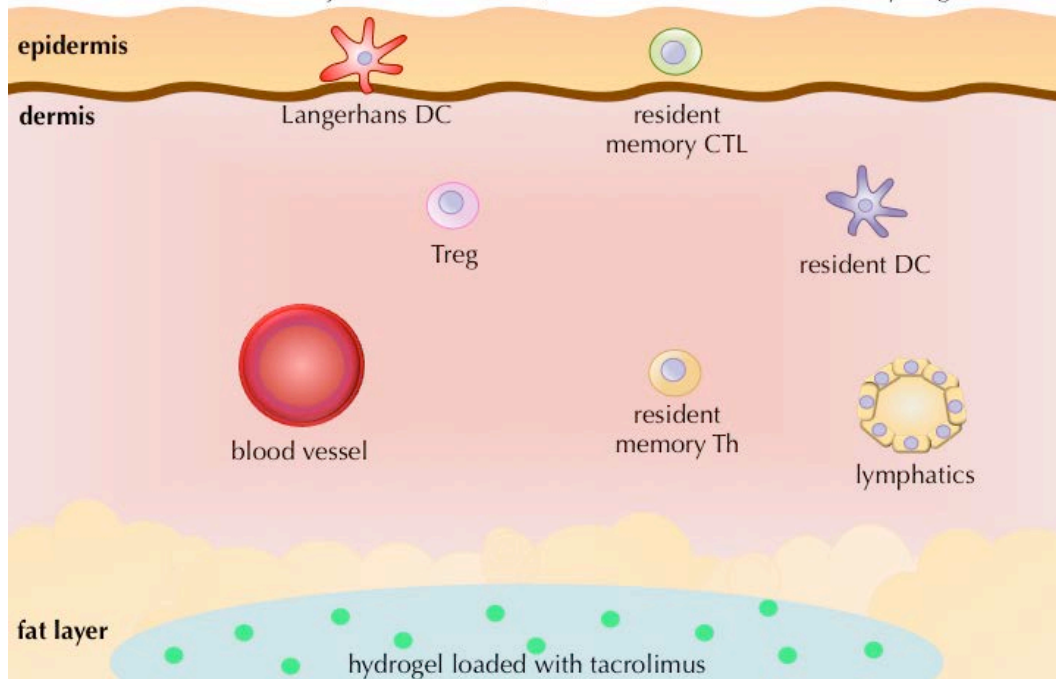


Figure 4. d) Teff cells are suppressed by tacrolimus. Inflammation and rejection are gone. The levels of inflammation-related enzymes decrease, therefore TGMS-TAC digestion and ultimately tacrolimus decrease. Local tacrolimus levels are directly regulated by the local inflammatory status.

1.9.5. *In situ* forming implants

Liquid materials, which are able to rapidly solidify when administered subcutaneously, are attractive DDS, as they can follow the physiological structure of the surrounding tissues, without exerting any pressure on them or provoking an inflammatory response. A recent study demonstrated that injected mesoporous silica rods (MSRs) could form *in situ* 3D scaffolds which, loaded with cytokines and antigens, could serve as artificial lymph node, attracting and presenting the antigen to immune cells in the presence of a polarizing environment¹⁵⁵. A downside of *in situ* forming materials is that if the transition between liquid and solid state takes too long, there is a possibility for an uncontrolled burst release upon injection. One of the projects included in this thesis describes an *in situ* forming implant, loaded with rapamycin for local IS and immunomodulation (see Results, part 3.2).

These promising technologies have triumphed in animal trials, but only in short-term, single-application studies. Delaying rejection episodes is not a sufficient argument for their translation into clinics. If such delivery systems are to enter in a direct competition to the standard of care today, they have to demonstrate equal if not superior efficiency, considerably reduced off-target effects, and easy and fast mass-production on competitive cost. Ultimately, the necessity and potential of these therapeutic modalities, paired to the morbidities threatening VCA patients today, postulate a need for a deeper understanding of the interactions of graft, host and DDS immunologically and toxicologically. This way we could convincingly answer the question whether local DDS could be used as a means of IS in VCA patients.

2. Aims

The aim of the work presented here was to examine the long-term outcomes of local DDS application in a rat model of VCA to better understand whether local DDS are attractive candidates for translation to a clinical VCA setting. We questioned whether continuous localized IS would prevent rejection by blocking local rejection triggers, and if not, would rejection under localized treatment present divergent histopathological outcomes in respect to systemic IS. Indicators of graft acceptance such as chimerism or Treg increase, as well as indicators of kidney, liver and metabolic welfare were of particular interest to us.

We performed series of studies, consistently employing a well-studied rat VCA model, and providing answers in a stepwise fashion:

- We started by asking whether administering IS directly in the graft could sustain extended graft survival, and whether it could affect Treg and/or chimerism counts, as well as kidney and liver function differently than systemic IS (see Results, part 3.3).
- Second we extended these questions to two promising local DDS:
 - An *in situ* forming implant for continuous release of rapamycin (see Results, part 3.2)
 - An inflammation responsive hydrogel for on-demand release of TAC (see Results, part 3.1)
- Finally, we studied the mechanism of action of TAC loaded hydrogel *in vivo*. Moreover, we introduced an attractive feature for clinical VCA – a near-infrared reporter dye, which visualizes the hydrogel depots and helps to estimate TAC availability in the graft, and even systemically in plasma (see Results, part 3.4).

3. Results

- 3.1. Local injections of tacrolimus-loaded hydrogel reduce systemic immunosuppression-related toxicity in vascularized composite allotransplantation
- 3.2. Delivery of rapamycin using in situ forming implants induces immunoregulatory mechanisms promoting vascularized composite allograft survival
- 3.3. Intra-graft injection of tacrolimus promotes survival of vascularized composite allotransplantation
- 3.4. In vivo characterization and non-invasive monitoring of tacrolimus-loaded hydrogel for localized immunosuppression

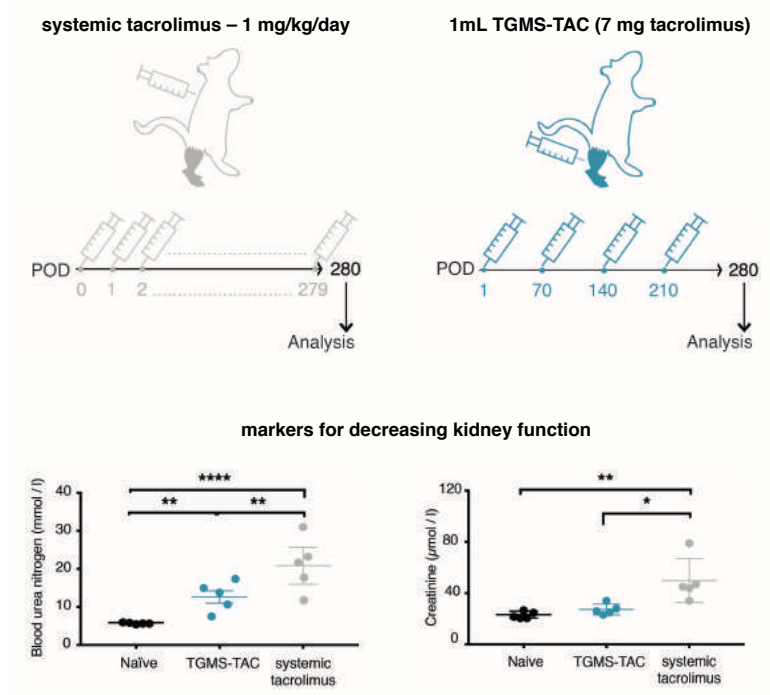
3.1. Local injections of tacrolimus-loaded hydrogel reduce systemic immunosuppression-related toxicity in vascularized composite allotransplantation

Dzhuliya V. Dzhonova, M.Sc.^{1,2}; Radu Olariu, M.D.³; Jonathan Leckenby, M.D.³; Yara Banz, M.D.-Ph.D.⁴; Jean-Christophe Prost, Ph.D.⁵; Ashish Dhayani, M.Sc.^{6,7}; Praveen K. Vemula, Ph.D.⁶; Esther Voegelin, M.D.³; Adriano Taddeo, Ph.D.^{1,3*}; Robert Rieben, Ph.D.^{1*}

¹Department for BioMedical Research, University of Bern, Murtenstrasse 50, 3008 Bern, Switzerland; ²Graduate School for Cellular and Biomedical Sciences, University of Bern, Freiestrasse 1, 3001 Bern, Switzerland; ³Clinic of Plastic and Hand Surgery; Inselspital, Bern University Hospital, University of Bern, Freiburgstrasse, 3010 Bern, Switzerland; ⁴Institute of Pathology, University of Bern, Murtenstrasse 31, 3008 Bern, Switzerland; ⁵Center of Laboratory Medicine, University Institute of Clinical Chemistry, University Hospital, Freiburgstrasse, 3010 Bern, Bern, Switzerland; ⁶Institute for Stem Cell Biology and Regenerative Medicine, Bellary Road, Bangalore 560065, India; ⁷The School of Chemical and Biotechnology, SASTRA University, Thirumalaisamudram, Thanjavur-613401, Tamil Nadu, India

Status: Submitted to *Transplantation*

Aim: To understand whether repeated intragraft injections of TAC-loaded inflammation-responsive hydrogel could promote long-term graft survival in a rat VCA model and to compare its toxicological and immunological impact to systemic TAC treatment.



Summary: Long-term graft survival was established with hydrogel treatment every 70 days. Superior levels of markers for kidney function and hematopoietic chimerism were observed with this treatment as compared to systemic treatment. Systemically treated animals but not hydrogel treated ones displayed typical IS-related side effects, such as lymphoma and opportunistic infections.

Local injections of tacrolimus-loaded hydrogel reduce systemic immunosuppression-related toxicity in vascularized composite allotransplantation

Dzhuliya V. Dzhonova, M.Sc.^{1,2}; Radu Olariu, M.D.³; Jonathan Leckenby, M.D.³; Yara Banz, M.D.-Ph.D.⁴; Jean-Christophe Prost, Ph.D.⁵; Ashish Dhayani, M.Sc.^{6,7}; Praveen K. Vemula, Ph.D.⁶; Esther Voegelin, M.D.³; Adriano Taddeo, Ph.D.^{1,3*}; Robert Rieben, Ph.D.^{1*}

¹Department for BioMedical Research, University of Bern, Bern, Switzerland

²Graduate School for Cellular and Biomedical Sciences, University of Bern, Bern, Switzerland

³Clinic of Plastic and Hand Surgery; Inselspital, Bern University Hospital, University of Bern, Bern, Switzerland

⁴Institute of Pathology, University of Bern, Bern, Switzerland

⁵Center of Laboratory Medicine, University Institute of Clinical Chemistry, University Hospital, Bern, Switzerland

⁶Institute for Stem Cell Biology and Regenerative Medicine, Bangalore, India

⁷The School of Chemical and Biotechnology, SASTRA University, Tamil Nadu, India

***Corresponding authors:**

Adriano Taddeo, Ph.D.

Department for BioMedical Research

University of Bern

Murtenstrasse 50

3008, Bern

Switzerland

Telephone: +41 31 632 02 99

Fax: +41 31 632 75 94

E-Mail: adriano.taddeo@dbmr.unibe.ch

Robert Rieben, Ph.D.

Department for BioMedical Research

University of Bern

Murtenstrasse 50

3008, Bern

Switzerland

Telephone: +41 31 632 96 69

Fax: +41 31 632 75 94

E-Mail: robert.riegen@dbmr.unibe.ch

Authorship:

D.V.D. performed and analyzed the *in vivo* experiments, flow cytometry, TGMS-TAC hydrogel preparation, DSA analyses.

R.O. and J.L. designed and performed the hind limb transplantations.

Y.B. performed and analyzed the histopathological evaluations.

J.-C.P. performed the tissue TAC analyses.

A.D. and P.K.V. designed and developed the TGMS-TAC hydrogel.

D.V.D., A.T. and R.R. wrote the manuscript.

E.V., P.K.V., A.T. and R.R. designed and supervised the studies, and reviewed the manuscript.

Disclosure:

The authors declare no conflicts of interest.

Funding:

This work was supported by Indo-Swiss Joint Research Program of the Swiss National Science Foundation (SNF, grant 156773) and the Department of Science and Technology, Govt. of India (grant INT/SWISS/SNSFP-51/2015) to R.R., E.V. and P.K.V., respectively. A.D. thanks the University Grant Commission for the senior research fellowship.

Abbreviations:

ALT, alanine aminotransferase

AST, aspartate aminotransferase

BUN, blood urea nitrogen

CTL, cytotoxic T lymphocytes

DSA, donor-specific antibody

POD, postoperative day

TAC, tacrolimus

Teff, effector T-cells

TGMS, triglycerol monostearate

TGMS-TAC, TAC-loaded TGMS hydrogel

Treg, regulatory T-cells

VCA, vascularized composite allotransplantations

Abstract

Background

Routine application of vascularized composite allotransplantation (VCA) is hampered by immunosuppression-related health comorbidities. To mitigate these we developed an inflammation-responsive hydrogel for local immunosuppression. Here we report on its long-term effect on graft survival, immunological and toxicological impact.

Methods

Brown Norway-to-Lewis rat hind limb transplantations were treated either systemically with daily injections of 1 mg/kg tacrolimus or with subcutaneous intragraft injections of hydrogel containing 7 mg tacrolimus, every 70 days. Animals were monitored for rejection or other pathology for 280 days. Systemic and graft tacrolimus levels, regulatory T-cells, and donor cell chimerism were measured periodically. At endpoint, markers for kidney, liver and metabolic state were compared to naïve age-matched rats.

Results

Both daily systemic tacrolimus and subcutaneous intragraft tacrolimus hydrogel at 70 day intervals were able to sustain graft survival for >280 days in 5 out of 6 recipients. In the hydrogel group one graft progressed to grade 3 rejection at postoperative day (POD) 149. In systemic tacrolimus group one animal was euthanized due to lymphoma on POD 275. Hydrogel treatment provided stable graft- and reduced systemic tacrolimus levels, and a 4 times smaller total tacrolimus dose compared with systemic immunosuppression. Hydrogel-treated animals showed preserved kidney function, absence of malignancies or opportunistic infections and increased hematopoietic chimerism compared to systemic immunosuppression.

Conclusions

Our findings demonstrate that localized immunosuppression with tacrolimus hydrogel is a long-term safe and reliable treatment. It may reduce the burden of systemic immunosuppression in VCA, potentially boosting the clinical application of this surgical intervention.

Introduction

Systemically administered tacrolimus (TAC) is the most commonly used immunosuppressant in vascularized composite allotransplantation (VCA)¹. However, of the 66 registered in the International Registry on Hand and Composite Tissue Transplantation hand transplant recipients, 26% suffered from elevated creatinine values, 32.3% – from opportunistic bacterial infections and three of them developed malignancies². These TAC-mediated morbidities are a barrier to the broader adoption of VCA. Transitioning patients from TAC to other immunosuppressants has been attempted, but with limited success². Consequently, the field has turned to “increasingly bold approaches in modifying immunosuppression”³, that need solid and conclusive pre-clinical data, demonstrating their feasibility, efficacy and safety.

Our group developed a graft-targeted inflammation-responsive hydrogel⁴⁻⁶ delivering TAC “on demand” – only when needed, with the aim to provide an effective future alternative or addition to systemic immunosuppression for patients. The hydrogelator – triglycerol monostearate (TGMS) – is biocompatible, biodegradable, generally recognized as safe by the US Food and Drug Administration, and can be loaded with therapeutically relevant amounts of TAC. TAC-loaded TGMS hydrogel (TGMS-TAC) releases TAC in response to inflammatory stimuli, and prolongs VCA survival with a single injection⁷.

Here we hypothesized that repeated subcutaneous intra-graft injections of TGMS-TAC maintain long-term graft survival in the Brown Norway-to-Lewis rat hind limb allotransplantation model. We expected that TGMS-TAC-treated animals would have higher TAC concentrations in the graft and lower in the blood compared to daily systemic TAC treatment (standard of care), which should result in reduced off-target effects and nephrotoxicity. Furthermore, we were interested in whether TGMS-TAC influences the dynamics of effector T-cells (Teff), regulatory T-cells (Treg), and chimerism.

Materials and Methods

Male Brown Norway and Lewis rats (6-8 weeks old weighing 200 to 250 g) were purchased from Charles Rivers Breeding Laboratories, Germany. Animals were kept in specific pathogen-free conditions. Experiments were planned and carried out in agreement with current 3R and ARRIVE guidelines and approved according to Swiss animal protection laws by the Veterinary Authorities of the Canton Bern, Switzerland, approval no. BE94/15.

Brown Norway-to-Lewis rat hind limb transplantations were performed and animals were treated either with 1 mg/kg/day TAC systemically in the neck fold or every 70 days with 1 ml TGMS-TAC containing 7 mg tacrolimus (n=6 for each group). In the TGMS-TAC group, four subcutaneous TGMS-TAC depots of 250 μ L each were injected in the zones of biceps femoris, gastrocnemius, tibialis anterior, and vastus muscles, taking great care to distribute the amount of drug as evenly as possible intra- and inter-individually. The re-injection time point was chosen based on a pilot study showing that transplanted animals (n=5) treated with a single intra-graft injection of 1 ml TGMS-TAC loaded with 7 mg TAC on post-operative day 1 (POD 1) rejected their graft on POD 83.4 ± 6.7 . Re-injection time point was defined as 14 days before rejection and set to POD 70. Graft rejection was evaluated macroscopically and graded as 0 = no rejection, 1 = erythema and edema, 2 = epidermolysis and exudation, and 3 = desquamation, necrosis, and mummification.

Rats were euthanized either once grade 3 rejection was reached or on day 280 (endpoint). Necropsy for immunosuppression-related side effects was performed. Kidney, as well as graft skin and muscle histology were evaluated by a blinded pathologist (Hematoxylin and Eosin and/or Periodic acid–Schiff staining, as necessary). Kidney samples were graded according to the semiquantitative calcineurin inhibitor toxicity score by Kambham et al.⁸. Histological grading of skin rejection was according to Banff classification⁹. Additionally skin and muscle lymphocyte infiltration, vasculopathy and necrosis were graded as 0 – none, 1 – minimal, 2 – moderate, 3 – extensive. Immunofluorescence analyses of IgG, IgM, C3b/c, C4b/c, C5b-9, CD45RA in graft skin and muscle were performed. Blood urea nitrogen (BUN) and creatinine; cholesterol and triglycerides; aspartate aminotransferase (AST) and alanine aminotransferase (ALT) as kidney, metabolism and liver markers, respectively, complete blood count, and donor-specific antibody formation were assessed in blood at endpoint.

Throughout the study TAC levels were measured in blood and skin biopsies retrieved from grafts and contralateral limbs at selected time points by LC-MS/MS.

Flow cytometry for obtaining Treg and chimerism levels was performed in blood at selected time points, and in graft and contralateral limb skin at endpoint.

Statistical analyses were executed with Prism software (GraphPad Software Inc., La Jolla, CA, United States). Statistically significant data were presented as follows: * $P < 0.05$; ** $P < 0.01$; *** $P < 0.001$; and **** $P < 0.0001$. Statistical tests are specifically indicated under each figure.

Detailed materials and methods are available under Supporting Information, in the online version of this article.

Results

Periodic TGMS-TAC injections promote long-term VCA survival

To test if 1 ml TGMS-TAC loaded with 7 mg TAC re-injected every 70 days promotes long-term graft survival in a rat hind limb transplantation model, we compared TGMS-TAC treatment to daily systemic immunosuppression using TAC at 1 mg/kg/day (Figure 1a). Five out of six animals survived until endpoint in each group (Figure 1b).

In the TGMS-TAC group one animal was sacrificed due to grade 3 rejection at POD 149 (Animal 1, Figure 1c). One animal experienced three rejection episodes (Animal 2, Figure 1c). One animal started rejecting at POD 262, which reached grade 2 at endpoint (Animal 3, Figure 1c). One animal experienced mild rejection, which resolved temporarily and later reoccurred (Animal 4, Figure 1c). Two animals had no rejection episodes (Animals 5 and 6, Figure 1c). No local complications due to TGMS-TAC-injections were observed in any of the rats. In systemic TAC group one animal was euthanized due to lymphoma on POD 275. Systemic immunosuppression was sufficient to maintain the grafts rejection-free throughout the duration of the treatment (Animals 7-12, Figure 1c).

Histopathological evaluation of graft skin at endpoint (POD 280) revealed no necrosis in any of the animals (Animals 1-12, Figure 1d). Two TGMS-TAC-treated animals were classified as Banff grade 3 (corresponding to macroscopic grade 2), and one as Banff grade 2 (corresponding to macroscopic grade 1) skin rejection (Animals 2-4, Figure 1d). One systemically treated animal was classified as Banff grade 2 skin rejection, although no macroscopic lesions were detectable (Animal 12, Figure 1d). No significant differences were found between the two groups in terms of lymphocyte infiltration ($P=0.2415$), vasculopathy ($P=0.1411$) or Banff grade ($P=0.1660$, Mann-Whitney test, Figure 1d). All observed rejection episodes were restricted to graft skin, with no signs of rejection in graft muscle (Supplementary Figure 1). However, TGMS-TAC-treated animals had significantly more pronounced atrophy of the muscle fibers as compared to systemic treatment ($P=0.0079$, Mann-Whitney test, Supplementary Figure 1).

As evident from Figure 1c, two rejection episodes in animal 2 markedly improved after TGMS-TAC re-injection. The first one – macroscopic grade 1 at the time of re-injection – was completely reverted within a week. The second one – macroscopic grade 2 – required two to three weeks to reduce to grade 1 (Figure 2) and within a month a complete recovery was observed, which, however, lasted only three weeks.

Reduced systemic but relevant tissue TAC levels with TGMS-TAC

To understand TAC distribution over time, TAC concentrations were measured in blood (bi-weekly), and in graft and contralateral limb skin (monthly). In blood, a burst release of TAC was detected in the first 72 h after the first TGMS-TAC injection. This peak was beyond the upper quantification limit of the LC-MS/MS analysis (i.e. 65 ng/ml) during the first 24-48 h, afterwards it normalized to therapeutic levels (5 – 20 ng/ml). At POD 46 most animals had sub-therapeutic levels (<5 ng/ml). Compared to the first TGMS-TAC injection, the following injections induced markedly weaker burst releases, followed by similar TAC

release kinetics ($P < 0.0001$ for first peak versus second, $P < 0.0001$ for first peak versus third, and $P = 0.0009$ for second peak vs. third, standard one-way ANOVA, Figure 3a). Trough levels of systemically treated animals were within the therapeutic range throughout the duration of the experiments (Figure 3a). Bi-weekly average TAC levels in blood of TGMS-TAC and animals showed that TGMS-TAC-treated animals had significantly lower TAC blood levels compared with systemically treated animals (9.29 ± 5.89 vs. 13.44 ± 4.44 ng/ml, respectively, $P = 0.0060$, Mann-Whitney test, Figure 3b).

In TGMS-TAC-treated animals there was a non-significant trend towards higher TAC concentrations in the graft as compared to the contralateral limb skin during the first week, corresponding to the burst release observed in blood ($P = 0.1532$, paired t-test, Figure 4a). For the rest of the measured time points there were no statistically significant differences between TAC levels in graft and contralateral limb skin. In systemically treated animals there were no statistically significant differences between the TAC levels in graft and contralateral limb skin at all time points (Figure 4b). Monthly average skin TAC levels in TGMS-TAC graft skin were higher than in the respective contralateral limb skin (1.1 ± 1.49 ng/mg vs. 0.25 ± 0.19 , respectively, $P = 0.0195$, Figure 4c). Under systemic treatment there was no significant difference between graft and contralateral limb skin (0.46 ± 0.39 ng/mg vs. 0.29 ± 0.16 ng/mg, respectively, $P = 0.1094$, Wilcoxon test, Figure 4c). When compared between groups, TAC levels in both graft and contralateral limb skin were comparable ($P = 0.7785$ and $P = 0.4755$ respectively, Mann-Whitney test, Figure 4c).

Low anti-donor antibody and complement activation

The formation of donor-specific antibody (DSA) was assessed by incubating donor thymocytes with plasma of transplanted animals and subsequent analysis by flow cytometry. There was no significant inter-group difference for binding of IgG to donor thymocytes, whereas IgM was significantly lower in the TGMS-TAC group at POD 280 as compared to systemic treatment (mean fluorescence – 75.56 ± 18.62 and 143.8 ± 41.09 respectively, $P = 0.013$, Student's t-test, Figure 5a). At endpoint no significant antibody (IgG and IgM, Figure 5b) and complement (C4b/c, C5b-9, Supplementary Figure 2) deposition, or B-cell infiltration was observed (CD45R, Supplementary Figure 3), except for increased C3b/c deposition under systemic treatment (integrated density 1018 ± 155.6 and 1500 ± 300.1 for TGMS-TAC and systemic treatment respectively, $P = 0.029$, Student's t-test, Supplementary Figure 2).

TGMS-TAC mitigates immunosuppression-related side effects

BUN in TGMS-TAC animals was higher than in naïve age-matched animals and lower than in systemically treated animals – 12.62 ± 1.6 , 5.9 ± 0.2 and 20.86 ± 4.86 mmol/l, respectively ($P = 0.0023$ TGMS-TAC vs. systemic treatment, $P = 0.0095$ TGMS-TAC vs. naïve, and $P < 0.0001$ systemic treatment vs. naïve, Figure 6a). Creatinine was lower in TGMS-TAC and naïve age-matched animals compared to systemic treatment (27.2 ± 4.21 , 23.2 ± 2.68 , and 49.8 ± 17.08 $\mu\text{mol/l}$, respectively, $P = 0.0117$ TGMS-TAC vs. systemic treatment, $P = 0.0039$ systemic treatment vs. naïve, Figure 6b). Histological analysis of

kidneys revealed only minimal damage under both treatments (Supplementary Figure 4).

Cholesterol was comparable between groups (2.48 ± 0.39 , 2.35 ± 0.48 , and 2.88 ± 0.47 mmol/l for TGMS-TAC, systemic treatment, and naïve Lewis rats, respectively, Figure 6c). Triglycerides were similar in TGMS-TAC and naïve rats and decreased in systemic treatment group as compared to naïve rats (1.22 ± 0.54 mmol/l, 0.44 ± 0.29 mmol/l, and 1.75 ± 0.99 mmol/l for TGMS-TAC, systemic treatment and naïve Lewis rats respectively, $P= 0.0236$ between naïve rats and systemic treatment, Figure 6d).

Hepatic enzymes were not significantly different between naïve rats and the two treatment groups. AST was 140.6 ± 97.18 U/L, 109 ± 52.72 U/L, and 80 ± 15.64 U/L for TGMS-TAC, systemic treatment, and naïve rats respectively, Figure 6e. ALT was 73.4 ± 29.57 U/L, 48.4 ± 29 U/L, and 50.4 ± 7.8 U/L for TGMS-TAC, systemic treatment, and naïve rats respectively, Figure 6f).

The complete blood count of TGMS-TAC and systemically treated animals at endpoint was comparable to naïve age-matched rats, except for total hemoglobin, mean corpuscular hemoglobin, platelet distribution width, and median platelet volume, which were lower under systemic treatment, compared either to naïve animals or to both naïve and TGMS-TAC-treated animals (one-way ANOVA, Table 1).

As mentioned above, under systemic treatment one of the six animals was euthanized at POD 275, due to markedly enlarged ipsilateral inguinal lymph node, accompanied by elevated white blood cell count (75.1×10^3 cells/ μ l) and apathetic behavior indicating pain and/or suffering. Histopathological analyses of the lymph node revealed aggressive lymphoma, most consistent with diffuse large B-cell lymphoma (Figure 6g). Another animal from the same group had an increasingly firm and growing solid mass circumventing the graft, accompanied by a slow but steady increase of the white blood cell count until endpoint. Necropsy revealed a large encapsulated granuloma-like formation filled with granulated yellow-green substance. Histopathological analysis confirmed that the formation was an infected pseudo-cyst (Figure 6h). PCR analyses of its content revealed *Staphylococcus aureus* and *Proteus mirabilis*, commensal skin bacteria. In the TGMS-TAC group neither malignant nor infectious complications were observed.

TGMS-TAC therapy favors hematopoietic chimerism

To understand the dynamics of Teff and Treg, and chimerism under both treatments we analyzed blood at selected time points throughout the study. The gating strategy for Teff and Treg enumeration is shown in Supplementary Figure 5, and for chimerism – in Supplementary Figure 6.

Both treatment groups had significantly decreased amounts of circulating T-cells compared to naïve rats. Initially there were significantly more T-cells in the TGMS-TAC group than in systemically treated group (for example in post-operative week 2: 2087 ± 427 T-cells/ μ l vs. 1163 ± 359 T-cells/ μ l respectively – $P=0.0074$, Student's t-test). After 17 weeks of gradual decrease the difference of T-cell counts between the TGMS-TAC and systemically treated group were no longer statistically significant (for example in post-operative week 19: 1825 ± 767 T-cells/ μ l vs. 1290 ± 336 T-cells/ μ l, $P=0.1486$, Student's t-test, Figure 7a). Three

T-cell populations – cytotoxic T lymphocytes (CTL), T helper cells and Treg – were separately analyzed, with additional focus on Helios⁺ and Helios⁻ Treg populations. The T helper cells were the most abundant T-cell population and followed the total T-cell dynamics (Figure 7b). There were no major differences in the CTL or the Treg populations between the two treatment groups over time (Figure 7c-f respectively).

In terms of chimerism, in the first 11 weeks there was a significantly higher amount of circulating donor-derived cells in the TGMS-TAC group (Figure 8a). Donor-derived B-cells, T helper cells, CTL, and monocytes were all significantly increased in the TGMS-TAC-treated group compared to systemic treatment for up to 23 weeks (Figure 8b-e). Circulating donor-derived granulocytes were initially high in both treatment groups (for example in post-operative week 2: 367 ± 92 and 314 ± 113 donor-derived granulocytes/ μ l for TGMS-TAC and systemic treatment, respectively). This number dropped to 58 ± 52 and 90 ± 36 cells/ μ l, respectively, at post-operative week 10 and remained low until termination of the experiment (Figure 8f). At endpoint peripheral blood monocytes isolated from graft and contralateral limb skin of both groups were analyzed using the same flow cytometry protocol. The cell count was low and revealed no significant differences between the two treatment groups (Supplementary Figure 7).

Discussion

Our data show that repeated intra-graft injections of TGMS-TAC sustain long-term graft survival with better toxicological and immunological outcomes as compared to systemic TAC delivery. Markers of kidney function (i.e. BUN and creatinine) and complete blood analysis at endpoint, showed preserved kidney and hematological parameters of TGMS-TAC-treated rats as compared to systemic treatment. Unlike humans¹⁰, rat models require sodium depletion in order to develop significant TAC-induced kidney damage¹¹⁻¹³. Therefore, we speculate that the toxic effects reported in this study may be underrepresented, and that the TGMS-TAC treatment may potentially have more visible benefits in humans, especially in the kidney on a histological level.

Our study was also of sufficient duration to reveal possible complications of long-term immunosuppression. One systemically treated animal developed an infected pseudo-cyst containing commensal skin bacteria. Another developed an aggressive lymphoma. Lymphomas can arise spontaneously in ageing Lewis rats; however, their incidence during the first year of life of a male Lewis rat is extremely low¹⁴, suggesting that systemic immunosuppression contributed to its development. Necropsy of TGMS-TAC-treated animals did not reveal any malignancy or opportunistic infection, suggesting that localized immunosuppression could mitigate immunosuppression-related complications.

Local complications related to TGMS-TAC treatment, such as rash, alopecia, discoloration, atrophy or thinning of skin, or extra-cutaneous hydrogel extrusions were not observed. Animals did not extensively groom or scratch the limb after injection indicating absence of local irritation. Stool was firm and urine was clear, suggesting no acute gastro-intestinal or renal complications resulting from TGMS-TAC either.

While providing better recipient outcomes, TGMS-TAC treatment resulted in inferior graft outcomes as compared to systemic treatment. Four of the six TGMS-TAC treated animals experienced at least one rejection episode. Rejecting TGMS-TAC treated animals had comparable systemic TAC levels to the non-rejecting TGMS-TAC treated animals. Moreover, we⁷ and others¹⁵ have demonstrated that localized immunosuppression promotes extended rejection-free graft survival in the setting of sub-therapeutic systemic TAC levels. Therefore, we hypothesize that these rejections are not due to sub-therapeutic systemic TAC levels, but rather to low intra-graft TAC levels. According to Capron et al., tissue levels of immunosuppression provide a more accurate insight into actual efficiency of immunosuppression¹⁶. Re-injecting TGMS-TAC guided by local TAC levels, instead of fixed time points, could mitigate the observed rejections. To test this hypothesis, we plan to conduct TGMS-TAC studies in a porcine VCA model. In addition to being more clinically relevant, pigs provide the opportunity to collect frequent biopsies, sufficient to identify minimal threshold for intra-graft TAC levels.

TGMS-TAC treated animals demonstrated increased muscle atrophy as compared to systemically treated animals. Calcineurin is involved in skeletal muscle hypertrophy and tacrolimus counteracts this effect¹⁷. However, to our knowledge, there have been no studies demonstrating that tacrolimus

monotherapy causes direct myotoxicity, as conversely reported for tacrolimus in conjunction with statins¹⁸. Moreover, clinical cases of tacrolimus overdose have not reported effects on skeletal musculature¹⁹, suggesting that muscle atrophy is not TAC related. Mechanical pressure of the hydrogel deposits on graft vessels or nerves resulting in muscle atrophy is not a likely explanation either, since grafts were all well-perfused and all animals used their limbs for walking until endpoint in both groups. The hydrogel itself has been previously described to be safe, biocompatible and biodegradable⁷. However, our data cannot rule out the possibility that muscle atrophy may be a hydrogel-related side effect, which could not develop in studies of shorter duration. Importantly, muscle atrophy is a known manifestation of chronic rejection, and we believe that this is the most likely explanation for our observations. Indeed, multiple acute rejection episodes have been correlated to chronic rejection, particularly in rat²⁰. However, non-rejecting TGMS-TAC treated animals also had high muscle atrophy scores, keeping the question of muscle atrophy a matter requiring further investigation.

A third and potentially problematic aspect of TGMS-TAC hydrogel could be the TAC burst release following TGMS-TAC injection. TGMS-TAC injections led to peaks in TAC blood levels that, with each subsequent injection, became significantly lower. Due to the enzyme responsiveness of the hydrogel, the most likely reason for the very high first peak is the elevated levels of inflammation-related enzymes resulting from the surgical trauma and ischemia-reperfusion injury. However, in our view, the burst release has arguably a negative impact, as high intra-graft peri-operative TAC levels were shown to prolong graft survival in the same experimental model²¹.

Each TGMS-TAC injection contained 7 mg of TAC and the total amount of TAC given over 280 days to TGMS-TAC-treated animals was 28 mg. In contrast, animals treated systemically with 1 mg TAC/kg/day received a total of 84 to 112 mg of TAC, depending on the weight of the rats, which ranged from 300 to 400 g. Consequently the systemic TAC levels in TGMS-TAC treated animals were significantly lower than the trough TAC levels in systemically treated animals. Nevertheless, TAC levels in skin were comparable between the two groups. Interestingly, while in non-rejecting TGMS-TAC treated animals TAC levels were similar in transplanted and contralateral limb skin, upon rejection levels increased in the transplanted limb as compared to non-rejecting grafts and contralateral limb skin (Supplementary Figure 8). This supports the idea that rejection triggers the local release of the drug. We also found that at endpoint systemically treated animals had significantly decreased tissue TAC levels ($P < 0.05$ in graft and $P < 0.001$ in contralateral limb skin as compared to previous time point by paired t-test). We do not have an explanation for this observation, as reduced systemic TAC levels, or any observable physiological changes, did not accompany it.

In terms of immunological outcomes, the amount of circulating and intra-graft Treg was comparable between TGMS-TAC and systemic treatment. However, TGMS-TAC treatment was associated with higher and more persistent hematopoietic chimerism compared to systemic treatment. Chimerism is a pro-tolerogenic factor²² and boosting it without aggressive pre-conditioning or bone marrow transplantation may be an attractive option to control anti-graft immunity

in VCA. Despite elevated chimerism, most TGMS-TAC-treated animals experienced rejection episodes. Chimerism alone is not sufficient to prevent rejection and requires the support of higher Treg counts²³, which was not the case under both treatments. Moreover, it has been shown that robust chimerism cannot prevent rejection once immunosuppression is tapered in a porcine VCA model²⁴. The levels of chimerism in TGMS-TAC-treated animals, despite being elevated compared to systemic treatment, were still below the threshold required for tolerance²⁵. Therefore rejection due to reaching low intragraft TAC levels was not preventable by the achieved increase in chimerism with TGMS-TAC. Nevertheless, the possibility to use localized immunosuppression to increase chimerism levels to the “tolerogenic threshold”²⁵ represents an interesting opportunity that deserves further investigation.

In 2014 for the first time the VCA society dealt with antibody-mediated rejection in a pre-sensitized face recipient, raising patient sensitization as the next frontier in the field²⁶. Recent studies in rat VCA model have clearly demonstrated that sensitized recipients experience accelerated rejection of both cell- and antibody-mediated nature²⁷. In our study we have not included a pre-sensitized group, neither did our animals develop *de novo* DSA. Complement deposition²⁸, and tertiary lymphoid structure formation²⁹, which were also described as participants in the VCA rejection process, were also not detected, consistent with previous studies³⁰. Future studies addressing the efficacy of TGMS-TAC in a sensitized animal model would provide a strong argument on the potential and limitations of this therapeutic modality.

In view of clinical application, a combination of “the best of both worlds” – combining use of reduced systemic immunosuppression and local ‘on demand’ immunosuppression – might be envisaged to balance the outcomes of graft and recipient. Moreover, single-drug immunotherapies are not successful in clinical VCA. Multi-drug immunosuppressive protocols are currently used in transplanted patients to guarantee an effective level of immunosuppression. Therefore, we believe that protocols involving localized immunosuppression in humans should further evolve by including multiple drugs to better control graft rejection.

In summary, this study demonstrates that the use of an enzyme-responsive drug delivery system for localized immunosuppression in VCA results in long-term graft survival with reduced drug-related side effects. These findings support the safety of this therapeutic possibility, and suggest a potential to mitigate immunosuppression-related morbidities in patients.

Acknowledgements:

The authors would like to thank Jane Shaw-Boden, Catherine Tsai and Tsering Wuethrich for technical assistance and proofreading. LC-MS/MS analyses were performed at the Clinical Metabolomics Facility, Center of Laboratory Medicine from the Bern University Hospital “Inselspital”. The authors thank Michael Hayoz for blood LC-MS/MS routine analyses, Alexander Leichtle for BUN, creatinine, cholesterol, triglycerides, AST and ALT analyses, and Gabriela Mäder for help with tissue LC-MS/MS TAC analyses.

References:

1. Howsare M, Jones CM, Ramirez AM. Immunosuppression maintenance in vascularized composite allotransplantation. *Current Opinion in Organ Transplantation*. July 2017;1-7. doi:10.1097/MOT.0000000000000456.
2. Petruzzo P, Sardu C, Lanzetta M, Dubernard J-M. Report (2017) of the International Registry on Hand and Composite Tissue Allotransplantation (IRHCTT). *Clin Transpl*. November 2017;1-10. doi:10.1007/s40472-017-0168-3.
3. Dean WK, Talbot SG. Vascularized Composite Allotransplantation at a Crossroad. *Transplantation*. 2017;101(3):452-456. doi:10.1097/TP.0000000000001610.
4. Qiu Y, Park K. Environment-sensitive hydrogels for drug delivery. *Adv Drug Deliv Rev*. 2001;53(3):321-339.
5. Patterson J, Hubbell JA. Enhanced proteolytic degradation of molecularly engineered PEG hydrogels in response to MMP-1 and MMP-2. *Biomaterials*. 2010;31(30):7836-7845. doi:10.1016/j.biomaterials.2010.06.061.
6. Purcell BP, Lobb D, Charati MB, et al. Injectable and bioresponsive hydrogels for on-demand matrix metalloproteinase inhibition. *Nat Mater*. 2014;13(6):653-661. doi:10.1038/nmat3922.
7. Gajanayake T, Olariu R, Leclere FM, et al. A single localized dose of enzyme-responsive hydrogel improves long-term survival of a vascularized composite allograft. *Sci Transl Med*. 2014;6(249):249ra110-249ra110. doi:10.1126/scitranslmed.3008778.
8. Kambham N, Nagarajan S, Shah S, Li L, Salvatierra O, Sarwal MM. A Novel, Semiquantitative, Clinically Correlated Calcineurin Inhibitor Toxicity Score for Renal Allograft Biopsies. *Clinical Journal of the American Society of Nephrology*. 2006;2(1):135-142. doi:10.2215/CJN.01320406.
9. Cendales LC, Kanitakis J, Schneeberger S, et al. The Banff 2007 working classification of skin-containing composite tissue allograft pathology. *Am J Transplant*. 2008;1396-1400. doi:10.1111/j.1600-6143.2008.02243.x.
10. Kershner RP, Fitzsimmons WE. Relationship of FK506 whole blood concentrations and efficacy and toxicity after liver and kidney transplantation. *Transplantation*. 1996;62(7):920-926.
11. Kędzierska K, Sindrewicz K, Sporniak-Tutak K, et al. Does Immunosuppressive Therapy Affect Markers of Kidney Damage? *Ann Transplant*. 2016;21:137-144. doi:10.12659/AOT.895275.
12. Andoh TF, Burdmann EA, Lindsley J, Houghton DC, Bennett WM. Functional and structural characteristics of experimental FK 506 nephrotoxicity. *Clin Exp*

- Pharmacol Physiol.* 1995;22(9):646-654.
13. Stillman IE, Andoh TF, Burdmann EA, Bennett WM, Rosen S. FK506 nephrotoxicity: morphologic and physiologic characterization of a rat model. *Lab Invest.* 1995;73(6):794-803.
 14. Baum A, Pohlmeier G, Rapp KG, Deerberg F. Lewis rats of the inbred strain LEW/Han: Life expectancy, spectrum and incidence of spontaneous neoplasms. *Experimental and toxicologic pathology.* 1995;47(1):11-18. doi:10.1016/S0940-2993(11)80275-7.
 15. Unadkat JV, Schnider JT, Feturi FG, et al. Single Implantable FK506 Disk Prevents Rejection in Vascularized Composite Allotransplantation. *Plastic and Reconstructive Surgery.* 2017;139(2):403e–414e. doi:10.1097/PRS.0000000000002951.
 16. Capron A, Haufroid V, Wallemacq P. Intra-cellular immunosuppressive drugs monitoring: A step forward towards better therapeutic efficacy after organ transplantation? *Pharmacol Res.* 2016;111:610-618. doi:10.1016/j.phrs.2016.07.027.
 17. Dunn SE, Burns JL, Michel RN. Calcineurin is required for skeletal muscle hypertrophy. *J Biol Chem.* 1999;274(31):21908-21912.
 18. Dalakas MC. Toxic and drug-induced myopathies. *J Neurol Neurosurg Psychiatry.* 2009;80(8):832-838. doi:10.1136/jnnp.2008.168294.
 19. Mrvos R, Hodgman M, Krenzelok EP. Tacrolimus (FK 506) overdose: a report of five cases. *J Toxicol Clin Toxicol.* 1997;35(4):395-399.
 20. Unadkat JV, Schneeberger S, Horibe EH, et al. Composite tissue vasculopathy and degeneration following multiple episodes of acute rejection in reconstructive transplantation. *Am J Transplant.* 2010;10(2):251-261. doi:10.1111/j.1600-6143.2009.02941.x.
 21. Olariu R, Denoyelle J, Leclère FM, et al. Intra-graft injection of tacrolimus promotes survival of vascularized composite allotransplantation. *Journal of Surgical Research.* 2017;218:e107-e107. doi:10.1016/j.jss.2017.05.046.
 22. Siemionow M, Cwykiel J, Madajka M. Bone Marrow-Derived Ex Vivo Created Hematopoietic Chimeric Cells to Support Engraftment and Maintain Long-Term Graft Survival in Reconstructive Transplantation. In: Brandacher G, ed. *The Science of Reconstructive Transplantation. Stem Cell Biology and Regenerative Medicine.* New York, NY: Springer New York; 2015:227-254. doi:10.1007/978-1-4939-2071-6_16.
 23. Pilat N, Farkas AM, Mahr B, et al. T-regulatory cell treatment prevents chronic rejection of heart allografts in a murine mixed chimerism model. *J Heart Lung Transplant.* 2014;33(4):429-437. doi:10.1016/j.healun.2013.11.004.

24. Shanmugarajah K, Powell H, Leonard DA, et al. The Effect of MHC Antigen Matching Between Donors and Recipients on Skin Tolerance of Vascularized Composite Allografts. *American Journal of Transplantation*. 2017;17(7):1729-1741. doi:10.1111/ajt.14189.
25. Lin J-Y, Tsai F-C, Wallace CG, Huang W-C, Wei F-C, Liao S-K. Optimizing chimerism level through bone marrow transplantation and irradiation to induce long-term tolerance to composite tissue allotransplantation. *J Surg Res*. 2012;178(1):487-493. doi:10.1016/j.jss.2012.02.064.
26. Chandraker A, Arscott R, Murphy GF, et al. The management of antibody-mediated rejection in the first presensitized recipient of a full-face allotransplant. *Am J Transplant*. 2014;14(6):1446-1452. doi:10.1111/ajt.12715.
27. Wang HD, Fidler SAJ, Miller DT, et al. Desensitization and Prevention of Antibody-mediated Rejection in Vascularized Composite Allotransplantation by Syngeneic Hematopoietic Stem Cell Transplantation. *Transplantation*. 2018; Publish Ahead of Print:1. doi:10.1097/TP.0000000000002070.
28. Sarhane KA, Tuffaha SH, Broyles JM, et al. A critical analysis of rejection in vascularized composite allotransplantation: clinical, cellular and molecular aspects, current challenges, and novel concepts. *Front Immunol*. 2013;4:406. doi:10.3389/fimmu.2013.00406.
29. Hautz T, Zelger BG, Nasr IW, et al. Lymphoid neogenesis in skin of human hand, nonhuman primate, and rat vascularized composite allografts. *Transpl Int*. 2014;27(9):966-976. doi:10.1111/tri.12358.
30. Unadkat JV, Schneeberger S, Goldbach C, et al. Investigation of Antibody-Mediated Rejection in Composite Tissue Allotransplantation in a Rat Limb Transplant Model. *TPS*. 2009;41(2):542-545. doi:10.1016/j.transproceed.2009.01.024.

Table 1 Complete blood count of TGMS-TAC and systemic tacrolimus treated groups at POD 280 vs. naive age-matched animals

	Naive Lewis rats (n=9)	TGMS-TAC (n=5)	Systemic tacrolimus (n=5)	Significance
WBC x 10 ³	9.6 ± 0.9	7.4 ± 3.4	14.8 ± 15.1	ns
RBC x 10 ³	9.5 ± 0.9	10.1 ± 0.6	9.6 ± 0.3	ns
HB g/dL	15.4 ± 0.4	15.8 ± 0.7	14.2 ± 0.7	†**, ‡**
HCT %	50.4 ± 3.7	53.4 ± 3.3	49.9 ± 1.5	ns
MCV fL	53.0 ± 2.0	53.1 ± 0.9	51.9 ± 2.1	ns
MCH pg	16.3 ± 1.4	15.7 ± 0.6	14.8 ± 1.1	ns
MCHC g/dL	30.7 ± 1.6	29.6 ± 1.0	28.5 ± 1.4	†*
PLT x 10 ³	709.2 ± 82.2	584.6 ± 124.6	629.6 ± 132.3	ns
RDW_SD fL	28.5 ± 0.4	28.7 ± 0.5	28.4 ± 0.5	ns
RDW_CV%	14.7 ± 2.0	14.9 ± 1.8	14.8 ± 2.1	ns
PDW fL	11.1 ± 0.4	11.0 ± 0.7	10.0 ± 0.3	†**, ‡**
MPV fL	8.2 ± 0.2	8.2 ± 0.3	7.7 ± 0.2	†**, ‡**

WBC - white blood cells

RBC - red blood cells

HB - hemoglobin

HCT - hematocrit

MCV- mean corpuscular volume

MCH - mean corpuscular hemoglobin

MCHC - mean corpuscular hemoglobin concentration

PLT - platelets

RDW - red blood cell distribution width

PDW - platelet distribution width

MPV - median platelet volume

† Statistical significance between Naive Lewis rats and systemic tacrolimus treated group

‡ Statistical significance between TGMS-TAC-treated group and systemic tacrolimus treated group

* $P < 0.05$

** $P < 0.01$

Figure legends:

Figure 1 Long-term graft survival and graft histology are comparable between TGMS-TAC and systemic tacrolimus treatment. (a) Experimental scheme of the two treatment groups. Group 1 – 1 ml hydrogel with 7 mg tacrolimus intra-graft treated group (TGMS-TAC). Group 2 daily systemic treatment with 1 mg/kg/day tacrolimus group (systemic tacrolimus), including treatment application frequencies and planned duration of the experiments. (b) Kaplan-Meier survival curve of TGMS-TAC-treated and systemic tacrolimus treated animals (n=6 /group). (c) Macroscopic grading of graft rejection over time in each of the rats (animals 1 to 6 – TGMS-TAC treated, animals 7 to 12 – systemically treated). Appearance of edema and erythema are defined as grade 1, epidermolysis and exudation as grade 2, desquamation, necrosis and mummification as grade 3. TGMS-TAC re-injection time points are indicated. Animal 1 was euthanized at postoperative day 149 after reaching grade 3 rejection. (d) Representative histological Hematoxylin and Eosin stained sections of graft skin collected at endpoint – postoperative day (POD) 280 from both treatment groups and their corresponding histopathological evaluation. Inter-group differences of the results presented are not significant as evaluated by Mann-Whitney test. Individual values are presented as dots with indication of the mean values by lines.

Figure 2 TGMS-TAC treatment does not completely prevent, but can revert rejection episodes. (a) Representative photographs of rejecting graft before (POD 204) and after (POD 234) TGMS-TAC re-injection and (b) corresponding histological Hematoxylin and Eosin stained sections of rejecting graft skin before and after TGMS-TAC re-injection.

Figure 3 Blood tacrolimus levels are lower with TGMS-TAC therapy. (a) Tacrolimus levels were measured by LC-MS/MS in blood of TGMS-TAC and systemic tacrolimus treated rats (trough levels) over time. TGMS-TAC re-injection time points are indicated by syringe symbols on the x-axis. Statistical analyses of the differences between the peaks of tacrolimus release under TGMS-TAC treatment are shown. Data are shown as individual values and means, *** $P < 0.001$, **** $P < 0.0001$ by ordinary one-way ANOVA. Individual values have been manually shifted to left or right to make each value visible. (b) Mean bi-weekly tacrolimus blood levels between TGMS-TAC and systemic tacrolimus treated rats are compared. Each data point represents the mean value of pooled tacrolimus measurements acquired over the course of each two consecutive weeks (starting from post-operative week 1 + 2, then 3 + 4 etc. until the end of the study). Statistical analyses of the differences between the two groups are shown. Data are presented as individual values, mean \pm SD. are indicated, ** $P < 0.01$ by Mann-Whitney test.

Figure 4 Tacrolimus levels in graft skin are higher with TGMS-TAC therapy. (a) LC-MS/MS tacrolimus measurements in graft and contralateral limb skin biopsies of TGMS-TAC-treated rats over time. TGMS-TAC re-injection time points are indicated. (b) LC-MS/MS tacrolimus measurements in graft and contralateral limb skin biopsies of systemic tacrolimus treated rats over time. Data are shown as

individual values and means. Individual values have been manually shifted to left or right to make each value visible. (c) Mean tacrolimus levels in graft and contralateral limb skin of TGMS-TAC-treated or systemic tacrolimus treated animals. Each data point represents the mean value across the experimental group at each time point of tacrolimus measurements in either graft or contralateral limb skin. Statistical analyses of the differences between the two groups are shown. Data are shown as individual values, mean \pm SD are indicated, * P <0.05, Mann-Whitney test is used for comparisons between the two treatment groups, Wilcoxon test is used for comparisons within a group between the two sites of biopsy collections.

Figure 5 Local and systemic tacrolimus treatment is associated with low donor-specific antibody (DSA) formation. (a) Levels of IgG and IgM DSA in the plasma of TGMS-TAC or systemic tacrolimus treated rats at POD 280. Donor-thymocytes have been incubated with heat-inactivated recipients' plasma isolated at POD 280, followed by staining with anti-IgG and anti-IgM antibody. DSA deposition on thymocytes have been analyzed by flow cytometry and expressed as mean fluorescence intensity (MFI). Lower threshold for positivity is defined as mean + 2x SD of the MFI measured in donor-thymocytes incubated with naïve Lewis rats' plasma. Data are shown as individual values, mean \pm SD are depicted, * P <0.05 by Student's t-test. (b) Representative results of immunostained graft skin and muscle cryosections with anti-IgG or anti-IgM antibody and (c) their corresponding quantification. Data are shown as individual values, mean \pm SD are depicted. Inter-group differences are not significant as evaluated by Student's t-test.

Figure 6 TGMS-TAC treatment mitigates elevation of kidney function markers and occurrence of malignancy and opportunistic infections. (a-f) Biochemical analyses of the plasma levels of (a) blood urea nitrogen, (b) creatinine, (c) cholesterol, (d) triglycerides, (e) aspartate aminotransferase, (f) alanine aminotransferase in plasma collected at POD 280 from TGMS-TAC and systemic tacrolimus treated rats. Data are shown as individual values, mean \pm SD are depicted, * P <0.05, ** P <0.01, **** P <0.0001 by one-way ANOVA. (g) Representative histological Hematoxylin and Eosin stained section of pseudocyst infected with *Staphylococcus aureus* and *Proteus mirabilis* in a systemic tacrolimus treated rat and of (h) ipsilateral inguinal lymph node with lymphoma in another systemic tacrolimus treated rat.

Figure 7 TGMS-TAC treatment depletes T-cells to a lesser extent than systemic TAC treatment. (a-f) Absolute number of T-cell populations in blood of TGMS-TAC and systemic tacrolimus treatment at selected time points. The values measured in naïve animals are reported (black dots). Cells are enumerated by flow cytometry as (a) T-cells (CD45⁺, CD3⁺), (b) Cytotoxic T-cells (CD45⁺, CD3⁺, CD8⁺), (c) T helper cells (CD45⁺, CD3⁺, CD4⁺), (d) Treg cells (CD45⁺, CD3⁺, CD4⁺, FoxP3⁺, CD25^{high}), (e) Helios⁺ Treg cells (CD45⁺, CD3⁺, CD4⁺, FoxP3⁺, CD25^{high}, Helios⁺), (f) Helios⁻ Treg cells (CD45⁺, CD3⁺, CD4⁺, FoxP3⁺, CD25^{high}, Helios⁻). Data are shown as mean \pm SD. Statistical analyses between naïve and the two treatment groups - one-way ANOVA. Highlighted in orange are the time points,

which are significantly different between TGMS-TAC and systemic tacrolimus treatment groups. Significant differences between naïve animals and treated animals are not shown.

Figure 8 TGMS-TAC boosts multilineage hematopoietic chimerism in blood. (a-f) Donor-derived white blood cell populations in blood from TGMS-TAC and systemic tacrolimus at selected time points. The values measured in naïve animals (unspecific-staining) are reported (black dots). Donor cells are enumerated by flow cytometry as (a) all donor-derived white blood cells (CD45⁺, RT1a⁺), (b) donor-derived B-cells (CD45⁺, CD3⁻, CD4⁻, SSC^{low}, RT1a⁺), (c) donor-derived T helper cells (CD45⁺, CD3⁺, CD4⁺, RT1a⁺), (d) donor-derived cytotoxic T-cells (CD45⁺, CD3⁺, CD8⁺, RT1a⁺), (e) donor-derived monocytes (CD45⁺, CD3⁻, CD4⁺, RT1a⁺), (f) donor-derived granulocytes (CD45⁺, CD3⁻, CD4⁻, SSC^{high}, RT1a⁺). Naïve Lewis rats' white blood cells are RT1a⁻. Data are shown as mean ± SD. Statistical analyses between naïve and the two treatment groups - one-way ANOVA. Highlighted in orange are the time points, which are significantly different between TGMS-TAC and systemic tacrolimus treatment groups. Significant differences between naïve animals and treated animals are not shown.

Figure 1

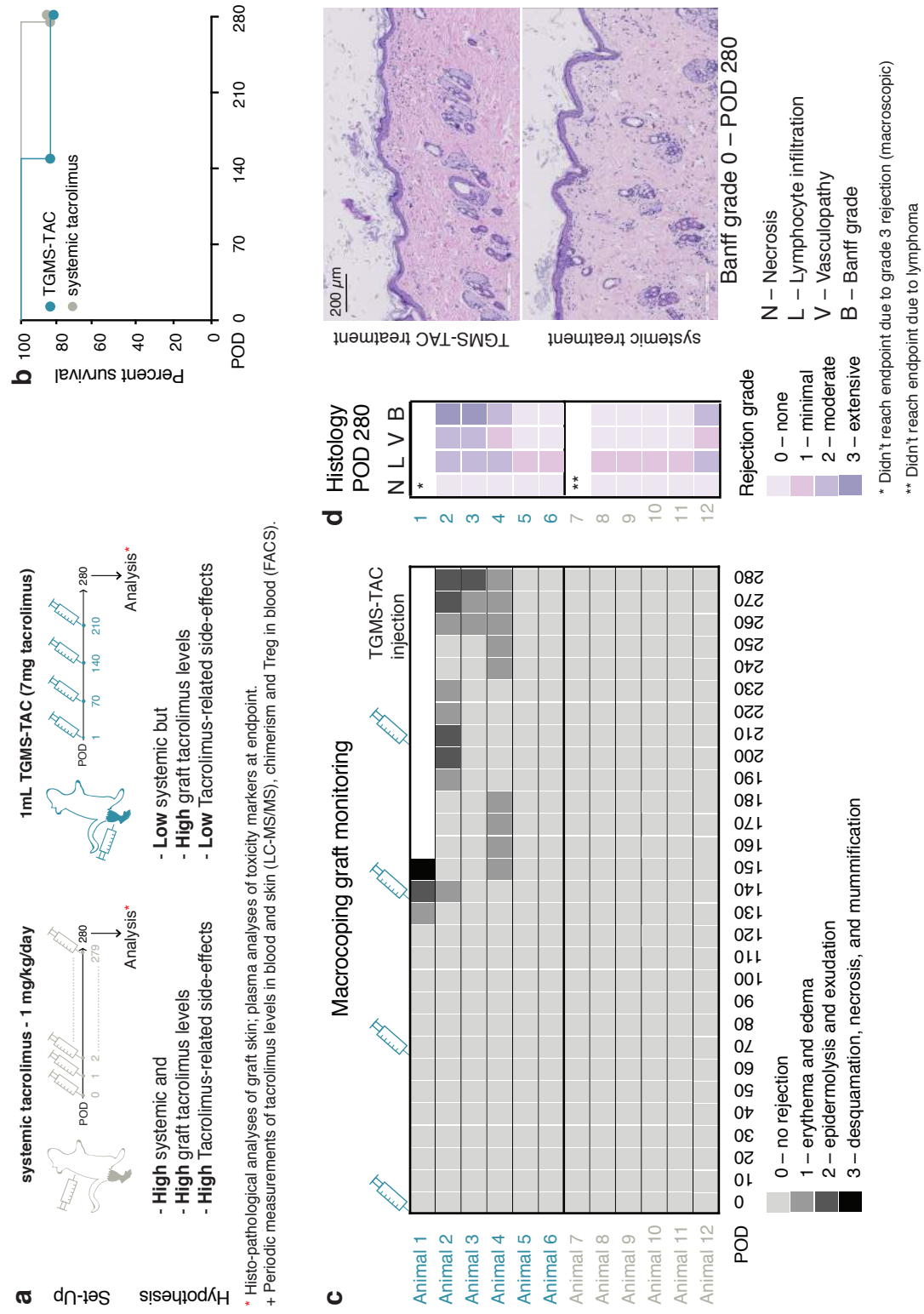


Figure 2

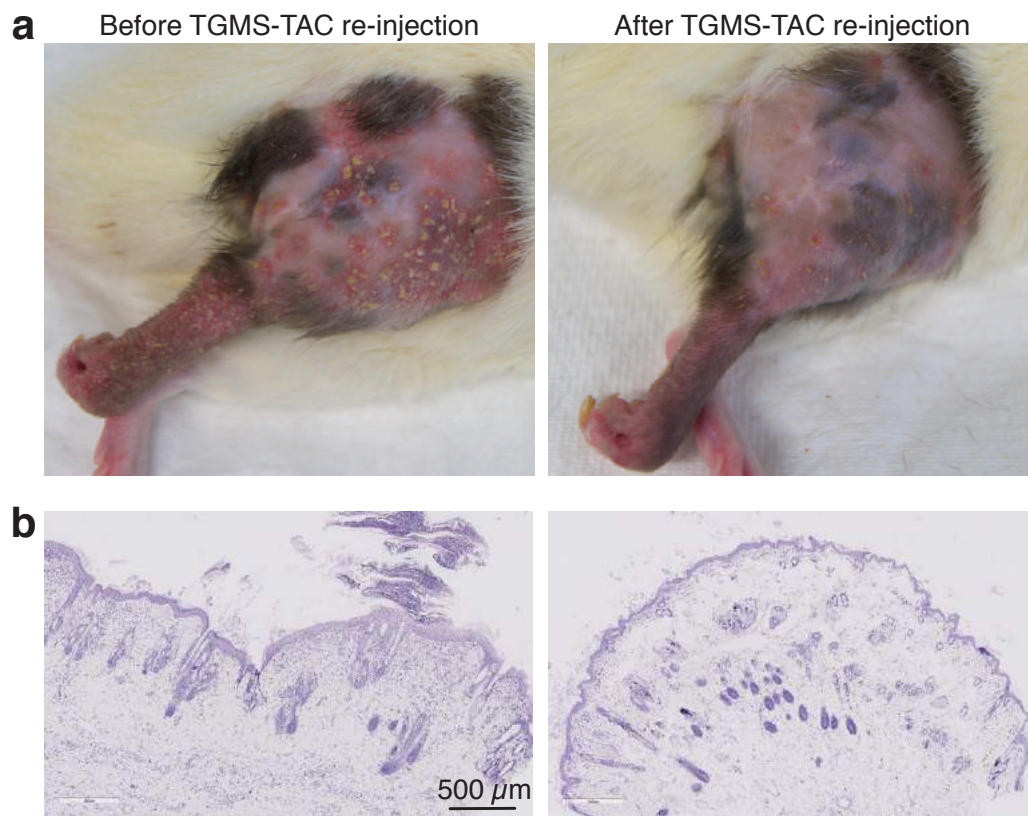


Figure 3

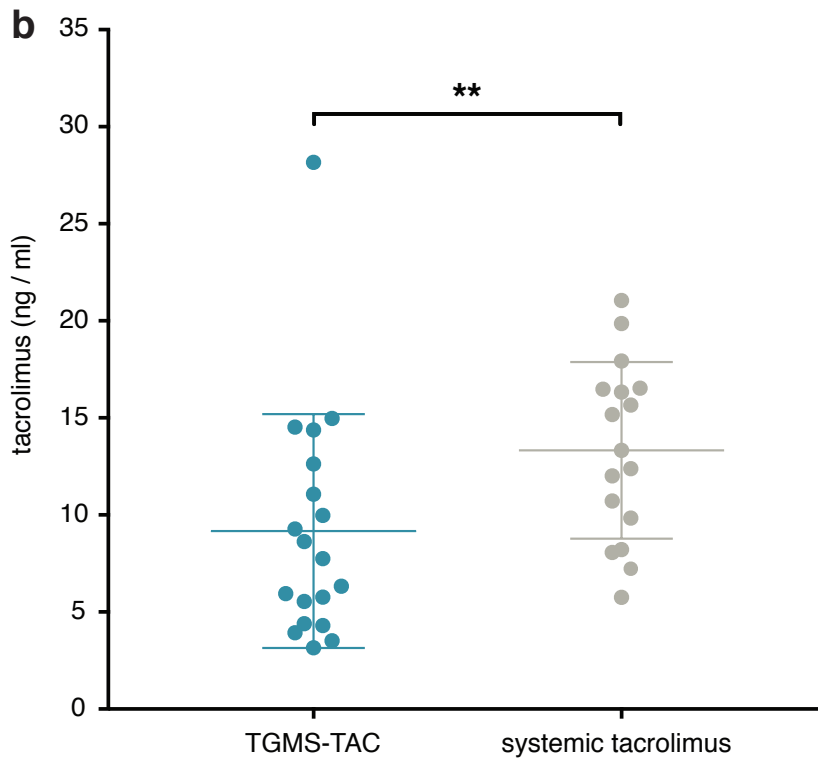
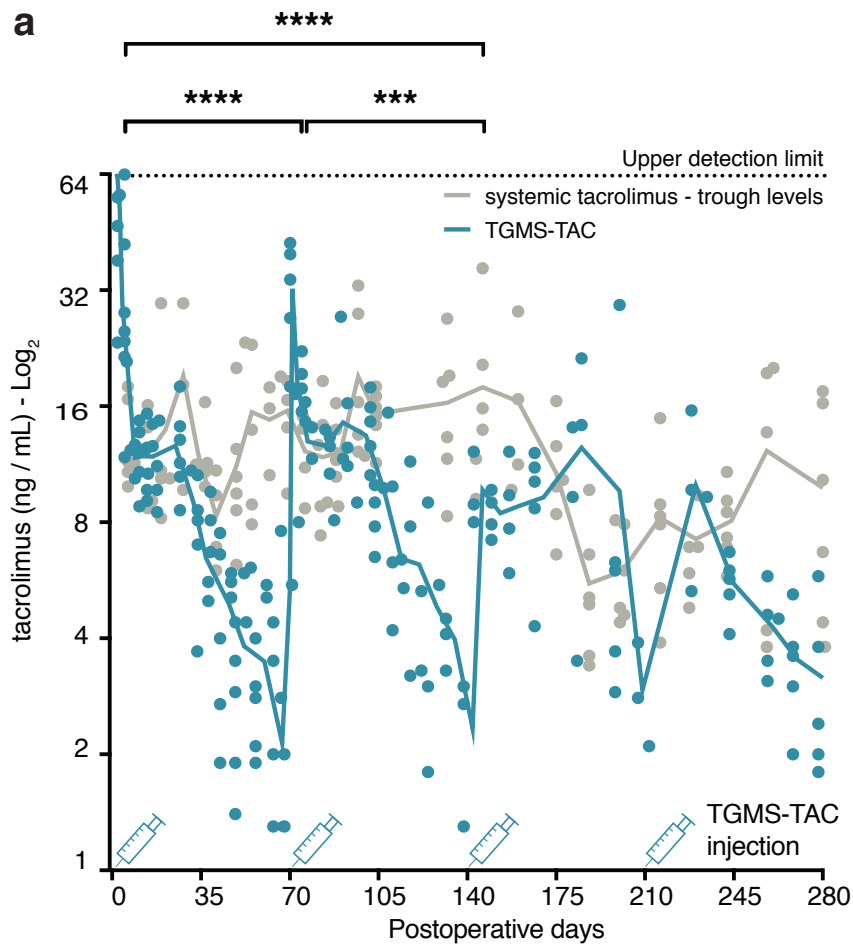


Figure 4

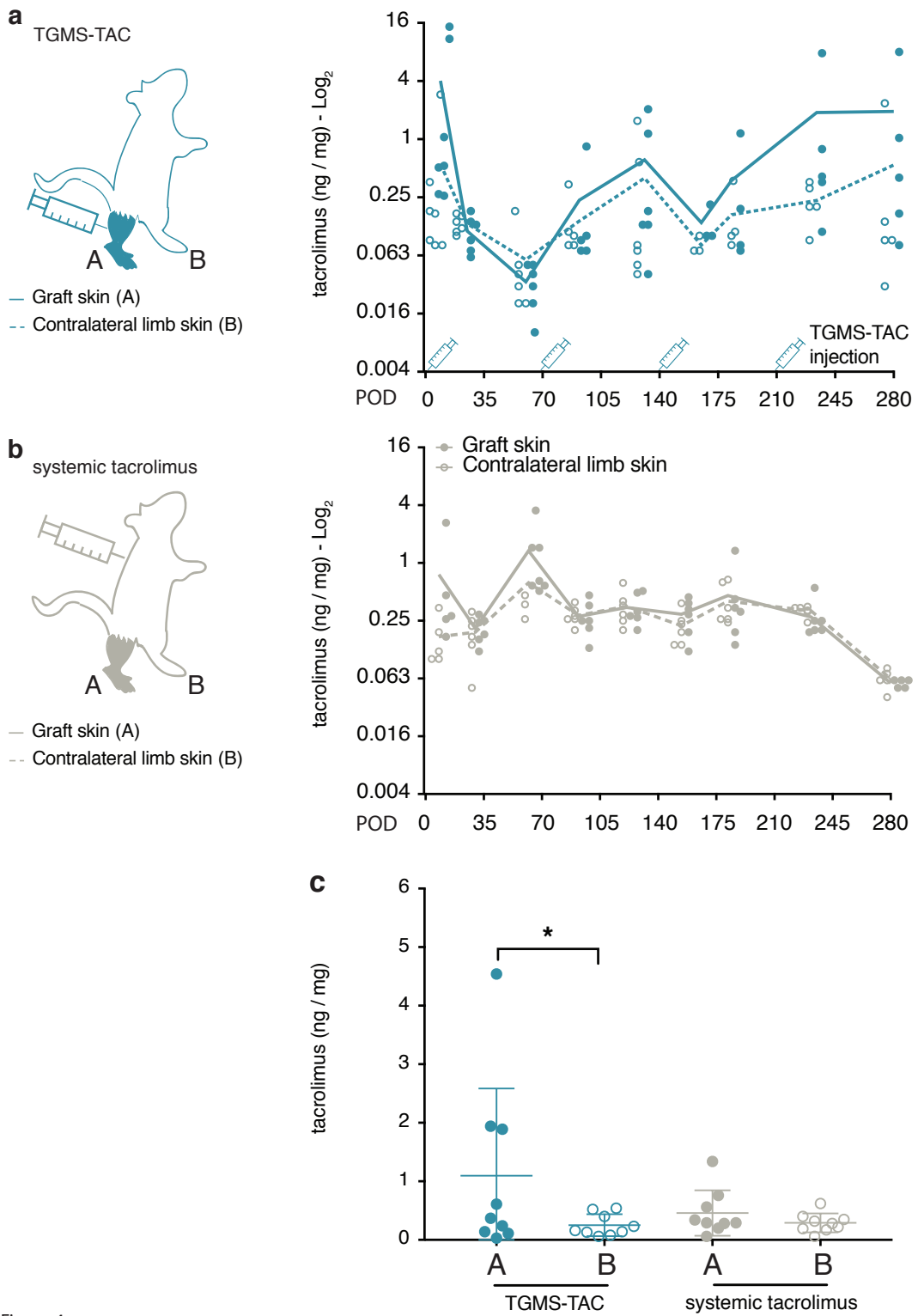


Figure 5

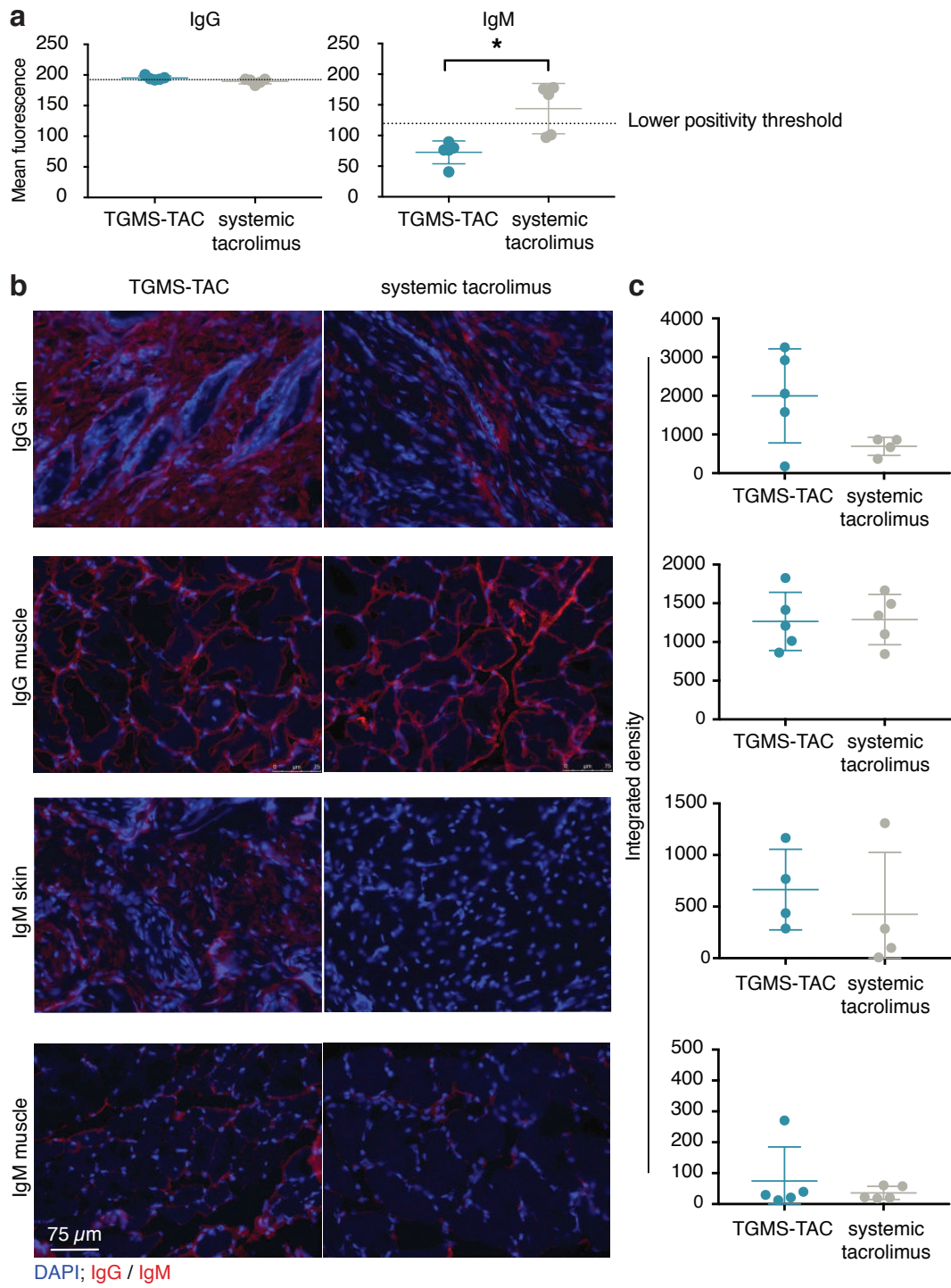


Figure 6

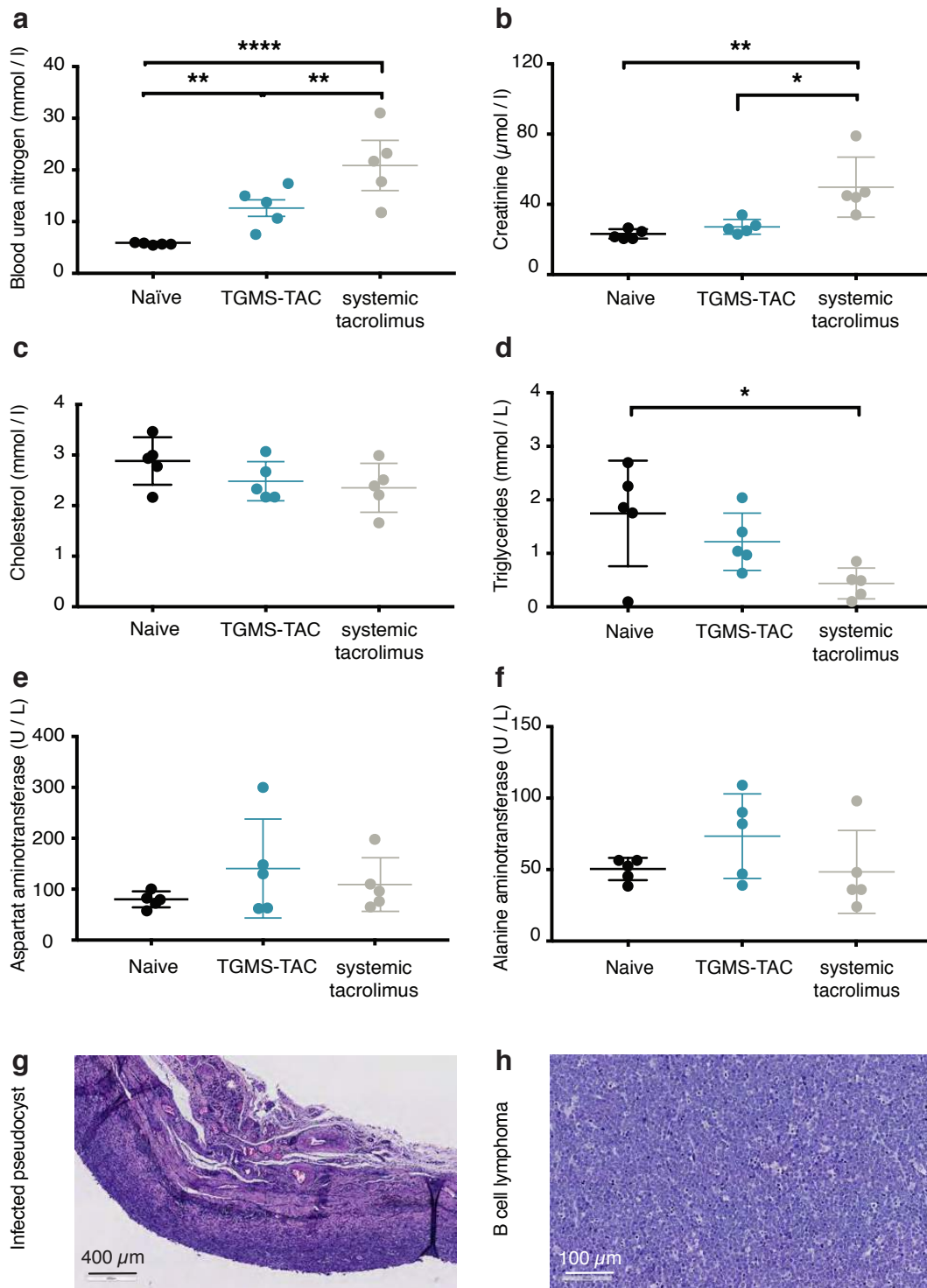


Figure 7

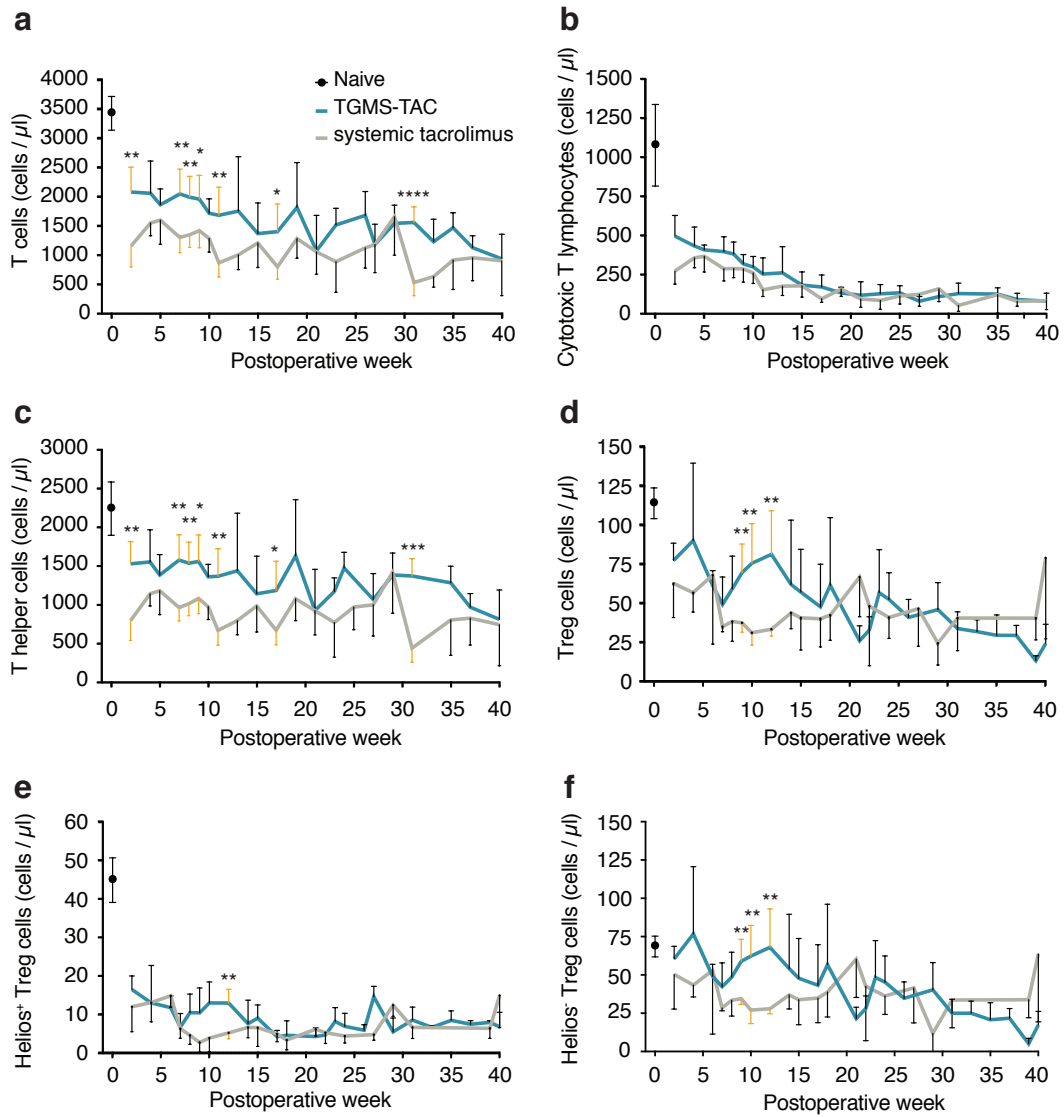
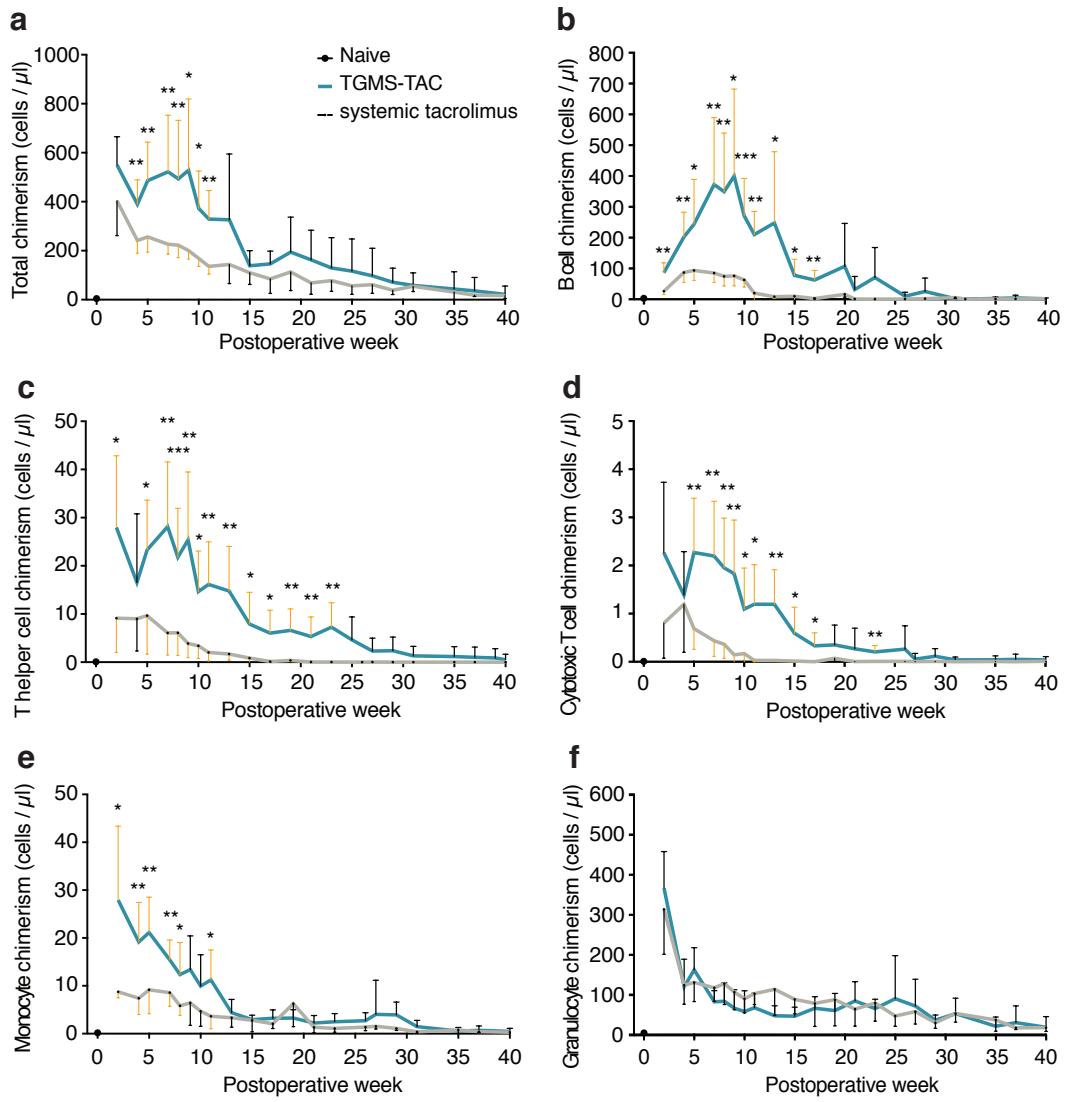


Figure 8



Supplementary Materials and Methods

Animals

Male Brown Norway and Lewis rats (6-8 weeks old weighing 200 to 250 g) were purchased from Charles Rivers Breeding Laboratories, Germany. Animals were kept in specific pathogen-free conditions and care was carried out in strict accordance with the Swiss Laws in Animal Protection. All experimental protocols were approved by the Veterinary Authorities of the Canton Bern.

Drug preparation

Tacrolimus (LC Laboratories, Woburn, MA, United States), TGMS (AK Scientific, Union City, CA, United States), EDTA Hybri-Max (Sigma, St. Louis, MO, United States) and sterile water (B.Braun, Melsungen, Germany) were used for TGMS-TAC preparation as described previously¹.

Limulus amoebocyte lysate test (Pyrogen 03 Plus, Lonza Group, Basel, Switzerland) was used for pyrogen detection according to manufacturer's instructions and TGMS-TAC was considered pyrogen-free if 1:10 dilution of hydrogel in sterile water resulted negative to the test.

TAC solution for systemic injections was prepared by dissolving TAC in Ethanol (absolute, Merck, Darmstadt, Germany) with addition of 1:1 Kolliphor EL (Sigma). The solution was further diluted in sterile saline 1:10 for injection.

Hind limb transplantation and monitoring

Hind limb transplantations were performed as described previously² using a two-surgeon method.

All the operations were performed under continuous inhalation anesthesia. Isoflurane 5% (AbbVie AG, North Chicago, IL, United States) with oxygen (0.8 L/min) was used for the induction of anesthesia. Maintenance anesthesia employed 1-1.5 % Isoflurane with 0.6 L/min oxygen. All the rats were maintained at a normal body temperature using thermal pads.

Surgeon one prepared both hind limbs of a donor Brown-Norway rat for transplantation. The hind limbs were harvested while keeping the whole inguinal fat pad with its lymph nodes in the graft and taking care not to injure the epigastric vessels that ensure its vascularization. The femoral artery and vein were prepared for anastomosis on a length of approximately 1-1.5 cm from the emergence of the epigastric vessels up to the inguinal crease. Concomitantly, surgeon two prepared the first Lewis recipient by removing the hind limb including the inguinal fat pad and performing a midfemoral amputation. The recipient vessels were prepared for anastomosis from the inguinal crease up to the emergence of the epigastric vessels. The first allograft was then reattached by surgeon two using and intramedullary osteosynthesis with a 19 G needle with blunted ends, after which preliminary fixation of the anterior muscle compartments was performed with resorbable 5-0 sutures. Venous anastomosis was performed next performed using the cuff technique with a polyimide cuff with an inner diameter of 1.19 mm (Vention Medical Inc Denver, United States). The arterial anastomosis was performed next in an end-to-end microsurgical technique using 10-0 ETHILON Nylon Suture (Ethicon Inc., Somerville, NJ, United States). The transplantation was completed after neurorrhaphy of the

femoral nerve, sciatic nerve and approximation of the posterior compartment thigh muscles. Skin closure was performed with resorbable 5-0 Coated VICRYL (polyglactin 910) Suture (Ethicon Inc.) in a continuous fashion. Surgeon one performed the same procedure of transplantation of the second hind limb allograft to a second Lewis recipient after finishing graft procurement and euthanasia of the Brown-Norway rat. The successfully transplanted rats were randomly assigned to the following two groups:

Group 1 - Systemically treated with daily subcutaneous injection in the neck fold of 1 mg/kg TAC solution (n=6); Group 2 – Treated with 1 ml TGMS-TAC loaded with 7 mg TAC subcutaneously in the graft every 70 days starting the day after the operation (n=6). In this group, four depots of TGMS-TAC of 250 μ L each were injected in the zones of biceps femoris, gastrocnemius, tibialis anterior, and vastus muscles, taking great care to distribute the amount of drug as evenly as possible intra- and inter-individually. Re-injection time point was decided upon a pilot study showing that transplanted animals (n=5) treated with a single intra-graft injection of 1 ml TGMS-TAC loaded with 7 mg TAC (POD 1) rejected their graft on $POD 83.4 \pm 6.7$. Re-injection time point was defined as 14 days before rejection and set to POD 70.

After transplantation, animals were inspected on a daily basis for weight loss and signs of pain or distress³. Graft survival was monitored until endpoint – POD 280 or macroscopic grade 3 rejection. Graft rejection was evaluated macroscopically as grade 0 = no rejection, 1 = erythema and edema, 2 = epidermolysis and exudation, and 3 = desquamation, necrosis, and mummification. At sacrifice skin and muscle from the graft were formalin fixed (24 h), paraffin-embedded, and sectioned (3 μ m). Hematoxylin-eosin as well as periodic acid-Schiff stained sections were graded by a pathologist blinded to the treatment regimens. Skin was graded according to Banff classification⁴, while muscle necrosis and lymphocyte infiltration were graded as grade 0 – none, 1 – minimal, 2 – moderate, and 3 – extensive.

Tacrolimus kinetics analyses

TAC in blood (systemic), in graft skin biopsies (local), and in contralateral hind limb skin biopsies was measured at selected time points.

Peripheral blood was collected from the sublingual vein in EDTA coated tubes (Sarstedt, Nümbrecht, Germany) and stored at -20° C until use. TAC concentrations in blood were assessed using the Kit MS1100 (ClinMass Complete Kit, advanced, for Immunosuppressants in Whole Blood, RECIPE Chemicals + Instruments GmbH, Munich, Germany) and quantified by LC-MS/MS.

Skin biopsies from the transplanted and contralateral limb were excised, weighed, snap frozen, and stored at - 20° C until use. The sample preparation was adapted using the MS1312 from Recipe as internal standard. TAC and internal standard were dissolved in 70 % (v/v) methanol solution. Standard spiking solution was prepared to build up a calibration curve between 0.3 and 65 ng/mL. The frozen tissues were gently thawed at room temperature. For blank matrix, samples skin samples without TAC treatment were used. A blank matrix was prepared adding 1000 μ L of precipitation solution to untreated tissue. A volume of 40 μ L of internal standard solution and 960 μ L of precipitation solution

were added to the treated samples. All samples were then grinded with five stainless steel balls for 30 minutes at 25 Hz. The tubes were centrifuged 5 minutes at 4° C and 20'000 rcf. 500 µL of the tissue extract was filtered with a Mini-Uni Prep G2 vials (GE Healthcare, Chicago, USA).

Chromatographic analysis was performed on an Acquity I-Class system (Waters, Milford, MA, USA) with ClinMass Complete Kits (Immunosuppressants in whole blood, advanced – on-line analysis). The autosampler temperature was set at 10 °C and the autosampler needle was washed with a strong needle wash solution of isopropanol:methanol:acetone:H₂O (1:1:1:1, v/v). A solution of 20 % (v/v) methanol was used as weak needle wash. Analytes were ionized by electrospray ionization (ESI) in the positive mode and detected on a triple quadrupole mass spectrometer (Xevo TQ-S, Waters, Milford, MA, USA). The capillary and the cone voltage were set at 3 kV and 40 V, respectively. The source offset was set at 60 V, the desolvation temperature at 400° C, the desolvation gas at 1000 L/h, the cone gas at 150 L/h, the nebulizer at 7 bar and the source temperature at 150° C. The instrument was controlled via MassLynx (version 4.1, Waters). Data were acquired, integrated and processed with TargetLynx (MassLynx v4.1).

Analyses of immunosuppression-related toxicity

At sacrifice complete blood count was acquired (Sysmex KX-21N automatic hematology analyzer, Sysmex Corporation, Kobe, Hyōgo Prefecture, Japan). Kidney and liver function markers in plasma (creatinine, blood urea nitrogen and alanine aminotransferase, aspartate aminotransferase respectively) were submitted for analysis to the Center of Laboratory Medicine at the University Hospital of Bern. Kidney and liver samples were formalin fixed (24 h), paraffin-embedded, and sectioned (3 µm). Histopathological analysis (Hematoxylin and Eosin, Periodic acid–Schiff) were graded by a pathologist blinded to treatment regimens as described previously⁵. Results were compared to naïve age-matched Lewis rats.

Flow Cytometry analyses

For blood analyses, freshly drawn blood was collected in EDTA coated tubes at pre-defined time points for chimerism and Treg analyses. Erythrocytes were lysed with 10X RBC Lysis Buffer (Multi-species, Thermo Fisher Scientific, Waltham, MA, United States) and the cells were incubated for 15 min with Fixable Viability Dye eFluor 506 (Thermo Fisher Scientific). After washing with 1xPBS 1%BSA, cells were incubated with the following anti-rat antibodies: Alexa Fluor 700 anti-rat CD45 antibody (BioLegend, San Diego, CA, United States), CD3-PerCP-Vio700, rat (Miltenyi Biotec, Bergisch Gladbach, Germany), APC/Cy7 anti-rat CD4 antibody (BioLegend), CD8b-PE-Vio770, rat (Miltenyi Biotec), and either FITC anti-rat CD25 antibody (BioLegend), or mouse anti rat MHC Class I RT1Ac:FITC (Bio-Rad Laboratories, Hercules, CA, United States) for 15 min at 4°C. Cells were washed and permeabilized (eBioscience FoxP3 / Transcription Factor Staining Buffer Set, Thermo Fisher Scientific) and incubated 30 min with anti-Helios-PE, human and mouse (Miltenyi Biotec) and FOXP3 monoclonal antibody (FJK-16s), eFluor 450 (Thermo Fisher Scientific), and acquired using a LSR II cytometer (BD Biosciences, San Jose, United States)

equipped with FACS Diva Software (BD Biosciences). Data were analyzed with Flow-Jo software (Tri-Star, Ashland, United States). Absolute cell number was estimated from the proportion of cells recorded by flow cytometry in the CD45+ gate multiplied by absolute mononuclear cell count measured using a Sysmex hematology analyzer in the same blood sample.

For skin analyses, at sacrifice graft and contralateral limb skin was minced (gentleMACS dissociator, Miltenyi Biotec, Bergisch Gladbach, Germany) and digested with Collagenase D (Roche, Basel, Switzerland) 1 mg/ml and DNase I (Sigma) 200 µg for 1h at 37° C on agitation. Resulting suspension was filtered through 40 µm cell strainers (Falcon, Corning Inc., Corning, NY, United States) and overlaid on top of Ficoll-Paque PLUS Separation Media (GE Healthcare, Little Chalfont, United Kingdom). After centrifugation the ring of cells was collected, washed, and used immediately. Cell were stained, acquired and analyzed as described above.

DSA analyses in plasma

Plasma isolated at sacrifice was complement inactivated (46° C, 30 min) and incubated (1:10 in PBS) for 15 min with donor thymocytes (1×10^6 cells) pre-treated with 3% BSA and purified mouse anti-rat CD32 (BD Biosciences) to block unspecific Fc receptors binding. After washing, cells were incubated for 15 min with Fixable Viability Dye eFluor 506 (Thermo Fisher Scientific), washed and stained with CD3-PerCP-Vio700, rat (Miltenyi Biotec), goat F(ab')₂ anti rat IgG:FITC (Bio-Rad Laboratories) and R-Phycoerythrin AffiniPure F(ab')₂ fragment goat anti-rat IgM, µ chain specific (Jackson ImmunoResearch Laboratories, West Grove, PA, United States) for 15 min at 4°C. After extensive washing, cells were acquired and analyzed as explained above. Minimum threshold of positivity for DSA in the plasma of transplant recipients was determined to be equal to the mean of naïve Lewis plasma plus two times its standard deviation.

Immunofluorescence analyses

Skin and muscle samples retrieved at sacrifice day were embedded in TissueTec - O.C.T. (Sakura Finetek, Alphen aan den Rijn, The Netherlands) on dry ice and sectioned (5 µm). Slides were stained with DAPI (4',6-diamidino-2-phenylindole, Boehringer Mannheim GmbH, Mannheim, Germany) and one of the following primary antibodies: goat anti-rat IgG-BIOT (Southern Biotech, Birmingham, AL, United States), goat anti-rat IgM-BIOT (Southern Biotech), mouse anti rat CD45RA (B Cells Only, Southern Biotech), polyclonal rabbit anti-human C3c complement (Multipurpose, Agilent, Santa Clara, California, United States), anti-complement C4c antibody (LifeSpan BioSciences, Seattle, WA, United States) or C5b-9, rat, mAb 2A1 (Hycult Biotech, Plymouth Meeting, PA, United States,). The following secondary antibodies were used: Streptavidin-Cy3 from *Streptomyces avidinii* (Sigma-Aldrich), anti-rabbit IgG (whole molecule), F(ab')₂ fragment-Cy3 antibody produced in sheep (Sigma-Aldrich), donkey anti-sheep IgG (H+L) cross-adsorbed secondary antibody, Alexa Fluor 488 (Thermo Fisher Scientific) or goat anti-mouse IgG (H+L) highly cross-adsorbed secondary antibody, Alexa Fluor Plus 488 (Thermo Fisher Scientific). Slides were visualized with Leica DMI4000, LAS AF Software, Wetzlar, Germany. All images were

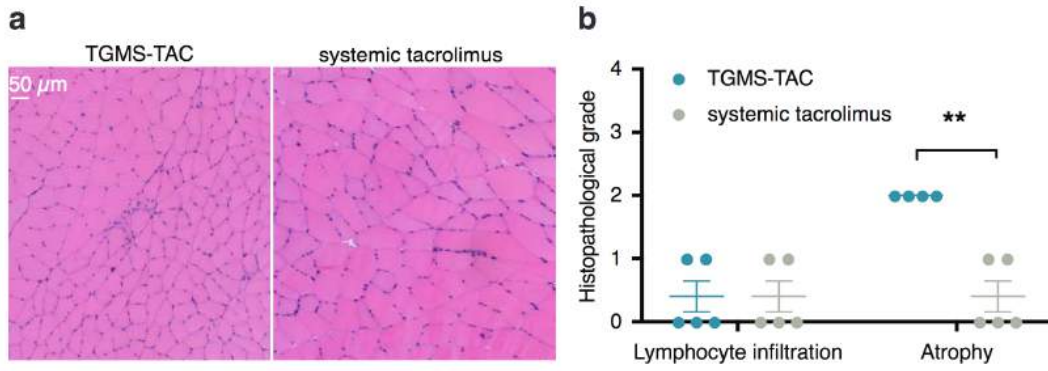
captured with identical exposure times. Quantitative analysis of fluorescence intensity (integrated density) was performed by ImageJ software (<https://imagej.nih.gov/ij/>).

Statistical analyses

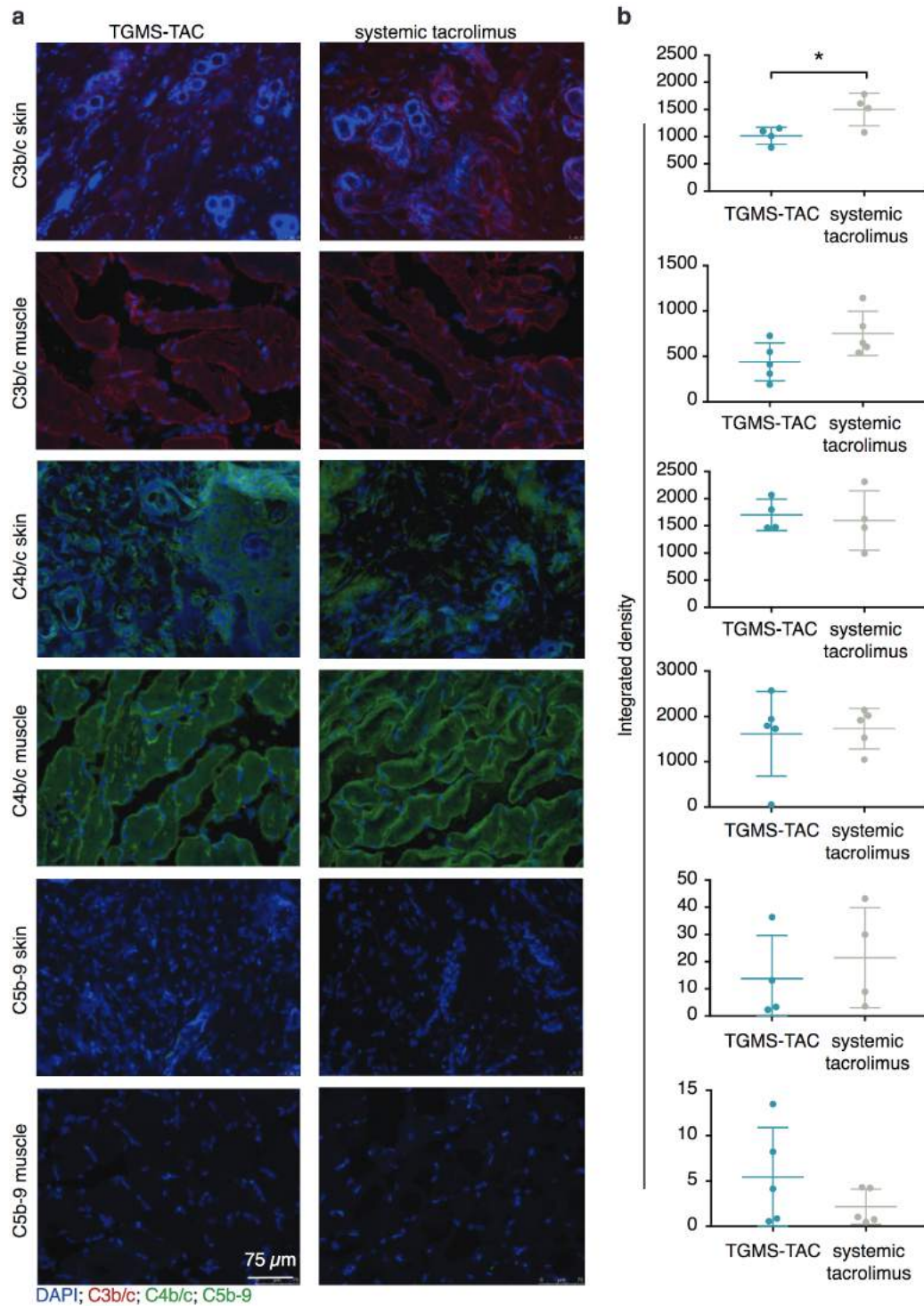
Statistical analyses were performed with Prism software (GraphPad Software Inc., La Jolla, CA, United States). Statistically significant data are presented as follows: * $P < 0.05$; ** $P < 0.01$; *** $P < 0.001$; and **** $P < 0.0001$. Tests are specifically indicated under each figure.

References to Supplementary Materials and Methods

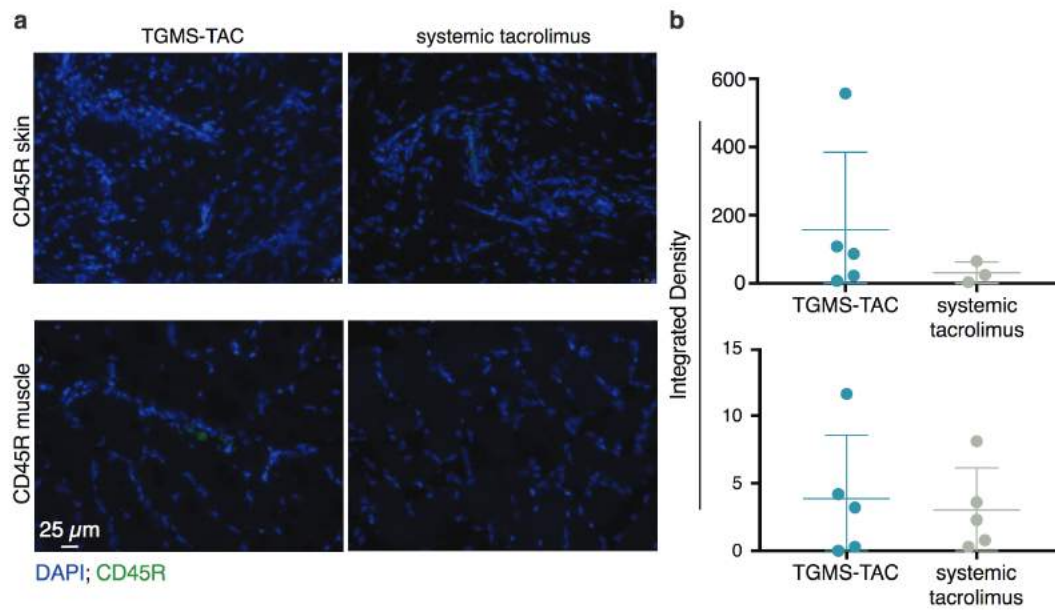
1. Gajanayake T, Olariu R, Leclere FM, et al. A single localized dose of enzyme-responsive hydrogel improves long-term survival of a vascularized composite allograft. *Sci Transl Med*. 2014;6(249):249ra110-249ra110. doi:10.1126/scitranslmed.3008778.
2. Olariu R, Denoyelle J, Leclère FM, et al. Intra-graft injection of tacrolimus promotes survival of vascularized composite allotransplantation. *Journal of Surgical Research*. 2017;218:e107-e107. doi:10.1016/j.jss.2017.05.046.
3. Sotocinal SG, Sorge RE, Zaloum A, et al. The Rat Grimace Scale: A partially automated method for quantifying pain in the laboratory rat via facial expressions. *Molecular Pain*. 2011;7(1):55. doi:10.1186/1744-8069-7-55.
4. Cendales LC, Kanitakis J, Schneeberger S, et al. The Banff 2007 working classification of skin-containing composite tissue allograft pathology. In: Vol 8. Blackwell Publishing Ltd; 2008:1396-1400. doi:10.1111/j.1600-6143.2008.02243.x.
5. Kambham N, Nagarajan S, Shah S, Li L, Salvatierra O, Sarwal MM. A Novel, Semiquantitative, Clinically Correlated Calcineurin Inhibitor Toxicity Score for Renal Allograft Biopsies. *Clinical Journal of the American Society of Nephrology*. 2006;2(1):135-142. doi:10.2215/CJN.01320406.



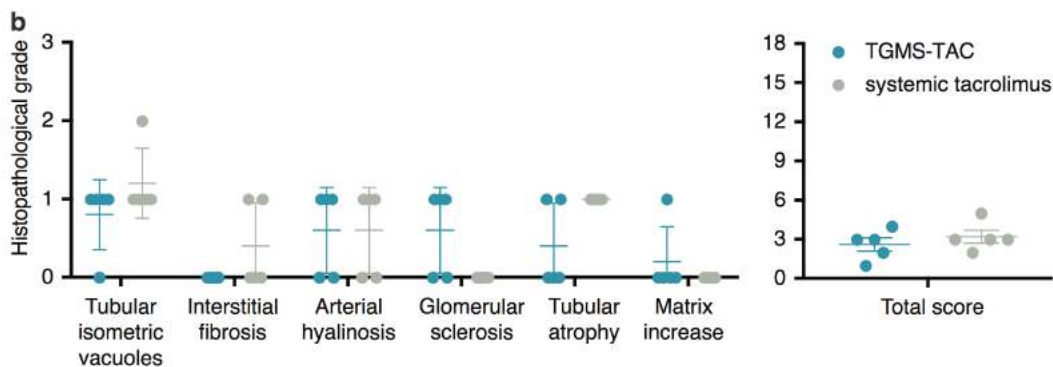
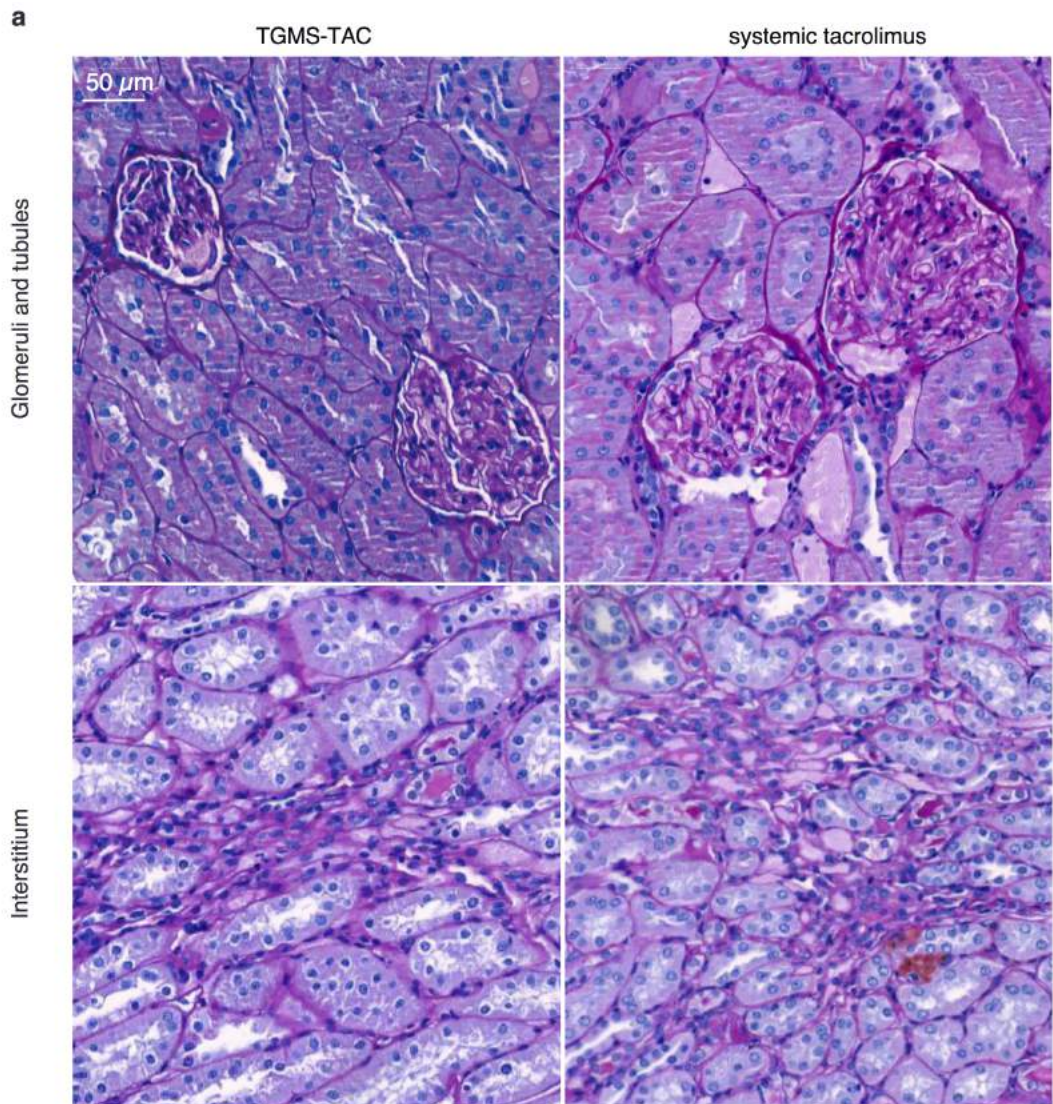
Supplementary Figure 1 Atrophy and no rejection in graft muscle. (a) Representative histological hematoxylin and eosin stained sections of graft muscle collected at POD 280 from animals treated with TGMS-TAC or systemic tacrolimus and their corresponding (b) histopathological evaluation. Data are presented as individual values, mean \pm s.d are indicated, **P<0.01 by Mann-Whitney test.



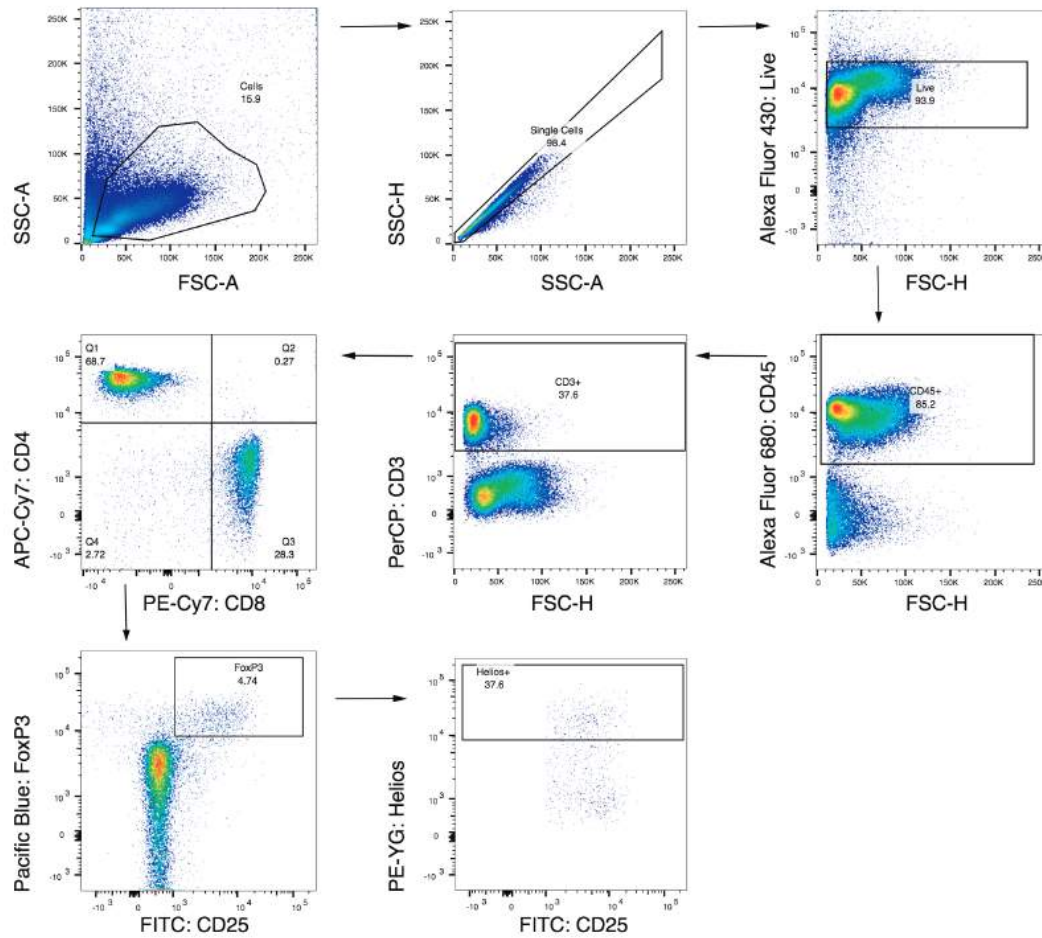
Supplementary Figure 2 No complement deposition is detectable in long-term surviving grafts. C4b/c, C3b/c, C5b-9 deposition in graft skin and muscle retrieved at POD 280 from TGMS-TAC and systemic tacrolimus treated rats. (a) Representative results of immunostained cryo-sections with DAPI (nucleus), anti-IgG and anti-IgM antibodies and (b) their corresponding quantification. Data shown as individual values, mean \pm s.d are depicted. * <0.05 by Student's t-test.



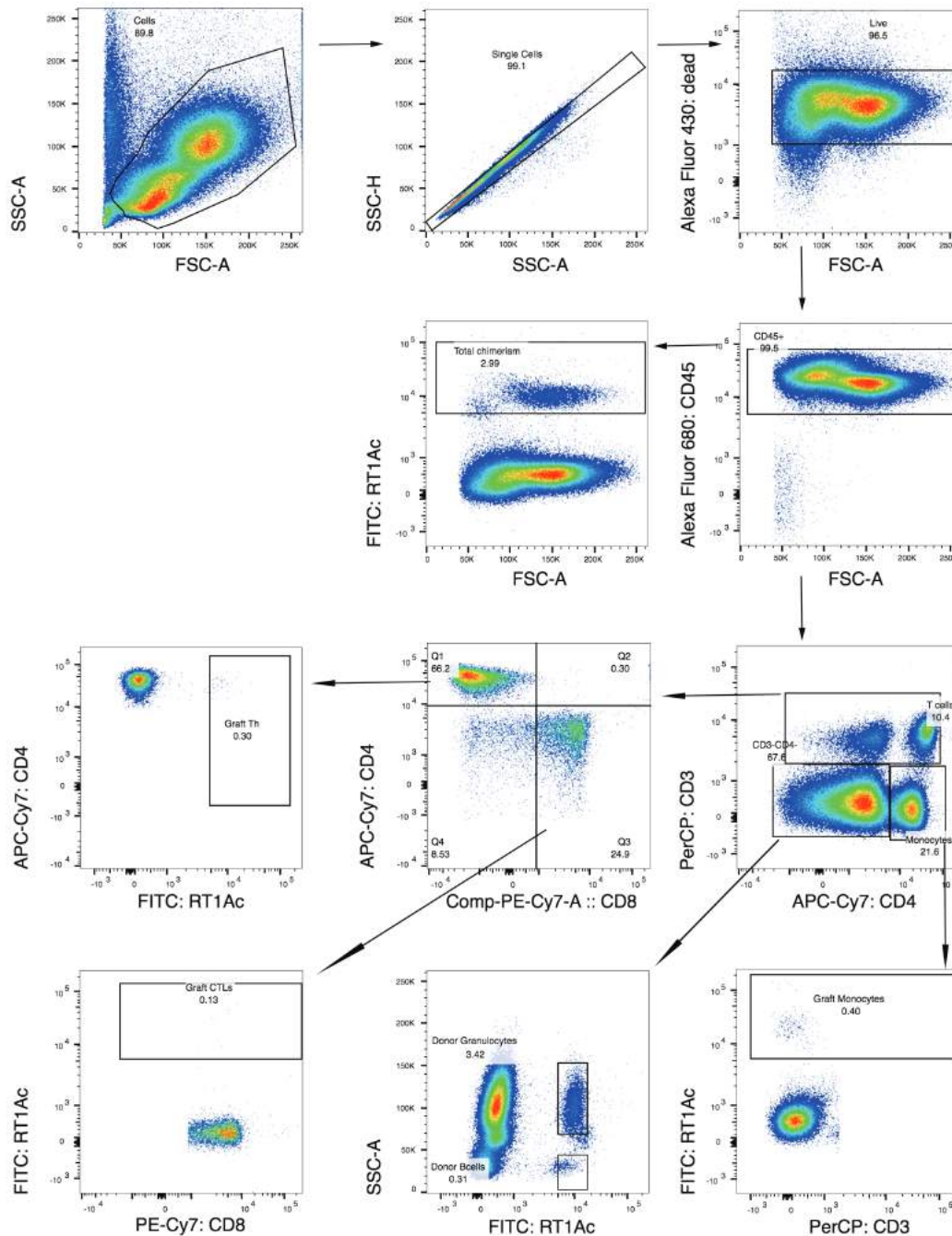
Supplementary Figure 3 No B cell infiltration is detectable in long-term surviving grafts. CD45R+ cells infiltration in graft skin and muscle retrieved at POD 280 from TGMS-TAC and systemic tacrolimus treated rats. (a) Representative results of immunostained cryo-sections with DAPI (nucleus) and anti-CD45R+ antibody and (b) their corresponding quantification in graft skin and muscle. Data shown as individual values, mean \pm s.d are depicted. Statistical analysis - Student's t-test.



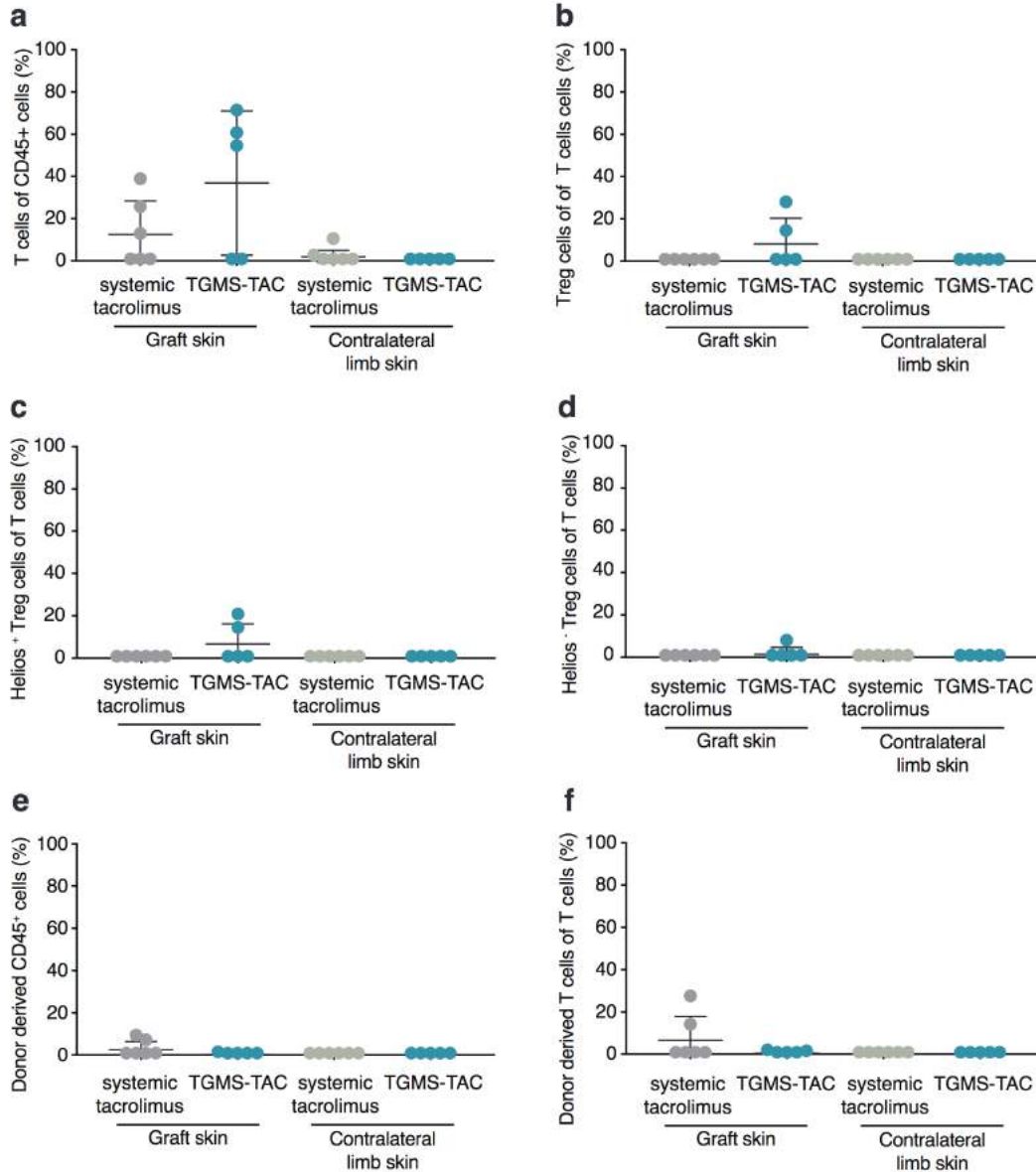
Supplementary Figure 4 Minimal damage was observed in kidney of rats from both experimental groups. (a) Representative histological Periodic acid–Schiff (PAS) stained sections of kidney at POD 280 of animals treated with TGMS-TAC or systemic tacrolimus and their corresponding (b) histopathological evaluation according to the following semiquantitative pathologic scoring system for Calcineurin Inhibitor Nephrotoxicity: Tubular isometric vacuoles, Interstitial fibrosis, Glomerulosclerosis, Tubular atrophy and Mesangial matrix increase - None - Score 0, 1 to 25% - Score 1, 26 to 50% - Score 2, >50% - Score 3; Arteriolar medial hyalinosis - None - Score 0, <10% - Score 1, 11 to 30% - Score 2, >30% - Score 3. Statistical analyses of the differences between the two groups are shown. Data are presented as individual values, mean \pm s.d. are indicated, ** $P < 0.01$, Mann-Whitney test.



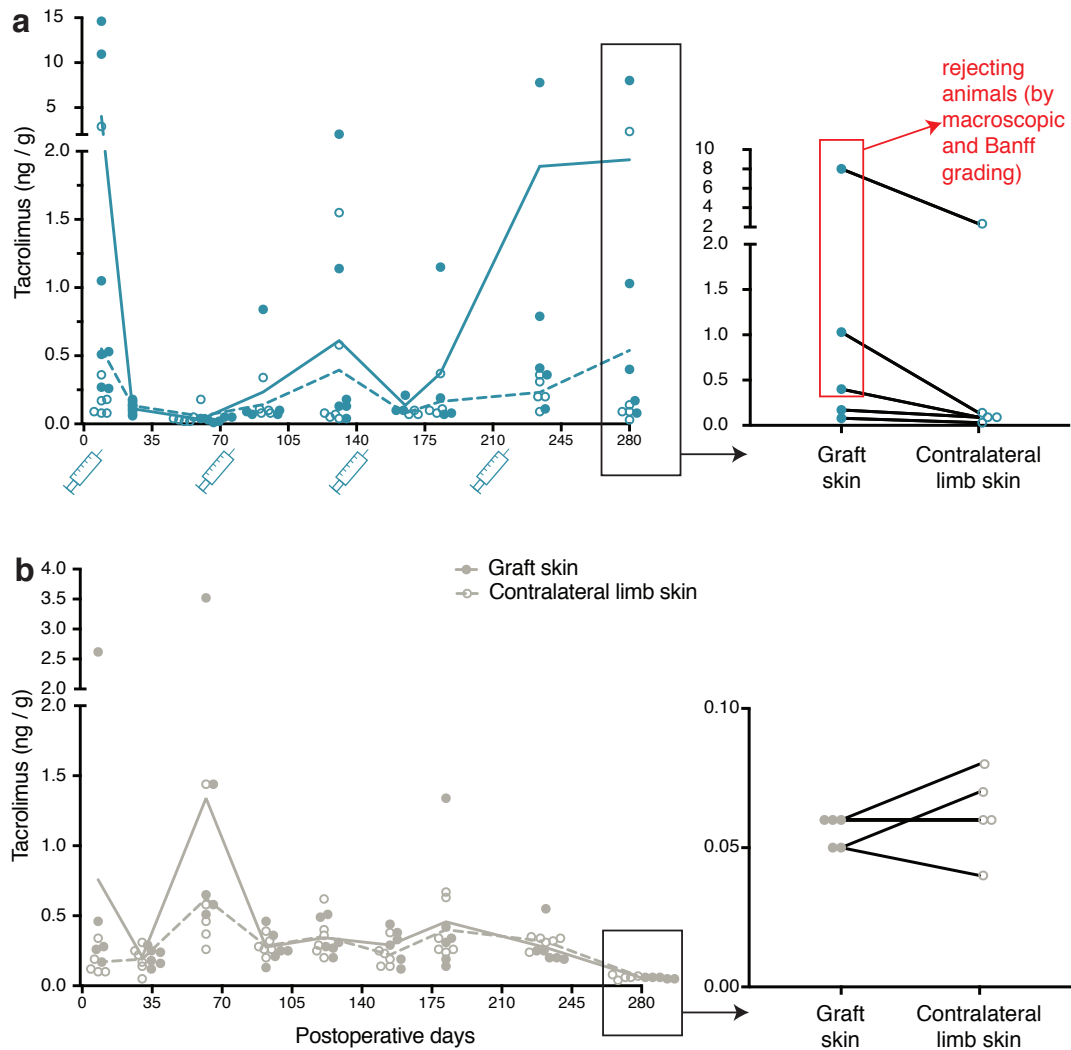
Supplementary Figure 5 Gating strategy for enumeration of Treg cells in the peripheral blood. After identification of cells by their physical parameters (i.e., forward and side scatter), single, viable (dim Viability Dye expression) CD45+ cells have been identified and gated. In the CD45+ gate, CD3+ cells have been selected and CD4+ population within them have been further investigated. Of those, FoxP3+, CD25high cells have been defined as Treg cells. Subsequently, Helios+ and Helios- Treg have been distinguished. All populations were expressed as frequency of CD45+ cells and the absolute cell number was determined using the complete blood cell count of the same blood sample. For skin analyses, due to inability to determine absolute white blood cell count, percent of parent population have been used to appreciate relative abundance of each population.



Supplementary Figure 6 Gating strategy for the analysis of chimerism in the peripheral blood of hind limb recipients. After identification of cell by their physical parameters (i.e., forward and side scatter), single, viable (dim Viability Dye expression) CD45+ cells have been identified and gated. In this gate the number of RT1Ac+ cells have been defined as “total chimerism” (i.e. all donor-derived white blood cells). CD45+ cells have been further separated by their expression of CD3 and CD4. CD3+ cells have been defined as T cells and further separated to CD4+ T helper cells and CD8+ cytotoxic T cells. CD3-CD4+ cells have been defined as monocytes. From the CD3-, CD4- cells, SSChigh have been defined as granulocytes and SSClow cells as B cells. In each of those populations RT1Ac+ cells have been defined as their donor-derived counterparts. For blood analyses, complete blood cell count has been used to determine the absolute white blood cells count, corresponding to the parent CD45+ population. All populations were expressed as frequency of CD45+ cells and the absolute cell number was determined using the complete blood cell of the same blood sample. For skin analyses, due to inability to determine absolute white blood cell count, percent of parent population have been used to appreciate relative abundance of each population.



Supplementary Figure 7 No significant changes in donor cell populations have been detected in graft skin. At sacrifice (POD 280) skin from both transplanted and contralateral native limb have been collected, minced and digested. Cells have been extracted and submitted to flow cytometric analyses, using the same antibodies and protocol from Figure 7 and 8. Total amount of T cells (a), Treg cells (b), Helios+ Treg cells (c) and Helios- Treg cells (d), as well as total donor-derived white blood cells (e) and T cells (f) have been analyzed according to the gating strategies described in supplementary figures 5 and 6. Populations have been presented as percent of their parent populations. Intragroup comparisons between graft and contralateral limb skin have been analyzed by paired Student's t-test. Intergroup comparisons between TGMS-TAC and systemic tacrolimus treated groups have been analyzed by unpaired Student's t-test.



Supplementary Figure 8. Trend towards higher tacrolimus levels in skin of transplanted limbs versus contralateral native limbs in rejecting TGMS-TAC treated animals. Tacrolimus measurements in graft and contralateral limb skin biopsies of (a) TGMS-TAC-treated and (b) systemic tacrolimus treated rats over time from Figure 4, with linear Y-axis. Zoomed in both panels are values from post-operative day 280 (endpoint). (a, zoomed-in panel) Tacrolimus levels in TGMS-TAC treated hind limbs are not significantly higher than in contralateral native limbs. However there appears to be a trend towards higher TAC skin levels in rejecting animals. (b, zoomed-in panel) No difference between TAC levels in transplanted and native limbs in systemically treated animals. TGMS-TAC re-injection time points are indicated. Data are shown as individual values and means. Individual values, when overlapping, have been manually shifted apart to left or right to increase visibility of each value.

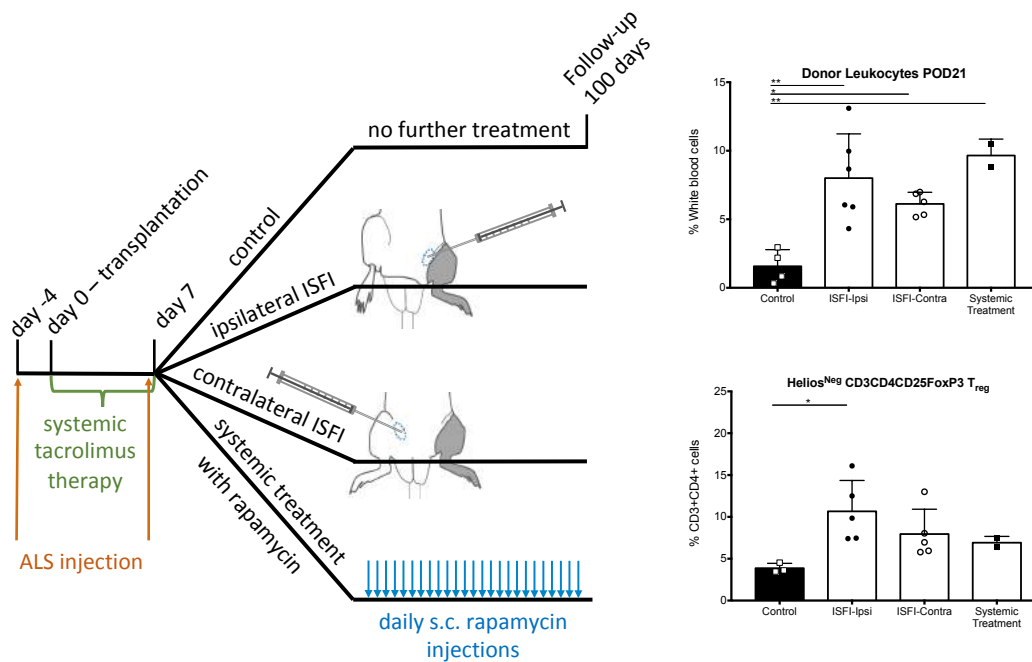
3.2. Delivery of rapamycin using in situ forming implants induces immunoregulatory mechanisms promoting vascularized composite allograft survival

Damian Sutter, M.D.^{1,2}; Dzhuliya V. Dzhonova, M.Sc.²; Cedric Bovet, Ph.D.³; Jean-Christophe Prost, Ph.D.³; Yara Banz, M.D.-Ph.D.⁴; Jean-Christophe Leroux, B.Pharm.-Ph.D.⁵; Robert Rieben, Ph.D.²; Esther Vögelin, M.D.^{1,2}; Jan Plock M.D.-Ph.D.⁶; Paola Luciani, Ph.D.^{5,7}; Adriano Taddeo, Ph.D.^{1,2*}; Jonas T. Schnider, M.D., M.B.A.^{1,2*}

¹Department of Plastic, Reconstructive and Hand Surgery, Inselspital, Bern University Hospital, University of Bern, Switzerland; ²Department of Clinical Research, University of Bern, Switzerland; ³University Institute of Clinical Chemistry, Inselspital, Bern University Hospital, University of Bern, Switzerland; ⁴Institute of Pathology, University of Bern, Switzerland; ⁵Institute of Pharmaceutical Sciences, Department of Chemistry and Applied Biosciences, ETH Zürich, Switzerland; ⁶Department of Plastic and Hand Surgery Zurich University Hospital, Switzerland; ⁷Department of Pharmaceutical Technology, University of Jena, Germany

Status: Revised version submitted to *Frontiers in Immunology*

Aim: To understand whether a single injection of rapamycin loaded in-situ forming implant (ISFI) could have immunoregulatory effects in a rat VCA model by boosting the levels of Treg and/or chimerism.



Summary: A single injection of ISFI resulted in prolonged graft survival and could induce acceptance, but not central tolerance to the graft, as evidenced by mixed lymphocyte reaction. Increased chimerism as well as increased levels of Helios⁺ regulatory T cells were observed in the animals treated with ISFI in the ipsilateral limb.

Delivery of Rapamycin Using In Situ Forming Implants Promotes Immunoregulation and Vascularized Composite Allograft Survival.

Damian Sutter^{1,2}, Dzhuliya V. Dzhonova², Jean-Christophe Prost³, Cedric Bovet³, Yara Banz⁴, Jean-Christophe Leroux⁵, Robert Rieben², Esther Vögelin^{1,2}, Jan A. Plock^{6*}, Paola Luciani^{5,7*}, Adriano Taddeo^{1,2†}, Jonas T. Schneider^{1,2,**†}**

¹Department of Plastic and Hand Surgery, Inselspital, Bern University Hospital, University of Bern, Switzerland.

²Department for BioMedical Research, University of Bern, Switzerland.

³University Institute of Clinical Chemistry, Inselspital, Bern University Hospital, University of Bern, Switzerland.

⁴Institute of Pathology, University of Bern, Switzerland.

⁵Institute of Pharmaceutical Sciences, Department of Chemistry and Applied Biosciences, ETH Zürich, Switzerland.

⁶Department of Plastic Surgery and Hand Surgery, University Hospital Zurich, University of Zurich, Switzerland.

⁷Department of Pharmaceutical Technology, Institute of Pharmacy, University of Jena, Germany.

*** Correspondence:**

Corresponding Authors:

esther.voegelin@insel.ch - jan.plock@usz.ch - paola.luciani@uni-jena.de - adriano.taddeo@dbmr.unibe.ch

[†]*These authors contributed equally to this work as senior authors*

Keywords: Vascularized Composite Allotransplantation, Immunoregulation, Drug Delivery System, Rapamycin, T_{reg}, Chimerism, In Situ Forming Implant.

Abstract

Vascularized composite allotransplantation (VCA), such as hand and face transplantations, has the potential to restore esthetic and function in patients that suffered severe injuries. However, adverse effects of chronic high-dose immunosuppression regimens strongly limit the access to these procedures in the clinic. In this study, we developed an *in situ* forming implant (ISFI) loaded with rapamycin to promote VCA acceptance. We hypothesized that the sustained delivery of low-dose rapamycin in proximity to the graft may induce an immunoregulatory microenvironment, boosting the expansion of T regulatory cells (T_{reg}) and, thus, graft acceptance. *In vitro* and *in vivo* analysis of rapamycin-loaded ISFI (Rapa-ISFI) showed sustained drug release with subtherapeutic systemic levels and persistent tissue levels. A single injection of Rapa-ISFI in the groin on the same side as a transplanted limb prolonged VCA survival with 83.3% of the rats reaching the 100 days endpoint as compared to 25.5 days graft survival of untreated rats. Treatment with Rapa-ISFI increased the levels of multilineage mixed chimerism and the frequency of Helios^{Neg} T_{reg} both in circulation and VCA-skin. Although we did not observe tolerance induction *in vitro*, a significant expansion of T_{reg} was present upon donor-specific stimulation. Our study shows that low-dose delivery of rapamycin by ISFI successfully promotes long-term acceptance of VCA inducing mixed chimerism and donor-specific T_{reg} that in turn may facilitate the establishment of peripheral tolerance. Rapa-ISFI therapy represents a promising approach for decreasing toxicity and increasing patient compliance, two of the major problems in VCA patient management. Importantly, the use of such delivery system may favor the reprogramming of allogeneic response toward regulatory function in VCA and, potentially, in other transplants and inflammatory conditions.

Introduction

Vascularized composite allotransplantation (VCA) has become a clinical reality during the last decade, and has been increasingly evaluated as a therapeutic reconstructive option for patients who have suffered extensive facial injuries or debilitating hand amputation (1). In particular, hand transplants have been successfully performed with excellent functional and esthetic outcomes by several centers around the world (2). However, long-term adverse effects of immunosuppressive treatment prevent a wider clinical application of this “life-enhancing” rather than “life-saving” procedure. Unlike solid organ transplantation, VCA offers unique opportunities for local delivery of immunosuppressive agents directly to the graft (3). We and other groups have shown that site-specific immunosuppression can be successfully used in VCA employing topical FK506 (4,5) and clobetasol (5), hydrogel-based drug delivery systems laden with FK506 (6), intra-graft injections of FK506 (7), and biodegradable disks containing FK506-loaded microspheres (8). All these approaches aim to reduce systemic exposure and global collateral or end-organ adverse effects while maintaining therapeutic levels in the different tissues of the grafts, especially skin.

Importantly, drugs administered directly into the graft may not only reduce potential side effects but also directly influence the magnitude and nature of an allogeneic immune response by promoting immune-regulation and tolerance through the expansion of donor-specific regulatory T cells (T_{reg}) (9). Indeed, accumulating evidence suggests that graft rejection is ultimately determined by the balance between allo-aggressive T cells and allospecific T_{reg} enabling donor-specific tolerance (10). Hence, several groups have focused their efforts on optimizing therapeutic protocols aimed at inducing allospecific T_{reg} for promoting transplant tolerance.

Rapamycin is a macrolide antibiotic structurally similar to FK506. It binds to FK506 Binding Protein-12 and affects the G1 phase of the cell cycle by acting on a unique cellular target called mammalian target of rapamycin (mTOR) (11). Recently, it has been demonstrated that, in contrast to cyclosporine and FK506, rapamycin can promote differentiation of T_{reg} both *in vivo* and *in vitro* while blunting Th17 differentiation and function (12-15). Moreover, a significant increase in T_{reg} numbers has been reported in kidney transplant patients under rapamycin therapy when compared to treatment with calcineurin inhibitors (15-19).

In this study, we developed an innovative drug delivery system that combines the advantage of *in situ* delivery with the potential to induce local immune-regulation and thus transplant survival. To this aim, we designed a solvent-induced phase inversion *in situ* forming implant (ISFI) using the US Food and Drug Administration approved polymer *poly(D,L-lactic-co-glycolic acid)* (PLGA). We loaded this ISFI with the immunoregulatory drug rapamycin and

injected it in close proximity to the transplant. We hypothesized that sustained low-dose delivered rapamycin may promote graft survival with minimal immunosuppression through the induction of immunoregulatory mechanisms such as T_{reg} expansion and increased chimerism levels.

Materials and Methods

Preparation and evaluation of rapamycin-loaded in situ forming implant (ISFI)

We developed a rapamycin-loaded *in situ* forming implant (Rapa-ISFI) analogous to the Atrigel® delivery system for long-term regional release (20,21). To this aim, rapamycin (5 mg, LC Laboratories, Woburn, MA, USA) was dissolved in 0.31 mL N-methyl-2-pyrrolidone (NMP, Sigma-Aldrich Chemie GmbH, Buchs, Switzerland) prior to being added to poly(D,L-lactic-co-glycolic acid) (PLGA, Resomer® RG 502, 50:50 mol% lactide/glycolide, 7-17 kDa, Sigma-Aldrich) at a final concentration of 45% (w/v) PLGA. The resulting viscous ISFI was transferred into 1 mL syringe and injected within 24h. The release kinetics of the implant were evaluated *in vitro* and *in vivo* (detailed information are provided in the *Supplementary material* for details).

Animal experiments

Inbred Lewis (recipient) and Brown Norway (donor) rats (all male) weighing between 200 g and 250 g were purchased from Charles River (Sulzfeld, Germany). All animals were housed in Specific Pathogen Free (SPF) conditions in cages of 2-4 rats with water and food ad lib. Animal experiments were performed in accordance with the terms of the Swiss animal protection law and were approved by the Animal Experimentation Committee of the Canton of Bern, Switzerland. Experimental protocols were refined according to the 3R principles and state-of-the-art anesthesia and pain management were used to minimize the number of animals and to reduce the exposure of the animals to stress and pain during the experiments.

Experimental design

To evaluate the clinical efficacy of the therapy in a VCA model. Brown Norway-to-Lewis hind limb transplantations were performed as described previously with modifications(6). Anti-lymphocyte serum (ALS) was injected 4 days before and 1 day after transplantation at 0.5 mL/rat intraperitoneally. The success of the ALS induction therapy was monitored by measuring the number of leukocytes in the peripheral blood on the day of transplantation. Rats with a leukocyte count lower than 2500 cells/ μ L of blood were used as recipients of hind limb transplants. After hind limb transplantation, animals were treated

with FK506 for 6 days (0.5 mg/kg subcutaneously) to bridge the time until complete wound healing to prevent impaired wound-healing caused by rapamycin(22,23). On day 7, animals were divided into 4 groups: Group 1 was left untreated (Control, n=6); Group 2 received an ISFI loaded with 5 mg of rapamycin subcutaneously into the groin of the transplanted limb (ISFI-Ipsilateral, n=6) and Group 3 into the groin of the contralateral limb (ISFI-Contralateral, n=6) (Supplementary Figure 1). Group 4 received daily injections of 0.5 mg/kg rapamycin subcutaneously (Systemic treatment, n=5). Clinical rejection was graded macroscopically and rats were sacrificed either once grade 3 rejection was reached or on day 100, which was defined as the endpoint. Rapamycin levels were measured in 1) blood at different time points, 2) skin-biopsies retrieved from the graft on postoperative day (POD) 21 and 49 and 3) skin, fat pad, muscle of the graft and of the contralateral side at the end of the experiment. To analyze the importance of ALS therapy in the therapeutic protocol, eight Lewis rats with unsuccessful ALS depletion (*i.e.*, blood leukocyte count higher than 7500 cells/ μ L, after the first ALS injection) underwent hind limb transplantation and were treated as described for Group 2 (*i.e.*, FK506 bridge therapy, Rapa-ISFI-ipsilaterally on day 7). Graft-versus-host disease (GvHD) was assessed macroscopically, by mixed lymphocyte reaction (MLR), and by analyzing the number and origin of infiltrating lymphocytes into injured sites by flow cytometry. Detailed material and methods are available in the *Supplementary material*.

Flow cytometry analysis of chimerism and T regulatory cells

EDTA-2K whole blood was collected and red cells were lysed using erythrocyte lysis buffer (eBioscience, Vienna, Austria). Cells were then stained with Fixable Viability Die eFluor 506 (eBioscience), washed and incubated with anti-rat fluorochrome-conjugated antibodies against CD3, CD8 (Miltenyi Biotec GmbH, Bergisch Gladbach, Germany), CD4 and CD25 (eBioscience) or the Brown Norway specific marker RT1Ac (MHC Class I, clone MCA 156/OX-27, AbD Serotec, Kidlington, UK). For T_{reg} staining, cells were fixed after extracellular staining and permeabilized using the FoxP3/Transcription Factor Staining Buffer Set (eBioscience) and incubated with anti-FoxP3 (eBioscience) and anti-Helios (Miltenyi) antibodies. After wash, cells were analyzed by flow cytometry using a SORP LSRII flow cytometer (BD Biosciences, San Diego, CA, USA) and BD Diva Software. Data were analyzed using FlowJo software (Tree Star, Ashland, OR, USA). Positivity for the RT1Ac marker was determined using cells from naïve Lewis rats as negative controls. Fluorescence minus one (FMO) controls were used to set the cut-off for the T_{reg} analysis. Skin (dermal and epidermal tissue), ear and tongue were collected and subcutaneous fat and hairs were carefully removed. Tissue was thoroughly minced in small pieces and incubated in DMEM (Thermo Fisher Scientific, Waltham, MA, USA)

containing 10% FBS (Thermo Fisher) and 1 mg/mL Dispase (StemCell Technology, Vancouver, Canada) overnight at 4 °C in agitation. Tissue was washed with DMEM medium (Thermo Fisher) and digested with DMEM containing 10% FBS, 1 mg/mL Collagenase D (Roche, Basel, Switzerland) and 200 µg DNase I (Sigma-Aldrich) for 1h at 37 °C in agitation. After filtration of the resulting single cell suspension through 40 µm cell strainers, cells were washed and mononuclear cells were isolated using Ficoll Separation Media (GE Healthcare, Europe GmbH, Switzerland). Isolated cells were processed for flow cytometry as described above. CD4 and CD8 expression was partially lost due to the digestion step. Therefore, in the tissue T_{reg} cells were identified as CD3⁺FoxP3⁺ cells.

Mixed lymphocyte reaction

MLR was performed as previously described with minor modification (24). Briefly, responder cells were isolated from peripheral blood of long-term survival animals and stained with 5 µM carboxyfluorescein succinimidyl ester (CFSE, Thermo Fisher). Stimulator cells were isolated from spleens of donor (Brown Norway) or third party rats (Wistar) using gently passing/mincing methods. Stimulator cell proliferation was blocked using 30Gy gamma-irradiation. After extensive washing, responder and stimulator cells were mixed in 1:1 ratio and incubated for 5 days in DMEM, 10% FBS, 1% PenStrep (Thermo Fisher) and 0.05 mM 2-mercaptoethanol (Sigma-Aldrich). Responder cell without stimulation (unstimulated control) were used as control of basal cell proliferation. After 5 days, cells were stained as described before for T_{reg} staining and analyzed by flow cytometry. Proliferation index was determined using FlowJo software. Stimulation Index (SI) was calculated by dividing the proliferation index of allogeneic combinations by those of unstimulated control.

Statistical Analysis

Statistical analysis was performed using the GraphPad Prism version 7. Unless noted otherwise, the results are expressed as means±SD. Survival of the allografts was examined using Kaplan-Meier analysis, and groups were compared using the log-rank test. Two-tailed *t* test was used to compare two groups, one-way ANOVA with Tukey's multiple comparisons test was used to compare means of more than 2 groups and one-way ANOVA with Dunnett's multiple comparisons unpaired test was to compare treatment groups (Groups 2-4) to the untreated group (Group 1). Paired or unpaired tests were used when appropriate as reported in the figure legend. Correlation was measured using Spearman's (rank) correlation. Significance was defined as *p*<0.05. Rats developing lethal GvHD in Group 4, were excluded from the chimerism and T_{reg} analysis. Moreover, considering that some sample was lost due to technical

problem during sample preparation, N number and scatter plot were show for all the figures. Significance was defined as $p < 0.05$.

Results

Design and drug release properties of ISFI

Rapa-ISFI loaded with 5 mg rapamycin were formulated and tested *in vitro* and *in vivo*. A schematic representation of the ISFI is presented in Figure 1A. The *in vitro* release kinetics showed a small initial burst during the first 24 h, which could be attributed to the release of the drug during implant formation and to the surface associated drug. The diffusion was then controlled for about 9 days after which the release rate transiently increased. $6.04 \pm 0.96\%$ of the drug was release during these 9 days burst-release. This is typical of PLGA implant and attributed to the bulk degradation of the system (25,26). From day 10 until the end of the experiment (ca. 1 month) the release rate was sustained at $9.51 \pm 2.07 \mu\text{g/d}$ (Mean \pm SEM) (Figure 1B). *In vivo* studies in naïve rats showed a release pattern comparable to the *in vitro* results. A burst release was observed within the first 24 h, reaching a blood concentration of $27 \pm 4 \text{ ng/mL}$. Systemic levels decreased gradually reaching levels below 5 ng/mL within 11 days. Thereafter, subtherapeutic systemic levels (range $1.8\text{-}1.5 \text{ ng/mL}$) were measurable up to 48 days (Figure 1C).

Rapamycin-loaded ISFI promote VCA survival.

To assess the effects of Rapa-ISFI treatment on the survival of a fully MHC-mismatched VCA, we performed Brown Norway-to-Lewis hind limb transplantation. The experimental protocol is shown in Figure 2A. Untreated hind limb allografts (Group 1, control) were rejected with 25.5 days median survival time (MST). In Group 2 (Rapa-ISFI injected on the ipsilateral side), 83.3% of the rats reached POD100 with an allograft MST >100 days ($p = 0.0007$ versus Group 1) (Figure 2B). Within Group 2, one rat rejected at POD32; one rat progressed to grade 2 rejection at POD28 and remained in this stage until the endpoint; two rats showed grade 1 rejection at POD21 followed by spontaneous resolution of the rejection episode; one rat showed no signs of rejection during the experiment (Supplemental Figure S2). Injection of Rapa-ISFI into the contralateral limb significantly prolonged graft survival with 50% of the rats reaching POD100 and a MST of 76.5 days ($p = 0.007$ versus Group 1 and $p = 0.33$ versus Group 2) (Figure 2B). In this group, three rats rejected their limbs; one rat showed a grade 2 rejection episode at POD30 that reverted to grade 0 at POD73 and the other two rats showed no signs of rejection during the entire experiment (Supplementary Figure 2). In the group treated with daily injection of rapamycin (Group 4, systemic treatment), 3 out of 5 rats

(60%) developed clear signs of acute GvHD and had to be sacrificed between POD33 and 41. The other two rats (40%) reached the endpoint without signs of GvHD or graft rejection. Median graft survival time was 100 days, significantly higher than control animals ($p=0.0295$ versus Group 1) and without significant differences as compared to Rapa-ISFI-treated animals (Figure 2B). However, general animal survival of Group 4 was 41 days, due to GvHD development. Specifically, macroscopic signs of GvHD started to appear around POD21 and included ear dermatomyeloma, diarrhea and tongue lesions. To further confirm the development of GvHD, we analyzed injured ears and tongues by flow cytometry, revealing infiltration of donor T cells in GvHD lesions (Supplementary Figure 3). Moreover, in these animals, we observed donor-specific hyporesponsiveness but normal response to third party stimulation at POD21 in an *in vitro* MLR assay (Supplementary Figure 4).

Histological grading of rejection based on the Banff working classification (27) confirmed the macroscopic findings. As compared to rats of Group 1, we observed a significant reduction of Banff score in rats from Group 2, with reduction of lymphocyte infiltration, tissue necrosis and vascular pathology (Figures 3A and B). Conversely, allografts from Group 3 showed a significant reduction only of tissue necrosis. Finally, in the two rats of Group 4 without GvHD we observed minimal tissue damage with only moderate lymphocytic infiltration. Muscle histopathology revealed only mild tissue damage upon rejection with minimal leukocyte infiltration and muscle necrosis and/or muscle atrophy. Rapamycin-treated allografts presented a tendency to reduced muscle pathology as compared to untreated rats (Supplementary Figure 5).

Rapamycin levels in hind limb transplanted rats.

As shown in Figure 4A, systemic daily injections of rapamycin (Group 4) generated an average trough concentration of 17.3 ± 3.9 ng/mL of drug (range 12.9-23.3 ng/mL). In transplanted animals that received a Rapa-ISFI, we observed an initial burst release of rapamycin with systemic blood levels at POD8 of 34.7 ± 10.4 and 31.8 ± 5.5 ng/mL in Groups 2 and 3, respectively ($p=0.6351$, by unpaired *t* test). After this, the levels decreased to 4.5 ± 1.0 and 3.3 ± 0.8 ng/mL at POD23 (Group 2 and 3, respectively, $p=0.0746$) and remained constant until POD58. Afterwards, the levels dropped below the quantification limit (*i.e.* 1.5 ng/mL).

In order to measure the tissue levels of rapamycin in the transplant, skin biopsies were analyzed at POD21, 49 and 100 in Groups 2 and 3. The injection of an ISFI either in the ipsilateral or in the contralateral limb generated VCA-skin concentrations of 0.06 ± 0.2 and 0.05 ± 0.02 ng/mg of tissue, respectively at POD21 ($p=0.7729$). The levels reached 0.07 ± 0.04 and 0.06 ± 0.04 ng/mg of tissue at POD 49 ($p=0.8547$), and then at endpoint dropped to 0.01 ± 0.01 and 0.01 ± 0.01 ng/mg, respectively (Figure 4B).

At the endpoint, skin, muscle and fat-pad tissues from the transplanted side and the contralateral side were recovered and analyzed for rapamycin concentrations. Similar levels of rapamycin were observed in skin and muscle (Figure 4C) of rats injected with Rapa-ISFI, independent of the Rapa-ISFI injection site (i.e. Groups 2 and 3) and tissue collection site (i.e. transplanted or contralateral limb). Fat pad levels showed high variation in the transplanted side of Group 2 but they were not significantly different as compared to Group 3. In the contralateral fat pad, values were similar in Groups 2 and 3. Systemically treated rats (Group 4) had uniform rapamycin tissue concentrations (average among the tissues was 0.48 ± 0.22 ng/mg) with no significant difference between tissues retrieved from the transplanted or contralateral side. However, skin and muscle tissue levels were significantly higher as compared to Groups 2 and 3 (Figure 4C).

Rapamycin treatment promotes multilineage mixed chimerism.

To verify whether Rapa-ISFI treatment influenced the levels of mixed chimerism, we measured the frequency of donor cells in the peripheral blood of recipient rats at different time points by flow cytometry (Supplementary Figure 6). At first, we focused our analysis on POD21, which allows for comparison of all 4 groups two weeks after the end of the bridging therapy and the start of specific treatments. As shown in Figure 5A, treatment with rapamycin in Groups 2, 3 and 4 was associated with higher frequency of RT1Ac⁺ donor cells in the peripheral blood at POD21 as compared to untreated rats ($8.0 \pm 3.2\%$, $6.1 \pm 0.5\%$ and $9.1 \pm 1.9\%$ vs $1.6 \pm 1.2\%$ of white blood cells, respectively). More specifically, we observed an increased frequency of donor granulocytes in all the groups treated with rapamycin and of monocytes in rats treated with Rapa-ISFI while no significant difference was observed in the frequency of donor T helper, T cytotoxic or B cells. In surviving rats, the percentage of donor leukocytes slightly decreased after POD21 but donor leukocytes were detectable until the endpoint (Figure 5B). Interestingly, in Groups 2 and 3, the frequency of donor granulocytes and monocytes decreased to undetectable levels, whereas the frequency of donor T helper and cytotoxic cells increased over time until the endpoint. The two long-term survival recipients of Group 4 showed a stable level of chimerism with decreased frequency of donor granulocytes only. As shown in Figure 5C, a significant correlation was found between graft-survival and the frequencies of donor leukocytes ($r=0.51$, $p=0.04$), in particular granulocytes ($r=0.61$, $p=0.01$) and monocytes ($r=0.65$, $p=0.006$), measured on POD21.

Induction therapy is needed to achieve high chimerism levels and long-term VCA survival

In order to understand the importance of ALS induction therapy to promote long-term VCA survival with Rapa-ISFI, in a new set of experiments we performed hind limb transplantation in recipients with unsuccessful ALS induction therapy. Rats were treated with bridging therapy and injection of Rapa-ISFI on the transplanted side at POD7 as described for Group 2. In rats with unsuccessful induction therapy, graft MST was 27.5 days, which is significantly shorter than rats of Group 2 (*i.e.*, MST >100 days, $p=0.007$) (Figure 6A). Moreover, the levels of multilineage chimerism in the blood were lower at POD21, with a significant reduction in the frequency of donor granulocytes (Figure 6B).

Rapa-ISFI treatment promotes the expansions of T regulatory cells

The frequency of circulating T_{reg} ($CD3^+CD4^+CD25^+FoxP3^+$), $Helios^{Pos}$ and $Helios^{Neg} T_{reg}$ was analyzed in the peripheral blood starting from POD21 (Supplementary Figure 7). As shown in Figure 7A, when compared to Group 1, rats of Group 2 had significantly higher frequency of T_{reg} in the peripheral blood ($p=0.044$), rats of Group 3 also had higher frequency of T_{reg} but it did not reach statistical significance ($p=0.145$) and rats of Group 4 had unchanged T_{reg} frequency. Notably, the injection of Rapa-ISFI on the transplanted side promoted the expansion of $Helios^{Neg}T_{reg}$, without affecting the frequency of $Helios^{Pos}T_{reg}$. Correlation analysis between the frequency of T_{reg} at POD21 and graft survival time showed a significant correlation ($r=0.71$, $p=0.006$). Specifically, the survival time correlated with the frequency of $Helios^{Neg} T_{reg}$ ($r=0.59$, $p=0.001$) and not with the frequency of $Helios^{Pos}T_{reg}$ (Figure 7B). The frequency of T_{reg} did not change significantly during the study and at POD100 the frequency of $Helios^{Neg}T_{reg}$ was similar to that at POD21 (Supplementary Figure 8).

At the time of rejection, the frequency of T_{reg} was analyzed in VCA skin of all rats after tissue digestion (Supplementary Figure 9). As shown in Figure 7C, rats from Group 2 showed a significant increase in the frequency of $Helios^{Neg}T_{reg}$ in the transplanted skin as compared to untreated rats (9.68 ± 2.8 vs $2.12\pm 0.6\%$, respectively; $p=0.007$). Notably, rats that rejected their grafts before the endpoint in Groups 2 and 3 presented lower frequency of $Helios^{Neg}T_{reg}$ in the skin (frequency was 5.45% in the rejecting rat of Group 2 and $4.35\pm 3.82\%$ in the three rejecting rats of Group 3).

Donor stimulation expands Treg in Rapa-ISFI treated rats in vitro

In order to assess the induction of donor specific tolerance, PBMC were isolated at POD100 and the T cell proliferative response to donor or third-party

antigens was assessed *in vitro* by MLR. In rats of Groups 2 and 3, stimulation index of CD4⁺ T lymphocytes in response to donor splenocytes (Brown-Norway) was not significantly different as compared to third-party (Wistar) stimulation (Figure 8A). However, in rats receiving Rapa-ISFI ipsilaterally the percentage of CD4⁺ T cells expressing FoxP3 significantly increased in response to donor antigens as compared to unstimulated controls while this frequency did not change in response to third party stimulation (14.2±7.7%, 1.7±1.1% and 6.2±2.3%, respectively, Figure 8B). The majority of the CD3⁺CD4⁺FoxP3⁺ cells were seen in the proliferating fractions. We did not observe T_{reg} expansion in PBMC isolated from surviving rats treated with Rapa-ISFI on the contralateral side.

Discussion

Rapa-ISFI as effective drug delivery system for site-specific immunosuppression in VCA

In this study, we investigated a biodegradable ISFI loaded with the immunoregulatory drug rapamycin to deliver low-dose immunosuppression and promote acceptance of VCA grafts by immunoregulatory mechanisms. Rapa-ISFI forms a drug depot that gradually releases rapamycin both *in vitro* and *in vivo*. The implant is simple to apply *via* subcutaneous injection and extends delivery times with systemic levels of the drug of about 30 ng/mL for the first 24h and subtherapeutic systemic levels for up to 50-60 days. Compared to other drug delivery vehicles such as nanoparticles, microspheres, liposomes or hydrogels, the ISFI can easily be surgically explanted should the need arise.

When used in a VCA model, the ipsilateral injection of Rapa-ISFI promoted graft survival for >100 days. This is in line with the results achieved by other drug delivery systems such as FK506-loaded hydrogels (6) or biodegradable disks containing FK506-loaded double-walled microspheres (8), confirming that *in situ* delivery of immunosuppressive drugs is a feasible and promising approach in VCA. However, in contrast to FK506 hydrogels, ISFI presented a limited burst release that remained in the clinically relevant range. Moreover, systemic concentrations reached subtherapeutic levels one week after injection and were measurable until POD58 whereas tissue levels were measurable until POD100, demonstrating a lower systemic drug exposure and higher tissue concentrations than FK506 disks (8).

Local rapamycin delivery to induce immunoregulatory mechanisms

Besides the development of innovative drug delivery systems for site-specific immunosuppression, the possibility to induce immunological graft tolerance (e.g. by promoting chimerism and/or expansion of regulatory cells) has been investigated as a potential solution for minimizing immunosuppression-related complications in VCA (28,29). In this study we argue that these two strategies may be combined. Thanks to a smart selection of the drug, the delivery system and the injection site we may delivery reduced but effective immunosuppression and promote immunoregulation and graft tolerance.

We show that sustained low-dose delivery of rapamycin by Rapa-ISFI could promote significantly higher levels of chimerism of both lymphoid and myeloid lineages in all at POD21. At this time, the levels of myeloid chimerism were elevated and positively correlated with graft survival, suggesting that initial high levels of donor granulocytes and monocytes may correlate with the engraftment of donor pluripotent hematopoietic stem cells (HSC) as recently demonstrated in mice receiving HSC transplantation after antibody-mediated clearance of recipient HSC (30-32). Importantly, donor T cell levels, although low at the beginning of treatment, increased with time, reaching the highest values at the endpoint in all rapamycin-treated groups, further confirming the capacity of rapamycin to promote engraftment of donor HSC and therefore graft survival (33).

Additionally, our study clearly shows that low-dose delivered rapamycin by ISFI induced T_{reg} cells in the peripheral blood and in VCA-skin. The capacity of rapamycin to induce T_{reg} alone or in combination with other treatments has been extensively reported (30-32). We demonstrated that the frequency of T_{reg} in blood and VCA-skin correlated with the promotion of graft survival. Notably, Rapa-ISFI treatment specifically promoted the expansion of $Helios^{Neg}T_{reg}$, as recently reported in a nonhuman primate model of kidney transplantation with rapamycin-only treatment or in combination with anti-CD28 therapy (33). It was previously proposed that Helios expression is restricted to thymus-derived natural T_{reg} (nT_{reg}) distinguishing them from peripheral T_{reg} (pT_{reg}) (34). Therefore, the accumulation of $Helios^{Neg}T_{reg}$ can be seen as a direct expansion of pT_{reg} . In line with this idea, the majority of the circulating and skin-resident T_{reg} were $Helios^{Neg}$ and the majority of thymus T_{reg} were $Helios^{Pos}$ in our model (unpublished observation), confirming a good correlation of this marker with pT_{reg} . However, recent studies excluded the value of Helios as a marker of nT_{reg} and proposed that $Helios^{Neg}T_{reg}$ may have an unstable but normal suppressive function (35-38). We believe that the two hypotheses are not mutually exclusive and that Rapa-ISFI can promote the generation of $Helios^{Neg} pT_{reg}$ with reduced stability, which accumulate in VCA-skin inducing peripheral graft tolerance. Accordingly, in the MLR experiment we observed a normal proliferating response to donor stimulation but a significant expansion of

donor specific T_{reg} in rats of Group 2, similar to what has been reported in rapamycin-treated human MLR (39). The stability of the peripheral tolerance mediated by $Helios^{Neg}T_{reg}$, especially after infection or by-stander activation (40,41), remains unclear and deserves further investigation.

Interestingly, the use of systemic rapamycin promoted similar mechanisms, apart from an evident induction of T_{reg} cells. However, lethal GvHD occurred in 60% of the rats treated with systemic rapamycin although drug systemic levels remained within the recommended therapeutic window (*i.e.* 10-20 ng/mL for regimens without calcineurin inhibitors(42)). Development of GvHD is rare after VCA and it has been reported mainly after recipient irradiation and bone marrow transplantation (43). Notably, rats treated with systemic rapamycin showed the highest levels of mixed chimerism, while unsuccessful induction therapy was associated with lower chimerism levels and lower graft survival. This suggests that a combination of systemic application of rapamycin with immunodepletive agents may promote an excessive engraftment of donor cells and thus development of GvHD. Conversely, Rapa-ISFI treatment did not induce GvHD, likely due to the lower rapamycin dose and lower systemic levels. Therefore, site-specific delivery of mTOR inhibitors may promote a better balance between multilineage mixed chimerism and GvHD development. Accordingly, also the contralateral injection of Rapa-ISFI prolonged graft-survival and induced multi-lineage chimerism without any signs of GvHD. However, as compared to injection on the transplanted site, contralateral Rapa-ISFI injection was less efficient in terms of induction of pT_{reg} , resembling the response of systemic rapamycin treatment. This suggests that the injection on the ipsilateral side may promote stronger immunoregulation due to the co-presence of rapamycin and abundant donor-antigens, especially in the draining lymph nodes. This may shift the lymph node and local microenvironment toward regulatory function, driving donor-specific peripheral tolerance. Although we did not specifically look to lymph node response in this study, this hypothesis is supported by recent findings clearly showing that co-delivery of the antigen with rapamycin can be used to induce antigen-specific immunological tolerance in peripheral lymph nodes (44,45). Further studies will be necessary to definitively prove this hypothesis.

Study limitations

The main limitation of this study is the lack of functional proof that the expansion of T_{reg} and the increased chimerism levels may directly control alloreaction promoting graft survival. It is a well-established paradigm that a balance of T_{reg} over T effector cells determines immune tolerance in transplantation (10,46). Similarly, it is clear that establishment of chimerism, even transient, can lead to tolerance induction in animal models and kidney-transplanted patients. An important question posed by our experiment is

whether the Rapa-ISFI induced pT_{reg}, would be able to specifically inhibit alloreaction. We did not specifically address this question, however the literature reports that T_{reg} isolated from rapamycin-treated MLR specifically inhibited newly prepared MLR assays and concurrently recruited more autologous responder T_{reg} (39,48). Similarly, T_{reg} accumulating in the periphery of long-term survivors with self-resolving acute rejection episodes receiving IL2 fusion protein showed donor-specific suppression *in vitro* (49). Therefore, we believe that Rapa-ISFI-induced donor-specific pT_{reg} may indeed control alloresponse in the periphery. Other limitations of the study are the limited observation time and the lack of a secondary donor skin graft to assess the capacity of the pT_{reg} to inhibit donor-specific response to a secondary *in vivo* challenge. The normal T cell proliferating response in the MLR assay and the observation of rejection episodes in Rapa-ISFI-treated rats suggest that the secondary challenge would be likely rejected, also due to by-stander activation secondary to surgical trauma. However, the recently proposed possibility that “memory of regulation” can dominate over memory of “infection-triggered rejection”(41) deserves further verification, and it will be explored in additional studies.

Conclusions

In this study we have developed a new therapeutic protocol combining induction regimens and regional delivery of rapamycin by ISFI. We showed that local drug delivery of immunosuppressive drugs could be used not only to promote less toxic immunosuppressive protocols increasing patient compliance, but also to favor the reprogramming of the local response toward regulatory function. Moreover, we provide evidence that delivery of rapamycin using an ISFI promotes immunoregulatory mechanisms such as establishment of multilineage chimerism and donor-specific pT_{reg}, which may facilitate the induction of peripheral tolerance resulting in long-term VCA survival.

Abbreviations:

GvHD: Graft-versus-Host Disease; HSC: Hematopoietic Stem Cells; ISFI: In Situ Forming Implant; MLR: Mixed Lymphocyte Reaction; MMF: Mycophenolate Mofetil; MST: Median Survival Time; mTOR: Mammalian Target of Rapamycin; NMP: N-methyl-2-pyrrolidone; nTreg: Natural T regulatory cells; PBMC: Peripheral Blood Mononuclear Cells; PLGA: Poly(D,L-lactic-co-glycolic acid); POD: Postoperative Day; pTreg: Peripheral T regulatory cells; Rapa-ISFI: Rapamycin-loaded in situ forming implant; Treg: T regulatory cells; VCA: Vascularized Composite Allotransplantation

Conflict of Interest

The authors declare that the research was conducted in the absence of any commercial or financial relationships that could be construed as a potential conflict of interest.

Author Contributions

D.S., J.A.P. A.T., and J.T.S designed the study and analyzed data; J-C.L. and P.L. designed and developed the drug delivery system; P.L. and D.S. analyzed the release data; D.S., A.T., D.V.D., J.T.S. designed and performed animal experiments, laboratory analysis and analyzed the respective data; Y.B. analyzed the histology; C.B. J-C.P. performed the LC-MS/MS analysis; R.R. provided essential support for the project and analyzed the laboratory data; J-C.L., E.V., J.A.P. and P.L. carried the overall responsibility for the project; A.T. wrote the manuscript. All Authors read and approved the final version of the manuscript.

Funding

Supported by Insel-grant to J.T.S., Grant-in-Aid of the Department of Clinical Research of the University of Bern to A.T., grant no. 32003B_138434 of the Swiss National Science Foundation to E.V. and R.R., grant no. 169805 of the Swiss National Science Foundation to J.A.P.

Acknowledgments

The Authors thank Maurizio Roveri for his valuable and extensive support with the set-up of HPLC for rapamycin quantification, Julie Denoyelle for her excellent technical help and Dr. Catherine Tsai for review of the manuscript and helpful comments. LC-MS/MS analyses were performed at the Clinical Metabolomics Facility, Center of Laboratory Medicine from the Bern University Hospital (Inselspital). The Authors thank Michael Hayoz for blood LC-MS/MS routine analysis. Lipoid GmbH is acknowledged the endowment to the University of Jena (P. L.).

Reference

1. Bohdan Pomahac RMG. Facial and Hand Allotransplantation. *Cold Spring Harbor perspectives in medicine* (2014)
doi:10.1101/cshperspect.a015651
2. Shores JT, Brandacher G, Lee WPA. Hand and Upper Extremity Transplantation: An Update of Outcomes in the Worldwide Experience. *Plastic and reconstructive surgery* (2015) **135**:351e–360e.
doi:10.1097/PRS.0000000000000892
3. Schnider JT, Weinstock M, Plock JA, Solari MG, Venkataramanan R, Zheng XX, Gorantla VS. Site-Specific Immunosuppression in Vascularized Composite Allotransplantation: Prospects and Potential. *Journal of Immunology Research* (2013) **2013**:e495212. doi:10.1155/2013/495212
4. Solari MG, Washington KM, Sacks JM, Hautz T, Unadkat JV, Horibe EK, Venkataramanan R, Larregina AT, Thomson AW, Lee WPA. Daily topical tacrolimus therapy prevents skin rejection in a rodent hind limb allograft model. *Plastic and reconstructive surgery* (2009) **123**:17S–25S.
doi:10.1097/PRS.0b013e318191bcbd
5. Gharb BB, Rampazzo A, Altuntas SH, Madajka M, Cwykiel J, Stratton J, Siemionow MZ. Effectiveness of topical immunosuppressants in prevention and treatment of rejection in face allotransplantation. *Transplantation* (2013) **95**:1197–1203.
doi:10.1097/TP.0b013e31828bca61
6. Gajanayake T, Olariu R, Leclère FM, Dhayani A, Yang Z, Bongoni AK, Banz Y, Constantinescu MA, Karp JM, Vemula PK, et al. A single localized dose of enzyme-responsive hydrogel improves long-term survival of a vascularized composite allograft. *Science Translational Medicine* (2014) **6**:249ra110. doi:10.1126/scitranslmed.3008778
7. Olariu R, Denoyelle J, Leclère FM, Dzhonova DV, Gajanayake T, Banz Y, Hayoz M, Constantinescu M, Rieben R, Vögelin E, et al. Intra-graft injection of tacrolimus promotes survival of vascularized composite allotransplantation. *Journal of Surgical Research* (2017) **218**:49–57.
doi:http://dx.doi.org/10.1016/j.jss.2017.05.046
8. Unadkat JV, Schnider JT, Feturi FG, Tsuji W, Bliley JM, Venkataramanan R, Solari MG, Marra KG, Gorantla VS, Spiess AM. Single Implantable FK506 Disk Prevents Rejection in Vascularized Composite Allotransplantation. *Plastic and reconstructive surgery* (2017) **139**:403e–414e.
doi:10.1097/PRS.00000000000002951
9. Dumont CM, Park J, Shea LD. Controlled release strategies for modulating immune responses to promote tissue regeneration. *J Control Release* (2015) **219**:155–166. doi:10.1016/j.jconrel.2015.08.014
10. Safinia N, Scotta C, Vaikunthanathan T, Lechler RI, Lombardi G. Regulatory T Cells: Serious Contenders in the Promise for Immunological

- Tolerance in Transplantation. *Frontiers in Immunology* (2015) **6**:438. doi:10.3389/fimmu.2015.00438
11. Sehgal SN. Sirolimus: its discovery, biological properties, and mechanism of action. *Transplantation Proceedings* (2003) **35**:7S–14S.
 12. Haxhinasto S, Mathis D, Benoist C. The AKT-mTOR axis regulates de novo differentiation of CD4+Foxp3+ cells. *The Journal of Experimental Medicine* (2008) **205**:565–574. doi:10.1084/jem.20071477
 13. Delgoffe GM, Kole TP, Zheng Y, Zarek PE, Matthews KL, Xiao B, Worley PF, Kozma SC, Powell JD. The mTOR kinase differentially regulates effector and regulatory T cell lineage commitment. *Immunity* (2009) **30**:832–844. doi:10.1016/j.immuni.2009.04.014
 14. Kopf H, la Rosa de GM, Howard OMZ, Chen X. Rapamycin inhibits differentiation of Th17 cells and promotes generation of FoxP3+ T regulatory cells. *Int Immunopharmacol* (2007) **7**:1819–1824. doi:10.1016/j.intimp.2007.08.027
 15. Zhao T, Yang C, Qiu Y, Xue Y, Zhao Z, Song D, Ma Z, Yang B, Xu M, Rong R, et al. Comparison of regulatory T cells and FoxP3-positive T-cell subsets in the peripheral blood of renal transplant recipients with sirolimus versus cyclosporine: a preliminary study. *Transplantation Proceedings* (2013) **45**:148–152. doi:10.1016/j.transproceed.2012.06.067
 16. Hendrikx TK, Velthuis JHL, Klepper M, van Gurp E, Geel A, Schoordijk W, Baan CC, Weimar W. Monotherapy rapamycin allows an increase of CD4 CD25 FoxP3 T cells in renal recipients. *Transplant International* (2009) **22**:884–891. doi:10.1111/j.1432-2277.2009.00890.x
 17. Chu Z-Q, Ji Q. Sirolimus did not affect CD4(+)CD25(high) forkhead box p3(+)T cells of peripheral blood in renal transplant recipients. *Transplantation Proceedings* (2013) **45**:153–156. doi:10.1016/j.transproceed.2012.07.145
 18. Gallon L, Traitanon O, Sustento-Reodica N, Leventhal J, Ansari MJ, Gehrau RC, Ariyamuthu V, De Serres SA, Alvarado A, Chhabra D, et al. Cellular and molecular immune profiles in renal transplant recipients after conversion from tacrolimus to sirolimus. *Kidney International* (2015) **87**:828–838. doi:10.1038/ki.2014.350
 19. Kim KW, Chung BH, Kim B-M, Cho M-L, Yang CW. The effect of mammalian target of rapamycin inhibition on T helper type 17 and regulatory T cell differentiation in vitro and in vivo in kidney transplant recipients. *Immunology* (2015) **144**:68–78. doi:10.1111/imm.12351
 20. Kranz H, Bodmeier R. A novel in situ forming drug delivery system for controlled parenteral drug delivery. *Int J Pharm* (2007) **332**:107–114. doi:10.1016/j.ijpharm.2006.09.033
 21. Kempe S, Mäder K. In situ forming implants - an attractive formulation principle for parenteral depot formulations. *J Control Release* (2012) **161**:668–679. doi:10.1016/j.jconrel.2012.04.016

22. Vögelin E, Jones NF, Rao UNM. Long-term viability of articular cartilage after microsurgical whole-joint transplantation and immunosuppression with rapamycin, mycophenolate mofetil, and tacrolimus. *The Journal of Hand Surgery* (2002) **27**:307–315.
23. Weinreich J, Löb S, Löffler M, Königsrainer I, Zieker D, Königsrainer A, Coerper S, Beckert S. Rapamycin-induced impaired wound healing is associated with compromised tissue lactate accumulation and extracellular matrix remodeling. *Eur Surg Res* (2011) **47**:39–44. doi:10.1159/000327972
24. Chen J-C, Chang M-L, Muench MO. A kinetic study of the murine mixed lymphocyte reaction by 5,6-carboxyfluorescein diacetate succinimidyl ester labeling. *Journal of Immunological Methods* (2003) **279**:123–133. doi:10.1016/S0022-1759(03)00236-9
25. Graham PD, Brodbeck KJ, McHugh AJ. Phase inversion dynamics of PLGA solutions related to drug delivery. *J Control Release* (1999) **58**:233–245.
26. Brodbeck KJ, DesNoyer JR, McHugh AJ. Phase inversion dynamics of PLGA solutions related to drug delivery. Part II. The role of solution thermodynamics and bath-side mass transfer. *J Control Release* (1999) **62**:333–344.
27. Cendales LC, Kanitakis J, Schneeberger S, Burns C, Ruiz P, Landin L, Rimmelink M, Hewitt CW, Landgren T, Lyons B, et al. The Banff 2007 working classification of skin-containing composite tissue allograft pathology. in (Blackwell Publishing Ltd), 1396–1400. doi:10.1111/j.1600-6143.2008.02243.x
28. Siemionow M, Klimczak A. Chimerism-based experimental models for tolerance induction in vascularized composite allografts: Cleveland clinic research experience. *Clin Dev Immunol* (2013) **2013**:831410–12. doi:10.1155/2013/831410
29. Keener AB. Saving face: The search for alternatives to life-long immunosuppression for face transplants. *Nature Medicine* (2016) **22**:448–449. doi:10.1038/nm0516-448
30. Lin CH, Wang YL, Anggelia MR, Chuang WY, Cheng HY, Mao Q, Zelken JA, Zheng XX, Lee WPA, Brandacher G. Combined Anti-CD154/CTLA4Ig Costimulation Blockade-Based Therapy Induces Donor-Specific Tolerance to Vascularized Osteomyocutaneous Allografts. *American Journal of Transplantation* (2016) **16**:2030–2041. doi:10.1111/ajt.13694
31. Pilat N, Klaus C, Schwarz C, Hock K, Oberhuber R, Schwaiger E, Gattringer M, Ramsey H, Baranyi U, Zelger B, et al. Rapamycin and CTLA4Ig Synergize to Induce Stable Mixed Chimerism Without the Need for CD40 Blockade. *American Journal of Transplantation* (2015)n/a–n/a. doi:10.1111/ajt.13154
32. Lin CH, Zhang W, Ng TW, Zhang D, Jiang J, Pulikkottil B, Lakkis F, Gorantla VS, Lee WPA, Brandacher G, et al. Vascularized osteomyocutaneous

- allografts are permissive to tolerance by induction-based immunomodulatory therapy. *American Journal of Transplantation* (2013) **13**:2161–2168. doi:10.1111/ajt.12275
33. Poirier N, Dilek N, Mary C, Ville S, Coulon F, Branchereau J, Tillou X, Charpy V, Pengam S, Nerriere-Daguin V, et al. FR104, an antagonist anti-CD28 monovalent fab' antibody, prevents alloimmunization and allows calcineurin inhibitor minimization in nonhuman primate renal allograft. *American Journal of Transplantation* (2015) **15**:88–100. doi:10.1111/ajt.12964
 34. Thornton AM, Korty PE, Tran DQ, Wohlfert EA, Murray PE, Belkaid Y, Shevach EM. Expression of Helios, an Ikaros transcription factor family member, differentiates thymic-derived from peripherally induced Foxp3+ T regulatory cells. *J Immunol* (2010) **184**:3433–3441. doi:10.4049/jimmunol.0904028
 35. Himmel ME, MacDonald KG, Garcia RV, Steiner TS, Levings MK. Helios+ and Helios- cells coexist within the natural FOXP3+ T regulatory cell subset in humans. *J Immunol* (2013) **190**:2001–2008. doi:10.4049/jimmunol.1201379
 36. Elkord E. Helios Should Not Be Cited as a Marker of Human Thymus-Derived Tregs. Commentary: Helios(+) and Helios(-) Cells Coexist within the Natural FOXP3(+) T Regulatory Cell Subset in Humans. *Frontiers in Immunology* (2016) **7**:276. doi:10.3389/fimmu.2016.00276
 37. Sebastian M, Lopez-Ocasio M, Metidji A, Rieder SA, Shevach EM, Thornton AM. Helios Controls a Limited Subset of Regulatory T Cell Functions. *J Immunol* (2016) **196**:144–155. doi:10.4049/jimmunol.1501704
 38. Kim H-J, Barnitz RA, Kreslavsky T, Brown FD, Moffett H, Lemieux ME, Kaygusuz Y, Meissner T, Holderried TAW, Chan S, et al. Stable inhibitory activity of regulatory T cells requires the transcription factor Helios. *Science* (2015) **350**:334–339. doi:10.1126/science.aad0616
 39. Levitsky J, Gallon L, Miller J, Tambur AR, Leventhal J, Flaa C, Huang X, Sarraj B, Wang E, Mathew JM. Allospecific regulatory effects of sirolimus and tacrolimus in the human mixed lymphocyte reaction. *Transplantation* (2011) **91**:199–206. doi:10.1097/TP.0b013e318200e97
 40. Young JS, Daniels MD, Miller ML, Wang T, Zhong R, Yin D, Alegre ML, Chong AS. Erosion of Transplantation Tolerance After Infection. *American Journal of Transplantation* (2017) **17**:81–90. doi:10.1111/ajt.13910
 41. Miller ML, Daniels MD, Wang T, Chen J, Young J, Xu J, Wang Y, Yin D, Vu V, Husain AN, et al. Spontaneous restoration of transplantation tolerance after acute rejection. *Nature Communications* (2015) **6**:7566. doi:10.1038/ncomms8566
 42. Chhabra A, Ring AM, Weiskopf K, Schnorr PJ, Gordon S, Le AC, Kwon H-S,

- Ring NG, Volkmer J, Ho PY, et al. Hematopoietic stem cell transplantation in immunocompetent hosts without radiation or chemotherapy. *Science Translational Medicine* (2016) **8**:351ra105–351ra105. doi:10.1126/scitranslmed.aae0501
43. Lin J-Y, Tsai F-C, Wallace CG, Huang W-C, Wei F-C, Liao S-K. Optimizing chimerism level through bone marrow transplantation and irradiation to induce long-term tolerance to composite tissue allotransplantation. *J Surg Res* (2012) **178**:487–493. doi:10.1016/j.jss.2012.02.064
 44. Maldonado RA, LaMothe RA, Ferrari JD, Zhang A-H, Rossi RJ, Kolte PN, Griset AP, O'Neil C, Altreuter DH, Browning E, et al. Polymeric synthetic nanoparticles for the induction of antigen-specific immunological tolerance. *Proceedings of the National Academy of Sciences* (2015) **112**:E156–E165. doi:10.1073/pnas.1408686111
 45. Tostanoski LH, Chiu Y-C, Gammon JM, Simon T, Andorko JI, Bromberg JS, Jewell CM. Reprogramming the Local Lymph Node Microenvironment Promotes Tolerance that Is Systemic and Antigen Specific. *Cell Reports* (2016) **16**:2940–2952. doi:10.1016/j.celrep.2016.08.033
 46. Scalea JR, Tomita Y, Lindholm CR, Burlingham W. Transplantation Tolerance Induction: Cell Therapies and Their Mechanisms. *Frontiers in Immunology* (2016) **7**:87. doi:10.3389/fimmu.2016.00087
 47. Oura T, Cosimi AB, Kawai T. Chimerism-based tolerance in organ transplantation: preclinical and clinical studies. *Clinical & Experimental Immunology* (2017) **189**:190–196. doi:10.1111/cei.12969
 48. Levitsky J, Miller J, Leventhal J, Huang X, Flaa C, Wang E, Tambur A, Burt RK, Gallon L, Mathew JM. The human “Treg MLR”: immune monitoring for FOXP3+ T regulatory cell generation. *Transplantation* (2009) **88**:1303–1311. doi:10.1097/TP.0b013e3181bbee98
 49. Jindal R, Unadkat J, Zhang W, Zhang D, Ng TW, Wang Y, Jiang J, Lakkis F, Rubin P, Lee WPA, et al. Spontaneous Resolution of Acute Rejection and Tolerance Induction With IL-2 Fusion Protein in Vascularized Composite Allotransplantation. *American Journal of Transplantation* (2015)n/a–n/a. doi:10.1111/ajt.13118

Figure legends

Figure 1: Design and evaluation of rapamycin-loaded ISFI (Rapa-ISFI). (A) Schematic representation of the Rapa-ISFI formation and drug release properties. 1) Upon injection into the subcutaneous tissue, 2) the biocompatible solvent *N*-methyl-2-pyrrolidone (NMP) diffuses out of solution into the surrounding tissue, causing the biocompatible and biodegradable PLGA-polymer to solidify in the aqueous environment of the interstitial tissue, trapping the drug within. Since the drug is soluble in NMP, a certain amount of drug will evade entrapment in the solid implant and account for an initial burst release. 3) As the implant is degraded over time, the drug is then released gradually. The drug can also be released via diffusion through the polymer matrix. (B) *In vitro* analysis of rapamycin release from Rapa-ISFI. Two Rapa-ISFI were prepared and injected into stainless steel mesh baskets suspended in release medium and rapamycin was quantified using high-performance liquid chromatography at different time point. The cumulative amount of rapamycin (total μg in the solution) is reported for the different sampling times. (C) *In vivo* rapamycin release from Rapa-ISFI. Three naïve Lewis rats were injected subcutaneously in one hind limb groin with Rapa-ISFI. Blood was sampled at designated time points and rapamycin concentration was measured by LC-MS/MS.

Figure 2: Rapa-ISFI treatment prolonged survival of vascularized composite allografts. (A) Experimental design. (B) Graft survival represented with Kaplan-Meier survival curves. (Group 1, n=6; Group 2, n=6; Group 3, n=6; Group 4, n=5). Median Survival time (MST) refers specifically to graft survival. The appearance of GVHD in three out of five rats of group 4 and the P value calculated by Mantel-Cox test are reported for each group.

Figure 3: Histological evaluation of the different treatments (A) Representative microphotographs of the histology sections of the skin stained with hematoxylin and eosin and histopathological grading of rejection based on Banff working classification for VCA rejection (27) in the 4 treatment groups. Skin was recovered from all the allografts at rejection or at the endpoint. Rats of Group 4 that developed lethal GvHD were excluded from the analysis. (B) Specific assessment of leukocyte infiltration, tissue necrosis and vascular, including endothelial cell (EC) pathology in the 4 treatment groups. For each of these categories a score from 0 to 3 was given (*i.e.*, 0= absent, 1=minimal, 2=moderate or 3=extensive). Data are presented as mean and SD. * $P < 0.05$ by one-way ANOVA with Tukey's multi-comparisons test.

Figure 4: Systemic and tissue levels of rapamycin. (A) Whole blood levels of rapamycin in rats from Group 2 (closed circles, continuous line, n=4-6), Group 3 (open circles, dotted line, n=1-5) and Group 4 (closed squares, interrupted line n=1-5). Rapamycin levels were measured by LC-MS/MS in the blood at different postoperative days (POD) and expressed as ng rapamycin per mL of blood. For Group 4 trough concentrations are shown (*i.e.*, blood collected about 18-24h after systemic rapamycin injection). (B) Skin rapamycin levels in rats treated with Rapa-ISFI. Skin biopsies were recovered from the allograft 21 (n=2 for Group 2 and n=4 for Group 3), 49 (n=2 for group 2 and n=2 for group 3) and 100 days (n=5 for Group 2 and n=2 for Group 3) after transplantation. Data presented as ng of rapamycin per mg of tissue. (C) Rapamycin levels in different tissues at the endpoint of long-term surviving rats of different treatment groups. Rapamycin was measured in skin, muscle and groin fat-pad recovered from the transplant side or the contralateral control limb. Data presented as mean and SD, *P<0.05, **P<0.01, *** P<0.001, **** P<0.0001 by one-way ANOVA with Tukey's multi-comparisons test. Rats from Group 1 were also tested as negative control and they show rapamycin levels under the quantification limit both in blood and tissue (not shown).

Figure 5: Rapamycin treatment promotes multilineage mixed chimerism. (A) Multilineage mixed chimerism levels at POD21 in the peripheral blood of the rats of different treatment groups. Donor leukocytes were identified as RT1Ac⁺ cells in the leukocytes gate; donor granulocytes as CD3⁻CD4⁻SSc^{High}RT1Ac⁺ leukocytes; donor monocytes as CD3⁻CD4⁺RT1Ac⁺ leukocytes; donor T helper (Th) cells as CD3⁺CD4⁺RT1Ac⁺ leukocytes; donor T cytotoxic (Tc) cells as CD3⁺CD4⁻RT1Ac⁺ leukocytes and donor B cells as CD3⁻CD4⁻SSc^{Low}RT1Ac⁺ leukocytes. Data presented as mean and SD, *P<0.05, **P<0.01 by one-way ANOVA with Tukey's multi-comparisons test. (B) Evolution of multilineage mixed chimerism. Flow cytometry analysis for measuring the frequency of donor cells was performed at POD21 (same data of Figure 4A), 63 and 100 in the rats from Groups 2 (n=5), 3 (n=5 POD 21 and n=3 POD 63 and 100) and 4 (n=2). (C) Correlation analysis between chimerism levels and allograft survival. Frequency of donor leukocytes, granulocytes and monocytes in peripheral blood of rats from Group 1 (open squares), Group 2 (closed circles), Group 3 (open circles) and Group 4 (closed square) at POD21 were correlated with allograft survival by nonparametric (Spearman) correlation, r values and P values are reported for each correlation.

Figure 6: Induction therapy with anti-lymphocyte serum (ALS) is necessary for Rapa-ISFI promotion of allograft survival and for efficient induction of multilineage chimerism. (A) Survival of hind limb allografts in Rapa-ISFI treated rats with unsuccessful ALS therapy. Kaplan-Meier survival curves comparing allograft survival in recipient rats with unsuccessful induction therapy (*i.e.*, white blood counts on the day of transplantation >7500 cells/ μ L) treated with ipsilateral injection of Rapa-ISFI as compared to rats of Group 2 (white blood counts on the day of transplantation <2500 cells/ μ L, from Figure 2). ** $P < 0.01$ by Mantel-Cox test. (B) Chimerism levels in rats with unsuccessful ALS therapy at POD21. The number of donor leukocytes, granulocytes and monocytes were measured in recipients with unsuccessful ALS therapy and compared to chimerism levels in rats of Group 2 (from Figure 5A). Data presented as mean and SD, * $P < 0.05$ by unpaired T-test.

Figure 7: Rapa-ISFI injection on the transplanted side promotes expansion of blood and tissue T_{reg}. (A) Frequency of T_{reg}, Helios^{Neg}T_{reg} and Helios^{Pos}T_{reg} in the peripheral blood at POD21. T_{reg} were identified as CD3⁺CD4⁺CD25⁺FoxP3⁺ cells. Helios^{Pos}T_{reg} and Helios^{Neg}T_{reg} were identified based on the expression of the transcription factor Helios. Data were expressed as frequency of CD3⁺CD4⁺ T cells and presented as mean and SD, * $P < 0.05$ by one-way ANOVA with Tukey's multi-comparisons test. (B) Correlation analysis between T_{reg} frequencies and allograft survival. Frequency of T_{reg}, Helios^{Neg}T_{reg} and Helios^{Pos}T_{reg} in peripheral blood of rats from Group 1 (open squares), Group 2 (closed circles), Group 3 (open circles) and Group 4 (closed square) at POD21 were correlated with allograft survival by nonparametric (Spearman) correlation, r values and P values are reported for each correlation. (C) Frequency of T_{reg}, Helios^{Neg}T_{reg} and Helios^{Pos}T_{reg} in skin recovered from allograft the day of sacrifice. Skin samples were recovered and analyzed both from rats rejecting their grafts at sacrifice (grey dots) and long-term survivors at the endpoint. T_{reg} were identified as FoxP3⁺ cells after exclusion of doublets and selection of viable CD3⁺ cells. Helios^{Neg} and Helios^{Pos} cells were identified based on the expression of the transcription factor Helios. Data were expressed as frequency of CD3⁺ cells and presented as mean and SD, * $P < 0.05$, ** $P < 0.01$ by one-way ANOVA with Tukey's multi-comparisons test.

Figure 8: *In vitro* donor-specific stimulation induces T_{reg} in ipsilateral Rapa-ISFI treated rats. Mixed lymphocyte reaction (MLR) was performed using responder PBMC isolated at POD100 from long term surviving rats. Responder cells were mixed with gamma-irradiated stimulator cells isolated from spleens of Brown Norway (BN) donor rats or third party Wistar rats. Responder cells without stimulation (unstimulated control) were used as control of basal cell proliferation. After 5 days, cells were stained and analyzed by flow cytometry. (A) Rats treated with Rapa-ISFI ipsilaterally (Group 2) or contralaterally (Group 3) show comparable proliferation response to donor and third party stimulation. (B) Representative flow cytometry picture and quantification of T_{reg} induction in response to donor BN or third party (Wistar) stimulation in MLR culture of ipsilateral or contralateral Rapa-ISFI treated rats. Each dot represents the frequency of CD3⁺CD4⁺FoxP3⁺ T_{reg} in MLR of PBMC isolated from rat treated with Rapa-ISFI ipsilaterally or contralaterally and stimulated with donor (BN) or third party (Wistar) cells. ** P<0.01 by one-way ANOVA with Dunnett's multiple comparisons test comparing BN or Wistar stimulation to unstimulated control.

Figure 1

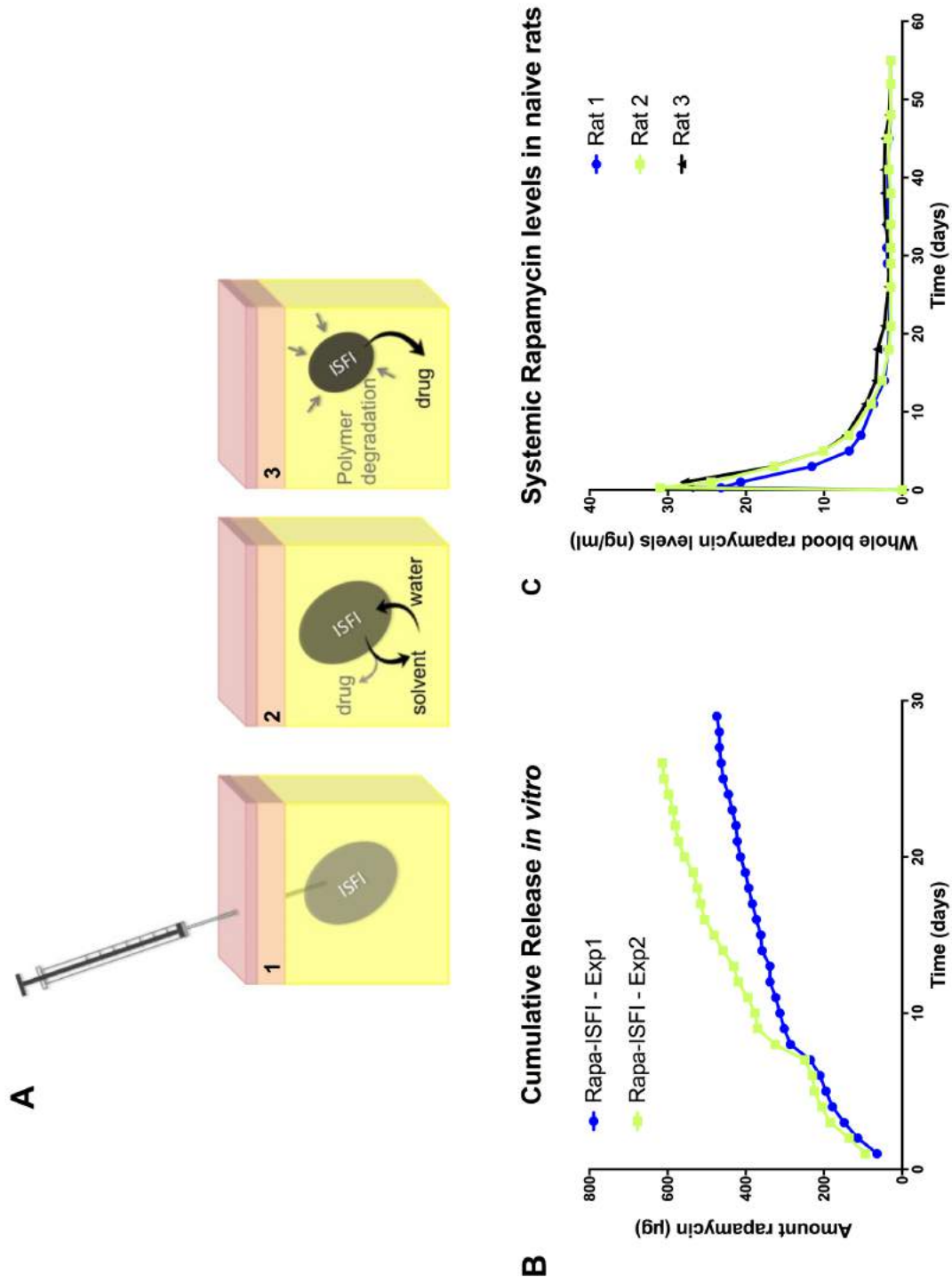
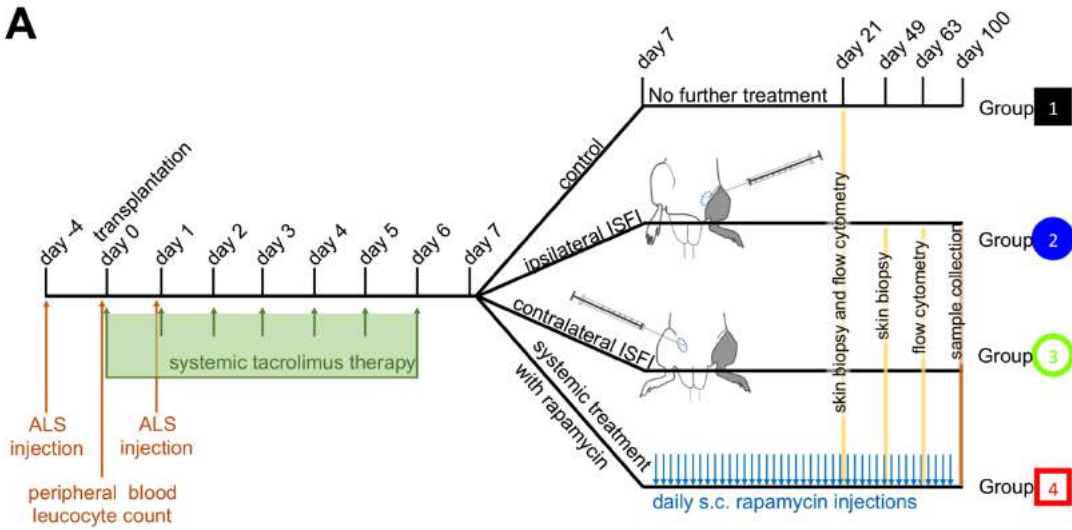
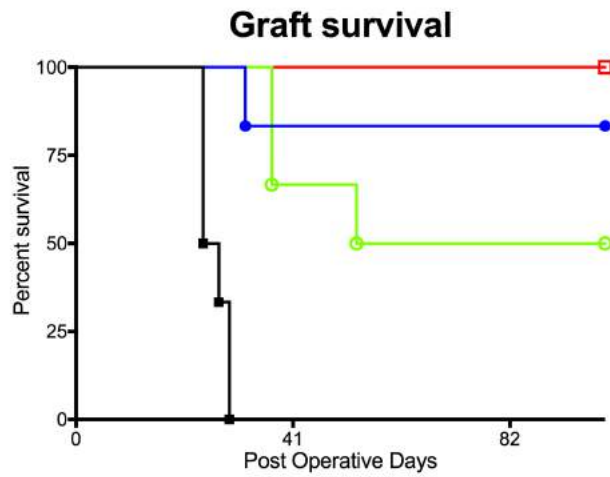


Figure 2

A



B



Group	Median Graft-Survival Time (days)	P value	n	Note
■ Control	25.5		6	all lost due to graft-rejection
● ISFI-Ipsilateral	Undefined	0.0007 vs Control 0.3206 vs ISFI-Contralateral 0.5637 vs Systemic Treatment	6	one lost due to graft-rejection
○ ISFI Contralateral	76.5	0.0007 vs Control 0.2584 vs Systemic Treatment	6	three lost due to graft-rejection
▣ Systemic Treatment	Undefined	0.0295 vs Control	5	three lost due to GvHD

Figure 3

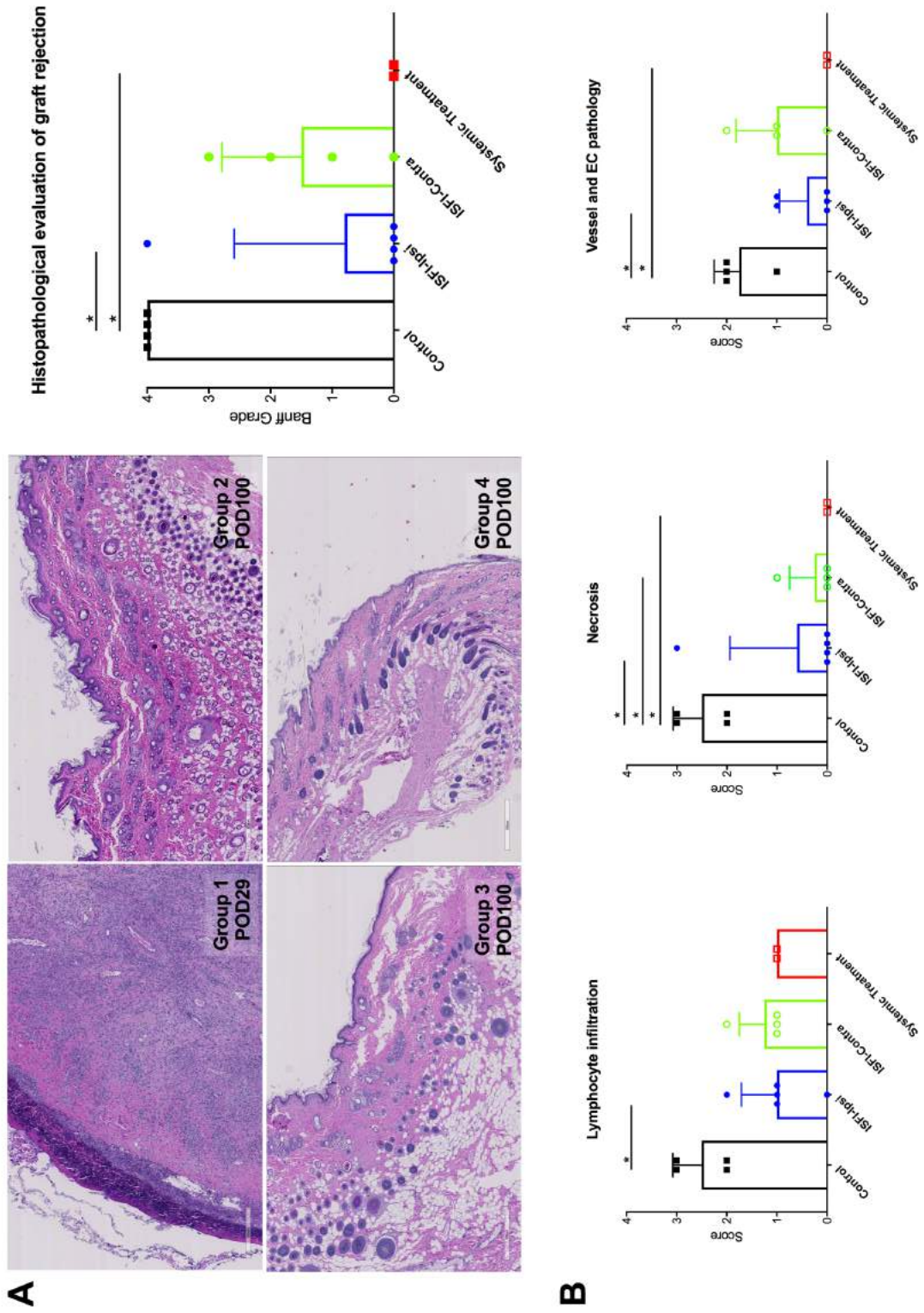


Figure 4

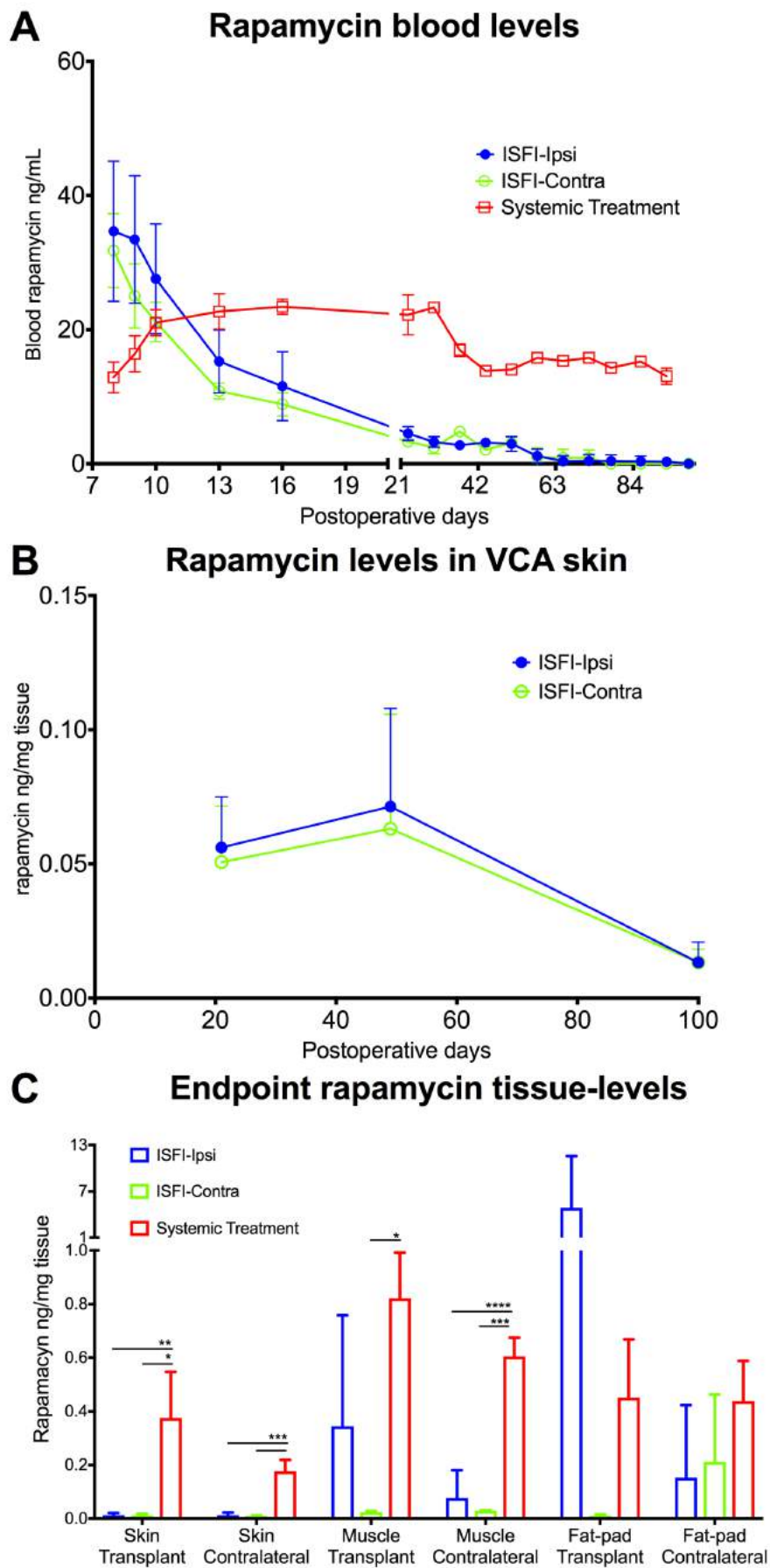


Figure 5

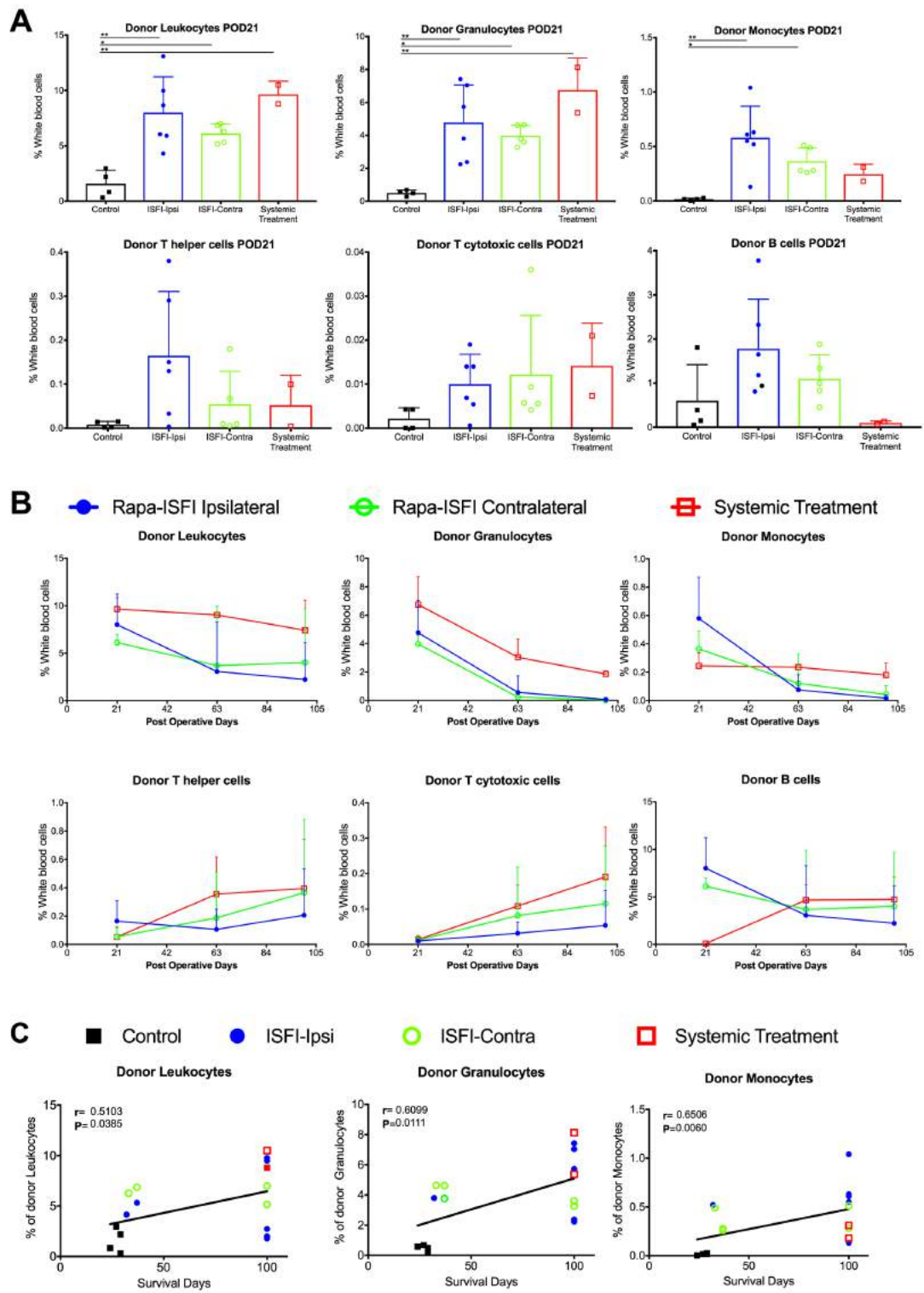


Figure 6

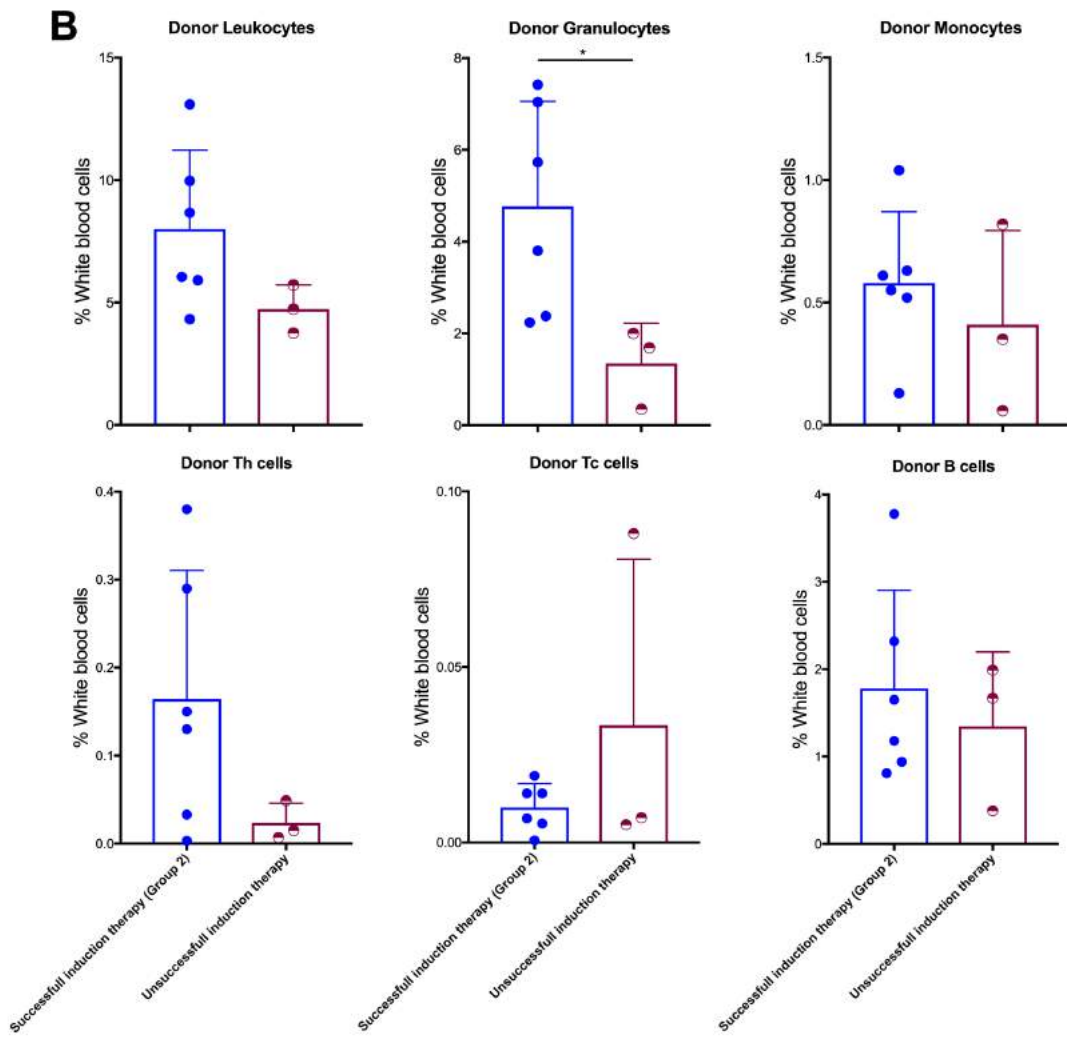
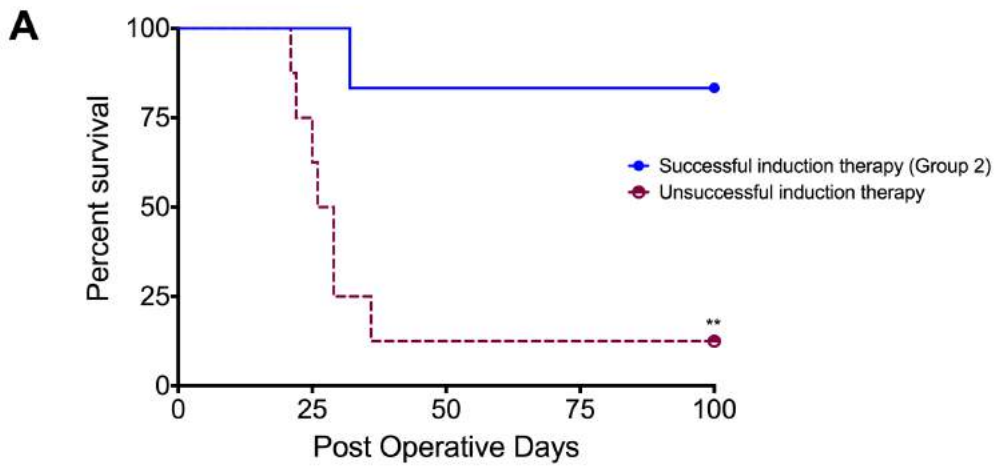


Figure 7

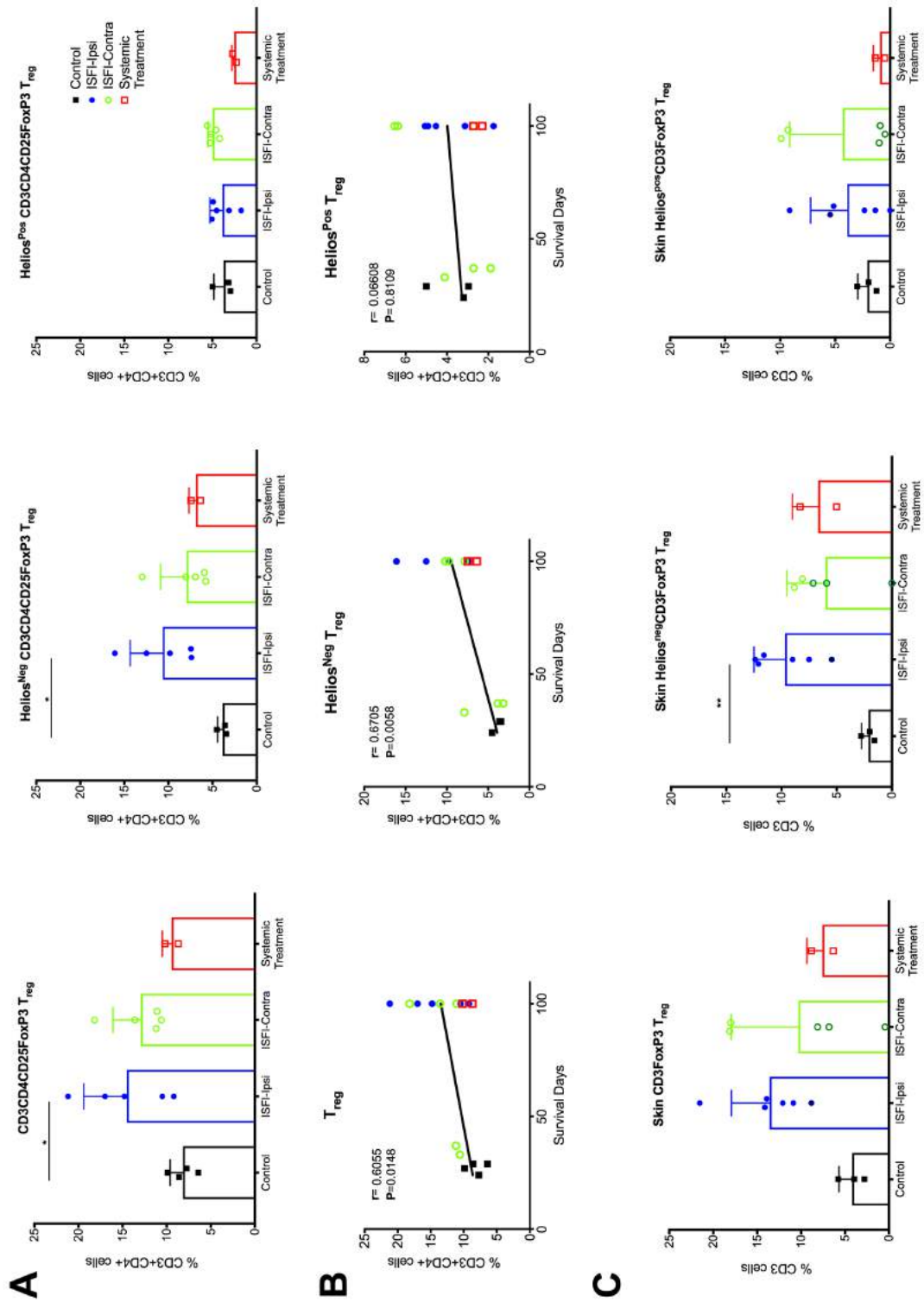
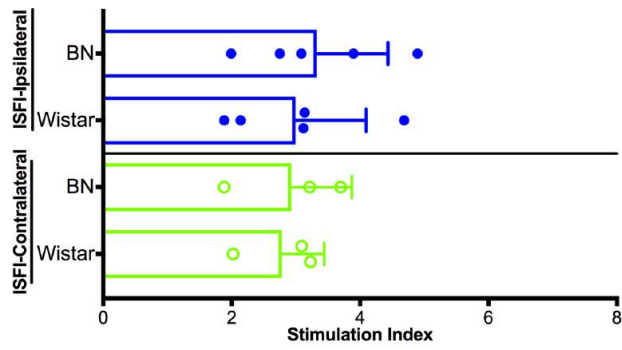


Figure 8

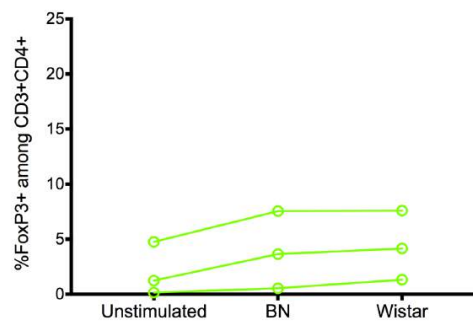
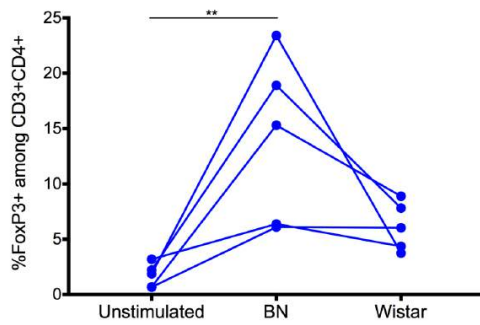
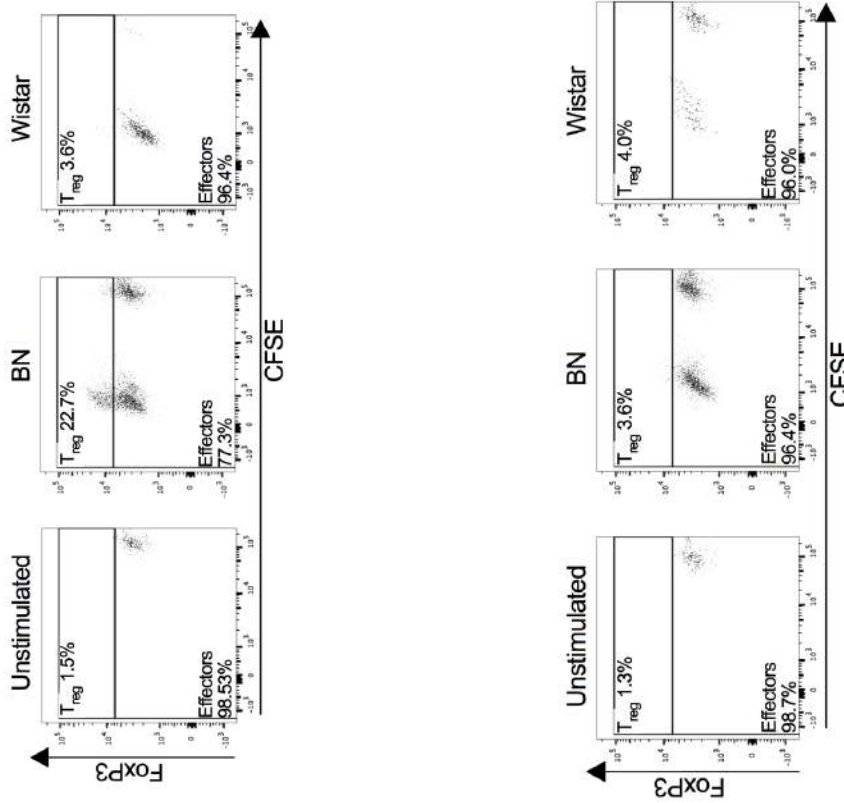
A

Mixed Lymphocyte Reaction POD100



B T_{reg} induction ISFI-Ipsilateral

T_{reg} induction ISFI-Contralateral



Supplementary Material

Delivery of Rapamycin Using In Situ Forming Implants Promotes Immunoregulation and Vascularized Composite Allograft Survival.

Damian Sutter, Dzhuliya V. Dzhonova, Jean-Christophe Prost, Cedric Bovet, Yara Banz, Jean-Christophe Leroux, Robert Rieben, Esther Vögelin, Jan A. Plock*, Paola Luciani*, Adriano Taddeo*, Jonas T. Schnider*

* **Correspondence:** Corresponding Authors: esther.voegelin@insel.ch - jan.plock@usz.ch - paola.luciani@uni-jena.de - adriano.taddeo@dbmr.unibe.ch

Supplementary Methods

In vitro analysis of ISFI release pattern

A release medium composed of 90% water, 0.9% sodium chloride (Sigma-Aldrich Chemie GmbH, Buchs, Switzerland), 0.5% polysorbate 80 (Sigma-Aldrich) and 10% methanol (Sigma-Aldrich) was prepared. Stainless steel mesh baskets(1) were suspended in 300 mL release medium and stored under horizontal shaking in an incubator at 37 °C. The prepared rapamycin-loaded ISFI (Rapa-ISFI) was injected into the baskets. Release medium was replaced with fresh medium at regular time intervals and aliquots of the release medium were sampled, lyophilized and stored at -20 °C. Samples were taken over the course of 29 days. At the end of the experiment, the lyophilized samples were reconstituted with methanol and tacrolimus 25 µg/mL as an internal standard to quantify rapamycin using high-performance liquid chromatography (HPLC-UV, Dionex UltiMate3000 HPLC, Thermo Fisher Scientific Inc, Waltham MA, USA). A YMC-ODS AQ column (150x4.6mm ID, 3µm particle size, YMC Co Ltd., Kyoto, Japan) was preheated to 50°C. The mobile phase consisted of 1mL/min 20% ultrapurified water, 50% MeOH and 30% Acetonitrile, set up as an isocratic method. Readout was measured at 278nm and analyzed using Chromeleon (Thermo Fisher Scientific Inc, Waltham MA, USA) software.

Evaluation of the systemic concentration of rapamycin in naive animals after ISFI injection

Rapa-ISFI was injected subcutaneously in the groin area of three naïve Lewis rats. 0.2-0.5 mL of whole blood was collected from the tongue vein at designated time points and rapamycin levels were measured by LC-MS/MS (see below for details).

Surgical procedure for hind limb transplantation

Rat hind limb transplantation was performed as described previously with several modifications (2,3). Briefly, buprenorphine at 50 mg/kg was given as a preemptive analgesic followed by 5% isoflurane in pure oxygen inhalation anesthesia for the induction and 1.5% for maintenance. Donors (Brown Norway) animals' hindlimbs were amputated at the midfemur level. The donor's inguinal fat pad was detached from the hind limb. Recipient (Lewis) rats were prepared by amputating the corresponding hindlimb leaving the autologous fat pad intact. Endomedullary osteosynthesis was performed with a blunted 18-gauge cannula. The femoral artery was anastomosed in an end-to-end technique with 10/0 interrupted sutures, and the vein anastomosis was performed with a cuff technique using a polyimide tube (RiverTech Medical, Chattanooga, TN USA) as described previously(4). After ensuring adequate vascularization of the transplanted limb, the femoral and sciatic nerves were anastomosed with interrupted 10/0 sutures followed by muscle and skin adaptation with 4/0 resorbable sutures (B. Braun Surgical, Rubi, Spain).

Experimental group treatment

All the recipients underwent an induction therapy with anti-lymphocyte serum (ALS) on day 4 preoperatively and postoperative day (POD) 1 (0.5 mL/rat i.p). Success of the induction therapy was measured right before operation (see below) and Brown Norway-to-Lewis hind limb transplantations were performed as described previously(3). After hind limb transplantation, all animals were treated with 0.5 mg/kg FK506 subcutaneously in the neck starting at day 0 until day 6 to bridge the time to complete wound healing. On day 7, rats were divided in 4 treatment groups: Group 1 was left untreated (Control, n=6); Group 2 received an ISFI loaded with 5 mg of rapamycin subcutaneously into the groin fat pad of the transplanted limb (ISFI-Ipsilateral, n=6); Group 3 received an ISFI loaded with 5 mg of rapamycin subcutaneously into the groin fat pad of the contralateral limb (ISFI-Contralateral); Group 4 received daily injections of 0.5 mg/Kg rapamycin subcutaneously (Systemic treatment, n=5). All animals were evaluated daily for general well-being and clinical rejection was graded macroscopically as 0=no rejection, 1=erythema and edema, 2=epidermolysis and exudation, and 3=desquamation, necrosis, and mummification. The rats were sacrificed either once grade 3 (rejection) was reached or at day 100 (end-point).

Evaluation of the number of lymphocyte after anti-lymphocyte serum (ALS) injection

In order to evaluate the success of the ALS therapy, blood was collected from all ALS treated Lewis rats right before the transplantation in dipotassium ethylenediamine tetraacetic acid (K₂EDTA, Sarstedt AG, Nümbrecht, Germany) and analyzed with a blood cell counter (Sysmex Suisse AG, Horgen, Switzerland) within 30 minutes of collection. Rats with a white blood cell count <2500 cells/ μ L were used as hind limb transplant recipients of Groups 1-4. Moreover, 8 rats with unsuccessful ALS depletion (i.e. with blood cell count >7500 cells/ μ L) were used to understand the importance of ALS induction therapy to promote long-term survival in ipilaterally injected Rapa-ISFI treated rats.

Histopathology

Tissue samples from the grafts, retrieved at the end of the experiments, were fixed in 4% buffered formaldehyde, processed according to standard histopathological specimen work-up, sectioned at 3 μ m thickness and stained with hematoxylin and eosin (H&E) for microscopic evaluation. A pathologist blinded to treatment groups, scored all the samples. Graft rejection was evaluated in skin samples based on the Banff 2007 working classification of skin(5). Moreover, skin samples were analyzed for lymphocyte infiltration, vessels and endothelial cells pathology and tissue necrosis. For each of these categories a score from 0 to 3 was given (i.e., 0= absent, 1=minimal, 2=moderate or 3=extensive). For muscle histology a score from 0 to 3 (i.e., 0= absent, 1=minimal, 2=moderate or 3=extensive) was given for necrosis and lymphocyte infiltration, the sum of these two categories gave the final muscle histopathological score.

Quantification of rapamycin in plasma and tissue

Whole blood samples were collected into tubes containing EDTA-2K at different time points and stored at -20°C until analysis. Rapamycin levels were measured by LC-MS/MS using the Kit MS1100 (ClinMass® Complete Kit, advanced, for Immunosuppressants in Whole Blood, RECIPE Chemicals + Instruments GmbH, Munich, Germany). The lower limit of quantification of rapamycin was 1.5 ng/mL.

Tissue levels were measured in skin biopsies retrieved from the transplant collected at POD21 and 49 as well as in skin, muscle, fat pad tissues, both from the transplanted and the contralateral sides. After tissue collection, 40 mg was aliquoted in a 2 mL Eppendorf tube and all samples were stored at -80°C. The sample preparation was adapted using the MS1312 from Recipe as internal standard (IS). Rapamycin and IS were dissolved in 70% (v/v) methanol

solution. Standard spiking solution were prepared to build up a calibration curve between 25 to 750 ng/mL, and the QC concentrations were set at 35, 150 and 700 ng/mL. The frozen tissues were gently thawed at room temperature. For blank matrix, calibration and QCs samples tissue without rapamycin treatment was needed. To prepare the calibration curve and the QC samples, 40 μ L of standard spiking solution (25 - 750 ng/mL), 40 μ L of IS solution, 920 μ L of precipitation solution (MS1021) were added to untreated tissue. A blank matrix is prepared adding 1000 μ L of precipitation solution to untreated tissue. A volume of 40 μ L of IS solution and 960 μ L of precipitation solution were added to the treated samples. All samples were then grinded with five stainless steel balls for 30 minutes at 25 Hz. The tubes were centrifuged 5 minutes at 4°C and 20'000 rcf. 500 μ L of the tissue extract was filtered with a Mini-Uni Prep G2 vials (GE Healthcare, Chicago, USA).

Chromatographic analysis was performed on an Acquity I-Class system (Waters, Milford, MA, USA) with ClinMass® Complete Kits (Immunosuppressants in Whole Blood, advanced – on-line analysis). The autosampler temperature was set at 10 °C and the autosampler needle was washed with a strong needle wash solution of isopropanol:methanol:acetone:nitrile:H₂O (1:1:1:1, v/v). A solution of 20% (v/v) methanol was used as weak needle wash. Analytes were ionized by electrospray ionization (ESI) in the positive mode and detected on a triple quadrupole mass spectrometer (Xevo TQ-S, Waters, Milford, MA, USA). The capillary and the cone voltage were set at 3 kV and 40 V, respectively. The source offset was set at 60 V, the desolvation temperature at 400 °C, the desolvation gas at 1000 L/h, the cone gas at 150 L/h, the nebulizer at 7 bar and the source temperature at 150 °C. The transition parameters for each transition are summarized in Table 1.

Table 1: SRM parameters for Rapamycin and Rapamycin 13C-d2 quantifiers and qualifiers ions

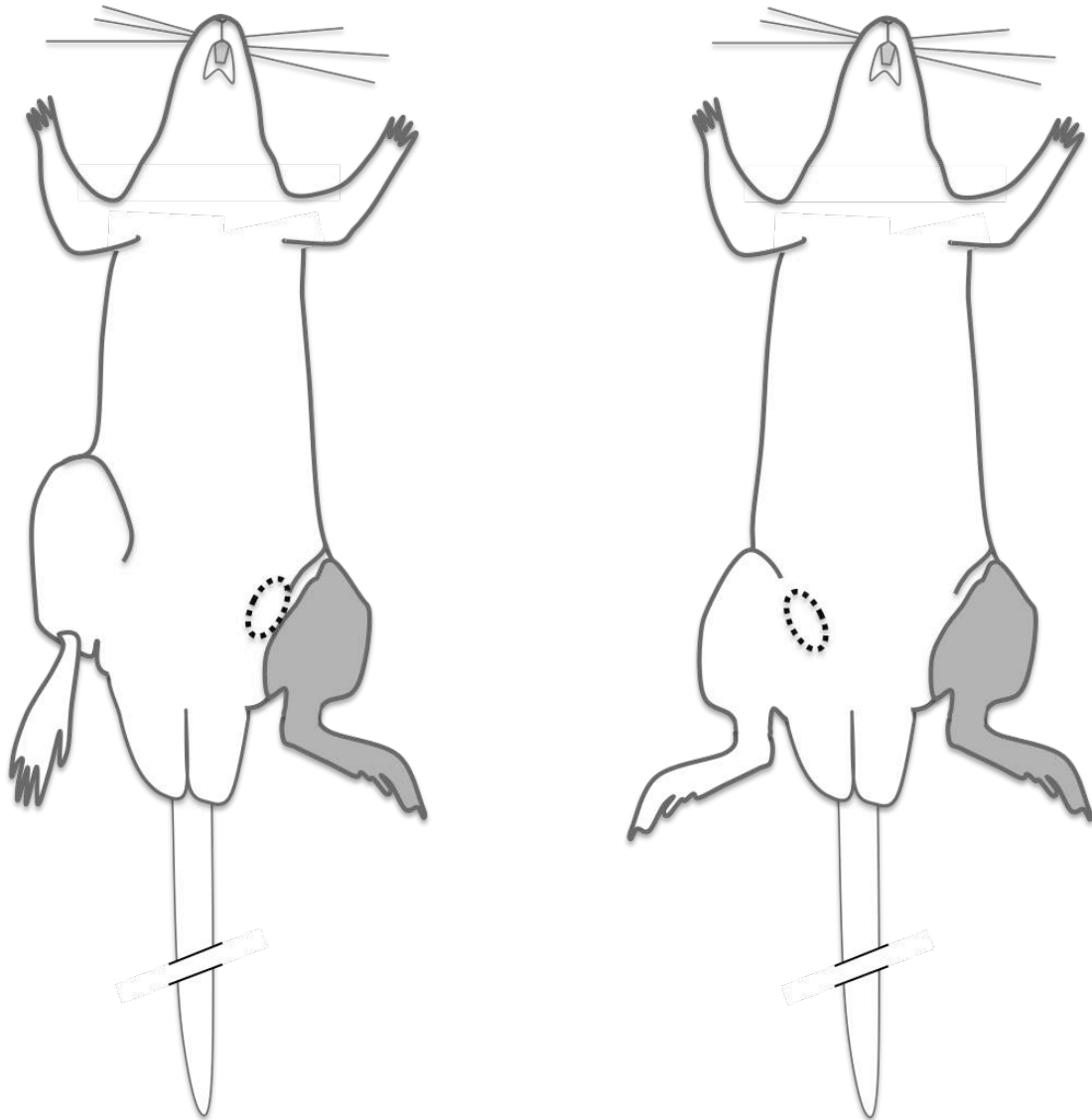
Name	Ion	Parent [m/z]	Daughter [m/z]	Collision [V]
Sirolimus	Quantifier	931.6	864.6	16
Sirolimus 13C-d2	Quantifier	935.6	864.6	16
Sirolimus	Qualifier	931.6	846.6	19
Sirolimus 13C-d2	Qualifier	935.6	846.6	19

The instrument was controlled via MassLynx (version 4.1, Waters). Data were acquired, integrated and processed with TargetLynx (MassLynx v4.1).

Supplementary References

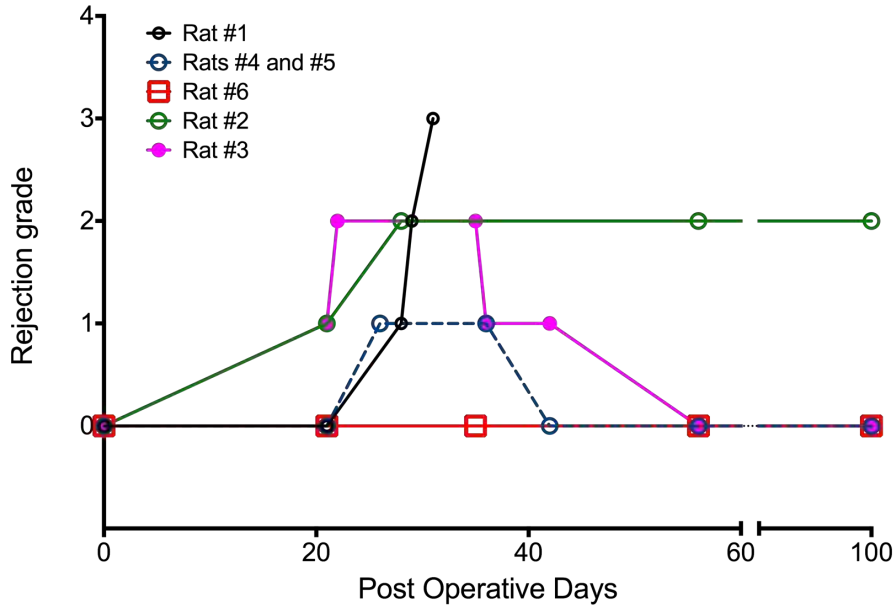
1. Karfeld-Sulzer LS, Ghayor C, Siegenthaler B, de Wild M, Leroux J-C, Weber FE. N-methyl pyrrolidone/bone morphogenetic protein-2 double delivery with in situ forming implants. *J Control Release* (2015) **203**:181–188. doi:10.1016/j.jconrel.2015.02.019
2. Sacks JM, Kuo Y-R, Horibe EK, Hautz T, Mohan K, Valerio IL, Lee WPA. An optimized dual-surgeon simultaneous orthotopic hind-limb allotransplantation model in rats. *Journal of Reconstructive Microsurgery* (2012) **28**:69–75. doi:10.1055/s-0031-1285822
3. Gajanayake T, Olariu R, Leclère FM, Dhayani A, Yang Z, Bongoni AK, Banz Y, Constantinescu MA, Karp JM, Vemula PK, et al. A single localized dose of enzyme-responsive hydrogel improves long-term survival of a vascularized composite allograft. *Science Translational Medicine* (2014) **6**:249ra110. doi:10.1126/scitranslmed.3008778
4. Sucher R, Oberhuber R, Margreiter C, Rumberg G, Jindal R, Lee WPA, Margreiter R, Pratschke J, Schneeberger S, Brandacher G. Orthotopic hind-limb transplantation in rats. *J Vis Exp* (2010) doi:10.3791/2022
5. Cendales LC, Kanitakis J, Schneeberger S, Burns C, Ruiz P, Landin L, Remmelink M, Hewitt CW, Landgren T, Lyons B, et al. The Banff 2007 working classification of skin-containing composite tissue allograft pathology. in (Blackwell Publishing Ltd), 1396–1400. doi:10.1111/j.1600-6143.2008.02243.x

Supplementary Figures

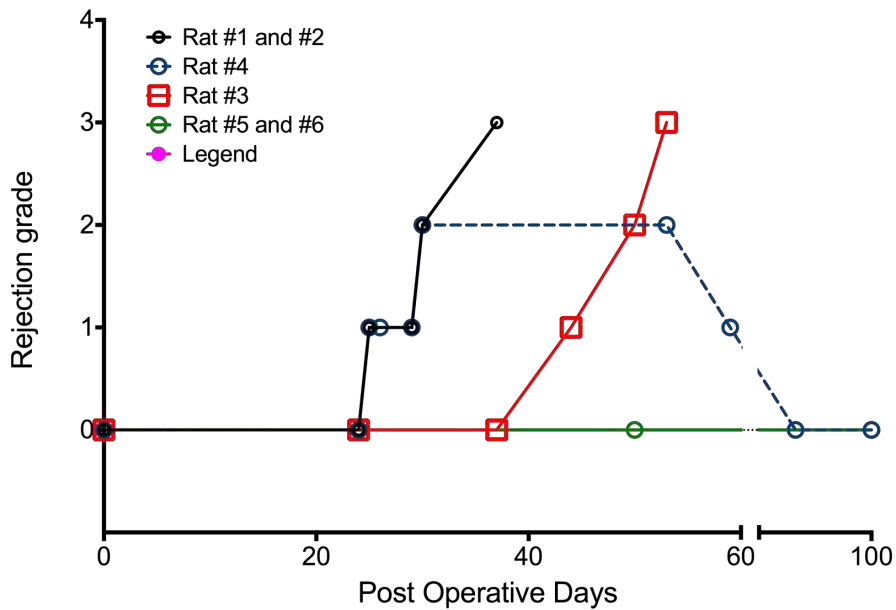


Supplementary Figure 1. Injection site of the Rapa-ISFI. Schematic of the injection site of the Rapa-ISFI at post-operative day (POD7) in rat of Group 2 (injection in the groin close to the transplanted limb) and rats of Group 3 (injection in the groin of contralateral native leg). Circle represents the injection site for each group.

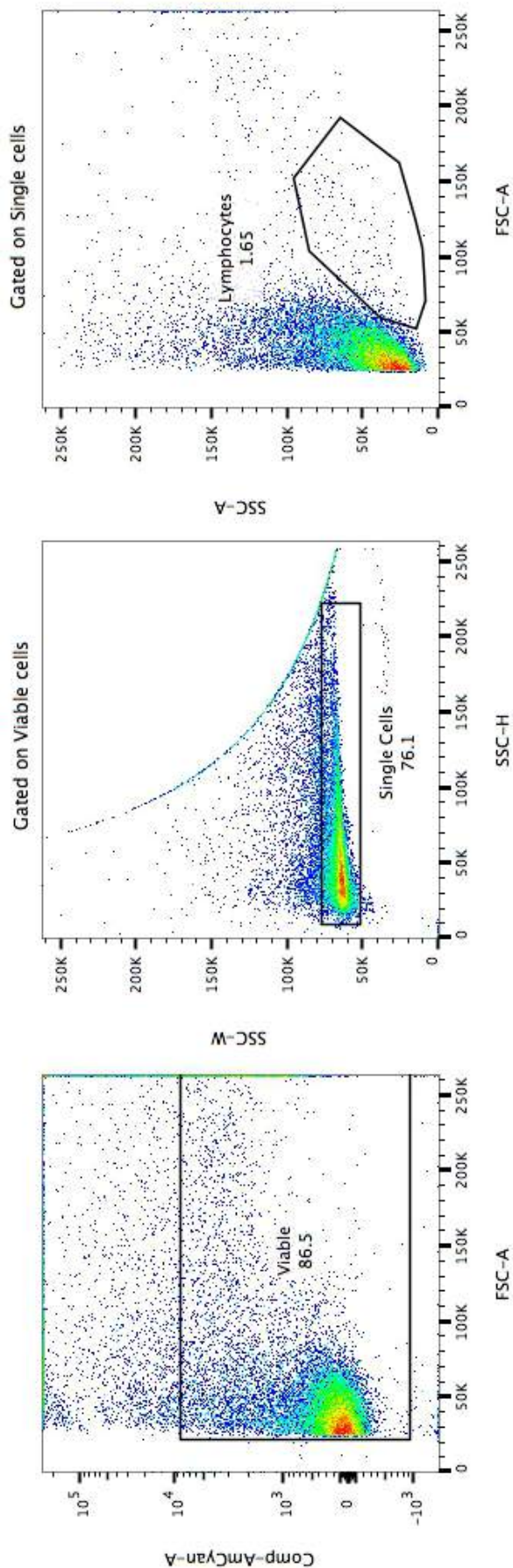
Rejection development in Group 2 (ISFI-Ipsi)



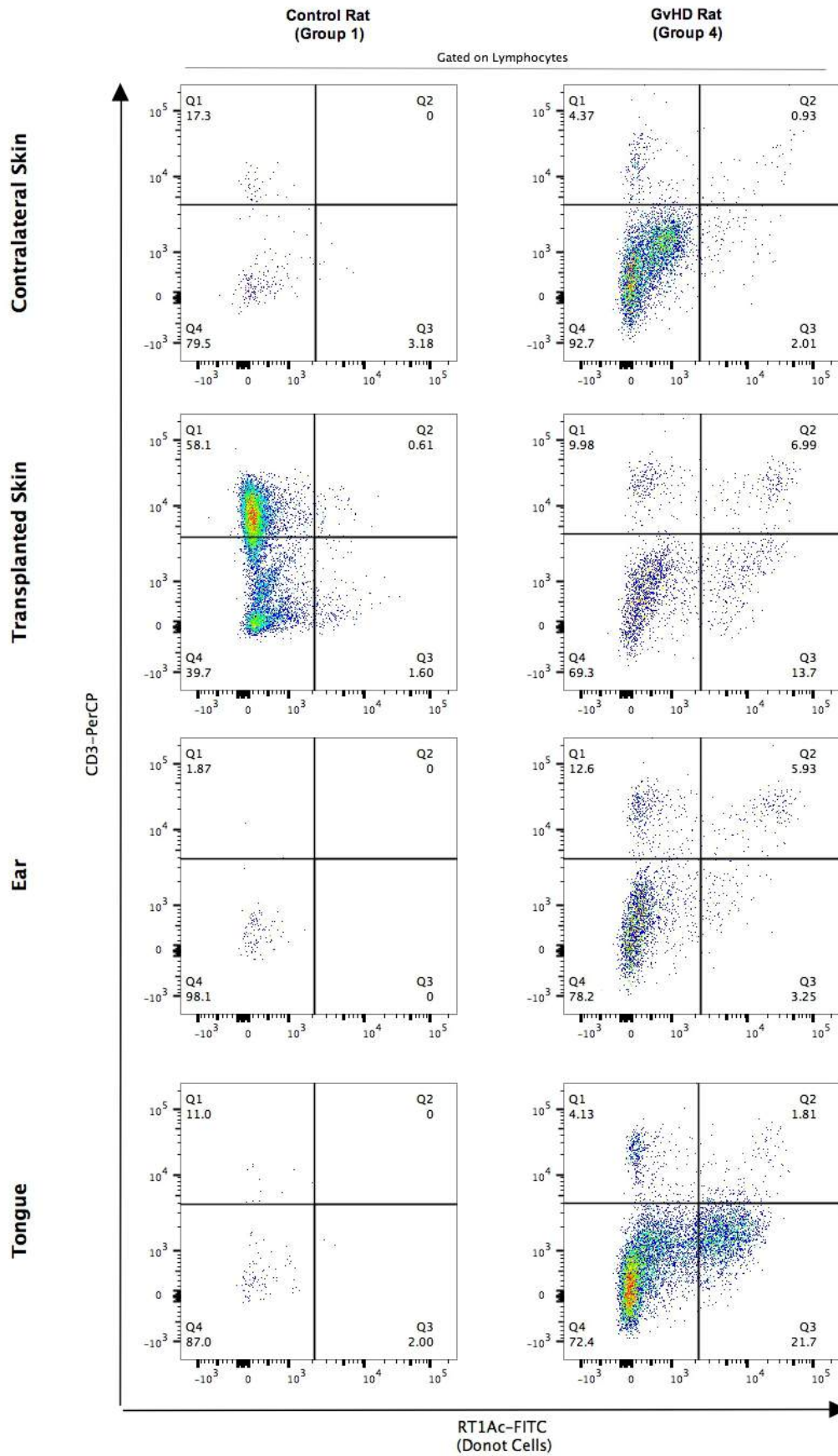
Rejection development in Group 3 (ISFI-Contralateral)

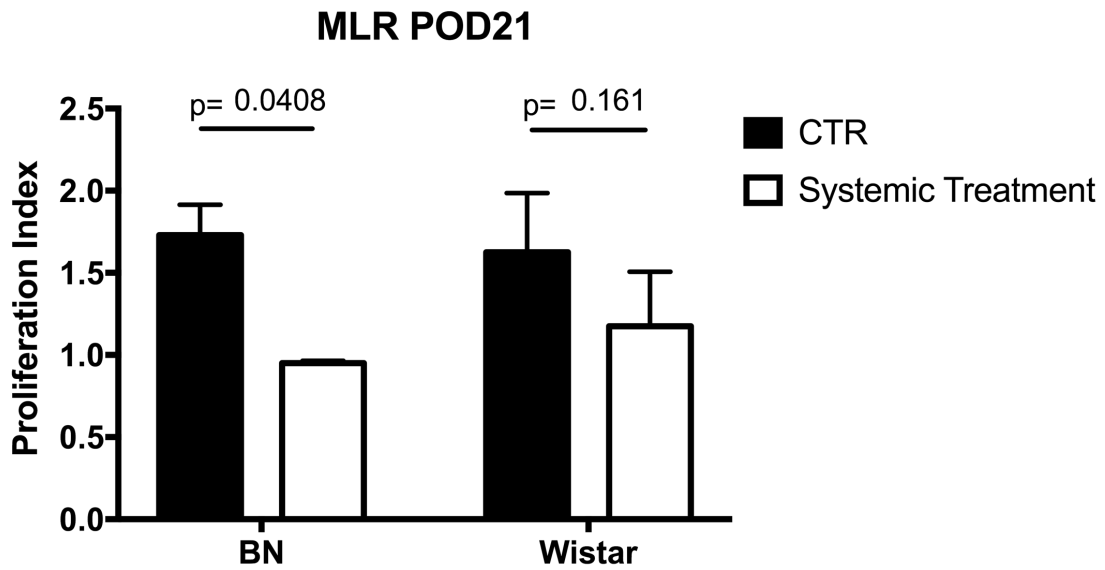


Supplementary Figure 2. Evaluation of macroscopic rejection in Rapa-ISFI treated rats. Development of rejection episodes in rats from Group 2 and 3. Graft rejection was graded daily as 0=no rejection, 1=erythema and edema, 2=epidermolysis and exudation, and 3=desquamation, necrosis, and mummification. Each line represents a single rat.

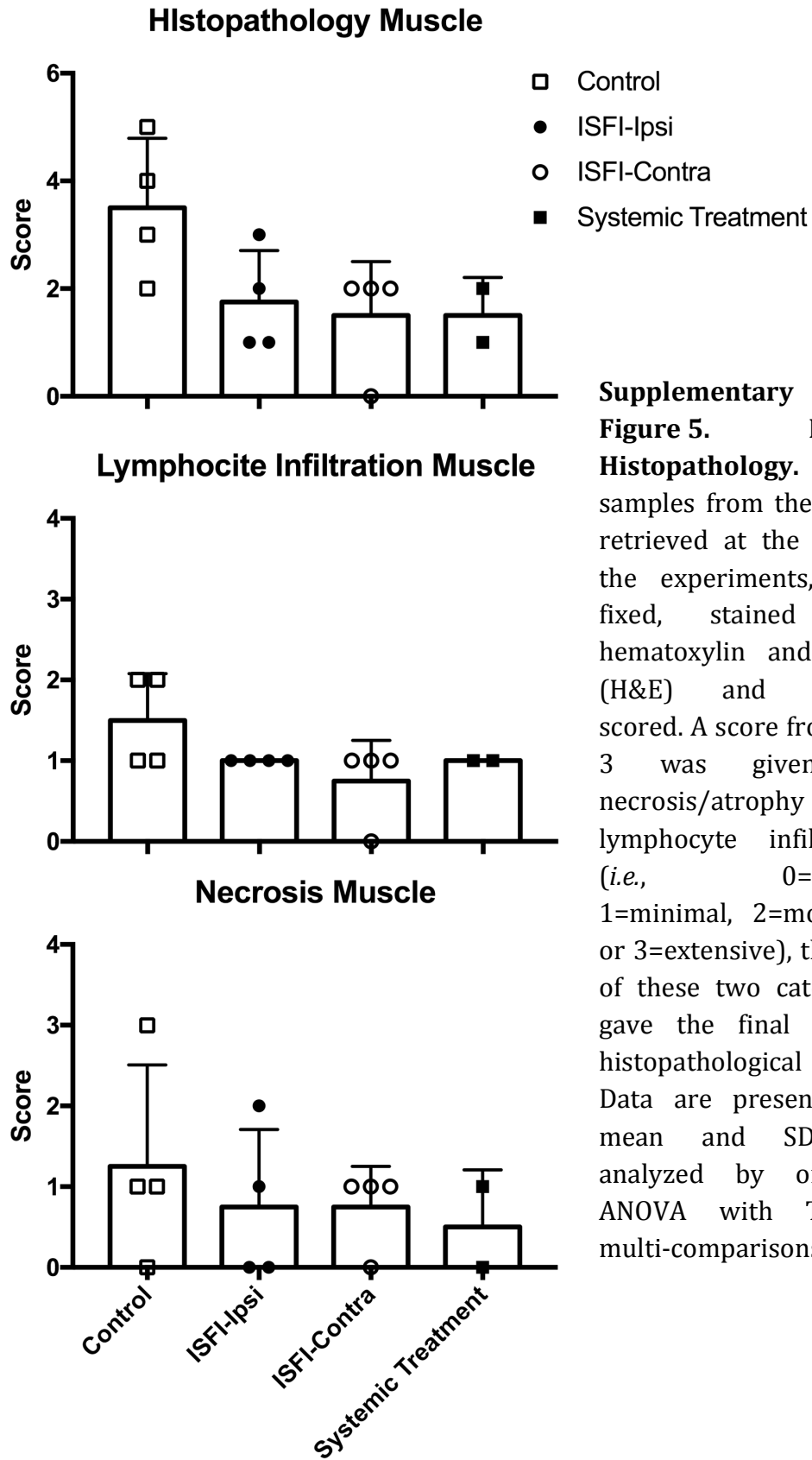


Supplementary Figure 3 (continued on next page). Donor lymphocyte infiltration in GvHD lesions. Flow-cytometry analysis of the lymphocyte infiltration in GvHD lesions in recipient ear and tongue. Tissues were retrieved at sacrifice, digested and stained for flow-cytometry. In all the samples dead cells were excluded by Fixable Viability Die (in AmCyan Channel), then single cells were selected and lymphocyte population was chosen based on physical parameters (first row). Among the lymphocytes, T cells were identified as CD3+ cells and donor cells as RT1Ac+ cells. Untreated rats rejecting their graft from Group 1, presented a great number of recipient T cells (CD3+RT1Ac- cells) in the transplanted skin and only a few in the contralateral skin, confirming the recipient T cell infiltration in the graft at rejection. In these rats the number of donor cells was relatively low in ear and tongue. Rats of Group 4 with macroscopic signs of GvHD showed clear infiltration of donor cells (RT1Ac+) and donor T cells (CD3+RT1Ac+) in the affected tissue (*i.e.*, ear and tongue) accompanied also by the infiltration of T cells of recipient origin due to strong inflammation. Representative pictures of 2 control rats and 3 rats with GvHD.



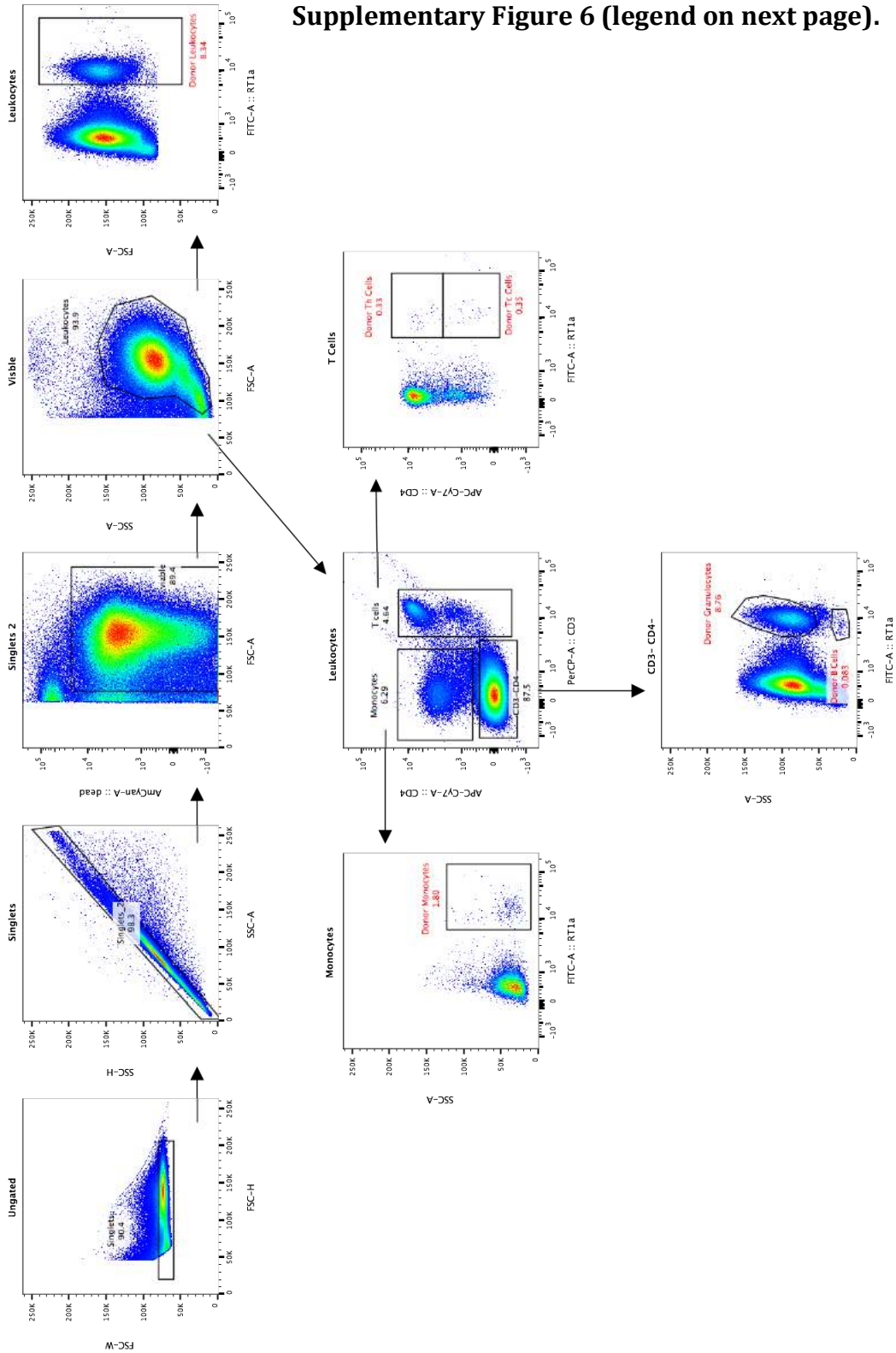


Supplementary Figure 4. Rats with GvHD showed significantly reduced response to BN cells as compared to untreated rats. Peripheral blood mononuclear cells were isolated at POD21 and stimulated either with donor cells (BN) or third party cells (Wistar). Proliferation was measured by evaluating CFSE dilution with Flow-Jo. Control rats from Group 1 (n=2) and rats from Group 4 treated with systemic rapamycin showing signs of GvHD (n=2) were compared. Data presented as mean and SD. P values were determined using the Holm-Sidak method.



Supplementary Figure 5. Muscle Histopathology. Muscle samples from the grafts, retrieved at the end of the experiments, were fixed, stained with hematoxylin and eosin (H&E) and blindly scored. A score from 0 to 3 was given for necrosis/atrophy and lymphocyte infiltration (*i.e.*, 0=absent, 1=minimal, 2=moderate or 3=extensive), the sum of these two categories gave the final muscle histopathological score. Data are presented as mean and SD and analyzed by one-way ANOVA with Tukey's multi-comparisons test.

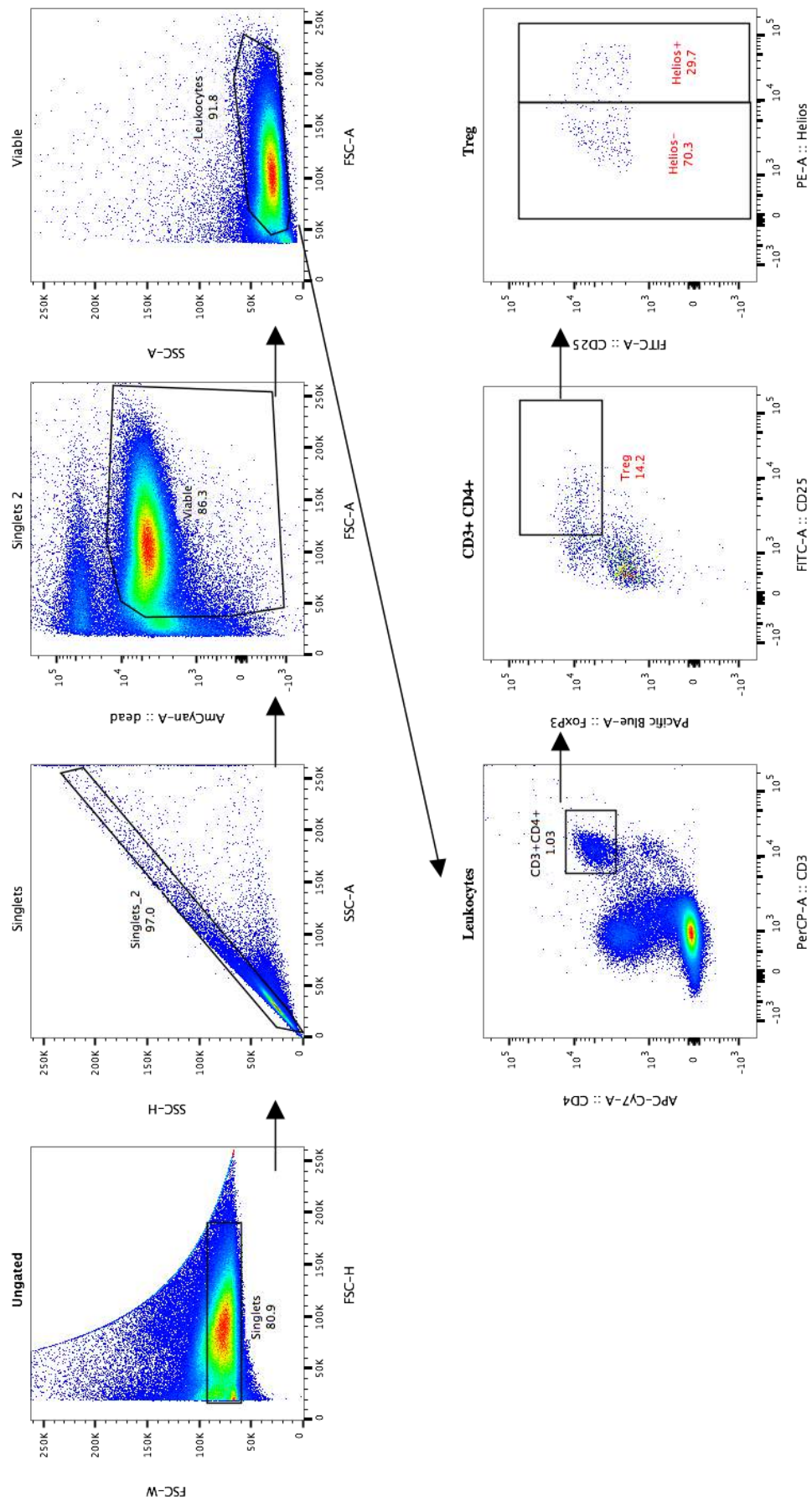
Supplementary Figure 6 (legend on next page).



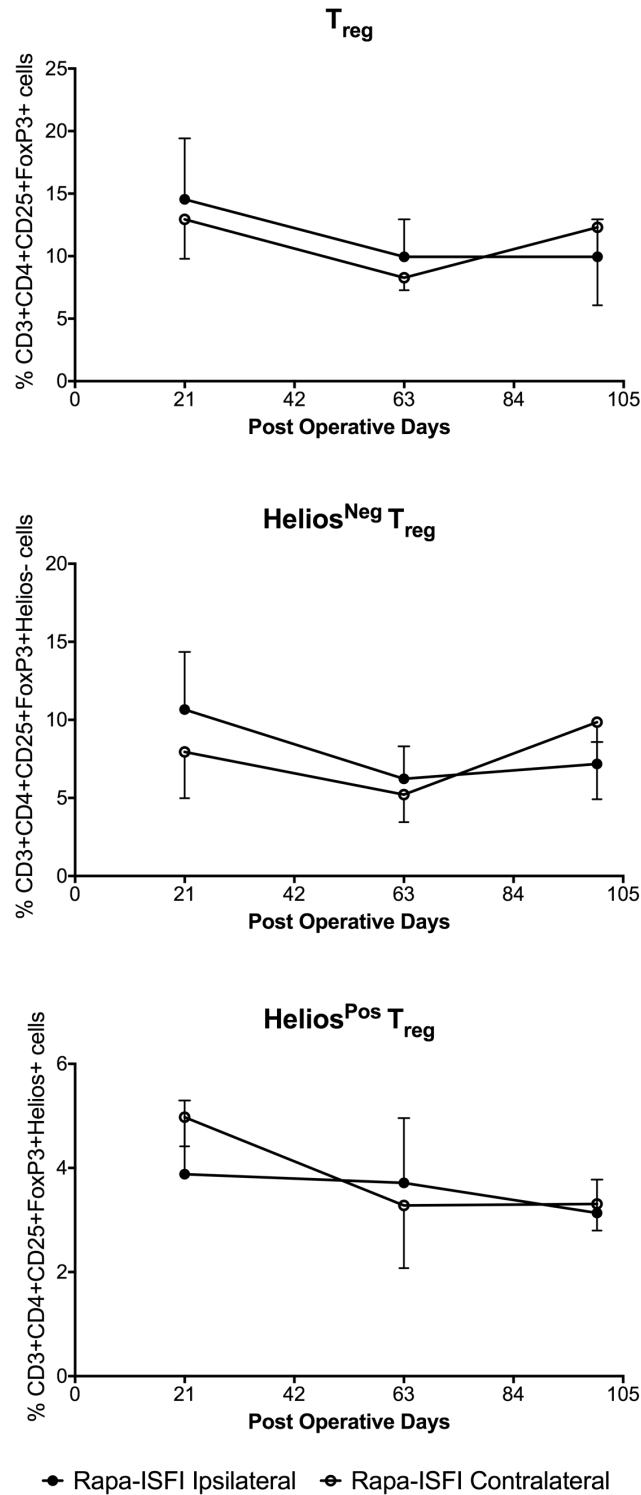
Supplementary Figure 6. Gating strategy for the quantification of multilineage chimerism levels in the peripheral blood of recipient rats.

Representative gating strategy for the quantification of multilineage chimerism levels in the peripheral blood of recipient rats at different time points after hind limb transplantation. After exclusion of doublets, dead cells and debris, donor cells (red names) were identified and quantified as frequency of circulating leukocytes. Positivity for the RT1Ac markers was set using naïve Lewis blood stained with the same panel as negative control. Donor leukocytes were identified as RT1Ac⁺ cells in the leukocytes gate; donor monocytes as CD3-CD4⁺RT1Ac⁺ leukocytes; donor T helper (Th) cells as CD3⁺CD4⁺ RT1Ac⁺ leukocytes; donor T cytotoxic (Tc) cells as CD3⁺CD4⁻ RT1Ac⁺ leukocytes. Donor B cells and granulocytes were identified in the CD3-CD4⁻ fraction based on their granularity (*i.e.*, side scatter) as CD3-CD4⁻SSC^{low}RT1Ac⁺and CD3-CD4⁻SSC^{high}RT1Ac⁺ leukocytes, respectively.

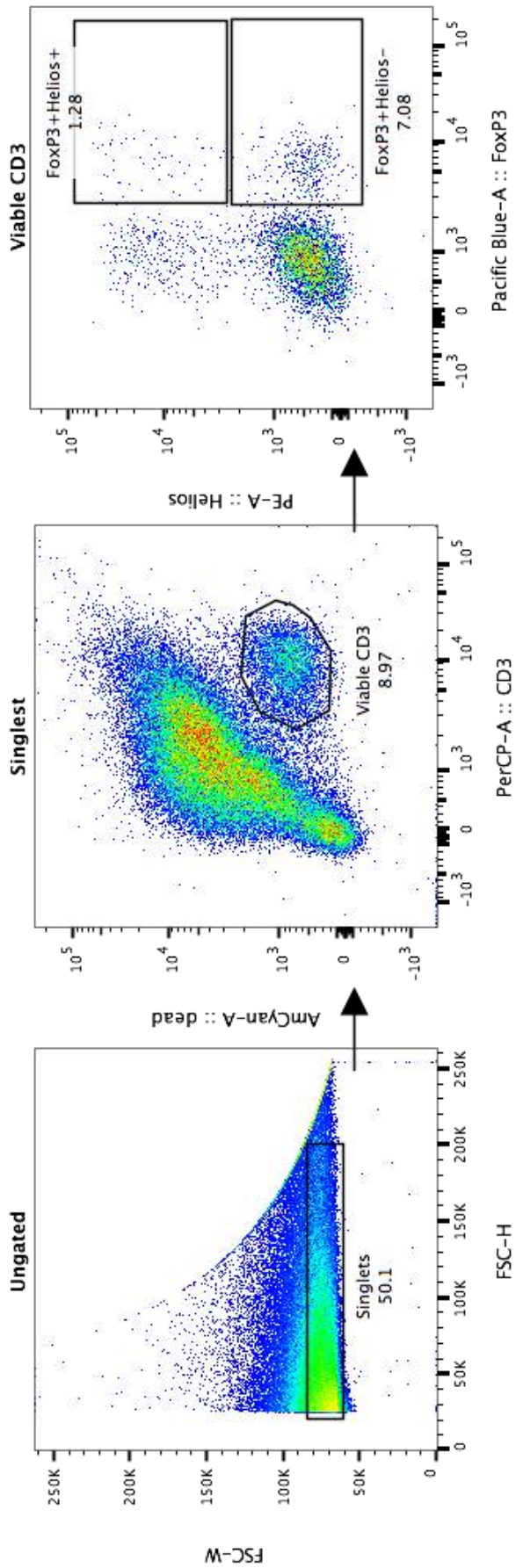
Supplementary Figure 7 (legend on next page).



Supplementary Figure 7. Gating strategy for the quantification of T_{reg}, Helios^{Pos} and Helios^{Neg} T_{reg} in the peripheral blood. T_{reg} were identified as CD3+CD4+CD25+FoxP3+ cells after exclusion of doublets, dead cells and debris. Helios^{Pos} and Helios^{Neg} cells were identified among the T_{reg} cells based on the expression of the transcription factor Helios. CD25 and FoxP3 positivity was set based on fluorescence minus one (FMO) controls. The frequency of all the T_{reg}, Helios^{Pos} T_{reg} and Helios^{Neg} T_{reg} was expressed as % of CD3+CD4+.



Supplementary Figure 8. The frequency of T_{reg}, Helios^{Pos} and Helios^{Neg} T_{reg} in the peripheral blood of the recipient rats treated with Rapa-ISFI remains stable during the experiment. T_{reg}, Helios^{Neg} T_{reg} and Helios^{Pos} T_{reg} were quantified at POD21, 63 and 100 in the peripheral blood of rats of Groups 2 (Rapa-ISFI Ipsilateral, black circles) and 3 (Rapa-ISFI-Cotralateral, open circle) as described. Data presented as mean and SD.



Supplementary Figure 9. Gating strategy for quantification of T_{reg}, Helios^{Pos} and Helios^{Neg} T_{reg} in the skin. Representative gating strategy for the enumeration of T_{reg} in the skin collected from VCA transplant. T_{reg} were identified as FoxP3+ cells after exclusion of doublets and selection of viable CD3+ cells. Helios^{Pos} and Helios^{Neg} cells were identified among the CD3+FoxP3+ T_{reg} based on the expression of the transcription factor Helios. The frequency of all the T_{reg} population was expressed as % Viable CD3+ cells.

3.3. Intra-graft injection of tacrolimus promotes survival of vascularized composite allotransplantation

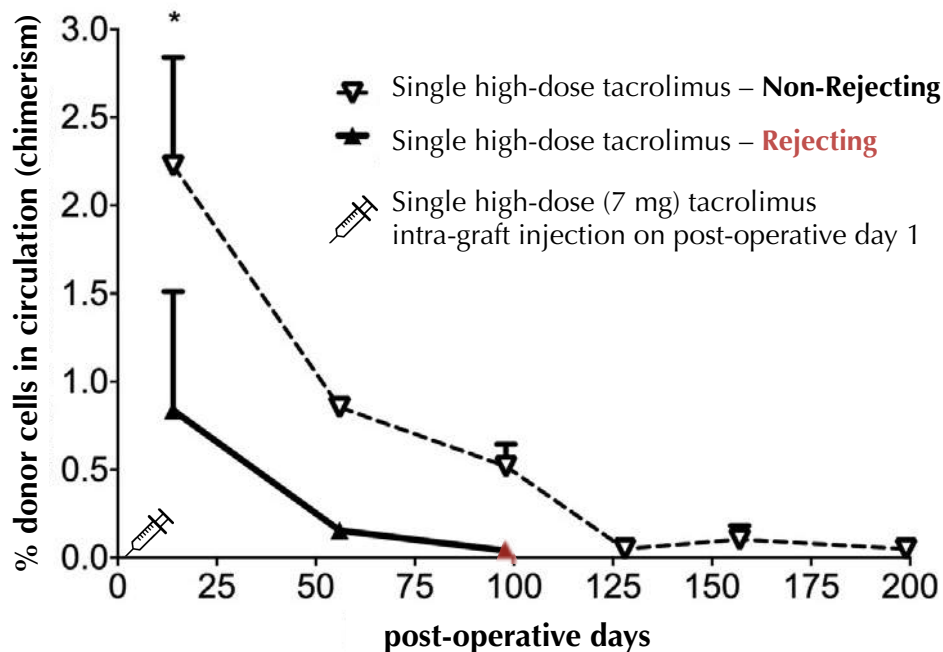
Radu Olariu, M.D.^{1,2}; Julie Denoyelle, M.Sc.²; Franck M. Leclère, M.D., Ph.D.^{1,2}; Dzhuliya V. Dzhonova, M.Sc.²; Thusitha Gajanayake, Ph.D.^{1,2}; Yara Banz, M.D.-Ph.D.³; Michael Hayoz, M.D.⁴; Mihai Constantinescu, M.D.^{1,2}; Robert Rieben, Ph.D.²; Esther Voegelin, M.D.^{1,2**}; Adriano Taddeo, Ph.D.^{1,2*}

¹Department of Plastic, Reconstructive, and Hand Surgery, Inselspital, Bern University Hospital, University of Bern, Bern, Switzerland; ²Department of Clinical Research, University of Bern, Bern, Switzerland; ³Institute of Pathology, University of Bern, Bern, Switzerland; ⁴University Institute of Clinical Chemistry, Inselspital, Bern University Hospital, University of Bern, Bern, Switzerland

Status: Published in *Journal of Surgical Research*, October 2017 (218) 49e57

Aim: To understand whether a TAC bolus injected intragraft could provide a long-term graft survival in a rat VCA model and whether it would have an influence on kidney and liver function. Here we sought an initial proof-of-concept and a potential mechanism (induction of Treg or chimerism) to develop long-term studies on localized DDS based on TAC.

Brown Norway-to-Lewis rat hind limb transplantation treated with a localized bolus injection of immunosuppression



Summary: A single bolus injection of TAC into the graft resulted in a dichotomy – half of the rats survived for 52–105 days, while the other half survived for >200 days after the transplantation. The later had significantly higher chimerism in post-operative day (POD) 14, which however did not induce central tolerance as evidenced by rejection of donor skin challenge at POD 215.

Available online at www.sciencedirect.com

ScienceDirect

journal homepage: www.JournalofSurgicalResearch.com

Intra-graft injection of tacrolimus promotes survival of vascularized composite allotransplantation

Radu Olariu, MD,^{a,b} Julie Denoyelle, MSc,^b Franck M. Leclère, MD, PhD,^{a,b}
Dzhuliya V. Dzhonova, MSc,^b Thusitha Gajanayake, PhD,^{a,b}
Yara Banz, MD, PhD,^c Michael Hayoz, MD,^d Mihai Constantinescu, MD,^{a,b}
Robert Rieben, PhD,^b Esther Vögelin, MD, PhD,^{a,b,**}
and Adriano Taddeo, PhD^{a,b,*}

^a Department of Plastic, Reconstructive, and Hand Surgery, Inselspital, Bern University Hospital, University of Bern, Bern, Switzerland

^b Department of Clinical Research, University of Bern, Bern, Switzerland

^c Institute of Pathology, University of Bern, Bern, Switzerland

^d University Institute of Clinical Chemistry, Inselspital, Bern University Hospital, University of Bern, Bern, Switzerland

ARTICLE INFO

Article history:

Received 16 February 2017

Received in revised form

12 April 2017

Accepted 11 May 2017

Available online 10 June 2017

Keywords:

Vascularized
composite allotransplantation
Drug delivery
Tacrolimus
Rat hind limb transplantation

ABSTRACT

Background: Immunosuppressive therapies derived from solid organ transplantation are effective in promoting survival of vascularized composite allotransplantation (VCA), but they cause serious side effects that are difficult to justify for this non-life-saving procedure. Unlike solid organ transplantation, hand and face transplants offer the possibility of site-specific immunosuppression for reducing systemic exposure while increasing intra-graft concentrations of the drug. Therefore, in this study, we tested whether a single intra-graft injection tacrolimus could promote VCA survival.

Methods: Brown Norway-to-Lewis hind limb transplantations were performed, and animals were left untreated (group I), treated with a daily injection of 1-mg/kg tacrolimus for 21 days (group 2) or injected with 7-mg tacrolimus directly into the transplanted limb on day 1 (group III). Graft rejection was monitored, and animals were sacrificed at grade 3 rejection or 200 days after transplantation.

Results: Intra-graft injection of tacrolimus significantly prolonged allograft survival as compared to untreated animals or animals treated with systemic tacrolimus. Half of the intra-graft-treated rats rejected their graft on average at day 70.5. Interestingly, the other half remained rejection-free for more than 200 days without signs of kidney or liver toxicity. In these animals, tacrolimus was detected in the VCA skin but not in the blood until day 200. Long-term survival was not linked to induction of donor-specific tolerance but to a higher level of lymphocyte chimerism.

* Corresponding author. Department of Clinical Research, University of Bern, Murtenstrasse 50, CH-3008, Bern, Switzerland. Tel.: +41 31 632 0299; fax: +41 31 632 7594.

** Corresponding author. Hand Surgery and Surgery of Peripheral Nerves, Inselspital, University Hospital of Bern, Freiburgstrasse 10, CH-3010 Bern, Switzerland. Tel.: +41 31 632 3534; fax: +41 31 632 3496.

E-mail addresses: esther.voegelin@insel.ch (E. Vögelin), adriano.taddeo@dkf.unibe.ch (A. Taddeo).

0022-4804/\$ – see front matter © 2017 Elsevier Inc. All rights reserved.

<http://dx.doi.org/10.1016/j.jss.2017.05.046>

Conclusions: Intra-graft delivery of tacrolimus may promote VCA survival by increasing tissue drug availability and promoting the establishment of transient chimerism and thus long-term graft acceptance.

© 2017 Elsevier Inc. All rights reserved.

Introduction

Vascularized composite allotransplantation (VCA) is emerging as a reconstructive option for patients suffering from extensive damage of nonvital body parts that cannot be treated with conventional surgical techniques.^{1,2} In the past 2 decades, several types of human VCA have been performed worldwide. These include hand and face transplantations, as well as arms, intestine and abdominal wall, knee, femur, larynx, uterus, and penis.³ Most of the hand (single or double) and face (partial or total) allotransplantations reported so far have achieved good functional and esthetic outcomes and considerably improved the patients' quality-of-life.⁴ However, due to its allogeneic nature, VCA needs both induction therapy and life-long immunosuppressive therapy (IST) to achieve long-term graft survival. As in solid organ transplantation (SOT), the use of IST to avoid rejection is associated with well-defined side effects, such as opportunistic infection, malignancy, and renal impairment.² Moreover, acute cellular rejection remains a major concern, with 85% of patients experiencing at least one episode during the first year.³ Similar to SOT, human VCA can also develop chronic rejection targeting preferentially skin and deep vessels and leading to graft vasculopathy and often to graft loss, as recently reviewed.⁵ The high incidence of acute rejection, the emerging evidence for chronic rejection, and the side effects of immunosuppression are the main limits to VCA development.

Inadequate immunosuppressive drug levels are one of the factors contributing to acute and chronic rejection of SOT, increasing the risk of therapeutic failure.⁶ Also in VCA, tacrolimus trough levels <5 ng/mL appear to be associated with a higher risk for acute rejection.⁷ Interestingly, higher tacrolimus trough levels in the first week after renal transplantation (>27.5 ng/mL) are associated with reduced 1-year acute rejection rates.^{8,9} This suggests that maintaining high-dose immunosuppression in the peritransplant period may promote changes in the early immunoresponse to donor antigens leading to long-term gains. However, the risks of moderate to severe adverse effects, particularly on the kidney, make it extremely difficult to further increase tacrolimus dosing.^{8,10}

Unlike SOT, VCA is readily accessible for local drug delivery. Transplant-targeted therapy may foster higher tissue levels of the drug reducing systemic exposure. In turn, this may reduce the intensity and frequency of acute rejection episodes and thus the development of chronic rejection, minimizing the risk for kidney toxicity. It has been reported that Banff grade 1-2 rejections can be treated solely with topical immunosuppressive drugs such as ointment containing tacrolimus and clobetasol, without increased systemic levels of immunosuppressive drugs.^{11,12} We have recently developed an injectable hydrogel that releases tacrolimus in response to inflammatory enzymes and prolongs VCA survival for more than 100 days.¹³ These encouraging studies make VCA transplants clear

candidates for the evaluation of novel transplant-targeted immunotherapeutic strategies. In this study, we hypothesized that the subcutaneous administration of high-dose tacrolimus immediately after transplantation may regulate the innate immunity/inflammatory responses in the peritransplant period promoting long-term survival of VCA.

Methods

Animal experiments

Inbred Lewis and Brown Norway rats (all male) weighing between 200g and 250g were purchased from Charles River. All animals were housed under standard conditions with water and food ad libitum. All animal experiments were performed in accordance with the terms of the Swiss animal protection law and were approved by the animal experimentation committee of the cantonal veterinary service (Canton of Bern, Switzerland). Experimental protocols were refined according to the 3R principles, and state-of-the-art anesthesia and pain management were used to minimize the number of animals and to reduce the exposure of the animals to stress and pain during the experiments.

Experimental design

Brown Norway-to-Lewis hind limb transplantation was performed as described previously.¹³ After hind limb transplantation, animals were randomly divided into three groups. In group I ($n = 4$), recipients were left untreated. In group II ($n = 6$), animals were treated with a daily subcutaneous injection in the neck of 1-mg/kg tacrolimus from day 1 to day 21. In group III ($n = 12$), 7-mg of tacrolimus dissolved in 200 μ L of sterile dimethyl sulfoxide (DMSO) was injected subcutaneously in four portions of 50 μ L circumferentially around the thigh region of the transplanted limb on postoperative day (POD) 1. Tacrolimus doses were decided based on our previous study showing that a hydrogel loaded with 7-mg tacrolimus could guarantee high-level tacrolimus in the first postoperative week, promoting long-term survival of an allogeneic limb.¹³ After the operation, rats were monitored, and clinical rejection was graded macroscopically as 0 = no rejection, 1 = erythema and edema, 2 = epidermolysis and exudation, and 3 = desquamation, necrosis, and mummification. The rats were sacrificed once grade 3 (rejection) was reached or at the end of the experiments (POD 200). Moreover, two long-term surviving rats underwent skin-transplantation (see [Full-thickness skin grafting](#)) and were kept beyond POD 200 for the time necessary to assess graft survival. Therefore, N number varied along the study because rats were sacrificed at different time points due to acute rejection. Donor skin challenge was performed only in two of six long-term surviving

animals due to the necessity to collect samples for skin and histology from the other animals ($n = 4$) to compare to animal from group I and animal from group III rejecting their graft. Experimental measurements (i.e., chimerism and regulatory T_{reg}) were performed in four animals per group. Importantly, rats of group III were retrospectively divided in (1) long-term survival or (2) rejection animals, leaving two rats per each subgroup.

Histopathology

Tissue samples from the grafts, retrieved at the end of the experiments, were fixed in 4% buffered formaldehyde, processed according to standard histopathological specimen work-up, sectioned at 3- μ m thickness, and stained with hematoxylin and eosin for microscopic evaluation. A pathologist blinded to treatment groups, scored all the samples. Skin samples were scored based on the Banff 2007 working classification of skin.¹⁴ Muscle samples were scored, and one point for any of the following manifestations was given: hemorrhage, vasculopathy, acute inflammation, necrosis, granulation tissue/chronic inflammation, fibrosis, and atrophy.

Biochemical analysis and quantification of plasma and skin levels of tacrolimus

Whole blood samples were collected into tubes containing EDTA-2K at different time points and stored at -20°C until analysis. Tacrolimus levels were measured by Liquid chromatography–mass spectrometry (LC-MS). Tacrolimus levels were prepared with the Kit MS1100 (ClinMass Complete Kit, advanced, for Immunosuppressants in Whole Blood, RECIPE Chemicals + Instruments GmbH, Munich, Germany) and quantified by LC-MS/MS.

Skin samples were collected on the day of sacrifice and were homogenized using a Qiagen TissueLyser II as described.¹⁵ Protein concentration was measured using a Bio-Rad DC Protein Assay kit, and 250 μ g of protein extract was analyzed using a PRO-Trac II Tacrolimus ELISA kit (DiaSorin) according to the manufacturer's instructions. Then, 250 μ g of total protein were resuspended in 100 μ L of buffer, and tacrolimus concentrations were expressed as ng/mL.

Full-thickness skin grafting

Donor-specific tolerance was assessed in two of six long-term survivors by skin graft challenge. Skin allografts with a dimension of 3×1.5 cm were harvested from the back of Brown Norway rats or syngeneic Lewis rats and transplanted onto the back of the long-term survivors 215 days after VCA. The grafts were thinned to encompass only skin and panniculus carnosus and were sutured with resorbable sutures into defects created in the recipient skin by excising skin on the back bilateral about 0.5 cm lateral to the posterior midline. A tie-over bolster dressing was applied and kept in place for 5 days after skin graft. On the fifth day after skin graft, the dressings were removed, and on ensuring adequate take, the grafts were evaluated daily for signs of rejection defined as secondary necrosis of the revascularized skin graft.

Flow cytometry analysis of chimerism and T regulatory cells

Peripheral blood mononuclear cells (PBMCs) were isolated from EDTA blood at different time points by Ficoll density gradient centrifugation. PBMCs were incubated with the Brown Norway specific marker RT1ⁿ (MHC Class I, clone MCA 156/OX-27, FITC conjugated, Serotec) to verify the chimerism levels. For the measurement of T regulatory cells (T_{reg}), PBMCs were incubated with anti-rat mAbs anti-CD4-PE and anti-CD25-APC (eBioscience) fix and permeabilized using the Foxp3/Transcription Factor Staining Buffer Set (eBioscience) and incubated with Anti-FoxP3 mAbs (eBioscience). After staining, PBMCs were analyzed by flow cytometry using a SORP LSRII flow cytometer (BD Biosciences) and BD Diva Software. Data were analyzed using FlowJo software (Tree Star). Positivity for the RT1ⁿ marker was determined using PBMC from naïve Lewis rats as negative controls. Fluorescence minus one controls were used to set the cutoff for the T_{reg} analysis.

Statistical analysis

Statistical analysis was performed using the GraphPad Prism, version 6 program (GraphPad Software). The results are expressed as means \pm standard deviation. Survival of the allografts was examined using Kaplan-Meier analysis, and groups were compared using the log-rank test. Groups were compared using one-way analysis of variance. Post hoc correction with Tukey's multiple comparisons test was used to compare means of all groups; Sidak multiple comparisons tests was used to compare mean of rejecting and long-term survival rats. Significance was defined as $P < 0.05$.

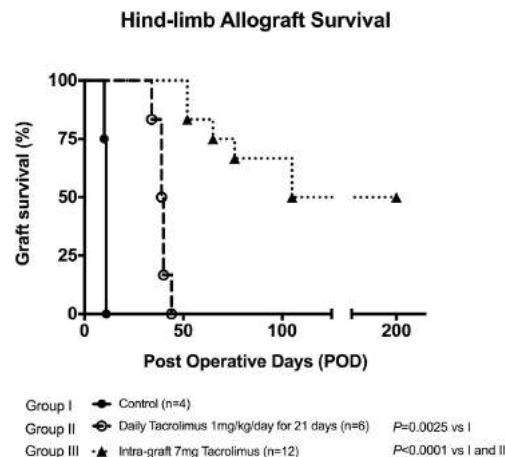


Fig. 1 – Vascular composite allograft survival. Kaplan-Meier graft survival curves for the allograft of Brown Norway-to-Lewis orthotopic hind limb transplantation of the three groups. Group I ($n = 4$) was left untreated. Group II ($n = 6$) was treated with daily subcutaneous injections in the neck of 1-mg/kg tacrolimus for 21 days. Group III ($n = 12$) was treated with a single subcutaneous injection of 7-mg tacrolimus directly into the transplanted limb on POD 1. P values were calculated by log-rank (Mantel-Cox) test.

Results

A single intra-graft injection of tacrolimus promotes VCA survival

To test the hypothesis that a single intra-graft injection of tacrolimus may prevent VCA rejection, hind limb transplantations were performed from Brown Norway-to-Lewis rats. As shown in Figure 1, transplanted limbs of untreated rats (group I) survived with a median survival time (MST) of 11 days. Transplanted hind limbs on rats treated with daily subcutaneous injection of tacrolimus for 21 days (group II) showed significant increase of graft survival (MST = 39.5 days; $P = 0.0025$). However, all the rats rejected their grafts after tacrolimus withdrawal. Rats injected with high-dose tacrolimus into the graft at POD 1 (group III), showed a graft MST of

152.5 POD and thus significantly higher than in the other two groups ($P < 0.0001$ both versus group I and II). Interestingly, in this group, half of the rats ($n = 6$) rejected their grafts between POD 52 and POD 105, with an MST of 70.5 days, showing a progressive rejection episode macroscopically similar to the untreated rats. The other half of the rats ($n = 6$) did not develop any rejection signs and remained rejection-free for more than 200 days posttransplantation without any further intervention.

To better characterize the rejection process in group III, skin and muscle samples of this group were histologically evaluated. Rats of group 3 were divided in rejecting or non-rejecting rats based on the macroscopic evaluation. Their histopathological score was compared to untreated controls. As shown in Figure 2A and B, skin collected from rats of the group III rejecting their graft presented similar histopathological features as compared to untreated rats (mean of histopathological score 3.7 and 4, respectively). Necrosis of the

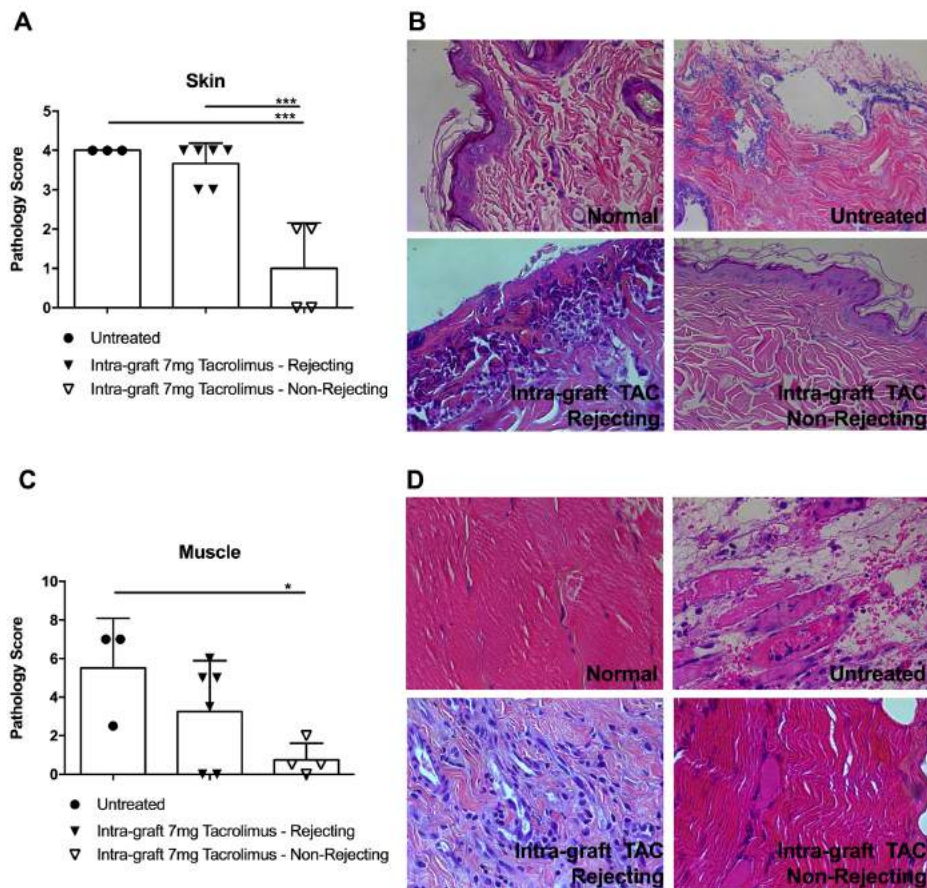


Fig. 2 – Histopathological evaluation. Histopathological score and representative photomicrographs of the skin (A and B) and gastrocnemius muscle (C and D). Untreated rats (● $n = 3$), rats treated with a single intra-graft injection of 7-mg tacrolimus (group III), which have rejected their grafts (▼ $n = 6$) or with long-term surviving VCA (▽ $n = 4$). Magnification 40x. Data were presented as means \pm SD. P values calculated by one-way ANOVA with Tukey's post hoc correction. * $P < 0.05$, *** $P \leq 0.001$.

tissue was evident in both of the groups with severe cell infiltration. Long-term survival grafts collected at POD 200 showed significantly lower histopathological injury scores as compared to the rejection rats of the group I and III (mean of histopathological injury score 1, $P \leq 0.001$ versus both group I and group III-rejecting). These rats showed minor signs of rejection with minimal mononuclear cell infiltration. Muscle tissue collected from the same rats showed similar differences among the groups, with a significant decrease in injury score of nonrejecting rats as compared to untreated rats (Fig. 2C and D). Skin and muscle from the contralateral limb was also analyzed. As expected, all the samples presented a normal histological structure, graded as 0 (not shown).

High-dose intra-graft tacrolimus does not induce liver and renal toxicity

To test whether the single, high-dose intra-graft tacrolimus injections could induce kidney or liver toxicity in rats from group III, we performed a biochemical analysis for creatinine, blood urea nitrogen, aspartate aminotransferase (AST), and alanine aminotransferase. Rats from group III did not show significant changes in any of the biochemical parameters studied, demonstrating a stable kidney and liver function. We observed an increase of AST at POD 70 only in the rats that

underwent rejection in the next few days. Conversely, the long-term surviving rats did not show any increase in AST levels, and all the biochemical parameters remained stable until the end of the experiment (Fig. 3). This AST increase in the rejecting rats is most likely secondary to chronic muscular injury due to VCA rejection (see Fig. 2), which could cause a direct release of the enzyme from necrotic muscular tissue.^{15,16}

Tacrolimus is persistently detectable in the skin but not in the blood

Plasma and skin levels of tacrolimus were measured in group III. We previously showed that administration of 7 mg of tacrolimus subcutaneously on POD 1 resulted in a peak of tacrolimus levels in the blood followed by a rapid decline over time.¹³ Here, we measured the blood levels of tacrolimus in group III at POD 57, 70, 98, 128, 170, and 200 using LC-MS. At these time points, all the analyzed samples ($n = 6$) showed undetectable tacrolimus in the blood (not shown), confirming that tacrolimus is not measurable systemically after POD 57. Tacrolimus concentrations in the skin of the transplanted limbs were measured at the different sacrifice points by ELISA. Tacrolimus concentration was higher than 30 ng/mL at POD 52 (Fig. 4). This value decreased to 5 ng/mL at POD 105 and remained constant in the long-term surviving grafts sacrificed at POD 200.

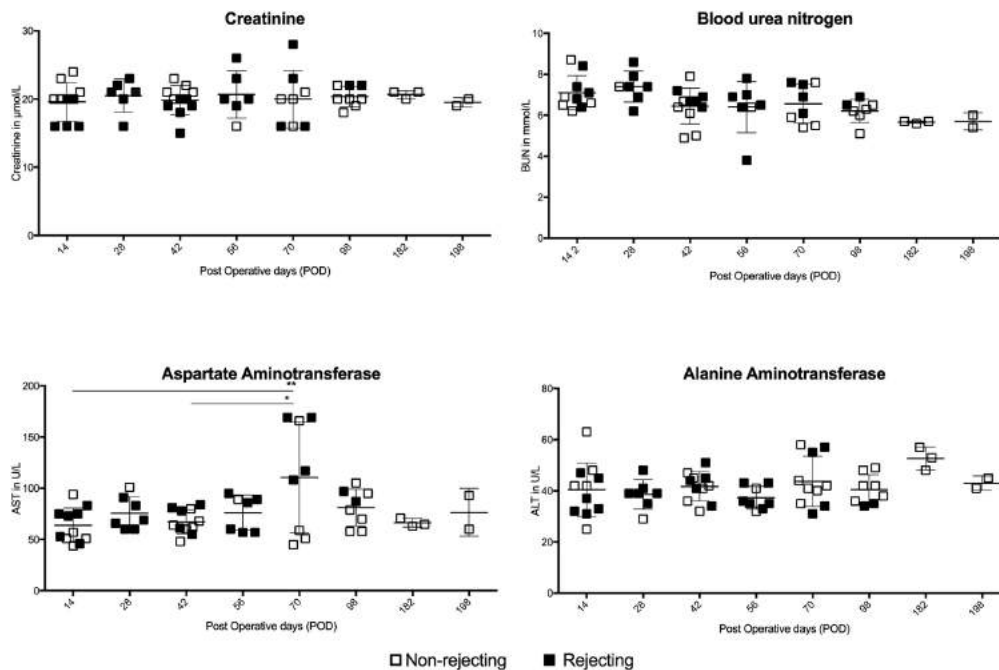


Fig. 3 – Blood biochemical parameters during the study in group III. Biochemical parameters were quantified on recipient rats treated with a single intra-graft injection of tacrolimus in plasma at different time points by LC-MS. Renal toxicity was analyzed by measuring creatinine and blood urea nitrogen (BUN). Liver toxicity was analyzed by measuring aspartate aminotransferase and alanine aminotransferase. Nonrejecting rats are represented with open symbols (□) and rats rejecting their graft are represented with full symbol (■). *N* number is reported in the graphs for each time point. Data were presented as means \pm SD. *P* values calculated by one-way ANOVA with Tukey's post hoc correction. * $P \leq 0.05$, ** $P \leq 0.01$.

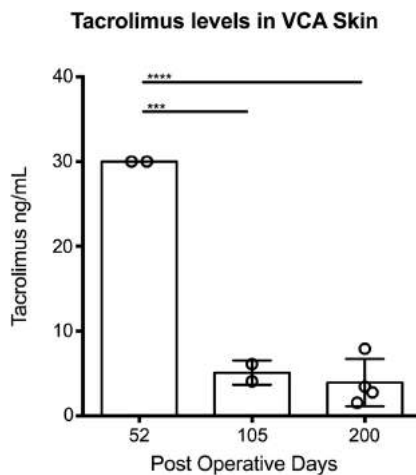


Fig. 4 – Levels of tacrolimus in the VCA skin in intra-graft-treated rats. Tissue levels of tacrolimus in the skin of the transplanted limbs were measured in group III at sacrifice time. Skin was collected from rats rejecting their graft at POD 52 ($n = 2$), 105 ($n = 2$), and from long-term surviving rats ($n = 4$). Tacrolimus concentration in 250- μ g of protein extract was measured by ELISA. Data were presented as means \pm SD. P values calculated by one-way ANOVA with Tukey's post hoc correction. **** $P \leq 0.001$, ***** $P \leq 0.0001$.

Higher hematopoietic chimerism in long-term surviving as compared to rejecting grafts

As we observed two different behaviors (long-term survival or rejection) within the group treated with a high dose of intra-graft tacrolimus, we sought to determine why only some recipients reached long-term allograft survival. Therefore, we

retrospectively analyzed the frequency of T regulatory cells and the level of peripheral chimerism in the rat from group III. As shown in Figure 5A, no significant changes were observed in the frequency of T_{reg} cells of long-term survival rats as compared to rejecting rats at any of the time point analyzed. However, a significantly higher level of peripheral chimerism was found in nonrejecting rats at POD 14 (2.23 ± 0.62 and $0.84 \pm 0.67\%$ of PBMC, respectively; $P = 0.03$; Fig. 5B). Moreover, in rats with long-term surviving allograft, donor cells were detectable until POD 98 as compared to POD 56 in rejecting rats ($0.52 \pm 0.13\%$ versus $0.16 \pm 0.02\%$ donor cells among PBMCs, respectively).

A single intra-graft injection of tacrolimus does not induce central tolerance

To test whether the promotion of long-term graft survival is due to the induction of donor-specific tolerance, two long-term survivors were transplanted with Brown Norway skin at POD 215. Both of the rats rejected the transplanted skin (Fig. 6). As expected, syngeneic Lewis-skin grafts were accepted.

Discussion

The side effects secondary to life-long immunosuppression are one of the main limitations to the widespread adoption of VCA as quality-of-life-improving procedure. To date, most of the VCA centers worldwide continue to use conventional immunosuppression regimens extrapolated from SOT.⁷ These protocols have proven to be effective in promoting graft survival. However, morbidity caused by the required drugs is high, making it desirable to develop immunosuppressive therapies able to avoid rejection, while reducing adverse events, such as infection and malignancy.²

In this study, we demonstrated that a single high dose of tacrolimus delivered into the graft 1 day after transplantation

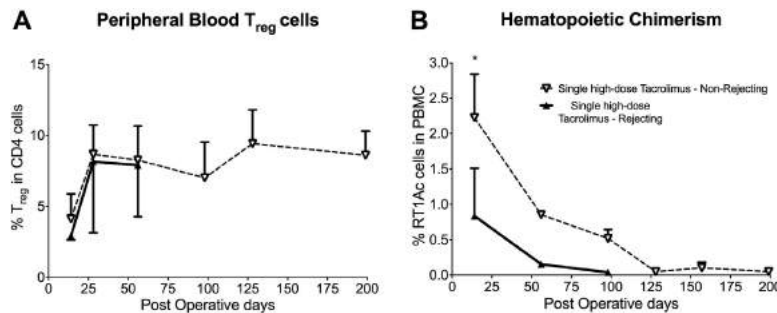


Fig. 5 – Analysis of the frequency of T_{reg} and donor cells in the PBMCs of rats from group III. T regulatory cells (T_{reg}) and donor-derived cells were measured in the PBMCs isolated at different time point from Lewis recipients treated with an intra-graft injection of tacrolimus at high dose ($n = 2$ per time point). Rats were divided based on the transplant outcome in rats rejecting their graft (\blacktriangle continuous line) or in long-term surviving graft (∇ dashed line). (A) T_{reg} were identified as $CD4+CD25 + Foxp3+$ cells based on FMO controls after exclusion of debris and doublets. Data are reported as percentage of T_{reg} in the CD4 population. (B) Brown Norway cells in transplant recipients were identified as $RT1^b$ positive cells, using naïve Lewis rats as negative controls after exclusion of debris and doublets. Data are reported as frequency on Brown Norway cells in the isolated PBMCs. Data presented as means \pm SD. P values calculated by one-way ANOVA with Sidak post hoc correction. * $P \leq 0.05$.

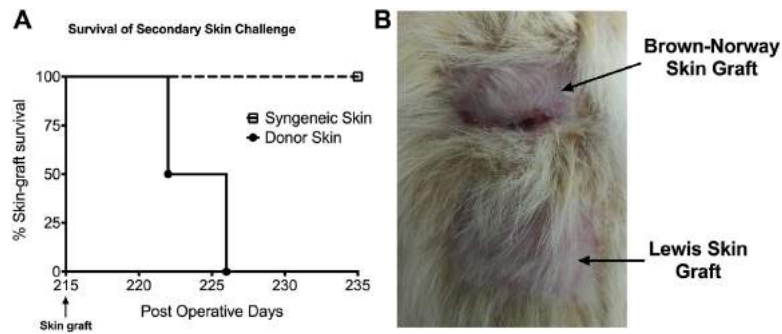


Fig. 6 – Absence of central immunological tolerance in long-term surviving graft recipients. Recipients bearing a long-term surviving hind limb allograft ($n = 2$) were challenged at POD 215 with secondary full-thickness skin from Brown Norway (BN) donor or Lewis syngeneic rats. (A) Kaplan-Meier graft survival curves of syngeneic or donor skin transplant. (B) Representative macroscopic picture of the graft showing that all the recipients rejected donor skin (upper transplant with contracted and scarred wound) and accepted the syngeneic Lewis skin (lower-transplant with hair growth and healed wound).

can promote long-term survival of VCA without inducing systemic toxicity in a rat model. Interestingly, half of the rats rejected their graft with an MST of 70.5 days. The other half displayed an extraordinary, uncomplicated postoperative follow-up with no evidence of rejection for >200 days despite the complete absence of further immunosuppressive therapy. Histological evaluation of these long-term surviving allografts confirmed the absence of histopathologically evident rejection.

Notably, only the intra-graft administration of tacrolimus promotes survival until the end of the experiment. Systemic administration of 1-mg/kg tacrolimus for 21 days for a total amount of about 6.3 mg of drug is able to prolong graft survival as compared to untreated animals. However, the graft is quickly rejected after drug withdrawal (MST = 40 days), in agreement with two previous studies in which 25 or 4 mg of tacrolimus were delivered systemically.^{17,18} Indefinite graft survival in hind limb transplantation using systemic immunosuppression has been reported in two studies. Both of the studies used a 2-week course including tacrolimus (2 mg/kg/d), mycophenolate mofetil (MMF) (15 mg/kg/d), and prednisolone (0.5 mg/kg/d). After these 2 weeks, prednisolone and MMF were gradually tapered, and by week 7, the animals were on tacrolimus only. Tacrolimus was then tapered to a maintenance dose, and then completely discontinued.^{19,20} Only one of these studies used the more stringent, high-responder Brown Norway-to-Lewis limb transplant model (as in our study). The authors reported that six of 23 rats (26%) achieved the 1-year end point with some rats experiencing single or multiple rejection episodes, which required a salvage therapy.²⁰ Therefore, when compared with these studies, the intra-graft delivery of 7-mg tacrolimus seems more efficient in prolonging graft survival with 50% of the rats reaching the end point of 200 days and the other 50% reaching an MST of 70.5 POD without added immunosuppression. Moreover, the quantity of immunosuppressive drug is drastically reduced, avoiding the 2-week course triple immunosuppression and any salvage therapy (only 7 mg of tacrolimus delivered in the

graft as compared to more than 226 mg of tacrolimus, 728 mg of MMF, and 24.3 mg of prednisone delivered systemically²⁰). Importantly, the injection of 7 mg of tacrolimus in the graft did not cause kidney or liver dysfunction. However, we did not analyze other side effects linked to the use of tacrolimus (e.g., hyperglycemia, hyperkalemia, and so forth), and further studies are warranted order to evaluate the long-term systemic toxicity of locally administered tacrolimus.

In rats treated with a single high-dose of tacrolimus, measurable concentrations of the drug were present in the VCA skin until the end point. At the same time points, tacrolimus was not measurable in the blood, suggesting that the intra-graft injection of the drug may promote a stable tissue concentration in absence of trough concentrations of tacrolimus. Hence, this long-lasting availability of tacrolimus in the tissue may play an important role in long-term graft survival. How a single intra-graft injection of tacrolimus can promote such long-lasting tissue availability remains unclear. Several studies have highlighted the interest of intracellular measurement and the lack of relationship between intracellular and blood concentrations for tacrolimus (reviewed in the study by Capron *et al.*²¹). Therefore, pharmacokinetic studies specifically designed at analyzing tacrolimus distribution after intra-graft application are needed. Notably, some of the rats rejected although tacrolimus was still detectable in the skin, suggesting that this is not the sole mechanism responsible for long-term survival.

In kidney transplant recipients, long-term stable kidney allograft survival without maintenance of immunosuppression can be achieved following transient mixed chimerism induction.^{22,23} Mixed chimerism is defined as the engraftment of donor hematopoietic stem cells in the recipient, leading to viable coexistence of both donor and recipient leukocytes.²⁴ Here, we show that the injection of a single high-dose of tacrolimus at POD 1 directly into the graft is able to promote transient mixed chimerism. Interestingly, a more persistent and significantly higher level of chimerism is observed in recipients with long-term surviving graft as compared to

rejecting recipients from the same group. In our study, chimerism was not associated with central tolerance induction, but with a state of immunological unresponsiveness to the graft. Hewitt *et al.* documented that development of a level of hematopoietic chimerism >60% was associated with development of graft versus host disease, whereas the presence of a stable chimerism level <14%, was associated with tolerance induction in limb allograft recipients.²⁵ Our therapy is able to promote chimerism levels ranging from 2% to 0.5% in the long-term surviving group. It is likely that such chimerism levels may not induce stable central tolerance. Recent evidence suggest that regulatory (i.e., nondeletional) mechanisms help promote long-term graft survival in chimeric recipient (reviewed in the study by Hock *et al.*²⁶). Although we could not demonstrate an increase in the frequency of T_{reg} in the peripheral blood, it is likely that the delivery of IST into the graft may induce the differentiation of tissue residence cells toward a regulatory rather than effector phenotype.

Based on the results of our study, we speculate that the intra-graft injection of tacrolimus at POD 1 may minimize the detrimental inflammation of the peritransplant period. This, together with the long-lasting availability of tacrolimus in the tissue, may lead to a balance between the graft and recipient-derived leukocytes, promoting the establishment of transient chimerism and the generation of tissue resident donor-specific regulatory cells and long-term graft survival.

One of the main limitations of this study is the use of a rodent model to test this new immunosuppressive approach to prevent rejection. Successful immunotherapies in animal models, when translated into the clinic, have produced limited success to date, likely in part because of the many species-specific differences between rodents and human immune responses.²⁷ Moreover, similar to other comparable studies,^{28,29} the necessity to retrospectively divide a group of rats in long-term surviving and rejecting animals after 200 days, decreased the statistical power of our study, and some of the reported immunological analysis should be confirmed in larger animal experiments. However, using this model, we could demonstrate that locally delivered immunosuppression may promote long-term graft survival, and we could gain the first insight in the mechanisms of the therapy.

Conclusions

In this study, we demonstrated that the direct availability of VCA for treatment may allow designing graft-targeted IST, to increase both the local availability of the drug and its immunomodulatory properties. This new approach can improve patient compliance and long-term outcomes reducing off-target toxicity and the intensity and frequency of acute rejection episodes as well as the development of chronic rejection.

Acknowledgment

LC-MS analyses and measurement of kidney and liver damage markers were performed at the Clinical Metabolomics Facility,

Center of Laboratory Medicine from the Bern University Hospital (Inselspital). Images were acquired on equipment supported by the Microscopy Imaging Center of the University of Bern. Histological samples were prepared with the help Markus Bänziger and the histopathology department as well as Prof. Zlobec's team at the translational research unit of the Institute of Pathology.

Funding: A.T. was supported by a grant-in-aid of the Department of Clinical Research of the University of Bern; E.V., M.C., and R.R. were supported by the Swiss National Science Foundation, grant no. 32003B_138434; and E.V. was supported by the American Society for Surgery of the Hand.

Authors' contributions: R.O., R.R., E.V., and A.T. designed the research and analyzed data; R.O., J.D., D.V.D., T.G., and A.T. designed and performed animal experiments, analyzed the respective data; F.M.L. designed and performed limb transplantation experiments; Y.B. analyzed the histology; M.H. performed the LC-MS analysis; M.A.C. designed and supervised the transplantation experiments; and R.R., E.V., and A.T. carried the overall responsibility for the project. R.O., E.V., and A.T. wrote the manuscript. All authors read and approved the final version of the manuscript.

Disclosure

The authors of this article have no conflicts of interest to disclose.

REFERENCES

- Murphy BD, Zuker RM, Borschel GH. Vascularized composite allotransplantation: an update on medical and surgical progress and remaining challenges. *J Plast Reconstr Aesthet Surg.* 2013;66:1449–1455.
- Pomahac B, Gobble RM, Schneeberger S. Facial and hand allotransplantation. *Cold Spring Harb Perspect Med.* 2014;4:1–14.
- Petruzzo P, Lanzetta M, Dubernard J-M, et al. The International Registry on hand and composite tissue transplantation. *Transplantation.* 2010;90:1590–1594.
- Breidenbach WC, Meister EA, Becker GW, et al. A statistical comparative assessment of face and hand transplantation outcomes to determine whether either meets the standard of care threshold. *Plast Reconstr Surg.* 2016;137:214e–222e.
- Kanitakis J, Petruzzo P, Badet L, et al. Chronic rejection in human vascularized composite allotransplantation (hand and face recipients): an update. *Transplantation.* 2016;100:2053–2061.
- O'Leary JG, Samaniego M, Barrio MC, et al. The Influence of Immunosuppressive Agents on the Risk of De Novo Donor-Specific HLA Antibody Production in Solid Organ Transplant Recipients. *Transplantation.* 2016;100:39–53.
- Kueckelhaus M, Fischer S, Seyda M, et al. Vascularized composite allotransplantation: current standards and novel approaches to prevent acute rejection and chronic allograft deterioration. *Transpl Int.* 2016;29:655–662.
- Gaynor JJ, Ciancio G, Guerra G, et al. Lower tacrolimus trough levels are associated with subsequently higher acute rejection risk during the first 12 months after kidney transplantation. *Transpl Int.* 2016;29:216–226.
- O'Seaghda CM, McQuillan R, Moran AM, et al. Higher tacrolimus trough levels on days 2-5 post-renal transplant are

- associated with reduced rates of acute rejection. *Clin Transplant*. 2009;23:462–468.
10. O'Regan JA, Canney M, Connaughton DM, et al. Tacrolimus trough-level variability predicts long-term allograft survival following kidney transplantation. *J Nephrol*. 2016;29:269–276.
 11. Solari MG, Washington KM, Sacks JM, et al. Daily topical tacrolimus therapy prevents skin rejection in a rodent hind limb allograft model. *Plast Reconstr Surg*. 2009;123:175–255.
 12. Gharb BB, Rampazzo A, Altuntas SH, et al. Effectiveness of topical immunosuppressants in prevention and treatment of rejection in face allotransplantation. *Transplantation*. 2013;95:1197–1203.
 13. Gajanayake T, Olariu R, Leclère FM, et al. A single localized dose of enzyme-responsive hydrogel improves long-term survival of a vascularized composite allograft. *Sci Transl Med*. 2014;6:249ra110.
 14. Cendales LC, Kanitakis J, Schneeberger S, et al. The Banff 2007 working classification of skin-containing composite tissue allograft pathology. *Am J Transplant*. 2008;8:1396–1400. Blackwell Publishing Ltd.
 15. Nathwani RA, Pais S, Reynolds TB, Kaplowitz N. Serum alanine aminotransferase in skeletal muscle diseases. *Hepatology*. 2005;41:380–382.
 16. Brancaccio P, Lippi G, Maffulli N. Biochemical markers of muscular damage. *Clin Chem Lab Med*. 2010;48:757–767.
 17. Fealy MJ, Umansky WS, Bickel KD, Nino JJ, Morris RE, Press BH. Efficacy of rapamycin and FK 506 in prolonging rat hind limb allograft survival. *Ann Surg*. 1994;219:88–93.
 18. Hautz T, Zelger B, Grahmmer J, et al. Molecular markers and targeted therapy of skin rejection in composite tissue allotransplantation. *Am J Transplant*. 2010;10:1200–1209.
 19. Lanzetta M, Ayrout C, Gal A, et al. Experimental limb transplantation, part II: excellent return of function and indefinite survival after withdrawal of immunosuppression. *Transplant Proc*. 2004;36:675–679.
 20. Kanatani T, Wright B, Lanzetta M, Molitor M, McCaughan GW, Bishop GA. Experimental limb transplantation, part III: induction of tolerance in the rigorous strain combination of Brown Norway donor to Lewis recipient. *Transplant Proc*. 2004;36:3276–3282.
 21. Capron A, Haufroid V, Wallemacq P. Intra-cellular immunosuppressive drugs monitoring: a step forward towards better therapeutic efficacy after organ transplantation? *Pharmacol Res*. 2016;111:610–618.
 22. Kawai T, Sachs DH, Sykes M, Cosimi AB. Immune Tolerance Network. HLA-mismatched renal transplantation without maintenance immunosuppression. *N Engl J Med*. 2013;368:1850–1852.
 23. Kawai T, Sachs DH, Sprangers B, et al. Long-term results in recipients of combined HLA-mismatched kidney and bone marrow transplantation without maintenance immunosuppression. *Am J Transplant*. 2014;14:1599–1611.
 24. Fuchs EJ. Transplantation tolerance: from theory to clinic. *Immunol Rev*. 2014;258:64–79.
 25. Black KS, Hewitt CW. Composite tissue (limb) allografts in rats. II. Indefinite survival using low-dose cyclosporine. *Transplantation*. 1985;39:365–368.
 26. Hock K, Mahr B, Schwarz C, Wekerle T. Deletional and regulatory mechanisms coalesce to drive transplantation tolerance through mixed chimerism. *Eur J Immunol*. 2015;45:2470–2479.
 27. Mestas J, Hughes CCW. Of mice and not men: differences between mouse and human immunology. *J Immunol*. 2004;172:2731–2738.
 28. Jindal R, Unadkat J, Zhang W, et al. Spontaneous Resolution of acute rejection and tolerance induction with IL-2 Fusion protein in vascularized composite allotransplantation. *Am J Transplant*. 2015;15:1231–1240.
 29. Lin CH, Zhang W, Ng TW, et al. Vascularized osteomyocutaneous allografts are permissive to tolerance by induction-based immunomodulatory therapy. *Am J Transplant*. 2013;13:2161–2168.

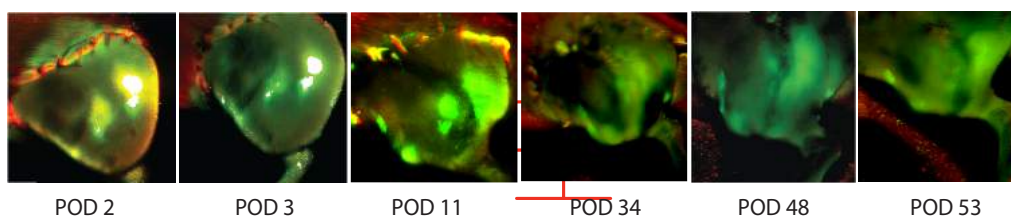
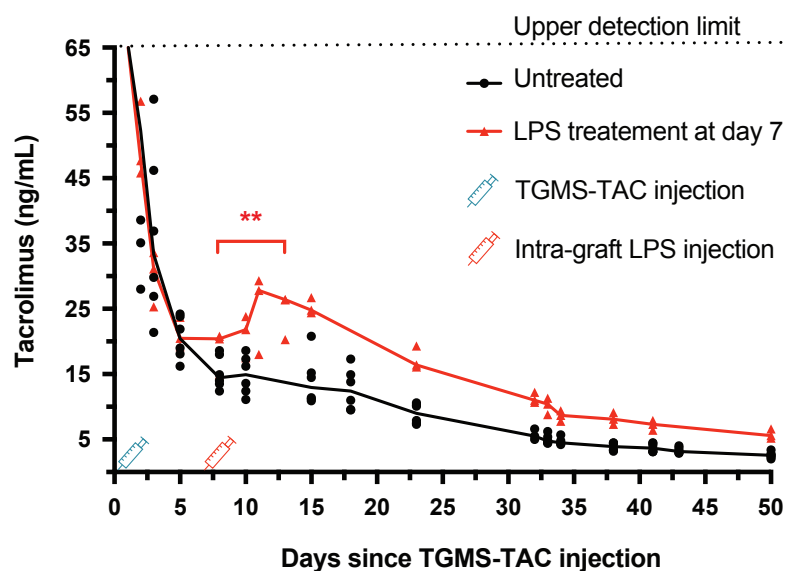
3.4. In vivo characterization and non-invasive monitoring of tacrolimus-loaded hydrogel for localized immunosuppression

Dzhuliya V. Dzhonova, M.Sc.^{1,2}; Radu Olariu³, Jonathan Leckenby³, Ashish Dhayani, M.Sc.^{4,5}; Praveen K. Vemula, Ph.D.⁴; Adriano Taddeo, Ph.D.^{1,3}; Robert Rieben, Ph.D.^{1*}

¹Department for BioMedical Research, University of Bern, Bern, Switzerland; ²Graduate School for Cellular and Biomedical Sciences, University of Bern, Bern, Switzerland; ³Clinic of Plastic and Hand Surgery, Inselspital, Bern University Hospital, University of Bern, Bern, Switzerland; ⁴Institute for Stem Cell Biology and Regenerative Medicine, Bangalore, India; ⁵The School of Chemical and Biotechnology, SASTRA University, Tamil Nadu, India

Status: Manuscript in preparation

Aim: To demonstrate the on-demand responsiveness of tacrolimus-loaded hydrogel *in vivo* and visualize hydrogel depots using near-infrared dye.



Summary: Tacrolimus-loaded hydrogel was injected in rats challenged or not with inflammatory stimulus. Tacrolimus release in whole blood was increased in response to inflammation, but not in unchallenged rats. Release of near-infrared dye from the hydrogel demonstrated good correlation with tacrolimus release *in vitro* and *in vivo* – in whole blood as well as locally in graft skin. Moreover, it allowed for convenient real-time non-invasive *in situ* monitoring of hydrogel deposits in transplanted animals.

In vivo characterization and non-invasive monitoring of tacrolimus-loaded hydrogel for localized immunosuppression

Dzhuliya V. Dzhonova, M.Sc.^{1,2}; Radu Olariu, M.D.³, Jonathan Leckenby, M.D.³, Ashish Dhayani, M.Sc.^{4,5}; Praveen K. Vemula, Ph.D.⁴; Adriano Taddeo, Ph.D.^{1,3}; Robert Rieben, Ph.D.^{1*}

¹Department for BioMedical Research, University of Bern, Murtenstrasse 50, 3008 Bern, Switzerland; ²Graduate School for Cellular and Biomedical Sciences, University of Bern, Freiestrasse 1, 3001 Bern, Switzerland; ³Clinic of Plastic and Hand Surgery; Inselspital, Bern University Hospital, University of Bern, Freiburgstrasse, 3010 Bern, Switzerland; ⁴Institute for Stem Cell Biology and Regenerative Medicine, Bellary Road, Bangalore 560065, India; ⁵The School of Chemical and Biotechnology, SASTRA University, Thirumalaisamudram, Thanjavur-613401, Tamil Nadu, India

***Corresponding author:**

Robert Rieben, Ph.D.
Department for BioMedical Research
University of Bern
Murtenstrasse 50
3008, Bern
Switzerland
Telephone: +41 31 632 96 69
Fax: +41 31 632 75 94
E-Mail: robert.riegen@dbmr.unibe.ch

Author contributions:

D.D. performed the *in vivo* experiments, TGMS-TAC hydrogel preparation and imaging, and wrote the manuscript. D.D. and A.D. performed the *in vitro* analyses. A.D. performed the HPLC analyses. R.O. and J.L. designed and performed hind limb transplantations. A.D. and P.V. designed and developed the TGMS-TAC hydrogel. P.V., A.T. and R.R. designed and supervised the studies, and reviewed the manuscript.

Abstract

Background

Local immunosuppression with tacrolimus-releasing hydrogel (TGMS-TAC) in response to inflammation-related enzymes could reduce systemic immunosuppression-related side effects in vascularized composite allotransplantation (VCA). We aimed to understand whether TGMS-TAC responds to inflammation *in vivo* and whether non-invasive monitoring of the hydrogel deposits is possible with encapsulated near-infrared dye.

Materials and Methods

Rats were injected with TGMS-TAC and challenged or not locally with lipopolysaccharides (LPS) 7 days later. Tacrolimus levels in blood and tissues were measured at selected time points.

Near-infrared dye encapsulated in the gel was used for imaging the hydrogel deposits in a rat VCA model and correlation of near-infrared signal and tacrolimus release from the gel was checked *in vitro* and *in vivo* in grafts and blood.

Results

LPS-treated but not untreated rats had increased blood tacrolimus levels (adj.p=0.0076, day 8 vs. day 13, one-way ANOVA). Tacrolimus levels in skin of LPS-treated animals were higher 48h after LPS compared to non-treated controls (p=0.0007 in treated, p=0.0254 in contralateral limbs, unpaired t-tests). LPS-treated animals had higher tacrolimus levels in treated limbs compared to contralateral limbs (p=0.0003 for skin and p=0.0053 for muscle, paired t-test). Correlation of tacrolimus and near-infrared dye release from TGMS-TAC was $R^2=0.6066$ *in vitro*, $R^2=0.6297$ in blood, and $R^2=0.5619$ in graft (Pearson's linear regression).

Conclusions

Here, we demonstrate *in vivo* responsiveness to inflammation of tacrolimus-loaded hydrogel and introduce a real-time *in situ* monitoring of the hydrogel deposits, using a near-infrared dye, with a reliable correlation of tacrolimus and dye release from the hydrogel.

Keywords: VCA, local immunosuppression, tacrolimus, hydrogel, near-infrared dye, imaging.

Introduction

Vascularized composite allotransplantation – the transplantation of tissue composites, such as face, hands and abdominal wall – has experienced an exhilarating development in the past two decades. By May 2017, 66 hand and 30 face transplantations have been registered, most of which demonstrating excellent survival, function and appearance¹. The recipients are typically young healthy people, who need life-long immunosuppression to protect their grafts from rejection. Unfortunately, the use of systemic immunosuppression is associated with enhanced risks of infections, metabolic disturbances, and cancer. As recently reported, 32.3% of hand transplant recipients experienced an opportunistic bacterial infection, 41.5% had hyperglycemia and two of the 66 patients included in the report developed malignancies¹.

To mitigate these health hazards, we are developing a novel drug delivery system for localized immunosuppression, aimed at reducing systemic immunosuppression adverse effects by decreasing the total drug uptake required to prevent rejection. It is composed of an injectable triglycerol monostearate (TGMS) hydrogel, loaded with the immunosuppressive drug tacrolimus (TAC), injectable subcutaneously into the VCA graft. TGMS hydrogel loaded with TAC (TGMS-TAC) releases the encapsulated TAC in response to elevated levels of inflammation-related enzymes *in vitro*². However, the mechanism of TAC release has not yet been demonstrated *in vivo*. Further, a single intra-graft TGMS-TAC injection in a Brown Norway-to-Lewis rat hind-limb transplantation model prolonged graft survival for >100 days, with sub-therapeutic drug levels in the blood for extended periods of time². Intra-graft levels have been described to be more accurate markers of immunosuppression than trough levels³, and could be particularly critical in the case of local immunosuppression. Nevertheless, frequent tissue biopsies collection for drug monitoring is an unpractical, painful and scaring procedure. A potential solution could be the incorporation of a surrogate marker, which can be non-invasively detected and provides information on the availability of TAC in the hydrogel deposit.

Near-infra-red dyes (NIRD) are used for *in vivo* imaging of hydrogels⁴, making them attractive candidates for visualizing drug delivery systems for local immunosuppression. NIRD are safe for administration in the body, emit light at wavelengths in which tissue autofluorescence is low, and can be detected by common instruments for fluorescence imaging. NIRD have proven to be effective for imaging of sentinel lymph nodes⁵, breast tissues⁶, and cancer⁷, with penetration in various tissues of up to several centimeters⁸.

Here, we aimed to better characterize the TGMS-TAC hydrogel *in vivo* and optimize it to improve its application in a clinical setting. To understand the TGMS-TAC release kinetics in response to inflammatory stimulus *in vivo*, we

injected TGMS-TAC subcutaneously in hind limbs of Lewis rats, which after 7 days received or not a subcutaneous injection of lipopolysaccharides (LPS) near the hydrogel deposits. We collected blood and tissue for TAC measurements on selected time points to understand whether LPS injection could increase TAC release from the hydrogel. In addition, we examined the hydrogel deposits for foreign-body reaction.

In addition, we questioned whether NIRD encapsulated in TGMS-TAC would allow non-invasive monitoring of hydrogel deposits in VCA and of TAC release. To this aim, we used an *in vitro* dialysis system, loaded with TGMS-TAC containing encapsulated NIRD and submerged in PBS or PBS with 10 μ L lipase. Lipase is an enzyme, which is upregulated during inflammation and rejection. It can digest the TGMS molecule and is a putative trigger of TAC release from the hydrogel *in vivo*. The dialysis systems were placed within containers filled with PBS that was collected and replenished on selected time points. The collected PBS was submitted to TAC and NIRD measurements and their levels were correlated. In addition, we injected NIRD-encapsulated TGMS-TAC subcutaneously in hind limbs of Brown Norway rats transplanted to Lewis rats. We monitored the hydrogel deposits and the NIRD release locally in the graft and systemically in blood plasma, and correlated it with TAC release.

Materials and methods

Animals

Male Brown Norway and Lewis rats (6-8 weeks old weighing 200 to 250 g) were purchased from Charles Rivers Breeding Laboratories, Germany. Animals were kept in specific pathogen-free conditions. Experiments were planned and carried out in agreement with current 3R and ARRIVE guidelines and approved according to Swiss animal protection laws by the Veterinary Authorities of the Canton Bern, Switzerland, approval no. BE94/15.

TGMS-TAC preparation

TAC (LC Laboratories, Woburn, MA, United States), TGMS (AK Scientific, Union City, CA, United States), EDTA Hybri-Max (Sigma, St. Louis, MO, United States) and sterile water (B.Braun, Melsungen, Germany) were used for TGMS-TAC preparation as described previously². For NIRD-encapsulated TGMS-TAC, 100µg/mL IRDye 800CW Carboxylate (LI-COR Biosciences, Lincoln, NE, United States) was added to the mixture.

Limulus amoebocyte lysate test (Pyrogent 03 Plus, Lonza Group, Basel, Switzerland) was used for pyrogen detection according to manufacturer's instructions and TGMS-TAC was considered pyrogen-free if 1:10 dilution of hydrogel in sterile water resulted negative to the test.

TAC release in response to local inflammatory stimulus *in vivo*

Naïve Lewis rats received 1 mL TGMS-TAC loaded with 7 mg TAC subcutaneously in the graft. Four deposits of TGMS-TAC of 250 µL each were injected in the zones of biceps femoris, gastrocnemius, tibialis anterior, and vastus muscles. Animals were randomly assigned in two groups – untreated control (n=12), and experimental group – receiving a subcutaneous injection of 100µg LPS (Lipopolysaccharides from *E.coli* O111:B4, γ-irradiated, BioXtra, Sigma) dissolved in 100µL PBS near the gel deposits (n=9). Peripheral blood was collected from the sublingual vein in EDTA coated tubes (Sarstedt, Nümbrecht, Germany) and stored at -20° C until use in 6 of the control and 3 of the LPS-treated animals. TAC concentrations in blood were assessed using the Kit MS1100 (ClinMass Complete Kit, advanced, for Immunosuppressants in Whole Blood, RECIPE Chemicals + Instruments GmbH, Munich, Germany) and quantified by LC-MS/MS. Blood TAC levels were measured for 50 days. The remaining 6 animals per group were sacrificed 9 days after TGMS-TAC injection (48h after LPS challenge) and skin, muscle and fat pad from the treated and contralateral untreated hind limbs was snap frozen and stored at -20°C for TAC measurements. At least one hydrogel deposit per animal was formalin fixed, paraffin embedded, and 5µm thick sections were stained with Hematoxylin and Eosin and submitted to a blinded pathologist for evaluation.

Hind limb transplantation and treatment

Hind limb transplantations were performed using a two-surgeon method as previously described⁹. The successfully transplanted rats received 1 ml TGMS-TAC loaded with 7 mg TAC and 100µg NIRD, subcutaneously in the graft (n=5). Four deposits of NIRD-containing TGMS-TAC of 250 µL each were injected in the zones of biceps femoris, gastrocnemius, tibialis anterior, and vastus muscles. Animals were inspected on a daily basis for weight loss and signs of pain or distress¹⁰ or rejection. Rejection was macroscopically determined as grade 0 – none; 1 – edema, erythema; 2 – epidermolysis, desquamation; 3 – frank necrosis and mummification. Near-infrared imaging of gel deposits, and NIRD and TAC measurements in graft and plasma were performed at selected time points and compared.

Near-infrared dye analyses

Blood: Peripheral blood was collected from the sublingual vein in EDTA coated tubes (Sarstedt) and centrifuged at 1500rpm for 10 minutes. Plasma was collected, placed in Corning 96 Well Black Polystyrene Microplate (clear flat bottom, black polystyrene, matrix active group TC-treated, Sigma) and immediately imaged with a LI-COR Odyssey instrument (LI-COR Biosciences) at 800nm. Imaging conditions: Laser – 800nm; Intensity – L2.0 (minimum), resolution – 169µm, quality – medium, focus offset – 4mm (maximum), identical brightness and contrast. Naïve Lewis rat blood plasma was used for subtraction of background fluorescence.

Graft: TGMS-TAC deposits were imaged *in situ* using LI-COR Odyssey instrument (LI-COR Biosciences) at 800nm. Imaging conditions were identical to blood imaging. Animals were kept under light anesthesia: 1-1.5 % Isoflurane (AbbVie AG, North Chicago, IL, United States) with 0.6 L/min oxygen, to prevent limb movement while image acquisition. Hind limbs were shaved before imaging for consistency.

Blood and graft infrared dye signal at 800nm was normalized for area and used for further analyses.

Tacrolimus analyses

Blood: Peripheral blood was collected, stored and quantified as previously described.

Tissue: Skin, muscle and fat biopsies from treated and untreated, contralateral limbs were excised, weighed, snap frozen, and stored at -20° C until use.

The sample preparation was adapted using the MS1312 from Recipe as internal standard. TAC and internal standard were dissolved in 70 % (v/v) methanol solution. Standard spiking solution was prepared to build up a calibration curve between 0.3 and 65 ng/mL. The frozen tissues were gently thawed at room temperature. For blank matrix, samples skin samples

without TAC treatment were used. A blank matrix was prepared adding 1000 μL of precipitation solution to untreated tissue. A volume of 40 μL of internal standard solution and 960 μL of precipitation solution were added to the treated samples. All samples were then grinded with five stainless steel balls for 30 minutes at 25 Hz. The tubes were centrifuged 5 minutes at 4° C and 20'000 rcf. 500 μL of the tissue extract was filtered with a Mini-Uni Prep G2 vials (GE Healthcare, Chicago, USA).

Chromatographic analyses were performed on an Acquity I-Class system (Waters, Milford, MA, USA) with ClinMass Complete Kits (Immunosuppressants in whole blood, advanced – on-line analysis). The autosampler temperature was set at 10 °C and the autosampler needle was washed with a strong needle wash solution of isopropanol:methanol:acetone:trifluoromethane:H₂O (1:1:1:1, v/v). A solution of 20 % (v/v) methanol was used as weak needle wash. Analytes were ionized by electrospray ionization (ESI) in the positive mode and detected on a triple quadrupole mass spectrometer (Xevo TQ-S, Waters, Milford, MA, USA). The capillary and the cone voltage were set at 3 kV and 40 V, respectively. The source offset was set at 60 V, the desolvation temperature at 400° C, the desolvation gas at 1000 L/h, the cone gas at 150 L/h, the nebulizer at 7 bar and the source temperature at 150° C. The instrument was controlled via MassLynx (version 4.1, Waters). Data were acquired, integrated and processed with TargetLynx (MassLynx v4.1).

Correlation of tacrolimus and near-infrared dye *in vitro*

Bottoms of 2mL tubes (Eppendorf, Hamburg, Germany) were excised and replaced with SnakeSkin Dialysis Tubing, 10K MWCO, 22 mm (Thermo Fisher Scientific, Waltham, MA, United States). Tubes were filled with 200 μL TGMS-TAC loaded with 1.4 mg TAC and 20 μg NIRD and randomly divided into two groups – control group (n=3) – gel submerged in 1mL PBS, and experimental group (n=3) – gel submerged in 1 mL PBS, containing 10 μL Lipase from *Thermomyces lanuginosus*, solution, $\geq 100,000$ U/g (Sigma). Tubes were placed within 50mL Falcon tubes (Thermo Fisher Scientific), containing 10mL PBS. Tubes were placed on a shaker under the following incubation conditions: 37°C, 5% CO₂ and 95% relative humidity under 50 rotations/minute. At selected time points, the PBS in the 50mL Falcon tubes was collected and replaced with fresh PBS. The collected PBS was used for NIRD measurements (using LI-COR Odyssey imager and a 96 well plate, as previously described) and for TAC measurements (HPLC).

Statistical analyses

Statistical analyses were performed with Prism software (GraphPad Software Inc., La Jolla, CA, United States). Statistically significant data are presented as follows: *p<0.05; **p<0.01; ***p<0.001; and ****p<0.0001. The used statistical tests are mentioned in the respective figure legends.

Results

TGMS-TAC releases tacrolimus in response to inflammatory stimulus *in vivo*

Naïve Lewis rats receiving a subcutaneous injection of TGMS-TAC in the hind limb demonstrated an initial systemic burst release of TAC in the first 72h. This peak was followed by normalization within therapeutic levels for over a month and a subsequent drop to sub-therapeutic TAC levels that continued to be detectable for at least 50 days. Importantly, animals receiving a subcutaneous injection of LPS in proximity to the TGMS-TAC deposits on day 7, demonstrated elevated systemic TAC levels in the subsequent days. At day 8 and at day 13 the mean \pm SD of systemic TAC levels in LPS-treated animals were 18.7 ± 3.3 (ng/ml), and 24.4 ± 3.5 (ng/ml), respectively (adj.p=0.0076, one-way ANOVA with Tukey's correction for multiple comparisons, Figure 1a). In addition, the area under the curve (AUC) of systemic TAC release was significantly higher in the LPS-treated animals compared to untreated animals (342.1 ± 13.3 , n=3 for LPS-treated versus 262.7 ± 14.6 , n=6 for untreated, p= 0.0108, unpaired t-test of AUC, Figure 1b).

Additionally, animals were sacrificed 48h after LPS challenge (or no challenge for control group, n=6 per group) and muscle, skin and fat pad from treated and contralateral untreated limbs were collected for TAC measurements (Figure 2a). TAC skin levels of LPS-challenged animals were significantly higher in the treated limbs compared to the contralateral limbs (p=0.0003, paired t-test, Figure 2b) and compared to the TAC skin levels in the treated limbs of the control group (p=0.0007, unpaired t-test, Figure 2b). TAC skin levels in contralateral limbs of LPS-challenged animals were also significantly higher than the respective levels in the control group (p=0.0254, unpaired t-test, Figure 2b). TAC levels in muscle of LPS-challenged animals were significantly higher in the limb receiving the LPS challenge in comparison to the contralateral limb (p=0.0053, paired t-test, Figure 2c). TAC levels in fat pad of LPS-challenged animals were comparable between the limbs receiving the LPS challenge, and the contralateral limbs (p=0.8134, paired t-test, Figure 2d). In the group without LPS challenge, there were no significant differences in TAC levels in skin, muscle, and fat pad between TGMS-TAC-treated limbs and untreated, contralateral limbs (p=0.2442, p=0.0771 and p=0.2319, respectively, paired t-test). TAC skin levels of LPS-challenged limbs were significantly higher compared to the TAC levels in the underlying muscle and fat pad (p=0.0173 and p=0.0015, paired one-way ANOVA with Tukey's post-hoc test).

TGMS-TAC injection leads to foreign body reaction

Explanted hydrogel deposits at day 9 after TGMS-TAC injection were analyzed histologically. All of them (n=14) had perifocal "capsule" formation

(Figure 3a), granulomatous in 64.3% (9 animals) and myofibroblastic in 57.1% (8 animals). Foreign body giant cells were noted in 35.7% of the cases (5 animals). Interestingly, despite capsule formation, the hydrogel was not isolated from its surroundings, given the presence of capillaries with circulating erythrocytes deep within the gel (Figure 3b).

Near-infrared dye release from TGMS-TAC and correlation to tacrolimus release *in vitro*

To understand whether NIRD incorporated in TGMS-TAC is released in response to inflammatory stimulus and whether it correlates to TAC release, we developed an *in vitro* installation, as described in Materials and Methods. Control installation contained PBS only (n=3), while experimental installation contained PBS with lipase (n=3). TAC release from lipase-spiked installation was not significantly elevated at any time point as compared to control installation (multiple t-test, Figure 4a). However, AUC analyses demonstrated that overall TAC release was significantly higher in lipase-spiked installation compared to control installation (mean \pm SD -26.09 ± 7.046 for control versus 51.21 ± 3.833 for experimental installation, respectively, p=0.0351, unpaired t-test of AUC, Figure 4b). NIRD release from lipase-spiked installation was not significantly elevated at any time point compared to control installation (multiple t-test, Figure 4c), neither was there a significant difference between the AUC (unpaired t-test of AUC, Figure 4d). Correlation of TAC and NIRD release from TGMS-TAC was $R^2=0.6066$ as computed by Pearson linear regression (Figure 4e).

Near-infrared dye release from TGMS-TAC and correlation to systemic and local tacrolimus levels *in vivo*

To assess the release kinetic of NIRD incorporated in TGMS-TAC *in vivo* and its potential value for hydrogel monitoring in VCA, we used Brown Norway-to-Lewis rat hind limb transplantation model (n=5). Animals received four deposits of 250 μ L TGMS-TAC with NIRD in the transplanted limb. Fluorescence emission at 800nm from TGMS-TAC into the surrounding graft tissue was monitored at selected time points (representative images in Figure 5a). Blood plasma was also collected at the same time points and imaged in a 96-wells plate to determine systemic NIRD release. Longitudinal analyses of plasma and graft fluorescence revealed that plasma fluorescence was no longer detectable after 60 days while intra-graft fluorescence persisted for more than 160 days (Figure 5b). Out of five grafts, four reached grade 3 of macroscopic rejection at post-operative days (POD) 94, 96, 96, and 481. One graft was accepted permanently. To correlate NIRD emission with TAC levels locally in the graft, and systemically in the blood, graft skin and peripheral blood were collected at selected time points for TAC measurements. Correlation of TAC and NIRD release from TGMS-

TAC in plasma was $R^2=0.6297$ (Figure 5d), and in graft was $R^2=0.5619$ (Figure 5e), as computed by Pearson linear regression.

Discussion

We have developed TGMS-TAC – a hydrogel for localized drug delivery directly into the graft. Our findings in a rat VCA model suggest that TGMS-TAC is an efficient and safe alternative to systemic immunosuppression². Here, we expand our understanding and the clinical translatability of this therapeutic modality. Previously, we have shown *in vitro*, that TGMS-TAC acts in an on-demand manner, by releasing TAC in response to enzymes typically elevated during rejection-induced inflammation². Here, we further confirm this mechanism of action of TGMS-TAC in Lewis rats. Animals treated with TGMS-TAC and challenged with LPS – a potent inflammatory stimulus – near the TGMS-TAC deposit clearly demonstrated an increase in the blood TAC levels after LPS challenge while such peak was not observed in control, unchallenged animals. Blood TAC levels in LPS-challenged animals were comparable to unchallenged animals prior the LPS injection. However, following LPS challenge, they remained slightly higher, following the same trend of decrease as the unchallenged animals. Consequently, more TAC was released from TGMS-TAC in LPS-challenged animals, as evidenced by higher AUC in comparison to the unchallenged group. In addition, tissue biopsies from the treated and the contralateral limbs revealed that the skin and muscle TAC levels in the LPS-treated limbs were significantly higher as compared to their respective levels in the contralateral, untreated limbs, while in the control animals they were comparable. The skin TAC levels seemed to be most responsive to the LPS challenge, which can be explained by the fact that LPS was given subcutaneously. Both the LPS-treated and contralateral limb skin TAC levels were higher as compared to the respective TAC levels in the control group. Moreover, skin from LPS-treated limb had higher TAC levels than the muscle or fat pad from the same limb. These findings underline that TAC release from TGMS-TAC animals is highly dependent on and titrated to the local inflammatory milieu.

Importantly, an initial burst release of TAC in blood was observed in the first 72h after TGMS-TAC injection. We did not collect biopsies, in order to avoid unanticipated inflammation and subsequent TAC release from the hydrogel. Therefore we were not able to determine whether and to what extent injecting the hydrogel deposits (foreign bodies) under the skin triggered an inflammatory response and potentially – the burst release. Indeed hydrogel deposits explanted at day 9 after injection triggered invariable foreign-body reaction with formation of large capsules. 50 days after injection, however, hydrogel deposits were almost completely resorbed, indicating that the

capsule did not isolate the hydrogel from its surrounding. It is, however, possible, that this burst release is a non-specific release of untrapped TAC. In such case further optimization of the hydrogel is due, before translation to clinical VCA setting.

Another moment in optimization of TGMS-TAC is making it possible to be monitored conveniently in a non-invasive fashion. To this aim we incorporated NIRD, which demonstrated a reasonable correlation with TAC release both *in vitro* and *in vivo*. An important observation, however, is that unlike TAC, NIRD did not respond to lipase with increased release from the hydrogel *in vitro*. A likely reason is that TAC is a highly lipophilic molecule, while the NIRD we used is a hydrophilic one. The hydrophilic NIRD could readily trespass the dialysis membrane in virtue of its own gradient, while hydrophobic TAC would preferentially remain within the hydrogel until it is released in the environment as a result of degradation of the hydrogel by lipase. Substituting the hydrophilic NIRD with a more hydrophobic one could be a potential way to solve this problem and improve the correlation between TAC and NIRD release from the hydrogel deposits. Ultimately, NIRD could serve as a potential surrogate marker for visualizing TGMS-TAC deposits *in situ* and estimating the remaining amount of TAC available locally and systemically.

This study has a few limitations, which have to be addressed. Firstly, we investigated the TAC release from TGMS-TAC in the context of local acute inflammatory stimulus, such as LPS. It remains to be elucidated whether inflammation in another anatomical site could influence the release of TAC from TGMS-TAC in a more “endocrine” fashion. This is a critical point, as the goal of TGMS-TAC is to provide relieved systemic immune depression in the context of environmental offenders, such as viruses, bacteria and fungi, as compared to systemic immunosuppression.

Further, as already mentioned, we used NIRD, which is highly hydrophilic in contrast to the very hydrophobic TAC, ultimately leading to differences in the distribution of the two molecules. Nevertheless, TAC and NIRD levels *in vitro* and *in vivo* (locally in the graft, and in peripheral blood) were correlating well with each other.

Finally, we could only partially reproduce our previous findings that TGMS-TAC injection prolongs vascularized composite allograft survival for >100 days. Out of five transplanted TGMS-TAC treated animals, three arrived to grade 3 rejection within 94-96 days. The remaining two progressed to grade 2 rejection at POD 97, which without any additional treatment reverted and completely recovered by POD 110. They received a second, back skin challenge from their donors after 200 days, which they accepted. However on POD 481 one of the animals arrived to grade 3 rejection of the original graft, while maintaining the secondary graft rejection free. The second animal showed no signs of rejection in either graft. These findings, although interesting and puzzling, are hard to interpret and replicate, and indicate that

batch-to-batch variations in the TGMS-TAC could lead to dramatically different outcomes.

Despite the limitations of our study, and the small sample size, we could demonstrate significant differences between TGMS-TAC behavior in inflammatory versus non-inflammatory conditions *in vitro* and *in vivo*. Moreover, we could visualize the hydrogel deposits *in situ*, allowing accurate estimation of the amount and distribution of TAC in the graft and in the blood. Further analyses that build on our knowledge on TGMS-TAC could help us bring this attractive localized inflammation-responsive drug delivery system closer to bedside.

Conclusion

Altogether our findings *in vivo* support the *in vitro* demonstrated mechanism of inflammation-triggered TAC release, and indicate that addition of NIRD in TGMS-TAC allows long-term *in situ* visualization of the hydrogel deposits.

Acknowledgements

The authors would like to thank Jean-Christophe Prost and Cédric Bovet for LC-MS/MS analyses of skin, performed at the Clinical Metabolomics Facility, Center of Laboratory Medicine from the Bern University Hospital “Inselspital”, as well as Yolanda Aebi and Michael Hayoz for blood LC-MS/MS routine analyses.

Disclosure

The authors have no conflicts of interest to disclose.

Funding

This work was supported by Indo-Swiss Joint Research Program of the Swiss National Science Foundation (SNF, grant 156773) and the Department of Science and Technology, Govt. of India (grant INT/SWISS/SNSFP-51/2015) to R.R. and P.V. respectively. A.D. thanks the University Grant Commission for the senior research fellowship.

References

1. Petruzzo, P., Sardu, C., Lanzetta, M. & Dubernard, J.-M. Report (2017) of the International Registry on Hand and Composite Tissue Allotransplantation (IRHCTT). 1–10 (2017). doi:10.1007/s40472-017-0168-3
2. Gajanayake, T. *et al.* A single localized dose of enzyme-responsive hydrogel improves long-term survival of a vascularized composite allograft. *Sci Transl Med* **6**, 249ra110–249ra110 (2014).
3. Capron, A. *et al.* Correlation of tacrolimus levels in peripheral blood mononuclear cells with histological staging of rejection after liver transplantation: preliminary results of a prospective study. *Transpl Int* **25**, 41–47 (2012).
4. Asai, D. *et al.* Protein polymer hydrogels by in situ, rapid and reversible self-gelation. *Biomaterials* **33**, 5451–5458 (2012).
5. Mieog, J. S. D. *et al.* Toward optimization of imaging system and lymphatic tracer for near-infrared fluorescent sentinel lymph node mapping in breast cancer. *Ann. Surg. Oncol.* **18**, 2483–2491 (2011).
6. Fang, Q. *et al.* Combined optical imaging and mammography of the healthy breast: optical contrast derived from breast structure and compression. *IEEE Trans Med Imaging* **28**, 30–42 (2009).
7. Bloch, S. *et al.* Whole-body fluorescence lifetime imaging of a tumor-targeted near-infrared molecular probe in mice. *J Biomed Opt* **10**, 054003 (2005).
8. Selvam, S., Kundu, K., Templeman, K. L., Murthy, N. & García, A. J. Minimally invasive, longitudinal monitoring of biomaterial-associated inflammation by fluorescence imaging. *Biomaterials* **32**, 7785–7792 (2011).
9. Olariu, R. *et al.* Intra-graft injection of tacrolimus promotes survival of vascularized composite allotransplantation. *Journal of Surgical Research* **218**, e107–e107 (2017).
10. Sotocinal, S. G. *et al.* The Rat Grimace Scale: A partially automated method for quantifying pain in the laboratory rat via facial expressions. *Molecular Pain* **7**, 55 (2011).

Figure Legends

Figure 1. Tacrolimus release in blood of rats challenged or not with LPS. a) Longitudinal measurements of tacrolimus in blood of rats injected subcutaneously in the hind limb with TGMS-TAC. Increased tacrolimus levels after LPS challenge in the same limb (n=3, red line), but no increase in unchallenged animals (n=6, black line). Upper limit of detection of tacrolimus in blood by LC-MS/MS was 65 ng/mL, higher values are not reliably measurable. b) AUC analyses of untreated and LPS-treated animals (*P<0.05, unpaired t-test).

Figure 2. Tacrolimus levels in tissues of rats challenged or not with LPS. a) Experimental set-up. TGMS-TAC treated animals received or not a subcutaneous injection of lipopolysaccharides (LPS) 7 days after TGMS-TAC injection. 48h after LPS challenge (or no challenge for controls), tissue levels of tacrolimus were measured by LC-MS/MS in b) skin, c) muscle and d) fat pad of TGMS-TAC treated and untreated, contralateral limbs (n=6 rats per group). b)-d) Shown are individual data points for each animal, with indication of mean \pm SD by lines. Paired t-tests were used for intra-group comparisons of same tissues; unpaired t-tests were used for inter-group comparisons of same tissues from either treated or contralateral limbs (*p<0.05, **p<0.01, ***p<0.001).

Figure 3. Hydrogel monitoring. Hydrogel deposits explanted for analyses on POD 9 show fibrotic capsule formation (a) and vascularization – capillaries formed inside the hydrogel deposit, indicated by an arrow (b). Shown are representative histological hematoxylin and eosin stained sections of hydrogel deposits at 3x (a) and 50x (b) magnification.

Figure 4. Tacrolimus and near-infrared dye release from TGMS-TAC hydrogel *in vitro*. a) Cumulative release of tacrolimus from TGMS-TAC under PBS or PBS spiked with lipase conditions over time and corresponding b) AUC analyses. c) Cumulative release of NIRD from TGMS-TAC under PBS or PBS spiked with lipase conditions over time and corresponding d) AUC analyses. e) Pearson correlation of tacrolimus and NIRD release from TGMS-TAC – linear regression with 95% confidence intervals.

Figure 5. Near-infrared dye release from TGMS-TAC in a Brown Norway-to-Lewis rat hind limb transplantation model. a) Representative images of longitudinal monitoring of fluorescence emission at 800nm from grafted limbs treated with NIRD-containing TGMS-TAC (n=5). POD – Post-operative day; green – emission of NIRD at 800nm; red – auto fluorescence of tissue, hair and sutures at 700nm; white – overexposure. b) Longitudinal

monitoring of fluorescence emission at 800nm from grafted limbs and plasma (n=5). Values are normalized for area, overexposed areas were excluded, and background subtraction was performed by imaging limbs and plasma before transplantation, and subtracting the mean obtained values. Featured is a close-up of the first 60 days, including analyses (**p<0.01; ***p<0.001; and ****p<0.0001; multiple t-test with Holm-Sidak correction, p values are indicated directly above the corresponding time points). c) Kaplan-Meier survival curve of graft survival (n=5). One graft reached grade 3 rejection at POD 94, two grafts on POD 96, one graft on POD 481 and one graft was permanently accepted. d) and e) Pearson correlation of tacrolimus and NIRD release from TGMS-TAC in plasma (d) and graft skin (e) – linear regression with 95% confidence intervals.

Figure 1

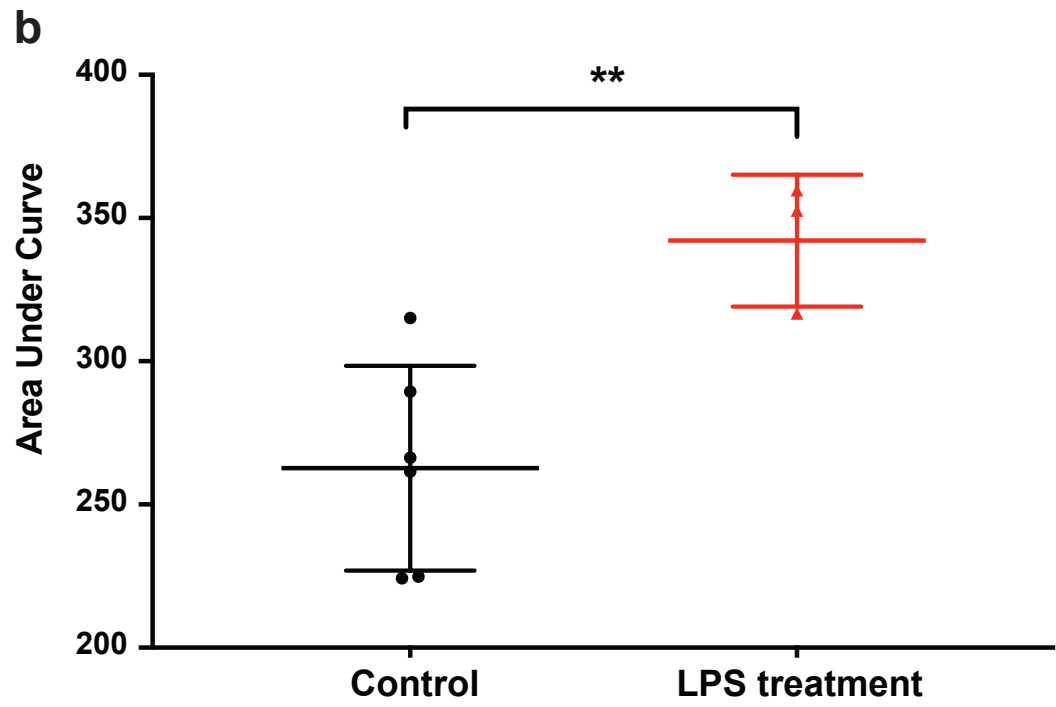
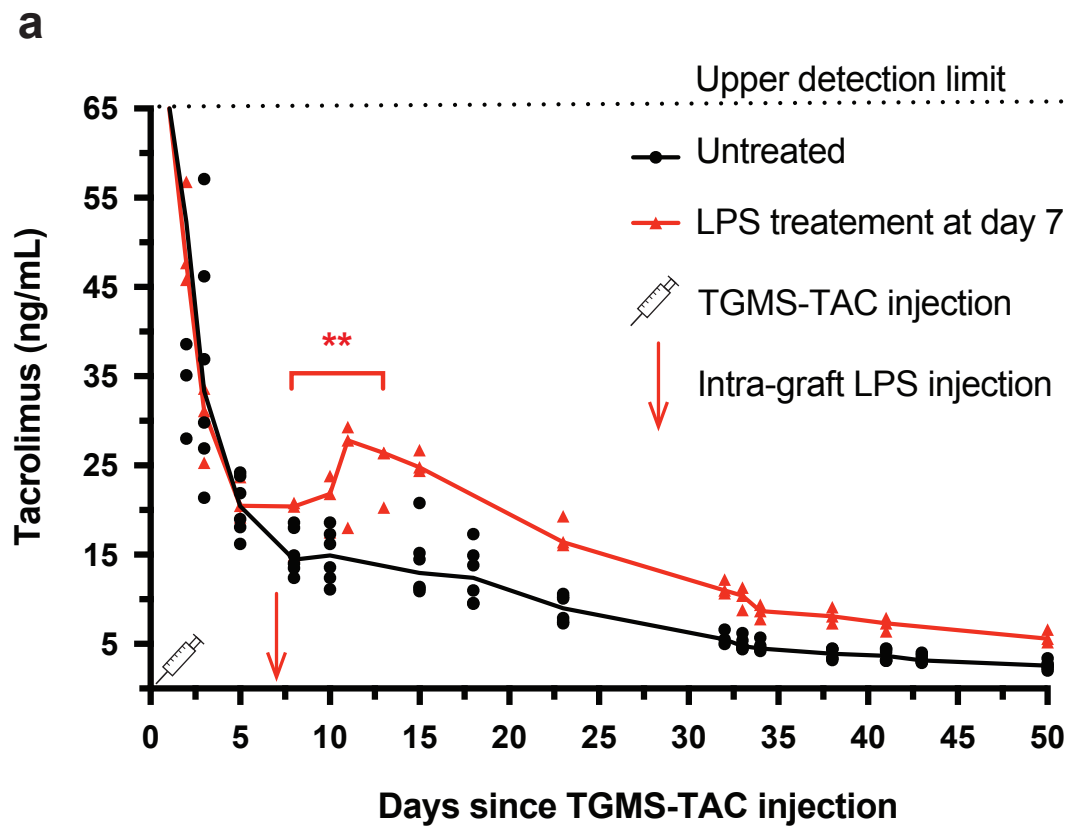


Figure 2

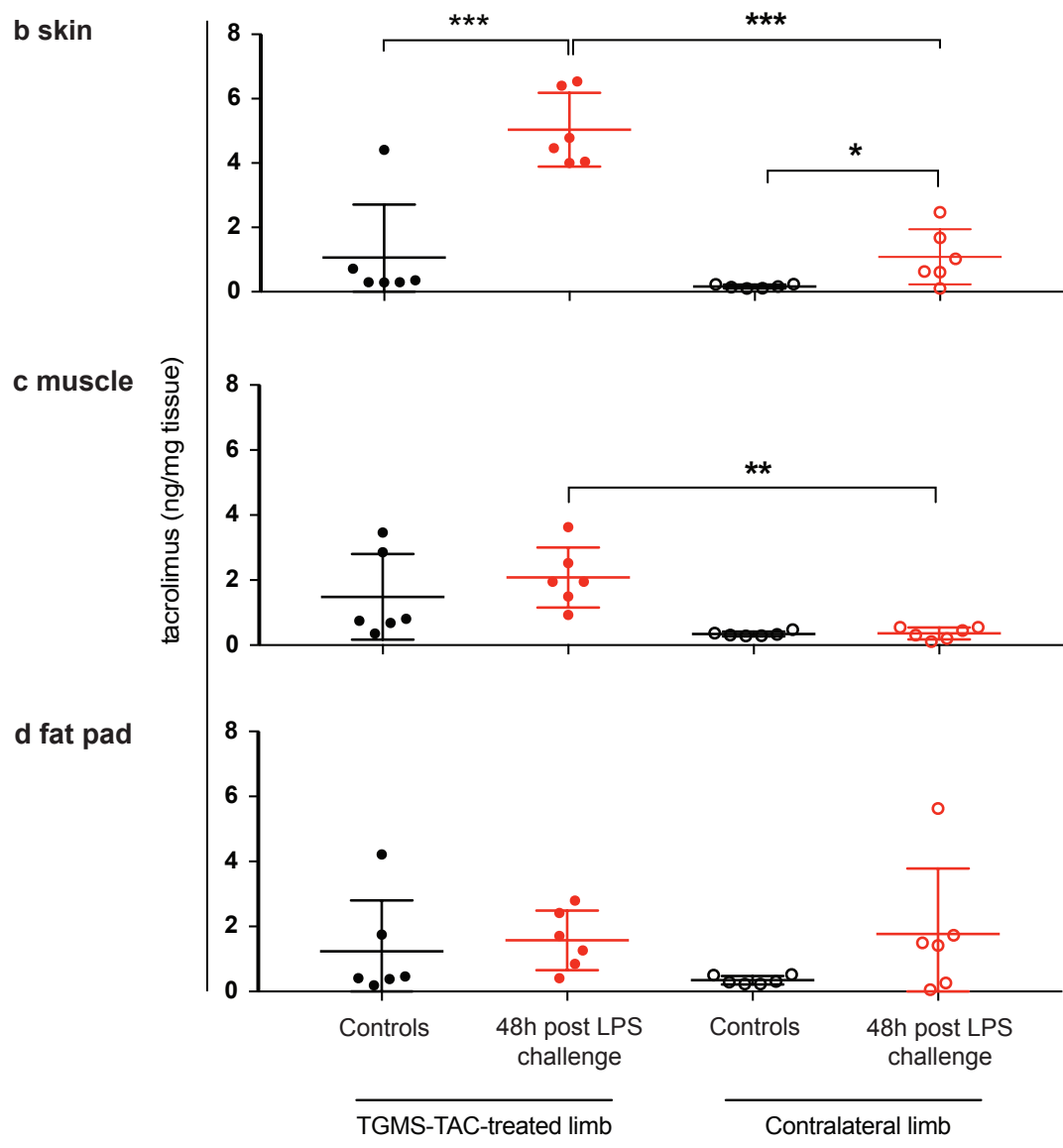
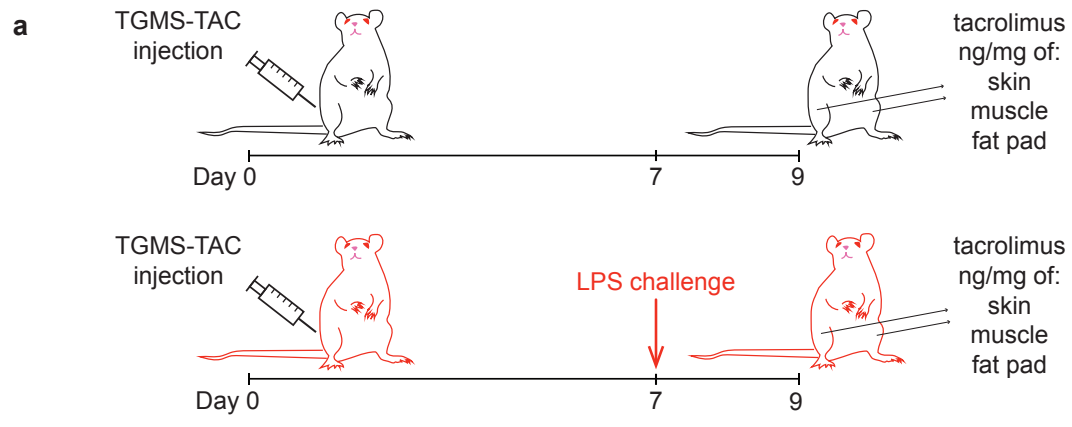
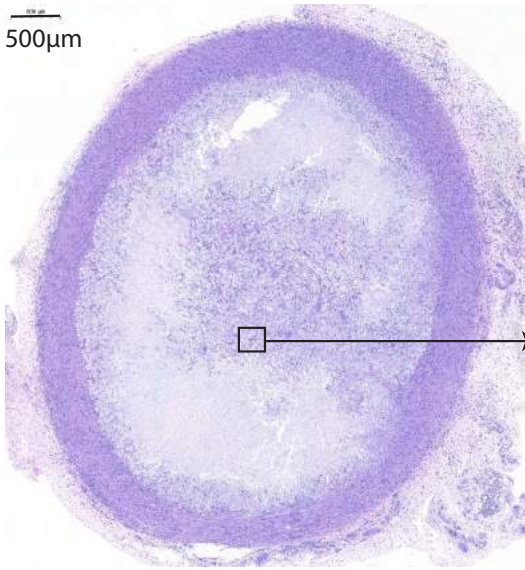


Figure 3

a

500µm



b

20µm

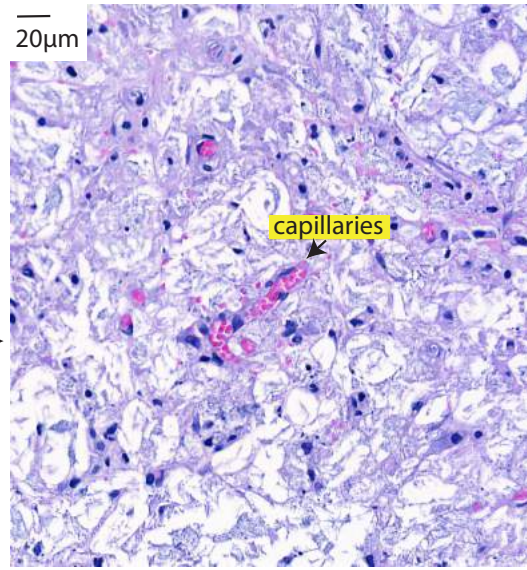


Figure 4

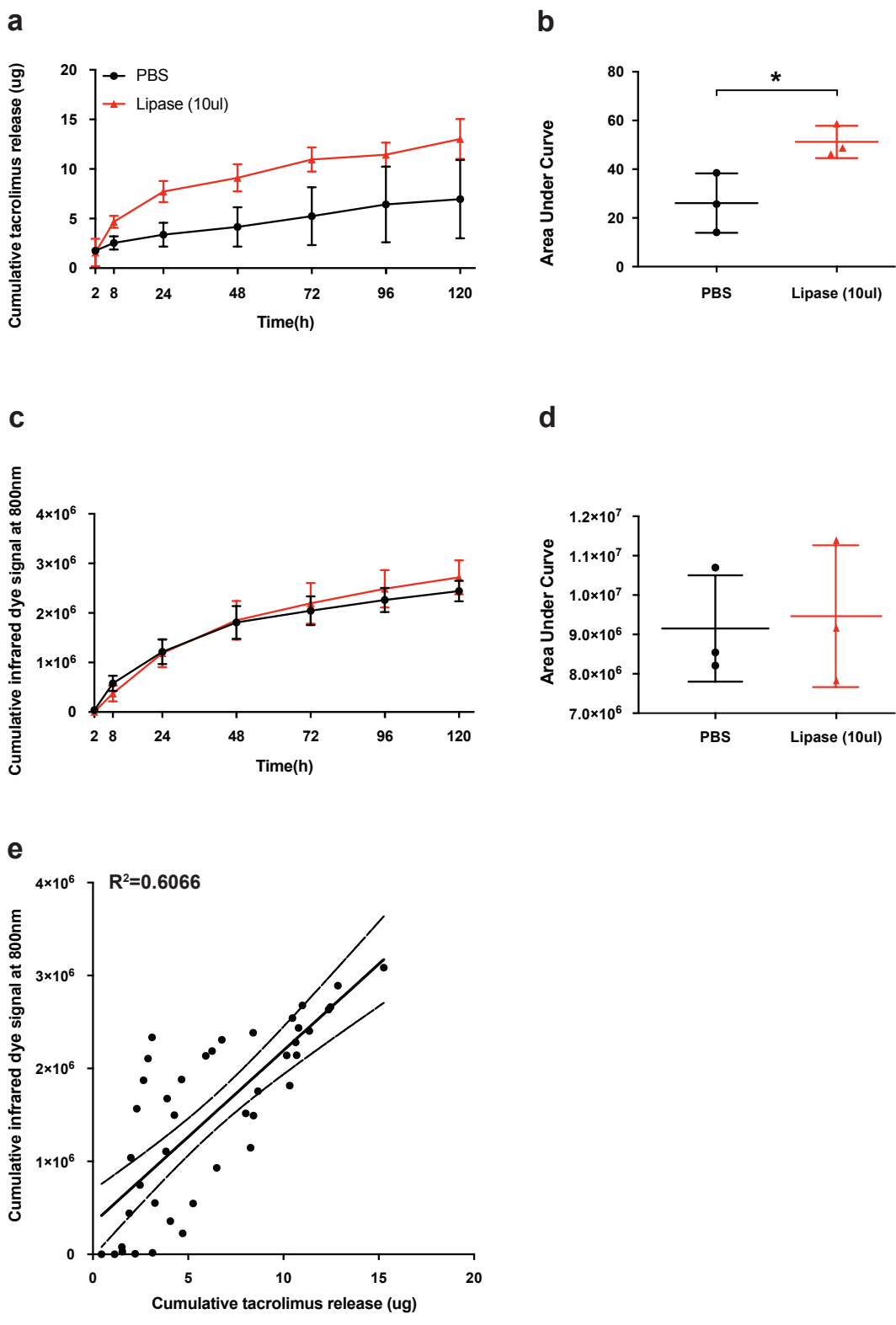
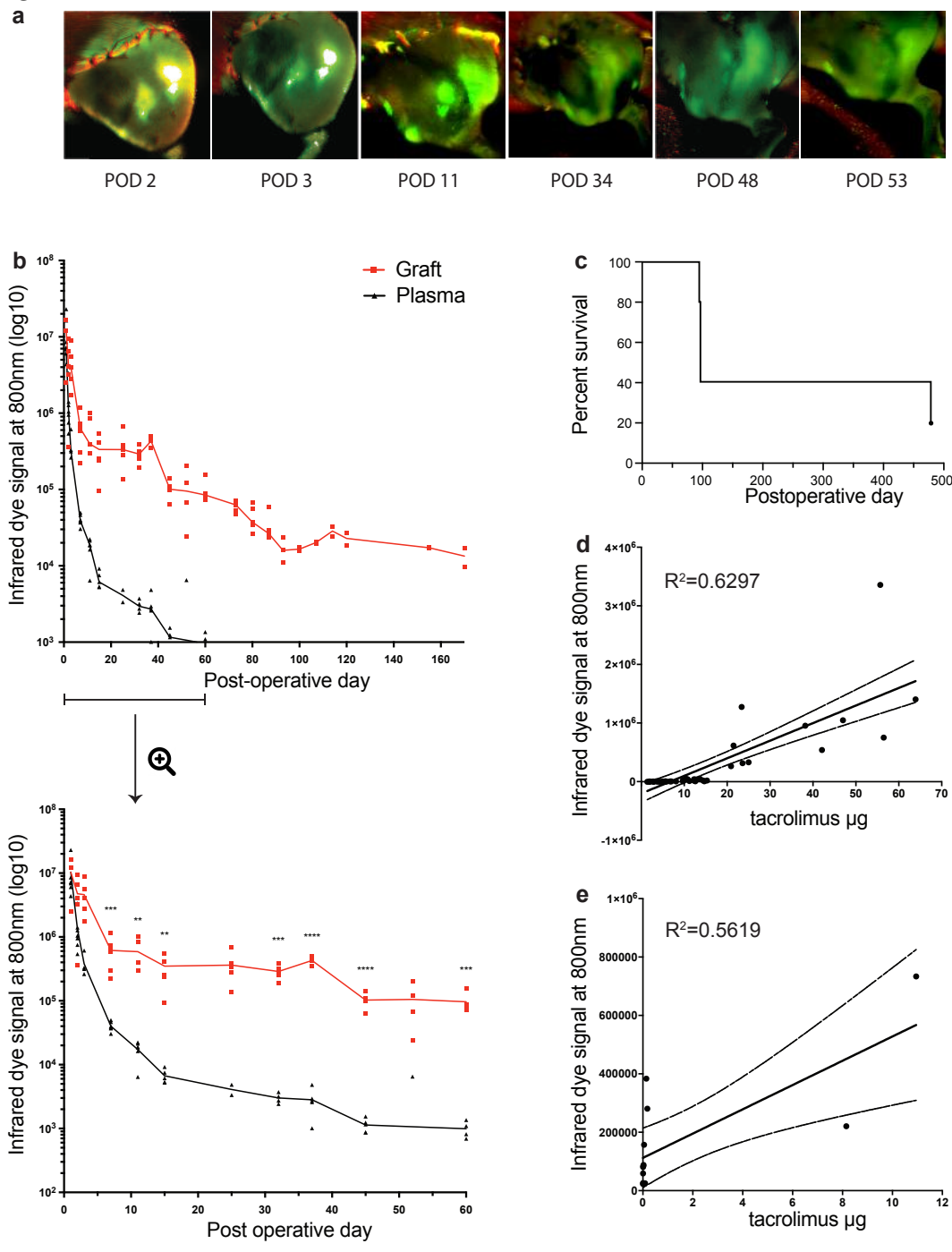


Figure5



4. Discussion and outlook

A leading problem in VCA transplantation stems from the high systemic levels of IS necessary to prevent graft rejection. Local DDS have inspired us and others to harness their potential benefits to devise IS with reduced systemic exposure, that could be used as a long-term maintenance IS in VCA.

First, we showed that an intra-graft injection of TAC bolus prolongs rejection-free graft survival, without induction depletion therapy and without any systemic treatment¹⁵⁶. We could stratify the animals into two groups – those who finally reject their grafts after 52–105 days, and those who after 215 days still didn't. There was a significant difference between the two groups in the levels of hematopoietic chimerism that we could detect early after transplantation (POD 14), however those levels were well under the levels suggested to induce tolerance⁹⁷. Indeed our animals rejected a secondary skin challenge from the donor strain, indicating that the bolus injection induced a local effect of hyporesponsiveness rather than tolerance. An alternative explanation that deserves investigation is the possibility that those animals indeed had systemic tolerance, but the inflammation caused by the surgical trauma during the skin grafting could broke it. Indeed Wang et al. and Young et al. have demonstrated unequivocally that tolerance is not a permanent state, but a moldable continuum, as inflammation caused by infection can erode tolerance and trigger rejection^{157,158}.

Further, we found that intragraft TAC levels at endpoint in animals rejecting early were higher than those measured in long-term surviving animals. These results suggest that more than just the immunosuppression levels mattered on a local level for rejection occurrence. It has been shown that TAC can inhibit the stimulatory effect of DC on T cells *in vitro*¹⁵⁹, and that TAC treated DC with tolerogenic phenotype suppressed T cells *in vivo* in a mouse model of arthritis¹⁶⁰. Future efforts should focus on understanding the impact of locally applied TAC IS on resident DC within transplanted skin as a potential mechanism to control anti-graft immunity. The conclusion of this study is that localized IS could indeed present a possibility as a standalone therapy. An intra-graft bolus of immunosuppressant is not a translatable to clinics approach. It is, however, an important proof of concept, which motivated us to push the envelope further.

Next, we investigated two local DDS, employing different strategies. TGMS-TAC relied on inflammation-triggered release of TAC in the graft,

titrated to the momentary local requirements (see Results, part 3.1). ISFI continuously releases low levels of the immunomodulatory drug rapamycin, promoting increased levels of circulating Treg, enhanced hematopoietic chimerism and local graft tolerance (see Results, part 3.2). **Table 5** summarizes the outcomes of the two studies and compares the performance of ISFI and TGMS-TAC to systemic IS.

Table 5. Back-to-back comparison of TGMS-TAC, ISFI and systemic IS

Variable	TGMS-TAC	ISFI	systemic IS
Induction therapy	✗	✓	✗
Release kinetics	on-demand	sustained	N/A
Graft survival with a single injection	>100 days	>100 days	N/A
Graft survival with repeated injections	280 days	not tested	infinite
Hematopoietic chimerism	✓	✓	✗
Treg promotion	✗	✓	✗
IS side effects reduction	✓	not tested	✗
Reduced systemic drug levels	✓	✓	✗
Adequate local drug levels	✓	✓	✓
Tolerance induction	✗	✗	✗
Acute rejection episodes	✓	✓	✗

Chimerism, although transient and low level was significantly increased with localized treatments in respect to systemic one, regardless of the drug and DDS chosen. This goes to show the importance of local immunomodulation on a global effect such as chimerism. However, despite elevated chimerism levels, our animals developed rejection episodes, highlighting that chimerism shouldn't be viewed as a goal or a promise, but as one of multiple factors pulling the lever of immune balance in one direction or another. In agreement with this, Shanmugarajah et al. have shown in a porcine VCA model, that rejection can occur even in the setting of a robust chimerism, depending on the type of MHC mismatch¹⁶¹.

In this line of thought, it is important to point out that we used a stringent model of full MHC incompatibility, without any depletive pre-treatment, and we could still demonstrate beneficial effects of local DDS on chimerism and Treg, albeit without tolerance. Multiple basic research papers report on achievement of tolerance in a variety of animal models and stress on its importance. They employ aggressive depleting protocols, which expose the graft recipients to health risks unacceptable in the setting of a “non-life saving procedure”, such as VCA. It has been already shown that as much as differences in gut microbiota result in changes in graft survival duration in a

murine model of skin transplantation¹⁶², emphasizing that alloimmunity is governed by known and unknown, controllable and uncontrollable factors. A clear gap in the collective knowledge is the relative and cumulative leverage of different influencers – primary transplantation- and ischemia-induced inflammation, cross-reactivity of memory T cells within the graft, infections, climate / environment, lifestyle, age and medical condition of the recipient, number and type of HLA and minor histocompatibility complex mismatches – on VCA rejection. As a result of that complexity, a standardized therapy provides very different outcomes for each patient. In contrast, an environment-sensing DDS, such as TGMS-TAC, can titrate the levels of drug released, to meet the individual and current needs of each graft. The excellent long-term graft and recipient outcomes of TGMS-TAC-treated rats lead us to believe that this treatment has a true potential for translation to clinical VCA and deserved a further exploration and development.

As was previously demonstrated, TGMS-TAC responds to enzymes, elevated during inflammation and rejection with TAC release *in vitro*¹⁵⁴. However, an open question remained whether that is indeed the trigger of TAC release *in vivo*. We demonstrated here, that local inflammation indeed led to increased release of TAC from the hydrogel, reinforcing the predictability of this therapeutic possibility (see Results, part 3.4). In addition, from our previous experiments we already remarked that TGMS-TAC promotes graft survival also with sub-therapeutic systemic TAC levels. That created a difficulty in determining the right timing for re-administration of TGMS-TAC. We reasoned that visualizing the hydrogel deposits and a reasonable estimation of the amount of remaining TAC in it, or available in the tissue and/or systemically in the blood can serve as a guidance. We incorporated a near-infrared dye in TGMS-TAC, which allowed an easy non-invasive visualization of TGMS-TAC deposits *in situ*, and demonstrated a sensible correlation to TAC *in vitro* and *in vivo*. We believe that this new feature of TGMS-TAC, after careful optimization, can dramatically improve the quality of life for VCA patients and relieve physicians, by reducing the time patients spent in hospital for therapeutic drug monitoring.

To conclude, our findings in a rat model of VCA consolidate the assertion that localized DDS for immunosuppression present a promising alternative to systemic IS, with the potential to mitigate noncompliance- and IS-related complications. These results should be further affirmed in a large animal model of VCA, that better mirrors the complex immune setting in patients.

5. References

1. Ali, S. & Fatima Haider, S. K. Psychological adjustment to amputation: variations on the bases of sex, age and cause of limb loss. *J Ayub Med Coll Abbottabad* **29**, 303–307 (2017).
2. Shukla, G. D., Sahu, S. C., Tripathi, R. P. & Gupta, D. K. A psychiatric study of amputees. *Br J Psychiatry* **141**, 50–53 (1982).
3. Hernigou, P. Ambroise Paré IV: The early history of artificial limbs (from robotic to prostheses). *International orthopaedics* **37**, 1195–1197 (2013).
4. Godfrey, S. B. *et al.* SoftHand at the CYBATHLON: a user's experience. *J Neuroeng Rehabil* **14**, 124 (2017).
5. Jiang, Y., Togane, M., Lu, B. & Yokoi, H. sEMG sensor using polypyrrole-coated nonwoven fabric sheet for practical control of prosthetic hand. *Front Neurosci* **11**, 33 (2017).
6. Germany, E. I., Pino, E. J. & Aqueveque, P. E. Myoelectric intuitive control and transcutaneous electrical stimulation of the forearm for vibrotactile sensation feedback applied to a 3D printed prosthetic hand. *Conf Proc IEEE Eng Med Biol Soc* **2016**, 5046–5050 (2016).
7. Beasley, R. W. & de Bese, G. M. Upper limb amputations and prostheses. *Orthop. Clin. North Am.* **17**, 395–405 (1986).
8. Benz, H. L. *et al.* Upper extremity prosthesis user perspectives on unmet needs and innovative technology. *Conf Proc IEEE Eng Med Biol Soc* **2016**, 287–290 (2016).
9. Engdahl, S. M. *et al.* Surveying the interest of individuals with upper limb loss in novel prosthetic control techniques. *J Neuroeng Rehabil* **12**, 53 (2015).
10. Dean, W. K. & Talbot, S. G. Vascularized composite allotransplantation at a crossroad. *Transplantation* **101**, 452–456 (2017).
11. da Varagine, J. *Leggenda aurea*. (1260-1298).
12. Ullman, E. Tissue and organ transplantation. *Annals of Surgery* **60**, 195–219 (1914).
13. Masson, J.C. Skin grafting, *JAMA* **70(22)**, 1581-1584 (1918). doi:10.1001/jama.1918.02600220003002
14. Loeb, L. The biological basis of individuality. *Science* **86**, 1–5 (1937).
15. Gibson, T. & Medawar, P. B. The fate of skin homografts in man. *J. Anat.* **77**, 299–310.4 (1943).
16. Medawar, P.B. The behaviour and fate of skin autografts and skin homografts in rabbits *J. Anat.* **78 (5)**, 176-199 (1944).

17. Billingham, R. E., Brent, L. & Medawar, P. B. Actively acquired tolerance of foreign cells. *Nature* **172**, 603–606 (1953).
18. Murray, J. E., Merrill, J. P. & Harrison, J. H. Renal homotransplantation in identical twins. *Journal of the American Society of Nephrology : JASN* **12**, 201–204 (1955).
19. Kuss, R., Legrain, M., Mathe, G., Nedey, R. & Camey, M. Homologous human kidney transplantation. Experience with six patients. *Postgrad Med J* **38**, 528–531 (1962).
20. Starzl, T. E., Marchioro, T. L. & Waddell, W. R. The reversal of rejection in human renal homografts with subsequent development of homograft tolerance. *Surg Gynecol Obstet* **117**, 385–395 (1963).
21. Shores, J. T., Brandacher, G., Schneeberger, S., Gorantla, V. S. & Lee, W. P. A. Composite tissue allotransplantation: hand transplantation and beyond. *J Am Acad Orthop Surg* **18**, 127–131 (2010).
22. Borel, J. F. & Kis, Z. L. The discovery and development of cyclosporine (Sandimmune). *TPS* **23**, 1867–1874 (1991).
23. Goto, T. *et al.* Discovery of FK-506, a novel immunosuppressant isolated from *Streptomyces tsukubaensis*. *TPS* **19**, 4–8 (1987).
24. Allison, A. C. & Eugui, E. M. Immunosuppressive and other effects of mycophenolic acid and an ester prodrug, mycophenolate mofetil. *Immunol. Rev.* **136**, 5–28 (1993).
25. Hewitt, C. W. *et al.* Composite tissue (limb) allografts in rats. I. Dose-dependent increase in survival with cyclosporine. *Transplantation* **39**, 360–364 (1985).
26. Black, K. S. *et al.* Composite tissue (limb) allografts in rats. II. Indefinite survival using low-dose cyclosporine. *Transplantation* **39**, 365–368 (1985).
27. Kahan, B. D. Cosmas and Damian in the 20th century. *The New England Journal of Medicine* **305**, 280–281 (1981).
28. Peacock, E. E. & Madden, J. W. Human composite flexor tendon allografts. *Annals of Surgery* **166**, 624–629 (1967).
29. Elliott, R. M., Tintle, S. M. & Levin, L. S. Upper extremity transplantation: current concepts and challenges in an emerging field. *Curr Rev Musculoskelet Med* **7**, 83–88 (2014).
30. Hofmann, G. O. *et al.* Vascularized knee joint transplantation in man: a report on the first cases. *Transpl Int* **11 Suppl 1**, S487–90 (1998).
31. Diefenbeck, M., Nerlich, A., Schneeberger, S., Wagner, F. & Hofmann, G. O. Allograft vasculopathy after allogeneic vascularized knee transplantation. *Transpl Int* **24**, e1–5 (2011).
32. Strome, M. *et al.* Laryngeal transplantation and 40-month follow-up. *The New England Journal of Medicine* **344**, 1676–1679 (2001).

33. Lorenz, R. R. & Strome, M. Total laryngeal transplant explanted: 14 years of lessons learned. *Otolaryngol Head Neck Surg* **150**, 509–511 (2014).
34. Dubernard, J.-M. *et al.* Human hand allograft: report on first 6 months. *The Lancet* **353**, 1315–1320 (1999).
35. Gazarian, A. *et al.* Hand allografts: experience from Lyon team. *Ann Chir Plast Esthet* **52**, 424–435 (2007).
36. Jones, J. W., Gruber, S. A., Barker, J. H. & Breidenbach, W. C. Successful hand transplantation. One-year follow-up. Louisville Hand Transplant Team. *The New England Journal of Medicine* **343**, 468–473 (2000).
37. Kaufman, C. L. & Breidenbach, W. World experience after more than a decade of clinical hand transplantation: update from the Louisville hand transplant program. *Hand Clin* **27**, 417–21–vii–viii (2011).
38. Dubernard, J.-M. *et al.* Functional Results of the First Human Double-Hand Transplantation. *Annals of Surgery* **238**, 128–136 (2003).
39. Bernardon, L. *et al.* Bilateral hand transplantation: Functional benefits assessment in five patients with a mean follow-up of 7.6 years (range 4-13 years). *J Plast Reconstr Aesthet Surg* **68**, 1171–1183 (2015).
40. Fageeh, W., Raffa, H., Jabbad, H. & Marzouki, A. Transplantation of the human uterus. *Int J Gynaecol Obstet* **76**, 245–251 (2002).
41. Levi, D. M. *et al.* Transplantation of the abdominal wall. *Lancet* **361**, 2173–2176 (2003).
42. Selvaggi, G. *et al.* Abdominal wall transplantation: surgical and immunologic aspects. *TPS* **41**, 521–522 (2009).
43. Birchall, M. Tongue transplantation. *Lancet* **363**, 1663 (2004).
44. Devauchelle, B. *et al.* First human face allograft: early report. *Lancet* **368**, 203–209 (2006).
45. Morelon, E. *et al.* Face Transplantation: Partial Graft Loss of the First Case 10 Years Later. *Am. J. Transplant.* **17**, 1935–1940 (2017).
46. Hu, W. *et al.* A preliminary report of penile transplantation. *Eur. Urol.* **50**, 851–853 (2006).
47. Barret, J. P. *et al.* Full face transplant: the first case report. *Annals of Surgery* **254**, 252–256 (2011).
48. Cavadas, P. C., Thione, A., Carballeira, A. & Blanes, M. Bilateral transfemoral lower extremity transplantation: result at 1 year. *Am. J. Transplant.* **13**, 1343–1349 (2013).
49. Cavadas, P. C., Thione, A., Blanes, M. & Mayordomo-Aranda, E. Primary central nervous system posttransplant lymphoproliferative disease in a bilateral transfemoral lower extremity transplantation recipient. *Am. J. Transplant.* **15**, 2758–2761 (2015).

50. Amaral, S. *et al.* 18-month outcomes of heterologous bilateral hand transplantation in a child: a case report. *The Lancet child and Adolescent Health* **1**, 35–44 (2017).
51. Petruzzo, P., Sardu, C., Lanzetta, M. & Dubernard, J.-M. Report (2017) of the International Registry on Hand and Composite Tissue Allotransplantation (IRHCTT). 1–10 (2017). doi:10.1007/s40472-017-0168-3
52. Howsare, M., Jones, C. M. & Ramirez, A. M. Immunosuppression maintenance in vascularized composite allotransplantation. *Current Opinion in Organ Transplantation* 1–7 (2017). doi:10.1097/MOT.0000000000000456
53. Kanitakis, J. *et al.* Clinicopathologic features of graft rejection of the first human hand allograft. *Transplantation* **76**, 688–693 (2003).
54. Sarhane, K. A. *et al.* A critical analysis of rejection in vascularized composite allotransplantation: clinical, cellular and molecular aspects, current challenges, and novel concepts. *Front. Immunol.* **4**, 406 (2013).
55. Chung, K. C., Oda, T., Saddawi-Konefka, D. & Shauver, M. J. An economic analysis of hand transplantation in the United States. *Plastic and Reconstructive Surgery* **125**, 589–598 (2010).
56. Salminger, S., Roche, A. D., Sturma, A., Mayer, J. A. & Aszmann, O. C. Hand Transplantation Versus Hand Prosthetics: Pros and Cons. *Current Surgery Reports* **4**, 1–7 (2016).
57. Salminger, S. Functional and Psychosocial Outcomes of Hand Transplantation Compared with Prosthetic Fitting in Below-Elbow Amputees: A Multicenter Cohort Study. *PLoS ONE* 1–13 (2016). doi:10.1371/journal.pone.0162507
58. Parnes, J. R. Molecular biology and function of CD4 and CD8. *Adv. Immunol.* **44**, 265–311 (1989).
59. Krensky, A. M., Weiss, A., Crabtree, G., Davis, M. M. & Parham, P. T-lymphocyte-antigen interactions in transplant rejection. *The New England Journal of Medicine* **322**, 510–517 (1990).
60. Landin, L., Cavadas, P. C., Nthumba, P., Ibañez, J. & Vera-Sempere, F. Preliminary results of bilateral arm transplantation. *Transplantation* **88**, 749–751 (2009).
61. Cendales, L. C. *et al.* The Banff 2007 working classification of skin-containing composite tissue allograft pathology. *Am. J. Transplant.* **8**, 1396–1400 (2008).
62. Clark, R. A. *et al.* The vast majority of CLA+ T cells are resident in normal skin. *The Journal of Immunology* **176**, 4431–4439 (2006).
63. Igyártó, B. Z. *et al.* Skin-resident murine dendritic cell subsets promote

- distinct and opposing antigen-specific T helper cell responses. *Immunity* **35**, 260–272 (2011).
64. Wakim, L. M., Waithman, J., van Rooijen, N., Heath, W. R. & Carbone, F. R. Dendritic cell-induced memory T cell activation in nonlymphoid tissues. *Science* **319**, 198–202 (2008).
 65. Nestle, F. O. *et al.* Plasmacytoid predendritic cells initiate psoriasis through interferon-alpha production. *J. Exp. Med.* **202**, 135–143 (2005).
 66. Campbell, D. J. & Butcher, E. C. Rapid acquisition of tissue-specific homing phenotypes by CD4(+) T cells activated in cutaneous or mucosal lymphoid tissues. *J. Exp. Med.* **195**, 135–141 (2002).
 67. Lian, C. G. *et al.* Biomarker evaluation of face transplant rejection: association of donor T cells with target cell injury. *Mod. Pathol.* **27**, 788–799 (2014).
 68. Valujskikh, A., Pantenburg, B. & Heeger, P. S. Primed allospecific T cells prevent the effects of costimulatory blockade on prolonged cardiac allograft survival in mice. *Am. J. Transplant.* **2**, 501–509 (2002).
 69. Masopust, D., Vezys, V., Marzo, A. L. & Lefrançois, L. Preferential localization of effector memory cells in nonlymphoid tissue. *Science* **291**, 2413–2417 (2001).
 70. Reinhardt, R. L., Khoruts, A., Merica, R., Zell, T. & Jenkins, M. K. Visualizing the generation of memory CD4 T cells in the whole body. *Nature* **410**, 101–105 (2001).
 71. Beura, L. K., Rosato, P. C. & Masopust, D. Implications of Resident Memory T Cells for Transplantation. *Am. J. Transplant.* **17**, 1167–1175 (2017).
 72. Schneeberger, S. *et al.* Atypical acute rejection after hand transplantation. *Am. J. Transplant.* **8**, 688–696 (2008).
 73. Wolfram, D. *et al.* Differentiation between acute skin rejection in allotransplantation and T-cell mediated skin inflammation based on gene expression analysis. *Biomed. Res. Int.* **2015**, 259160–11 (2015).
 74. Brehm, M. A. *et al.* Allografts stimulate cross-reactive virus-specific memory CD8 T cells with private specificity. *Am. J. Transplant.* **10**, 1738–1748 (2010).
 75. Lopdrup, R. G. *et al.* Seasonal Variability Precipitating Hand Transplant Rejection? *Transplantation* **101**, e313 (2017).
 76. Dijke, E. I. *et al.* B cells in transplantation. *J. Heart Lung Transplant.* **35**, 704–710 (2016).
 77. Sacks, S. H., Chowdhury, P. & Zhou, W. Role of the complement system in rejection. *Curr. Opin. Immunol.* **15**, 487–492 (2003).

78. Schneeberger, S. *et al.* Upper-Extremity Transplantation Using a Cell-Based Protocol to Minimize Immunosuppression. *Annals of Surgery* **257**, 345–351 (2013).
79. Weissenbacher, A. *et al.* Antibody-mediated rejection in hand transplantation. *Transpl Int* **27**, e13–7 (2014).
80. Etra, J. W., Raimondi, G. & Brandacher, G. Mechanisms of rejection in vascular composite allotransplantation. *Current Opinion in Organ Transplantation* **23**, 28–33 (2018).
81. Benichou, G., Yamada, Y., Aoyama, A. & Madsen, J. C. Natural killer cells in rejection and tolerance of solid organ allografts. *Current Opinion in Organ Transplantation* **16**, 47–53 (2011).
82. Hautz, T. *et al.* Lymphoid neogenesis in skin of human hand, nonhuman primate, and rat vascularized composite allografts. *Transpl Int* **27**, 966–976 (2014).
83. Kanitakis, J. *et al.* Chronic Rejection in Human Vascularized Composite Allotransplantation (Hand and Face Recipients). *Transplantation* **100**, 2053–2061 (2016).
84. Kaufman, C. L. *et al.* Graft vasculopathy in clinical hand transplantation. *Am. J. Transplant.* **12**, 1004–1016 (2012).
85. Petruzzo, P. *et al.* Clinicopathological Findings of Chronic Rejection in a Face Grafted Patient. *Transplantation* **99**, 2644–2650 (2015).
86. Hori, S., Nomura, T. & Sakaguchi, S. Control of regulatory T cell development by the transcription factor Foxp3. *Science* **299**, 1057–1061 (2003).
87. Vignali, D. A. A. Mechanisms of T(reg) Suppression: Still a Long Way to Go. *Front. Immunol.* **3**, 191 (2012).
88. Baecher-Allan, C., Viglietta, V. & Hafler, D. A. Inhibition of human CD4(+)CD25(+high) regulatory T cell function. *The Journal of Immunology* **169**, 6210–6217 (2002).
89. Sakaguchi, S. Naturally arising Foxp3-expressing CD25+CD4+ regulatory T cells in immunological tolerance to self and non-self. *Nature Immunology* **6**, 345–352 (2005).
90. Sawant, D. V. & Vignali, D. A. A. Once a Treg, always a Treg? *Immunol. Rev.* **259**, 173–191 (2014).
91. Toker, A. *et al.* Active demethylation of the Foxp3 locus leads to the generation of stable regulatory T cells within the thymus. *J. Immunol.* **190**, 3180–3188 (2013).
92. Bui, J. D., Uppaluri, R., Hsieh, C.-S. & Schreiber, R. D. Comparative analysis of regulatory and effector T cells in progressively growing versus rejecting tumors of similar origins. *Cancer Res.* **66**, 7301–7309 (2006).

93. Goodman, W. A. *et al.* IL-6 signaling in psoriasis prevents immune suppression by regulatory T cells. *J. Immunol.* **183**, 3170–3176 (2009).
94. Battaglia, M., Stabilini, A. & Roncarolo, M.-G. Rapamycin selectively expands CD4+CD25+FoxP3+ regulatory T cells. *Blood* **105**, 4743–4748 (2005).
95. Bestard, O. *et al.* Presence of FoxP3+ regulatory T Cells predicts outcome of subclinical rejection of renal allografts. *J. Am. Soc. Nephrol.* **19**, 2020–2026 (2008).
96. Akimova, T. *et al.* Differing effects of rapamycin or calcineurin inhibitor on T-regulatory cells in pediatric liver and kidney transplant recipients. *Am. J. Transplant.* **12**, 3449–3461 (2012).
97. Lin, J.-Y. *et al.* Optimizing chimerism level through bone marrow transplantation and irradiation to induce long-term tolerance to composite tissue allotransplantation. *J. Surg. Res.* **178**, 487–493 (2012).
98. Mohty, M. Mechanisms of action of antithymocyte globulin: T-cell depletion and beyond. *Leukemia* **21**, 1387–1394 (2007).
99. Brennan, D. C. & Schnitzler, M. A. Long-term results of rabbit antithymocyte globulin and basiliximab induction. *The New England Journal of Medicine* **359**, 1736–1738 (2008).
100. Hanaway, M. J. *et al.* Alemtuzumab induction in renal transplantation. *The New England Journal of Medicine* **364**, 1909–1919 (2011).
101. Lee, P., Murase, N., Todo, S., Makowka, L. & Starzl, T. The immunosuppressive effects of FR 900506 in rats receiving heterotopic cardiac allografts. *Surg Res Commun* **1**, 325–331 (1987).
102. Rusnak, F. & Mertz, P. Calcineurin: form and function. *Physiol. Rev.* **80**, 1483–1521 (2000).
103. Rincón, M. & Flavell, R. A. AP-1 transcriptional activity requires both T-cell receptor-mediated and co-stimulatory signals in primary T lymphocytes. *EMBO J.* **13**, 4370–4381 (1994).
104. Shaw, K. T. *et al.* Immunosuppressive drugs prevent a rapid dephosphorylation of transcription factor NFAT1 in stimulated immune cells. *Proc Natl Acad Sci USA* **92**, 11205–11209 (1995).
105. Boyman, O. & Sprent, J. The role of interleukin-2 during homeostasis and activation of the immune system. *Nature Publishing Group* **12**, 180–190 (2012).
106. Palkowitsch, L. *et al.* The Ca²⁺-dependent phosphatase calcineurin controls the formation of the Carma1-Bcl10-Malt1 complex during T cell receptor-induced NF-kappaB activation. *J. Biol. Chem.* **286**, 7522–7534 (2011).
107. Messer, G., Weiss, E. H. & Baeuerle, P. A. Tumor necrosis factor beta

- (TNF-beta) induces binding of the NF-kappa B transcription factor to a high-affinity kappa B element in the TNF-beta promoter. *Cytokine* **2**, 389–397 (1990).
108. Sica, A. *et al.* Interaction of NF-kappaB and NFAT with the interferon-gamma promoter. *J. Biol. Chem.* **272**, 30412–30420 (1997).
 109. Matsuda, S. *et al.* Two distinct action mechanisms of immunophilin-ligand complexes for the blockade of T-cell activation. *EMBO Rep.* **1**, 428–434 (2000).
 110. Khanna, A., Cairns, V. & Hosenpud, J. D. Tacrolimus induces increased expression of transforming growth factor-beta1 in mammalian lymphoid as well as nonlymphoid cells. *Transplantation* **67**, 614–619 (1999).
 111. Wu, C.-Y. & Benet, L. Z. Predicting drug disposition via application of BCS: transport/absorption/ elimination interplay and development of a biopharmaceutics drug disposition classification system. *Pharm. Res.* **22**, 11–23 (2005).
 112. Venkataramanan, R. *et al.* Clinical pharmacokinetics of tacrolimus. *Clin Pharmacokinet* **29**, 404–430 (1995).
 113. Antignac, M., Barrou, B., Farinotti, R., Lechat, P. & Urien, S. Population pharmacokinetics and bioavailability of tacrolimus in kidney transplant patients. *Br J Clin Pharmacol* **64**, 750–757 (2007).
 114. Staatz, C. E. & Tett, S. E. Clinical pharmacokinetics and pharmacodynamics of tacrolimus in solid organ transplantation. *Clin Pharmacokinet* **43**, 623–653 (2004).
 115. Lampen, A. *et al.* Metabolism of the immunosuppressant tacrolimus in the small intestine: cytochrome P450, drug interactions, and interindividual variability. *Drug Metab. Dispos.* **23**, 1315–1324 (1995).
 116. Hebert, M. Contributions of hepatic and intestinal metabolism and P-glycoprotein to cyclosporine and tacrolimus oral drug delivery. *Adv. Drug Deliv. Rev.* **27**, 201–214 (1997).
 117. Iwasaki, K. *et al.* Further metabolism of FK506 (tacrolimus). Identification and biological activities of the metabolites oxidized at multiple sites of FK506. *Drug Metab. Dispos.* **23**, 28–34 (1995).
 118. Nagase, K., Iwasaki, K., Nozaki, K. & Noda, K. Distribution and protein binding of FK506, a potent immunosuppressive macrolide lactone, in human blood and its uptake by erythrocytes. *J. Pharm. Pharmacol.* **46**, 113–117 (1994).
 119. Lusco, M. A., Fogo, A. B., Najafian, B. & Alpers, C. E. AJKD atlas of renal pathology: calcineurin inhibitor nephrotoxicity. *Am. J. Kidney Dis.* **69**, e21–e22 (2017).

120. Hoorn, E. J. *et al.* The calcineurin inhibitor tacrolimus activates the renal sodium chloride cotransporter to cause hypertension. *Nat Med* **17**, 1304–1309 (2011).
121. Jindal, R. M., Sidner, R. A. & Milgrom, M. L. Post-transplant diabetes mellitus. The role of immunosuppression. *Drug Saf* **16**, 242–257 (1997).
122. Radu, R. G. *et al.* Tacrolimus suppresses glucose-induced insulin release from pancreatic islets by reducing glucokinase activity. *Am. J. Physiol. Endocrinol. Metab.* **288**, E365–71 (2005).
123. Capron, A. *et al.* Correlation of tacrolimus levels in peripheral blood mononuclear cells with histological staging of rejection after liver transplantation: preliminary results of a prospective study. *Transpl Int* **25**, 41–47 (2012).
124. Kelly, P. A., Gruber, S. A., Behbod, F. & Kahan, B. D. Sirolimus, a new, potent immunosuppressive agent. *Pharmacotherapy* **17**, 1148–1156 (1997).
125. Neuhaus, P., Klupp, J. & Langrehr, J. M. mTOR inhibitors: an overview. *Liver Transpl.* **7**, 473–484 (2001).
126. Webster, A. C., Lee, V. W. S., Chapman, J. R. & Craig, J. C. Target of rapamycin inhibitors (sirolimus and everolimus) for primary immunosuppression of kidney transplant recipients: a systematic review and meta-analysis of randomized trials. *Transplantation* **81**, 1234–1248 (2006).
127. Davis, M. M. & Bjorkman, P. J. T-cell antigen receptor genes and T-cell recognition. *Nature* **334**, 395–402 (1988).
128. Lafferty, K. J. & Cunningham, A. J. A new analysis of allogeneic interactions. *Aust J Exp Biol Med Sci* **53**, 27–42 (1975).
129. Jenkins, M. K., Taylor, P. S., Norton, S. D. & Urdahl, K. B. CD28 delivers a costimulatory signal involved in antigen-specific IL-2 production by human T cells. *The Journal of Immunology* **147**, 2461–2466 (1991).
130. Janeway, C. A. & Bottomly, K. Signals and signs for lymphocyte responses. *Cell* **76**, 275–285 (1994).
131. Larsen, C. P. *et al.* Rational development of LEA29Y (belatacept), a high-affinity variant of CTLA4-Ig with potent immunosuppressive properties. *Am. J. Transplant.* **5**, 443–453 (2005).
132. Grahammer, J. *et al.* Benefits and limitations of belatacept in 4 hand-transplanted patients. *Am. J. Transplant.* **17**, 3228–3235 (2017).
133. de Graav, G. N. *et al.* Down-regulation of surface CD28 under belatacept treatment: an escape mechanism for antigen-reactive T-cells. *PLoS ONE* **11**, e0148604 (2016).

134. Stegall, M. D., Morris, R. E., Alloway, R. R. & Mannon, R. B. Developing new immunosuppression for the next generation of transplant recipients: the path forward. *Am. J. Transplant.* **16**, 1094–1101 (2016).
135. Ghazal, K. *et al.* Treatment with mTOR inhibitors after liver transplantation enables a sustained increase in regulatory T-cells while preserving their suppressive capacity. *Clin Res Hepatol Gastroenterol* (2017). doi:10.1016/j.clinre.2017.10.001
136. Noyan, F. *et al.* Prevention of allograft rejection by use of regulatory T cells with an MHC-specific chimeric antigen receptor. *Am. J. Transplant.* **17**, 917–930 (2017).
137. Castro-Manreza, M. E. & Montesinos, J. J. Immunoregulation by mesenchymal stem cells: biological aspects and clinical applications. *Journal of Immunology Research* **2015**, 1–20 (2015).
138. Plock, J. A. *et al.* Adipose- and bone marrow-derived mesenchymal stem cells prolong graft survival in vascularized composite allotransplantation. *Transplantation* **99**, 1765–1773 (2015).
139. Cavanagh, L. L., Saal, R. J., Grimmett, K. L. & Thomas, R. Proliferation in monocyte-derived dendritic cell cultures is caused by progenitor cells capable of myeloid differentiation. *Blood* **92**, 1598–1607 (1998).
140. Schultze, J. L. *et al.* CD40-activated human B cells: an alternative source of highly efficient antigen presenting cells to generate autologous antigen-specific T cells for adoptive immunotherapy. *J. Clin. Invest.* **100**, 2757–2765 (1997).
141. Sicard, A. *et al.* B cells loaded with synthetic particulate antigens: a versatile platform to generate antigen-specific helper T cells for cell therapy. *Nano Lett.* **16**, 297–308 (2016).
142. Diaz-Siso, J. R. *et al.* Initial experience of dual maintenance immunosuppression with steroid withdrawal in vascular composite tissue allotransplantation. *Am. J. Transplant.* **15**, 1421–1431 (2015).
143. Solari, M. G. *et al.* Daily topical tacrolimus therapy prevents skin rejection in a rodent hind limb allograft model. *Plastic and Reconstructive Surgery* **123**, 17S–25S (2009).
144. Kim, S.-M. & Kim, H.-S. Engineering of extracellular vesicles as drug delivery vehicles. *Stem Cell Investig* **4**, 74–74 (2017).
145. Pang, L. *et al.* A novel strategy to achieve effective drug delivery: exploit cells as carrier combined with nanoparticles. *Drug Delivery* **24**, 83–91 (2017).
146. Cremel, M., Guérin, N., Horand, F., Banz, A. & Godfrin, Y. Red blood cells as innovative antigen carrier to induce specific immune tolerance. *Int J Pharm* **443**, 39–49 (2013).

147. Jhunjhunwala, S. *et al.* Controlled release formulations of IL-2, TGF- β 1 and rapamycin for the induction of regulatory T cells. *J Control Release* **159**, 78–84 (2012).
148. Zamorano-Leon, J. J. *et al.* New strategy of tacrolimus administration in animal model based on tacrolimus-loaded microspheres. *Transpl. Immunol.* **36**, 9–13 (2016).
149. Miyamoto, Y. *et al.* Pharmacokinetic and immunosuppressive effects of tacrolimus-loaded biodegradable microspheres. *Liver Transpl.* **10**, 392–396 (2004).
150. Segers, V. F. M. & Lee, R. T. Biomaterials to enhance stem cell function in the heart. *Circ. Res.* **109**, 910–922 (2011).
151. Liu, J. M. H. *et al.* Transforming growth factor-beta 1 delivery from microporous scaffolds decreases inflammation post-implant and enhances function of transplanted islets. *Biomaterials* **80**, 11–19 (2016).
152. Unadkat, J. V. *et al.* Single implantable FK506 disk prevents rejection in vascularized composite allotransplantation. *Plastic and Reconstructive Surgery* **139**, 403e–414e (2017).
153. Vemula, P. K., Li, J. & John, G. Enzyme catalysis: tool to make and break amygdalin hydrogelators from renewable resources: a delivery model for hydrophobic drugs. *J. Am. Chem. Soc.* **128**, 8932–8938 (2006).
154. Gajanayake, T. *et al.* A single localized dose of enzyme-responsive hydrogel improves long-term survival of a vascularized composite allograft. *Sci Transl Med* **6**, 249ra110–249ra110 (2014).
155. Kim, J. *et al.* Injectable, spontaneously assembling, inorganic scaffolds modulate immune cells in vivo and increase vaccine efficacy. *Nat Biotechnol* **33**, 64–72 (2015).
156. Olariu, R. *et al.* Intra-graft injection of tacrolimus promotes survival of vascularized composite allotransplantation. *Journal of Surgical Research* **218**, e107–e107 (2017).
157. Wang, T. *et al.* Infection with the intracellular bacterium, *Listeria monocytogenes*, overrides established tolerance in a mouse cardiac allograft model. *Am. J. Transplant.* **10**, 1524–1533 (2010).
158. Young, J. S. *et al.* Erosion of Transplantation Tolerance After Infection. *American Journal of Transplantation* **17**, 81–90 (2016).
159. Tiefenthaler, M. *et al.* In vitro treatment of dendritic cells with tacrolimus: impaired T-cell activation and IP-10 expression. *Nephrol. Dial. Transplant.* **19**, 553–560 (2004).
160. Ren, Y., Yang, Y., Yang, J., Xie, R. & Fan, H. Tolerogenic dendritic cells modified by tacrolimus suppress CD4(+) T-cell proliferation and

- inhibit collagen-induced arthritis in mice. *Int. Immunopharmacol.* **21**, 247–254 (2014).
161. Shanmugarajah, K. *et al.* The effect of MHC antigen matching between donors and recipients on skin tolerance of vascularized composite allografts. *American Journal of Transplantation* **17**, 1729–1741 (2017).
 162. Alhabbab, R. *et al.* Diversity of gut microflora is required for the generation of B cell with regulatory properties in a skin graft model. *Nature Publishing Group* 1–12 (2015). doi:10.1038/srep11554

6. Acknowledgements

Lieber Robert,

Danke, dass du mir seit dem ersten Tag dein Vertrauen geschenkt hast! Du erlaubtest mir so unabhängig zu arbeiten wie ich es möchte, und gleichzeitig war deine Unterstützung immer in Reichweite, was immens beruhigend war.

Caro Adriano,

Grazie per essere il mio "partner in crime" e un vero amico. Mi hai insegnato tanto, non solo come essere uno scienziato decente, ma anche come essere un essere umano decente. Grazie di tutto!

Dear Giorgio, Hans-Rudolf and Praveen,

Having the opportunity to learn from you and improve my own work through your invaluable contributions was nothing short of a huge stroke of luck for me! It was such a privilege to have you as inspiring scientists and people! Thank you for your time, support and advice!

Dear teammates,

You were my big, cool lab family and I will miss you sincerely! Thank you Tsering, Catherine, Riccardo, Jane, Mai, Alain, Yvonne, Uyen, Marla, Shengye, Oliver, Julie, Pavan and many others who were part of the lab at some point. Also I'd like to thank Dr. Vögelin, Dr. Olariu, Dr. Leckenby, Dr. Sutter, Dr. Schnider, Dr. Banz, Jean-Christophe, Cedric, Yolanda, Michael, Alexander, and Ashish. Working with you was an extremely rewarding experience!

Cher Michel,

Merci pour ton temps, ton soutien, ton amour et surtout de rester à mes côtés dans mes moments de folie durant ma thèse.

Мамо, татко, Мими,

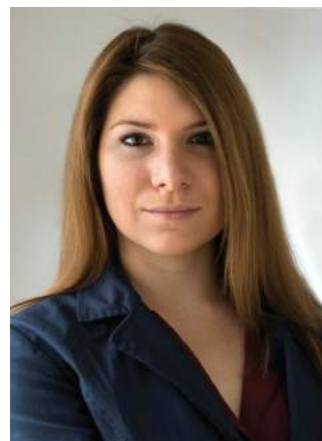
Съжалявам, че все нямам достатъчно време да прекарам с вас и да ви покажа колко много ви обичам и колко много значите за мен. Посвещавам тази работа на вас и ви благодаря, че винаги сте вярвали в мен, винаги сте ме оставяли да бъда и да правя това, което искам, и ми дадохте свободата да правя изборите за живота си самостоятелно. Надявам се един ден да върна част от това, което вие сте ми дали.

7. Curriculum Vitae

Dzhuliya Dzhonova

+ 41 (0) 77 955 29 99, dzhuliya.dzhonova@gmail.com

English (proficient); German (B1 - B2); French (beginner);
Bulgarian (mother tongue)



EMPLOYMENT HISTORY

Hepatitis B lab specialist – 8 / 2014 - 4 / 2015

pRED, Roche, Basel - Infectious Diseases Department

Supervisor: Miriam Triyatni, MD, PhD

PCR, immunosorbent analyses, viral extraction and purification for *in vitro* iPSC-derived, Hepatitis B infected hepatocyte based platform for compound screening of potential anti-Hepatitis B drug.

Analytical Support – 8 / 2013 – 7 / 2014

Roche Diagnostics AG, Rotkreuz - Process & Support

Supervisor: Sheila Isepponi; Stephen Will, PhD

Support internal clients for PCR analyses with electrophoresis and UPLC.

Inventor for US Patent # 14189671.2 -1404 – “PCR verification by UPLC”.

Bulgarian Academy of Sciences – Internship – 5 / 2013 - 8 / 2013

Biophysics & Biomedical Engineering Department

Supervisor: Stefka Taneva, Prof.

Serum NAD(P)H fluorescence / proteome calorimetry as potential diagnostic tools for IgM multiple myeloma in a mouse model.

EDUCATION

PhD – Biomedical Sciences – 2015 – 2018

Department for BioMedical Research, University of Bern

Supervisor: Robert Rieben, Prof.

Preclinical validation of inflammation-responsive hydrogels for local immunosuppression in rat model of vascularized composite allotransplantation, incl. immunological, toxicological and PK/PD analyses.

MSc – Cell Biology & Pathology – 2012 – 2014

Sofia University – GPA: 5.57; Master work at Roche Diagnostics AG, Rotkreuz –

Thesis Grade: 6.00

Developed and patented a new technology for analysis of false positive RT-PCR samples with UPLC for HIV, later transferred for Hepatitis A& B and other viruses.

BSc – Molecular Biology – 2008 – 2012

Sofia University, GPA: 5.16; State Exam: 6.00 (2.00 – min; 6.00 – max)

PROFESSIONAL COMPETENCES

Experienced in broad variety of molecular (PCR, ELISA and like, Luminex, Western blot), analytical (HPLC, electrophoresis) and cell-biology techniques (flow cytometry, MLR, cell-culture), *in vivo* research (FELASA / LTK1 certified), immunofluorescence imaging, viral and exosomes purification (incl. nanoparticle tracking analyses). Trying to gradually switch from Prism7 to R and looking forward to develop expertise in biostatistics with R.

Additional strengths: technical presentation, project management

REFERENCES

Robert Rieben, Prof. - Cardio-vascular Research Group Leader, DBMR
University of Bern, Murtenstrasse 50, 3008, Bern, CH
Telephone: +41 31 632 96 69, e-mail: robert.rieben@dbmr.unibe.ch

Miriam Triyatni, MD-PhD - Safety Science Leader, Licensing and Early Development
F. Hoffmann-La Roche Ltd B686, Centralbahnstrasse 4, 4070, Basel, CH
Telephone +41 61 688 17 24, e-mail: miriam.triyatni@roche.com

Sheila Isepponi - Principal Scientist II & Team Leader, Analytics Support Team
Roche Diagnostics International AG, Forrenstrasse 2, 6343, Rotkreuz, CH
Telephone +41 41 798 5269, e-mail: sheila.isepponi@roche.com

8. Publications, abstracts, presentations

PUBLICATIONS

Dzhonova D. et al. Local injections of tacrolimus-loaded hydrogel reduce systemic immunosuppression-related toxicity in vascularized composite allotransplantation. Under revision.

Dzhonova D. et al. In vivo characterization and non-invasive monitoring of tacrolimus-loaded hydrogel for localized immunosuppression immunosuppression. Manuscript in preparation.

Sutter D; **Dzhonova D.** et al. Delivery of rapamycin using in situ forming implants induces immunoregulatory mechanisms promoting vascularized composite allograft survival. Under revision.

Olariu R; Denoyelle J; Leclère F; **Dzhonova D.** et al. Intra-graft injection of tacrolimus promotes survival of vascularized composite allotransplantation. J Surg Res 218,49-57(2017)

PRESENTATIONS

INTERNATIONAL

19/23.08.2016 – 26th International Congress of The Transplantation Society – Poster

10/12.11.2016 – Basic Science in Transplantation Congress – Poster

03/05.11.2016 – American Society for Reconstructive Transplantation 5th Biennial Meeting – Oral

24/27.09.2017 – 18th Congress of the European Society for Organ Transplantation – Oral

26/27.10.2017 – International Society of Vascularized Composite Allotransplantation congress – Poster

NATIONAL

21.04.2016 – **Award finalist:** Spring Meeting of Swiss Society of Pharmacology and Toxicology – Oral

20.04.2017 – Spring Meeting of Swiss Society of Pharmacology and Toxicology – Poster

LOCAL

04.11.2015 – University of Bern – Day of Clinical Research – Poster

06.04.2016 – University of Bern – Progress Report

02.11.2016 – University of Bern – Day of Clinical Research – Poster

31.10.2017 – **Award finalist:** University of Bern – Day of Clinical Research – Poster

02.02.2017 – University of Bern – GCB Symposium – Oral (Slam)

29.08.2017 – University of Bern – 8 x 8[!] - Junge Forschende erzählen – Oral